

Role of Transcription Factors AP-2 and NFI in Development and Glioblastoma

by

Saket Jain

A thesis submitted in partial fulfillment of the requirements for the degree of

Doctor of Philosophy

in

Experimental Oncology

Department of Oncology  
University of Alberta

©Saket Jain, 2018

# Abstract

Gene regulation pathways involved in embryonic development are commonly implicated in cancer. Transcription factors play key roles in all aspects of development including cell proliferation, migration and differentiation. Aberrant expression of many developmentally-regulated transcription factors contributes to many malignancies. In this thesis, we studied the role of transcription factor family AP-2 in retinal development and glioblastoma (GBM) and the role of transcription factor family NFI in GBM. Four of the five members of the AP-2 family (AP-2 $\alpha$ , AP-2 $\beta$ , AP-2 $\gamma$  and AP-2 $\delta$ ) have previously been shown to be expressed in developing retina. In Chapter 2, we show that the fifth member of the AP-2 family, AP-2 $\epsilon$ , is also expressed in the developing mammalian retina. Our data point to a specialized role for AP-2 $\epsilon$  in a subset of amacrine cells, with AP-2 $\epsilon$  being restricted to the GABAergic amacrine lineage. AP-2 $\epsilon$  is co-expressed with AP-2 $\alpha$ , AP-2 $\beta$  and AP-2 $\gamma$  in subsets of amacrine cells, suggesting roles for both AP-2 homodimers and AP-2 heterodimers in the regulation of AP-2 target genes in the retina. Our work suggests spatially- and temporally-coordinated roles for combinations of AP-2 transcription factors in amacrine cells during retinal development.

Several studies have implicated aberrant regulation of AP-2 with cancer. In Chapter 4, we examined the role of AP-2 in GBM progression. GBMs are the most aggressive brain cancers with a dismal prognosis. Despite aggressive treatment including surgery followed by radiotherapy and chemotherapy the median survival remains ~14 months. In low grade astrocytoma, AP-2 $\alpha$  is primarily found in the nucleus, whereas in GBM, it has a cytoplasmic pattern. Based on our results, three members of the AP-2 family, AP-2 $\alpha$ , AP-2 $\beta$ , and AP-2 $\gamma$ , are widely expressed in GBM cell lines and patient-

derived neurosphere cultures. Interestingly, AP-2 $\beta$  levels are particularly high in patient-derived neurosphere cultures when compared to adherent cells derived from the same patient. Furthermore, AP-2 $\beta$  primarily localizes to the nucleus of cells cultured under neurosphere conditions compared to cells cultured under adherent conditions. Depletion of AP-2 $\beta$  results in reduced expression of stem cell markers Nestin and SOX2. As well, cell migration is significantly reduced upon AP-2 $\beta$  depletion in patient-derived GBM cultures. As hypoxia is a hallmark of GBM tumours, we examined the effect of AP-2 $\beta$  on cell migration markers and well as stem cell markers under hypoxia. Overall, our results indicate a role for AP-2 $\beta$  in stem cell maintenance in GBM.

Next, we studied the role of NFI, in GBM. The NFI family consists of four family members NFIA, NFIB, NFIC and NFIX. In the developing CNS, NFI family members are involved in glial cell differentiation. Studies from our lab and other labs suggest a role for NFIs in GBM. In Chapter 3, we used ChIP-on-chip to identify additional NFI targets in GBM cells. Of ~400 putative targets identified using this approach, we focused on HEY1, a Notch effector gene associated with maintenance of neural stem cells. We showed that all four NFIs can bind to the NFI recognition sites in the *HEY1* promoter and that NFI negatively regulates the expression of HEY1. We further showed that depletion of HEY1 in GBM cells results in reduced cell proliferation and increased cell migration. We also found a correlation between elevated HEY1 levels and expression of B-FABP, a stem/progenitor cell marker in GBM cells, and also showed that HEY1 depletion results in increased levels of astrocyte differentiation marker GFAP. Overall our results indicate that NFI negatively regulates HEY1 and expression of HEY1 is associated with the expression of stem cell markers in GBM.

# Preface

The research in this thesis was conducted with assistance or in collaboration as noted below.

Chapter 2 has been published as **Jain S**, Glubrecht DD, Germain, D and Godbout R. *AP-2 $\epsilon$  expression in developing retina: Contributing to molecular diversity of amacrine cells*. **Scientific Reports**, (2018) Feb 21;8(1):3386. Darryl Glubrecht performed the co-immunofluorescence and immunohistochemistry experiments. Devon Germain carried out the analysis of the sequencing data. I designed all the experiments, prepared the constructs, and performed *in situ* hybridization, western blot analysis, RT-PCRs, qPCRs, analyzed the co-immunofluorescence data, prepared all figures, and wrote the manuscript with input from the other authors. Dr. Roseline Godbout supervised the study and was involved at all stages of the project including experimental design, analysis and in writing the manuscript.

Chapter 3 is currently under review as Brun M\*, **Jain S\***, Monckton E and Godbout R. *Nuclear Factor I represses the notch effector HEY1 in glioblastoma*. **Neoplasia**, (\* **Co-first author**). Miranda Brun and I contributed equally to the manuscript and were involved with designing the experiments and analysis of the data. Miranda carried out the ChIP-on-chip, gel shifts and some of the luciferase reporter gene assays. I carried out the reporter gene assays, the cell proliferation assay, scratch assay and Transwell migration assay, cell cycle analysis, qPCR and western blot analysis. Elizabeth Monckton provided assistance with the gel shifts and reporter gene assays. Dr. Roseline Godbout supervised the study and was involved at all stages of the project including experimental design, analysis and in writing the manuscript.

Chapter 4 is expected to be submitted as a manuscript in the near future. Experiments carried out in this chapter were carried out by me except for the immunohistochemistry experiments which were performed by Darryl Glubrecht. Dr. Roseline Godbout supervised the study and was involved at all stages of the project including experimental design and analysis.

# Acknowledgments

I would like to thank my supervisor Dr. Roseline Godbout for her continued support during my Ph.D. program. Dr. Godbout has always been a source of motivation throughout the graduate school. Her dedication towards science has always inspired me to be disciplined and focused in my research interests. She has always been prompt in answering queries, providing feedback on results and especially in reviewing the papers and my thesis. She has always encouraged me to explore new ideas and think independently. Moreover, she has been very patient when the experiments didn't work and provided her constructive criticism when needed. I would also like to thank my committee members Dr. Gordon Chan and Dr. Alan Underhill for their help with their technical expertise and suggestions in steering the project in the right direction. I am also grateful to Dr. Sun and Gerry from the cell imaging facility at the Cross Cancer Institute for providing their expertise at various points during my Ph.D.

I would like to express my gratitude to my lab mates Dr. Lei Li, Dr. Rongzong Liu, Elizabeth Monckton, Darryl Glubrecht, Kevin Vo, Jack wang, Xia Xu, Daniel Choi and Stanley for the numerous discussions and help with the experiments when needed.

I am grateful to my friends specially Pritam, Arun, Indrani and Nishant for being with me through the best and the worst times since I arrived in Edmonton. Their immense emotional support and encouragement has made my difficult times easier in Edmonton.

Last but not the least, I would like to thank my parents and my younger brother for always believing in me. Their never-ending support has helped me to stay motivated and work hard towards my goal.

# Table of Contents

<b>Abstract</b> .....	<b>ii</b>
<b>Preface</b> .....	<b>iv</b>
<b>Acknowledgments</b> .....	<b>vi</b>
<b>List of Figures</b> .....	<b>x</b>
<b>List of Tables</b> .....	<b>xii</b>
<b>List of Abbreviations</b> .....	<b>xiii</b>
<b>Chapter 1 Introduction</b> .....	<b>1</b>
<b>1.1 Retina Development</b> .....	<b>2</b>
1.1.1 Genesis of retinal cells .....	2
1.1.2 Escaping the cell cycle .....	5
1.1.3 Retinal differentiation .....	7
1.1.4 Retinal amacrine cells .....	9
<b>1.2 Glioblastoma</b> .....	<b>11</b>
1.2.1 Epidemiology and classification .....	11
1.2.2 Glioblastoma current treatment and survival .....	16
1.2.3 GBM cell migration .....	17
<b>1.3 Transcription factor Activator Protein 2 (AP-2; TFAP2)</b> .....	<b>19</b>
1.3.1 Structure and function of AP-2 .....	19
1.3.2 AP-2 in embryonic development and AP-2 knockout mice .....	25
<b>1.4 Role of AP-2 in cancer</b> .....	<b>27</b>
1.4.1 AP-2 aberrant expression and subcellular localization .....	28
1.4.2 AP-2 in glioblastoma.....	29
<b>1.5 Transcription factor Nuclear Factor I</b> .....	<b>30</b>
1.5.1 Structure and function .....	30
1.5.2 Role of NFI in gliogenesis .....	32
1.5.3 NFI in glioblastoma.....	35
<b>1.6 HEY1: A Notch effector</b> .....	<b>37</b>
1.6.1 HEY family .....	37
1.6.2 HEY in brain development.....	38
1.6.3 HEY1 in glioblastoma.....	39
<b>1.7 Research objectives</b> .....	<b>42</b>
1.7.1 Chapter 2: AP-2 $\epsilon$ expression in developing retina .....	42
1.7.2 Chapter 3: NFI represses Notch effector HEY1 in glioblastoma .....	43
1.7.3 Chapter 4: Role of AP-2 $\beta$ in stem cell maintenance in glioblastoma.....	44
<b>Chapter 2 AP-2<math>\epsilon</math> Expression in Developing Retina</b> .....	<b>45</b>
<b>2.1 Introduction</b> .....	<b>46</b>
<b>2.2 Material and Methods</b> .....	<b>48</b>
2.2.1 Ethics statement .....	48
2.2.2 Semi-quantitative and quantitative RT-PCR.....	48
2.2.3 In situ hybridization .....	49
2.2.4 Immunostaining.....	50
2.2.5 Analysis of AP-2 expression in mouse retinal cells .....	51
2.2.6 Data availability statement .....	52
<b>2.3 Results</b> .....	<b>53</b>

2.3.1	AP-2 $\epsilon$ is expressed in amacrine cells .....	53
2.3.2	Co-expression of AP-2 $\epsilon$ and other AP-2 family members in retina.....	57
2.3.3	AP-2 $\epsilon$ is expressed in GABAergic amacrine cells .....	62
2.3.4	Co-expression analysis of AP-2 transcription factors using single cell RNA sequencing data 64	
2.3.5	AP-2 $\epsilon$ RNA is expressed in retinoblastoma cell lines.....	67
<b>2.4</b>	<b>Discussion .....</b>	<b>70</b>
<b>Chapter 3</b>	<b>Nuclear Factor I represses Notch effector HEY1 in glioblastoma .....</b>	<b>74</b>
<b>3.1</b>	<b>Introduction .....</b>	<b>75</b>
<b>3.2</b>	<b>Material and Methods.....</b>	<b>77</b>
3.2.1	Cell lines, constructs, siRNAs, and transfections.....	77
3.2.2	Chromatin immunoprecipitation-on-chip (ChIP-on-chip) and ChIP-PCR.....	78
3.2.3	Electrophoretic mobility shift assay (EMSA) .....	81
3.2.4	Western blot analysis .....	82
3.2.5	Quantitative real time-PCR (qPCR).....	82
3.2.6	Reporter gene assay.....	83
3.2.7	Cell proliferation assay.....	83
3.2.8	Scratch assay .....	83
3.2.9	Transwell migration assay.....	84
3.2.10	Neurosphere formation assay.....	84
3.2.11	Statistical analysis.....	85
<b>3.3</b>	<b>Results.....</b>	<b>86</b>
3.3.2	Chromatin immunoprecipitation (ChIP)-on-chip of NFI binding regions in GBM cells.....	86
3.3.3	NFI binds to the HEY1 promoter in vivo.....	99
3.3.4	NFI binds to NFI recognition sequences in the HEY1 promoter .....	101
3.3.5	NFI represses HEY1 expression and promoter activity .....	106
3.3.6	HEY1 expression in GBM cells .....	108
3.3.7	HEY1 depletion decreases cell proliferation and increases cell migration in GBM.....	111
3.3.8	HEY1 depletion results in decrease neurosphere formation .....	115
<b>3.4</b>	<b>Discussion .....</b>	<b>117</b>
<b>Chapter 4</b>	<b>Role of AP-2<math>\beta</math> in GBM pathogenesis.....</b>	<b>123</b>
<b>4.1</b>	<b>Introduction .....</b>	<b>124</b>
<b>4.2</b>	<b>Material and methods .....</b>	<b>127</b>
4.2.1	Cell lines, siRNAs, and transfections.....	127
4.2.2	Semi-quantitative and quantitative RT-PCR.....	128
4.2.3	Western blot analysis .....	128
4.2.4	Cell proliferation assay.....	129
4.2.5	Scratch assay .....	129
4.2.6	Transwell migration assay.....	132
4.2.7	Immunostaining.....	132
4.2.8	Phosphatase and sumoylation assays .....	133
<b>4.3</b>	<b>Results.....</b>	<b>134</b>
4.3.1	Expression of AP-2 transcription factors in GBM .....	134
4.3.2	Expression of AP-2 $\beta$ correlates with survival in low grade gliomas and is associated with proneural GBM subtype .....	139
4.3.3	AP-2 $\beta$ localizes to the cytoplasm of adherent GBM cells.....	142
4.3.4	Effect of AP-2 $\beta$ on GBM cell growth properties .....	145
4.3.5	Effect of AP-2 $\beta$ on GBM stem cell markers .....	148
4.3.6	Hypoxia induces AP-2 $\beta$ expression .....	151

4.3.7	Post-translational modification of AP-2 $\beta$ .....	151
<b>4.4</b>	<b>Discussion .....</b>	<b>154</b>
<b>Chapter 5</b>	<b>Discussion and Future directions .....</b>	<b>167</b>
<b>5.1</b>	<b>Summary and key findings .....</b>	<b>169</b>
<b>5.2</b>	<b>Regulation of AP-2 transcription factor activity .....</b>	<b>172</b>
5.2.1	Activation of AP-2 by retinoic acid and cAMP .....	172
5.2.2	AP-2 dimerization and binding specificity.....	174
<b>5.3</b>	<b>AP-2 family members show redundant roles during amacrine cell development .....</b>	<b>176</b>
<b>5.4</b>	<b>AP-2 and NFI in glioblastoma .....</b>	<b>178</b>
<b>5.5</b>	<b>NFI-HEY1-Notch.....</b>	<b>181</b>
<b>5.6</b>	<b>Targeting transcription factors for cancer treatment.....</b>	<b>182</b>
<b>5.7</b>	<b>Future directions .....</b>	<b>184</b>
5.7.1	Validation of target genes and identification of additional AP-2 target genes.....	184
5.7.2	To study the functional significance of AP-2 $\epsilon$ in retinal development.....	185
5.7.3	Validation of additional NFI targets.....	186
5.7.4	Examination of specific NFI family members involved in HEY1 expression.....	187
5.7.5	Characterization of AP-2 sumoylation in GBM cells .....	187
5.7.6	To further characterize the role of AP-2 $\beta$ in GBM cells and mouse models .....	188
<b>References</b> .....		<b>190</b>

# List of Figures

<b>Figure 1.1</b> Structure of the retina .....	3
<b>Figure 1.2</b> Order of birth of retinal cell types in mammals .....	6
<b>Figure 1.3</b> Various interacting factors regulating cell proliferation and differentiation in retinal development.....	8
<b>Figure 1.4</b> Classification of glioma based on the new 2016 WHO classification.....	12
<b>Figure 1.5</b> Molecular abnormalities associated with primary and secondary glioblastoma.....	14
<b>Figure 1.6</b> Structural organization of AP-2.....	21
<b>Figure 1.7</b> Sequence alignment of AP-2 proteins.....	22
<b>Figure 1.8</b> Structural organization of NFI protein.....	31
<b>Figure 2.1</b> <i>AP-2<math>\epsilon</math></i> RNA is expressed in mouse and chick retina.....	54
<b>Figure 2.2</b> Immunohistochemical analysis of AP-2 $\epsilon$ in retina.....	56
<b>Figure 2.3</b> Co-immunostaining of AP-2 $\alpha$ and AP-2 $\epsilon$ in P1, P7 and P14 mouse retina.....	58
<b>Figure 2.4</b> Quantification of AP-2 expression data obtained from co-immunofluorescence analysis.....	59
<b>Figure 2.5</b> Co-immunostaining of AP-2 $\beta$ and AP-2 $\epsilon$ in P1, P7 and P14 mouse retina.....	60
<b>Figure 2.6</b> Co-immunostaining of AP-2 $\gamma$ and AP-2 $\epsilon$ at P1, P7 and P14 in mouse retina.....	61
<b>Figure 2.7</b> Co-immunofluorescence showing AP-2 $\epsilon$ expression in glycinergic and GABAergic amacrine cells.....	63
<b>Figure 2.8</b> Co-immunostaining of AP-2 $\alpha$ and AP-2 $\gamma$ in P1 and P7 mouse retina.....	66
<b>Figure 2.9</b> Semi-quantitative RT-PCR showing expression of <i>AP-2<math>\gamma</math></i> and <i>AP-2<math>\epsilon</math></i> in RB cells.....	68
<b>Figure 3.1</b> NFI binds to the <i>HEY1</i> promoter <i>in vivo</i> .....	100
<b>Figure 3.2</b> Binding of NFI to putative NFI binding sequences in the <i>HEY1</i> promoter.....	102
<b>Figure 3.3</b> Binding of NFIA, NFIB, NFIC, and NFIX to NFI binding sites in the <i>HEY1</i> promoter.....	105
<b>Figure 3.4</b> Regulation of <i>HEY1</i> promoter activity by NFI.....	107
<b>Figure 3.5</b> <i>HEY1</i> expression and effect of <i>HEY1</i> knockdown on <i>GFAP</i> RNA levels and cell proliferation.....	110
<b>Figure 3.6</b> <i>HEY1</i> knockdown results in increased cell migration.....	113
<b>Figure 3.7</b> <i>HEY1</i> knockdown reduces neurosphere formation.....	114
<b>Figure 3.8</b> Immunofluorescence analysis of MG tumour neurospheres.....	121
<b>Figure 4.1</b> RT-PCR analysis of AP-2 transcription factors in GBM cell lines.....	135
<b>Figure 4.2</b> Expression of AP-2 in A4-004 adherent vs neurospheres.....	137
<b>Figure 4.3</b> <i>AP-2<math>\beta</math></i> RNA levels in GBM cell lines.....	138
<b>Figure 4.4</b> Immunohistochemical analysis of AP-2 $\beta$ in GBM patient tumour tissues.....	140
<b>Figure 4.5</b> Expression of <i>AP-2<math>\beta</math></i> correlates with survival in glioma patients.....	141
<b>Figure 4.6</b> Subcellular localization of AP-2 transcription factors.....	143
<b>Figure 4.7</b> Subcellular localization of AP-2 $\beta$ in A4-004 adherent and neurosphere cultures.....	144
<b>Figure 4.8</b> Effect of AP-2 $\beta$ depletion on cell proliferation and migration in GBM cells.....	146

<b>Figure 4.9</b> Effect of AP-2 $\beta$ knockdown on stem cell markers in GBM cells. ....	147
<b>Figure 4.10</b> A4-004 cell sorting based on ALDH activity.....	149
<b>Figure 4.11</b> AP-2 $\beta$ mRNA and protein are induced under hypoxia.....	150
<b>Figure 4.12</b> Effect of AP-2 $\beta$ on target genes in GBM cells. ....	153
<b>Figure 4.13</b> Analysis of AP-2 $\beta$ post-translational modification.....	155
<b>Figure 4.14</b> Inhibition of sumoylation affects AP-2 $\beta$ subcellular localization.....	156
<b>Figure 4.15</b> Effect of Rolipram on AP-2 proteins. ....	161
<b>Figure 4.16</b> Western blot analysis showing the effect of AP-2 knockdown on SOX2 expression.....	164
<b>Figure 4.17</b> AP-2 $\alpha$ and AP-2 $\gamma$ affects GBM growth properties. ....	165

# List of Tables

<b>Table 1.1</b> Major subtypes of glioblastoma along with their molecular signatures and response to treatment. ....	15
<b>Table 1.2</b> Interacting partners of AP-2 transcription factors .....	23
<b>Table 1.3</b> Phenotypes of AP-2 knockout mice .....	24
<b>Table 2.1</b> Analysis of 21 clusters of amacrine cells. ....	65
<b>Table 3.1</b> Putative NFI target genes identified by CHIP-on-chip .....	88
<b>Table 3.2</b> PANTHER enrichment analysis of putative NFI target genes identified by ...	98
<b>Table 4.1</b> List of primer sequences used for RT-PCR analysis.....	130
<b>Table 4.2</b> List of primer sequences used for quantitative RT-PCR analysis .....	131

# List of Abbreviations

<b>2-HG</b>	2-Hydroxyglutarate
<b>AMPK</b>	5' AMP-activated protein kinase
<b>AP-2</b>	Activating protein 2
<b>APCDD1</b>	Adenomatosis polyposis coli down-regulated 1
<b>ASCL1</b>	Achaete-scute homolog 1
<b>ATH5</b>	Activating transcription factor 5
<b>B-FABP</b>	Brain fatty acid binding protein
<b>BCL2</b>	B-cell lymphoma 2
<b>bHLH</b>	Basic helix-loop-helix
<b>BMP</b>	Bone morphogenetic protein
<b>BOFS</b>	Branchio-Oculo-Facial Syndrome
<b>bp</b>	Base pair
<b>br</b>	Binding region
<b>BTSC</b>	Brain tumour stem cell
<b>cAMP</b>	Cyclic adenosine monophosphate
<b>CBP</b>	CREB-binding protein
<b>Ccnd1</b>	CyclinD1
<b>CDK</b>	Cyclin-dependent kinase
<b>CDKN1A</b>	Cyclin-dependent kinase inhibitor IA (p21)
<b>CEBP<math>\alpha</math></b>	CCAAT-enhancer binding protein alpha
<b>ChIP</b>	Chromatin immunoprecipitation
<b>CITED</b>	CREB-binding protein/p300-interacting transactivator with Asp/Glu-rich C-terminal domain
<b>CNS</b>	Central nervous system
<b>CoRE</b>	Composite response element
<b>CREB</b>	Cyclic AMP response element binding protein
<b>CT</b>	Computerized tomography scan
<b>DAPI</b>	4'6-diamidino-2-phenylindole
<b>DDX1</b>	Dead box 1
<b>DLL</b>	Delta like ligand
<b>DMEM</b>	Dulbecco's modification of Eagle's minimum essential medium
<b>DMSO</b>	Dimethyl sulfoxide
<b>DNA</b>	Deoxyribonucleic acid
<b>dNTP</b>	deoxyribose nucleotide triphosphate
<b>E2F</b>	E2 promoter binding factor
<b>ECL</b>	Enhanced chemiluminescence
<b>ECM</b>	Extracellular matrix
<b>EDTA</b>	Ethylenediaminetetraacetic acid
<b>EGF</b>	Epidermal growth factor
<b>EGFR</b>	Epidermal growth factor receptor
<b>EMSA</b>	Electrophoretic mobility shift assay
<b>EMT</b>	Epithelial-mesenchymal transition
<b>ER-<math>\alpha</math></b>	Estrogen receptor alpha

<b>ERBB2</b>	Avian erythroblastic leukemia viral oncogene homolog 2
<b>ERK</b>	Extracellular signal-regulated kinase
<b>ESR1</b>	Estrogen Receptor 1
<b>EZH2</b>	Enhancer of zest homolog 2
<b>FGF</b>	Fibroblast growth factor
<b>FGFR3</b>	Fibroblast growth factor receptor 3
<b>FOXC</b>	Forkhead-box C
<b>GABA</b>	Gamma-aminobutyric acid
<b>GABRA6</b>	Gamma-aminobutyric acid type a receptor 6
<b>GAD1</b>	Glutamate decarboxylase 1
<b>GAPDH</b>	Glyceraldehyde 3-phosphate dehydrogenase
<b>GBM</b>	Glioblastoma multiforme
<b>GCL</b>	Ganglion cell layer
<b>GE</b>	Ganglionic eminence
<b>GFAP</b>	Glial fibrillary acidic protein
<b>GLAST</b>	Glutamate aspartate transporter
<b>Glyt1</b>	Glycine transporter 1
<b>GO</b>	Gene ontology
<b>GTP</b>	Guanine triphosphate
<b>Gy</b>	Gray
<b>HA</b>	Hemagglutinin
<b>HDAC1</b>	Histone deacetylase 1
<b>HER2</b>	Human epidermal growth factor receptor 2
<b>HES</b>	Hairy and enhancer of split
<b>HEY</b>	Hairy/E(spl)-related with YPRW motif
<b>HIF-1<math>\alpha</math></b>	Hypoxia inducible factor 1 $\alpha$
<b>HRP</b>	Horseradish peroxidase
<b>IB</b>	Immunoblot
<b>ID4</b>	Inhibitor of differentiation 4
<b>IDH</b>	Isocitrate dehydrogenase
<b>IGF-5</b>	Insulin-like growth factor 1
<b>IgG</b>	Immunoglobulin G
<b>IL</b>	Interleukin
<b>INL</b>	Inner nuclear layer
<b>IP</b>	Immunoprecipitation
<b>JAG-1</b>	Jagged-1
<b>JAK</b>	Janus kinase
<b>LKB1</b>	Liver kinase B1
<b>LM-PCR</b>	Ligation mediated-polymerase chain reaction
<b>MADM</b>	Mosaic analysis of double markers
<b>MASH1</b>	Mammalian homolog of achaete-scute homolog 1 (ASCL1)
<b>Math3</b>	Neurogenic Differentiation 4
<b>MCAM</b>	Melanoma Cell Adhesion Molecule
<b>MDM2/4</b>	Mouse double minute 2/4 homolog
<b>MEK</b>	Mitogen-activated protein kinase kinase
<b>MG</b>	Malignant glioma

<b>MGMT</b>	O <sup>6</sup> -methylguanine-DNA methyltransferase
<b>MMD2</b>	Monocyte to macrophage differentiation associated 2
<b>MMP</b>	Matrix metalloproteinase
<b>MMTV</b>	Mouse mammary tumour virus
<b>MRI</b>	Magnetic resonance imaging
<b>mRNA</b>	Messenger ribonucleic acid
<b>N-CoR</b>	Nuclear receptor co-repressor
<b>NEB</b>	New England Biolabs
<b>NEFL</b>	Neurofilament light polypeptide
<b>NES</b>	Nuclear export sequence
<b>NEUROD4</b>	Neuronal differentiation 4
<b>NF1</b>	Neurofibromatosis 1
<b>NLS</b>	Nuclear localization sequence
<b>NFI</b>	Nuclear factor I
<b>NFκB</b>	Nuclear factor kappa-light-chain-enhancer of activated B cells
<b>NICD</b>	Notch intracellular domain
<b>Notch</b>	Notch homolog 1, translocation-associated
<b>Nrl</b>	Neural Retina Leucine Zipper
<b>OLIG2</b>	Oligodendrocyte transcription factor
<b>ONL</b>	Outer nuclear layer
<b>Otx2</b>	Orthodenticle Homeobox 2
<b>PAI1</b>	Plasminogen activator inhibitor
<b>PANTHER</b>	Protein analysis through Evolutionary Relationships
<b>PAX6</b>	Paired box protein-6
<b>PBS</b>	Phosphate buffered saline
<b>PcG</b>	Polycomb group complex
<b>PDGFRA</b>	Platelet derived growth factor receptor alpha
<b>PEI</b>	Polyethylenimine
<b>PET</b>	Polyethylene terephthalate
<b>PI3K</b>	Phosphoinositide 3-kinase
<b>PKA</b>	Protein kinase A
<b>PKC</b>	Protein kinase C
<b>PLP1</b>	Proteolipid protein 1
<b>PNS</b>	Peripheral nervous system
<b>PPase</b>	Phosphatase
<b>pRB</b>	Retinoblastoma protein
<b>PRC2</b>	Polycomb repressive complex 2
<b>PSA-NCAM</b>	Polysialylated isoforms of Neural Cell Adhesion Molecule
<b>PTEN</b>	Phosphatase and tensin homolog
<b>PVDF</b>	Polyvinylidene fluoride
<b>qPCR</b>	Quantitative real-time polymerase chain reaction
<b>RARE</b>	Retinoic acid response elements
<b>RAX</b>	Retina and anterior neural fold homeobox protein
<b>RB1</b>	Retinoblastoma protein
<b>RBP-Jκ</b>	Recombining binding protein suppressor of hairless
<b>RIPA</b>	Radioimmunoprecipitation assay

<b>RNA</b>	Ribonucleic acid
<b>RPC</b>	Retinal progenitor cell
<b>RPE</b>	Retinal pigmented epithelium
<b>RRT-PCR</b>	Reverse transcriptase polymerase chain reaction
<b>RX1</b>	Retinal homeobox protein
<b>SDS</b>	Sodium dodecyl sulfate
<b>SELEX</b>	Systematic evolution of ligands by exponential enrichment
<b>Shh</b>	Sonic hedgehog
<b>siRNA</b>	Small interfering ribonucleic acid
<b>SIX3</b>	SIX Homeobox 3 protein
<b>SIX6</b>	SIX Homeobox 6 protein
<b>SMAD2</b>	Mothers against decapentaplegic homolog 2
<b>SOX2</b>	Sex determining region Y-box 2
<b>SP1</b>	specificity protein 1
<b>SPARCL1</b>	SPARC like protein 1
<b>STAT</b>	Signal transducer and activator of transcription
<b>SUMO</b>	small ubiquitin-like modifiers
<b>SV40</b>	Simian Virus 40
<b>SWI/SNF</b>	SWItch/Sucrose Non-Fermentable
<b>Tac1</b>	tachykinin
<b>TBE</b>	Tris-borate-EDTA buffer
<b>TBP</b>	TATA-binding protein
<b>TCGA</b>	The Cancer Genome Atlas Research Network
<b>TFAP2</b>	Transcription factor AP2
<b>TFIIB</b>	Transcription factor II B
<b>TGF</b>	Transforming growth factor
<b>TNF-<math>\alpha</math></b>	Tumour necrosis factor alpha
<b>TP53</b>	Tumour Protein 53
<b>TSA</b>	Tyramide Signal Amplification
<b>VACht</b>	Vesicular acetylcholine transporter
<b>VEGF</b>	Vascular endothelial growth factor
<b>VEGFR</b>	Vascular endothelial growth factor receptor
<b>VER</b>	Visual potential response
<b>VSX1</b>	Visual system homeobox 1
<b>VZ</b>	Ventricular zone
<b>WAP</b>	Whey acidic protein gene
<b>WHO</b>	World Health Organization
<b>WWOX</b>	WW Domain Containing Oxidoreductase
<b>YB1</b>	Y-Box Binding Protein 1
<b>ZEB1</b>	Zinc Finger E-Box Binding Homeobox 1

# **Chapter 1 Introduction**

## **1.1 Retina Development**

The vertebrate retina is a complex structure that originates from neuro-ectodermal progenitor cells and is composed of seven different classes of cells, of which six are neuronal [photoreceptors (rods and cones), horizontal, bipolar, amacrine and ganglion cells] with one class of glial cells (Müller glia)<sup>1, 2</sup> (Figure 1.1). The neuronal cell types are arranged in three different layers: the outer nuclear layer (ONL) made up of photoreceptors, the inner nuclear layer (INL) made up of horizontal, bipolar and amacrine cells and the innermost ganglion cell layer (GCL) made up mostly of ganglion cells. These three layers are separated by the inner and outer plexiform layers. The different cell types of the retina receive, process and transmit the visual signal to the optic centers in the brain. The different classes of retinal cells originate from retinal progenitor cells (RPC) which undergo proliferation, migration and differentiation in a highly-specified spatio-temporal manner<sup>3</sup>. All processes related to retinal differentiation are tightly regulated by spatial and temporal expression of transcription factors.

### ***1.1.1 Genesis of retinal cells***

Retinal development starts from proliferating neural cells in the neural plate which are designated to form the eye field. The neural field divides into two lateral domains which give rise to an optical vesicle. The optical vesicle bulges to form the cup structure of the retina with the outer layer of epithelial cells giving rise to retinal pigmented epithelium (RPE) and the inner neuroepithelial cells forming the retina.

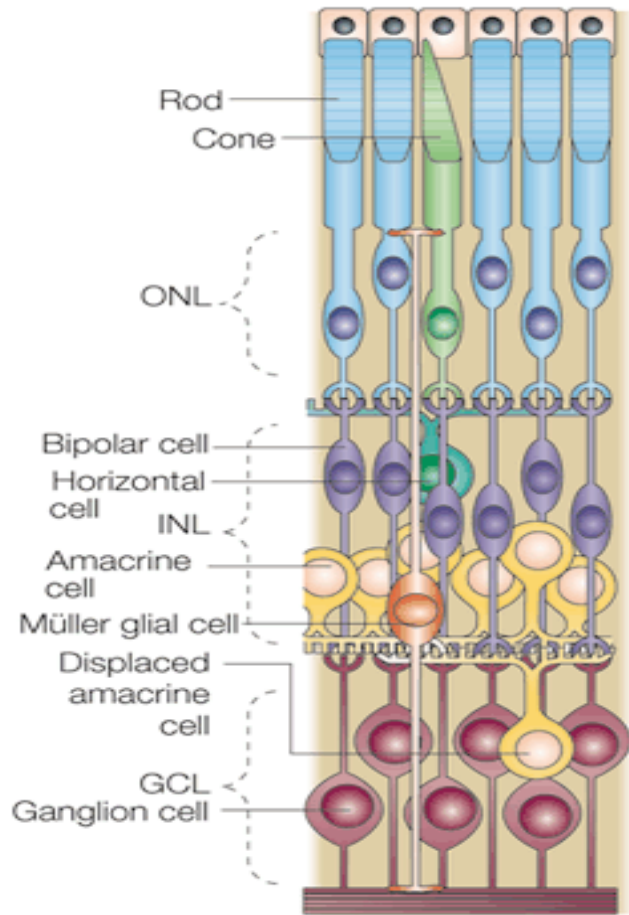


**Figure 1.1 Structure of the retina**

There are six major types of neuronal cells and one type of glial cell in the retina. These cell types are arranged in a layered structure. The figure shows the different layers of cells in the vertebrate retina. This figure has been reproduced with permission from Springer Nature (Nature Reviews Neuroscience) (Livesey et. al.)<sup>1</sup>

Retinal progenitor cells undergo cell division to expand the retinal tissue. RPC division gives rise to clones of different size and composition. The size of the clones ranges from 1 to >200 cells<sup>4</sup>. Interestingly, all retinal cell fates are possible within a single clone<sup>4, 5</sup>. The birth of the different retinal cell types follows an evolutionarily conserved pattern, with the onset of neurogenesis marked by the birth of ganglion cells, followed by the birth of horizontal cells, cones, amacrine cells and rods, followed by bipolar cells and Müller glial cells (Figure 1.2)<sup>6</sup>. The proliferation and identity of retinal cells is tightly regulated by several early transcription factors including PAX6, SIX6, SIX3, RAX, RX1, TLX and SOX2<sup>7-9</sup>. These transcription factors mainly regulate RPC proliferation and identity specification but at the same time allow expression of genes which are important for early differentiation. *Pax6* and *Tlx* knockout mice show reduced cell proliferation during neurogenesis<sup>10</sup>. *Rx1* and *Pax6* knockout mice have also been shown to suppress differentiation<sup>11</sup>. *Six6* and *Six3* induce early proliferation and retinal growth<sup>12, 13</sup>, while *Sox2* is necessary for suppression of neuronal differentiation<sup>14, 15</sup>. Cell proliferation of RPC also depends on the levels of CyclinD1 (*Ccnd1*) along with cyclin dependent kinases CDK4/6<sup>16</sup>. Cyclin-cdk complexes regulate progression through the G1 phase of cell cycle. Interestingly, *Ccnd1* is expressed at much higher levels in RPC compared to other embryonic tissues<sup>17</sup>. *Ccnd1* knockout mice show severe hypocellularity in the retina<sup>17</sup>. E2F and *N-Myc* transcription factors redundantly activate RPC proliferation downstream of *Ccnd1*<sup>18</sup>.

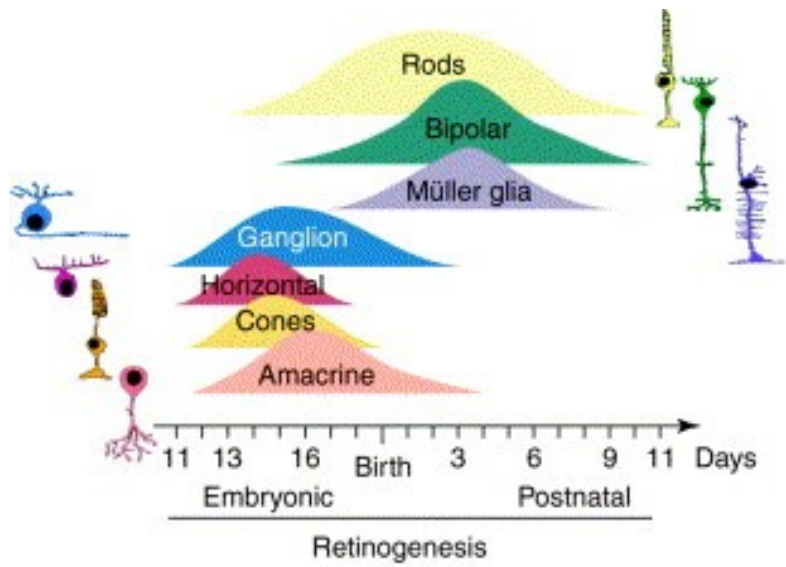
The Notch and Wnt signaling pathways play important roles during retina development. Wnt signaling has been shown to activate cell proliferation and inhibit differentiation<sup>19</sup>. Notch signaling promotes the maintenance of RPC and inhibits neuronal

differentiation<sup>20</sup>. Differentiated cells secrete additional signals like vesicular endothelial growth factor (VEGF), which induces the proliferation of RPCs via the MEK/ERK pathway<sup>21</sup>.

### **1.1.2 Escaping the cell cycle**

The process of differentiation is initiated at specific times in different locations across the retina and follows a central to peripheral gradient, with central retina differentiating first and peripheral retina differentiating last<sup>22</sup>. Two extracellular signaling pathways, fibroblast growth factor (FGF) and hedgehog, are key to neurogenesis in the retina. FGF expression acts as a trigger for differentiation, with FGF3/8 promoting the differentiation of ganglion cells in the central retina<sup>23</sup>. The newly born ganglion cells then start a wave by signaling neighboring proliferating cells to leave the cell cycle. Sonic hedgehog (Shh) expression in newly-differentiated ganglion cells induces Shh in the neighboring cells creating a ripple effect<sup>24</sup>. Shh signaling is necessary for ganglion cell cycle exit, with inhibition of Shh signaling shown to block differentiation of ganglion cells<sup>25</sup>,<sup>26</sup>. Regulatory mechanisms in the retina are set up to allow proliferation of progenitor cells at the same time as well-coordinated differentiation of the various retinal cell types is taking place.

The control of proliferation and differentiation in the retina is a complex process. As discussed earlier, CyclinD1 and Cdk expression in RPC is regulated by transcription factors that control proliferation in the retina. Concomitantly, other components of the cell cycle can influence differentiation. For example, the tumour suppressor gene *Rb1* regulates differentiation of rods by inhibiting RPC entry into S phase<sup>27</sup>. Also, the cells that



*TRENDS in Neurosciences*

**Figure 1.2 Order of birth of retinal cell types in mammals**

Timelines for birth of different retinal cells during development. This figure has been reproduced with permission from Elsevier (*Trends in Neuroscience*) (Marquardt et. al.)<sup>28</sup>

have undergone differentiation are prevented from re-entering the cell cycle, by the regulation of components of G1-S transition<sup>29</sup>. Apart from the cues for cell division, the duration of the cell cycle has also been shown to influence differentiation. Late RPC have a slower cell cycle, leading to the accumulation of CDK inhibitors, in turn leading to exit from the cell cycle<sup>30</sup>. Also, longer cell cycles result in accumulation of proteins such as *Vsx1* and *Otx2*, which in turn directs differentiation into late retinal cell types<sup>31</sup>.

### **1.1.3 Retinal differentiation**

A cell undergoing differentiation activates a number of genes essential for its morphology and function. Numerous transcription factors are involved in differentiation of RPCs along specific neuronal cell lineages. Many of these transcription factors belong to the bHLH (basic helix-loop-helix) and forkhead transcription factor families<sup>32</sup>. Temporal expression of different transcription factors regulates the balance between different neuronal cell fates. Single transcription factors have been shown to be essential for lineage specification; for example, *Math5* is essential for specification of ganglion cells<sup>33</sup>, *Nrl* for rod photoreceptors<sup>34</sup> and *Vsx2* for bipolar cells<sup>35</sup>. Crosstalk between transcription factors is necessary; for example, *Pax6* is required for the expression of bHLH transcription factors and directly activates *Ath5* (member of bHLH family), a proneural gene that is necessary for differentiation<sup>36</sup>. While essential for the specification of ganglion cells, *Ath5* further regulates the transcription of downstream genes including *Brn3*, which is also essential for ganglion cell differentiation<sup>37</sup>.

Epigenetic modifications play a key role in the transition from proliferation to differentiation and ensures that the process is irreversible<sup>38</sup>. Components of cellular

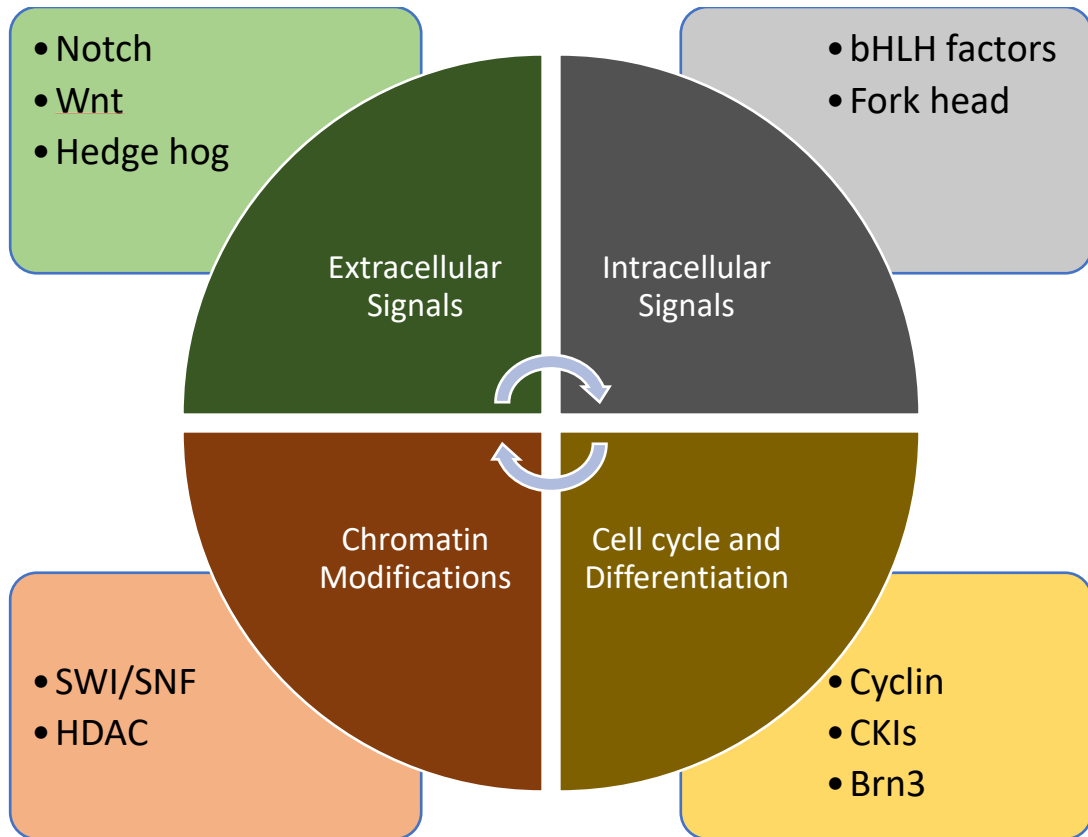


**Figure 1.3 Various interacting factors regulating cell proliferation and differentiation in retinal development.**

Diagram showing that cell proliferation, differentiation and lineage specification in retina is governed by different cellular processes including various transcription factors, signaling pathways, cell cycle proteins and epigenetic factors<sup>39</sup>.

epigenetic machinery change as the cell decides its fate. Histone deacetylation represses genes during differentiation, with loss of *HDAC1* associated with increased proliferation and differentiation inhibition<sup>40</sup>. The SWI/SNF chromatin remodeling complex also plays a role in neural differentiation<sup>41</sup>. Brm, a subunit of the SWI/SNF complex, promotes differentiation of retinal progenitor by inhibiting Notch and activating Brn3<sup>42</sup>.

#### **1.1.4 Retinal amacrine cells**

Amacrine cells are defined as a class of interneurons that mediate the visual signal within the retina. These cells are located in the innermost part of the inner nuclear layer. Amacrine cells form synapses in the inner plexiform layer where they process and relay the visual signal to the ganglion cells. Amacrine cells are the most diverse cell type in the retina<sup>43, 44</sup>. In 1890, Ramon y Cajal demonstrated the various sizes, shapes and stratification patterns of vertebrate amacrine cells<sup>45</sup>. Golgi studies have resulted in the identification of additional morphological classes of amacrine cells<sup>46</sup>. Today more than 30 different morphological subtypes of amacrine cells have been described<sup>43</sup>. Different amacrine subtypes play specific roles and add to the diversity and complexity of integration of visual signals in the retina. Amacrine cells are divided into four main categories based on the diameter of their dendritic field (classified as narrow field, small field, medium field and wide field), with each of these four categories shown to have specific functions<sup>45</sup>. Signal transfer by amacrine cells is mediated through the neurotransmitters secreted by these cells. These neurotransmitters can be either inhibitory or excitatory. Most amacrine cells secrete the inhibitory neurotransmitters GABA (*Gad1* expressing; GABAergic) or glycine (*Glyt1* expressing: Glycinergic).

Excitatory amacrine cells secrete glutamate (glutamatergic) as their neurotransmitter. Single cell sequencing approaches can distinguish different subtypes of amacrine cells based on their different molecular signatures<sup>47-49</sup>. GABAergic cells can be further divided based on their expression of vesicular acetylcholine transporter (*VACht*) in the case of cholinergic amacrine cells, or neuropeptide tachykinin (*Tac1*) in the case of tachykinin amacrine cells. Transcription factors *Isl1* and *Sox2* are required for the differentiation of cholinergic amacrine cells. Profiling of amacrine cells based on the expression markers *Gad1* and *Glyt1* has revealed that GABAergic amacrine cells are born before glycinergic amacrine cells, showing a temporal expression pattern during development.

A study by Cherry *et al.*<sup>48</sup> showed the molecular heterogeneity of amacrine cells by single cell sequencing. Of the 32 single amacrine cells profiled in their study, they identified 467 amacrine marker genes, with none of these genes expressed in all amacrine cells. This study demonstrates heterogeneity within amacrine cells and points to specific gene expression patterns during development<sup>48</sup>. In another study, Macosko *et al.*<sup>49</sup> used a drop-sequencing approach to profile the genes expressed in individual retinal cells of a P14 (postnatal day 14) mouse. Amacrine cells were divided into 21 clusters based on gene expression patterns<sup>49</sup>. In keeping with previous studies, and based on gene expression, 12 out of the 21 clusters were defined as GABAergic (*Gad1*-positive), 5 as glycinergic (*Slc6a9*-positive) and one as glutamatergic (*Slc7a8*-positive), with the remaining 3 clusters showing low levels of all three neurotransmitters<sup>49</sup>. They further identified a candidate marker for each cluster of amacrine cells. In summary, the molecular signatures of different kinds of amacrine cells during development suggest specific functions for these genes in determining amacrine cell subtype specificity.

## 1.2 Glioblastoma

### 1.2.1 Epidemiology and classification

Gliomas are the most common type of brain tumour, comprising approximately 60% of central nervous system malignancies<sup>50</sup>, with an estimated annual incidence of ~6.6 per 100,000 individuals in North America<sup>51</sup>. According to the 2007 WHO classification, gliomas are divided into three major types based on morphological features: astrocytomas, oligodendrogliomas, and mixed oligoastrocytomas. These major types of gliomas are given a histological grade based on increasing malignancy. Thus, astrocytomas are further classified into grade I (pilocytic astrocytoma), grade II (diffuse astrocytoma), grade III (anaplastic astrocytoma) and grade IV (glioblastoma, GBM). Grade III and grade IV astrocytomas are collectively referred to as high-grade astrocytomas or malignant gliomas (MG). Oligodendroglial and mixed oligoastrocytomas are classified as either grade II or grade III.

In the past decade, genome wide molecular profiling studies have helped to better understand gliomas. New biomarkers have been identified that allow improved classification of tumours which more closely correlates with patient outcome. In 2016, WHO revised the classification of CNS tumours based on the recent advances in molecular profiling of these tumours. This classification incorporates molecular parameters along with the classical histological information. The major additions in the new classification includes *IDH-wildtype/mutant*, *1p/19q-codeletion*, addition of diffuse midline glioma H3 K27M-mutant (Figure 1.4)<sup>52</sup>.

In most cases, GBM arise *de novo* and are referred to as primary GBM. Cancers that result from the progression of low grade astrocytomas or oligodendrogliomas are

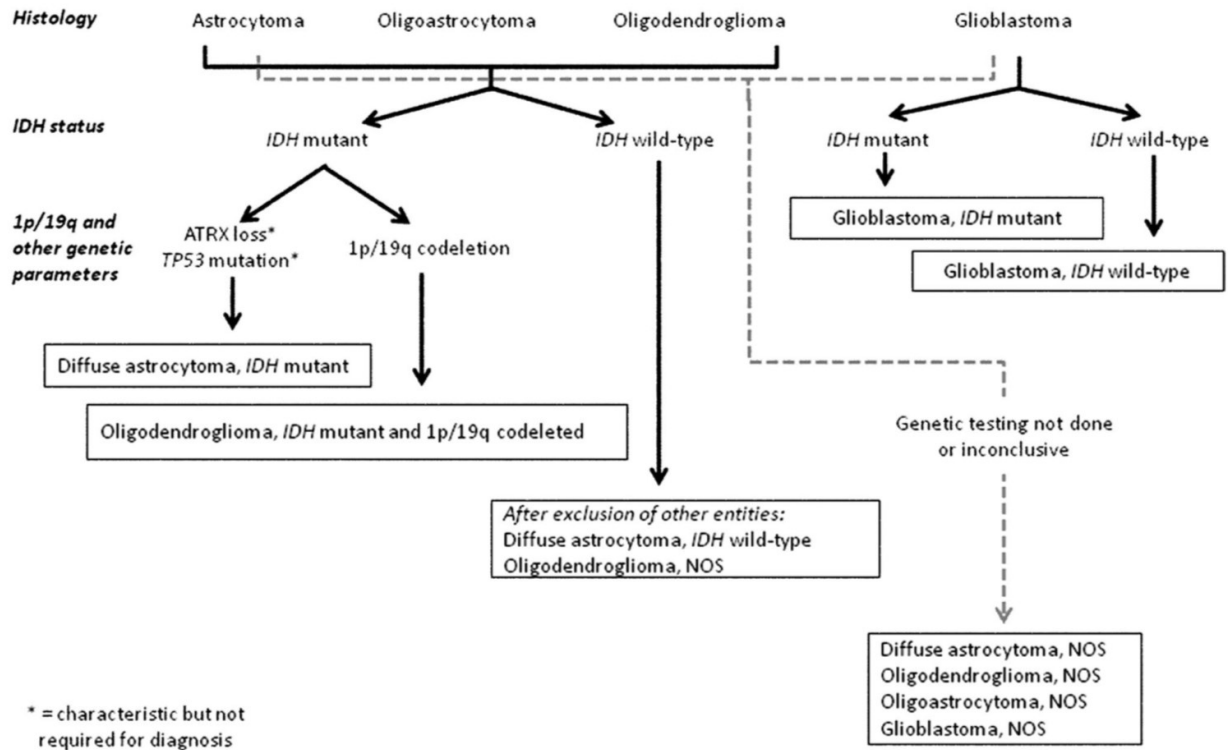


**Figure 1.4 Classification of glioma based on the new 2016 WHO classification.**

This figure has been reproduced with permission from Springer Nature (Acta Neuropathologica) (Louis et. al.)<sup>52</sup>

called secondary GBMs (Figure 1.5). To date, a few biomarkers have been identified as potent prognostic factors. Mutations in the isocitrate dehydrogenase gene (*IDH1*)<sup>53, 54</sup> are mainly associated with low-grade gliomas and secondary GBM and are a strong indicator of better prognosis whereas the methylation status of the O<sup>6</sup>-methylguanine DNA methyltransferase (*MGMT*) promoter predicts response to temozolomide adjuvant chemotherapy<sup>55, 56</sup>.

Genetic profiling is also used to better understand clinical outcomes in GBM patients. GBMs are divided into four distinct subtypes based on distinct genetic aberrations (Table 1.1)<sup>57, 58</sup>. The classical subtype is characterized by mutations or amplifications in the *EGFR* gene. The proneural subtype is characterized by frequent mutations in *TP53*, *PDGFRA* and *IDH1*. The third subtype, mesenchymal, is characterized by mutations in the neurofibromatosis type 1 (*NF1*) gene. Studies have shown that the proneural subtype is associated with increased overall survival, although these cancers do not respond well to chemotherapy. The classical and mesenchymal subtypes show improved clinical outcome in response to chemotherapy.

The discovery of major genetic alterations in GBM has contributed to increased understanding of the complexities involved in malignant transformation<sup>59, 60</sup>. However, new combined therapeutic approaches over the last 30 years have provided little benefit to the patient in terms of survival<sup>61, 62</sup>. Further studies are needed to understand the highly infiltrative nature of the disease.

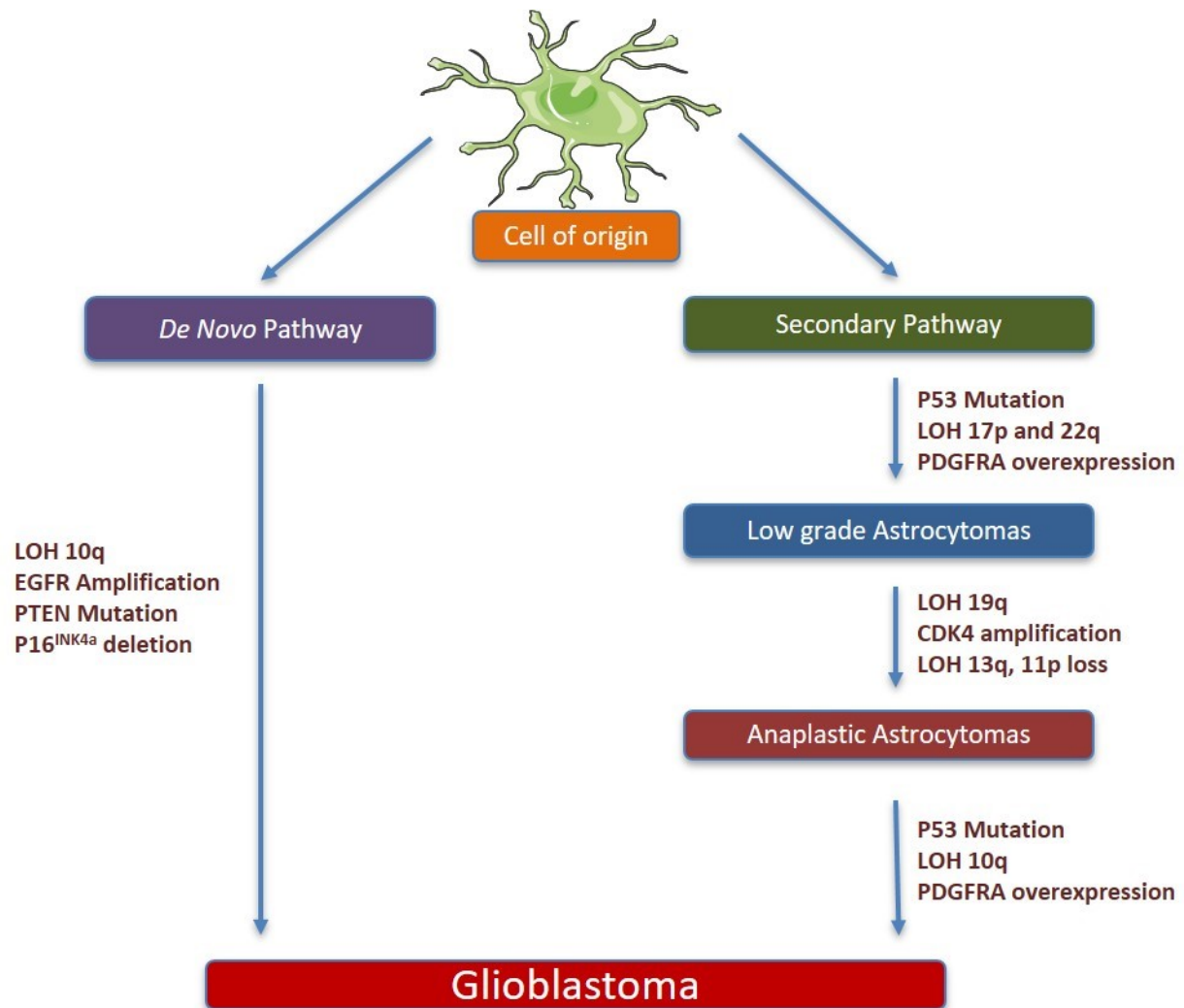


**Figure 1.5 Molecular abnormalities associated with primary and secondary glioblastoma.**

This figure has been modified with permission from Wolters Kluwer Medknow Publications (Indian Journal of Cancer) (Sarkar et. al.)<sup>63</sup>

	Proneural	Neural	Classical	Mesenchymal
Histological Markers	OLIG2, DLL3, SOX2, BCAN	MBP, MAL	EGFR, AKT, PCNA	YKL40, CD44, VEGF
Mutation signatures	P53, PDGFRA		Chr 7 gain, Chr 10 loss, PDGFRA	NFkB, NFI
Cellular Morphology	Oligodendroglial	Mixed	Astrocytic	Astrocytic
Treatment response	No response to TMZ		Improved clinical outcome	Improved clinical outcome

**Table 1.1 Major subtypes of glioblastoma along with their molecular signatures and response to treatment<sup>57, 59</sup>.**

### **1.2.2 Glioblastoma current treatment and survival**

GBM is the most aggressive form of brain tumours<sup>64</sup>. These tumours are highly infiltrative and show aberrantly high vascularization. Patients with GBM have a very poor prognosis, with a median survival of ~14 months<sup>65, 66</sup>. Current treatment regimens involve surgical resection followed by radiation therapy (total dose of 60 Gy fractionated in 2 Gy doses 5 days a week for 6 weeks) and concurrent chemotherapy with temozolomide (75 mg/square meter of body-surface area /day). This is followed by adjuvant therapy with temozolomide (6 cycles, 150-200 mg/square meter of body-surface area for 5 days of each 28 day cycle)<sup>67, 68</sup>. Despite this aggressive treatment regime, the median survival of GBM patients remains less than 2 years. The main reason behind this poor survival is the infiltration of tumour cells into the surrounding normal tissue. These infiltrative cells escape both surgical and radiation therapy leading to tumour recurrence<sup>69-71</sup>. Most of the DNA damaging agents target highly proliferative cells. However, invasive GBM cells have been shown to be less proliferative and thus may account for tumour recurrence<sup>72, 73</sup>. While primary GBMs often respond to chemotherapeutic agents, recurrent GBMs are resistant to these chemotherapeutic drugs including temozolomide. GBMs show alterations in their molecular signature upon recurrence. For example, a comprehensive study by Phillips *et al.* showed that recurrent GBM tumours shift toward the mesenchymal GBM subtype<sup>57</sup>. Similarly, a study by Halliday *et al.*<sup>74</sup> showed that a mouse model of proneural GBM resulted in a shift towards mesenchymal subtype upon radiation treatment<sup>74</sup>. Anti-angiogenic therapies including Bevacizumab (VEGF inhibitor) have shown some promise for treatment of primary tumours but result in even more aggressive forms for recurrent tumours<sup>75</sup>.

### **1.2.3 GBM cell migration**

The dismal prognosis of GBM is due to highly infiltrative tumour cells which escape surgery and radiotherapy, as well as the presence of cancer stem cells<sup>72, 76</sup>. GBM stem cells share properties with neural stem or progenitor cells, including self-renewal potential and ability to differentiate into different cell types. Many studies have shown that cancer stem cells are responsible for the aggressive infiltration associated with GBM tumours<sup>76, 77</sup>. GBM stem cells localize to the perivascular niche outside the hypoxic areas in GBM tumours and are resistant to radiation and chemotherapy<sup>78</sup>. Several signaling pathways have been shown to promote GBM cell invasion and migration<sup>72</sup>. TGF-beta signaling activates SMAD2 and ZEB1 which results in increased cell migration and invasion potential of GBM stem cells<sup>79</sup>. ZEB1 plays a significant role in regulating cell invasion and stemness in GBM stem cells by upregulating EMT (epithelial mesenchymal transition) related genes and stem cell markers like SOX2 and OLIG2<sup>80</sup>. The Wnt/ $\beta$ -catenin pathway is important for maintenance of proliferation and self-renewal of GBM stem cells<sup>81, 82</sup>. Recent studies indicate that Wnt5a, a Wnt ligand, serves as a regulator of GBM stem cell invasive potential *in vivo*. Wnt5a promotes GBM cell migration by upregulating the expression of MMPs<sup>83</sup>.

Several *in vitro* studies indicate that GBM cells have opposing proliferation and migration rates. The cells which are actively migrating tend to proliferate slowly, whereas rapidly proliferating cells tend to be non-migratory<sup>84, 85</sup>. The core of the tumour consists of rapidly proliferating cells while the outer rim consists of cells with invasive potential<sup>85, 86</sup>. Rapidly dividing GBM cells undergo metabolic stress due to limited availability of glucose<sup>87</sup>. Cancer cells adapt to this metabolic stress using alternate strategies so that

they can maintain tumour growth. An example of cancer adaptation is downregulation of miRNA-451, which is a negative regulator of LKB1/AMPK pathway<sup>87</sup>. Godlewski *et al.*<sup>88</sup> have shown that miRNA-451 regulates the balance between GBM cell migration and proliferation in response to glucose availability<sup>88</sup>. GBM cells express high levels of miRNA-451 under regular glucose availability, which results in high proliferation, while scarcity of glucose causes downregulation of miRNA-451 which in turn results in increased cell migration through activation of the LKB1-AMPK pathway and reduced cell proliferation through inhibition of mTOR activity<sup>88</sup>. EMT transformation in GBM has also been shown to be induced in response to therapy. For example, several studies indicate that administration of the anti-angiogenic drug bevacizumab increases the aggressive nature of recurring GBM tumours<sup>75</sup>.

### **1.3 Transcription factor Activator Protein 2 (AP-2; TFAP2)**

AP-2, also referred to as TFAP-2, was first identified as a 52-kDa protein bound to the enhancer region of Simian Virus 40 (SV40) and human metallothionein IIA<sup>89</sup>. Five AP-2 genes have been identified in mice and humans (*AP-2 $\alpha$* , *AP-2 $\beta$* , *AP-2 $\gamma$* , *AP-2 $\delta$*  and *AP-2 $\epsilon$* )<sup>90-94</sup>. AP-2s are sequence-specific DNA binding proteins that interact with cellular enhancer and promoter elements to regulate transcription. AP-2 transcription factors are predominantly localized in the nucleus where they bind as homodimers and heterodimers to the consensus sequence GCCNNGGC<sup>89, 95</sup>.

#### **1.3.1 Structure and function of AP-2**

All AP-2 genes in mammals have 7 exons, with the exception of AP-2 $\delta$  which has 6 exons. Orthologs of AP-2s are found in a variety of species including fish, amphibians and insects. Similarity between orthologs ranges from 60% to 90%. Based on sequence conservation and expression patterns, AP-2 $\alpha$ , AP-2 $\beta$ , AP-2 $\gamma$  are more closely related and belong to the same class while AP-2 $\delta$  and AP-2 $\epsilon$  have their own classes, with AP-2 $\delta$  being the most divergent of the AP-2 family members. The *AP-2 $\alpha$*  (*TFAP2A*), *AP-2 $\beta$*  (*TFAP2B*) and *AP-2 $\delta$*  (*TFAP2D*) genes are located on chromosome 6p, whereas the *AP-2 $\gamma$*  (*TFAP2C*) and *AP-2 $\epsilon$*  (*TFAP2E*) genes are located on chromosomes 20q and 1p, respectively. Structurally, AP-2 proteins have a well-conserved helix-span-helix dimerization motif at the carboxyl terminal region preceded by a central basic region (Figure 1.6). The helix-span-helix motif along with the central basic region constitutes the DNA binding domain. The conserved DNA binding domain suggests that AP-2 proteins bind to the same target genes. The N-terminus of AP-2 proteins is less conserved and

has a proline- and glutamine-rich transactivation domain (Figure 1.7). Within the transactivation domain lies a conserved PY motif (XPPXY) found in all AP-2's with the exception of AP-2 $\delta$ <sup>96</sup>. Differences in the AP-2 transactivation domains account for their different transactivation potential. AP-2 transcription factors bind as homodimers or heterodimers to a G/C-rich consensus sequence 5'-GCCN<sub>3</sub>GGC-3' usually located upstream of their target genes. Additional AP-2 binding motifs have been discovered based on *in vitro* binding assays, including 5'-GCCN<sub>4</sub>GGC-3' and 5'-GCCN<sub>3/4</sub>GGG-3'<sup>95</sup>. AP-2 has also been shown to bind to the SV40 enhancer element 5'-CCCCAGGC-3'<sup>89</sup> suggesting that AP-2 can bind to a variety of G/C-rich sequences with different binding affinities.

AP-2 proteins have been postulated to regulate the expression of a plethora of genes involved in a variety of biological functions during early embryonic development, cell proliferation, cell differentiation and apoptosis. A key gene known to be regulated by AP-2 is cell cycle inhibitor *CDKN1A* (*p21<sup>WAF1</sup>*). AP-2 inhibits cell growth by inducing *p21* expression either by direct interaction with p53 or independent of p53<sup>97, 98</sup>. *TGF $\alpha$* , *ER- $\alpha$* , *HER2*, *C-KIT*, *c-MYC*, *CEBP $\alpha$* , *IGF-5* are other key targets of AP-2. The regulatory activity of AP-2 is mediated through physical interaction with other proteins<sup>99-105</sup>. AP-2 has been shown to directly interact with YB1, p53, c-Myc, Sp1, PAX-6, RB1, WWOX, PARP, CREB, CITED (Table 1.2). Interaction of AP-2 with other proteins alters its activity. For example, interaction of AP-2 with c-MYC results in impairment of MYC/MAX DNA binding<sup>106</sup>. Interaction of AP-2 with pRB is important for transactivation of the *E-cadherin* gene<sup>107</sup>. AP-2 activity can further be regulated by post-translational modifications such as phosphorylation<sup>108</sup> and sumoylation<sup>109, 110</sup>. AP-2 is phosphorylated by protein kinase A

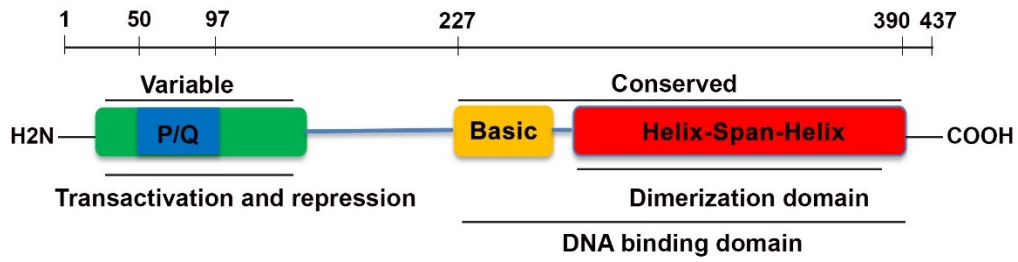


**Figure 1.6 Structural organization of AP-2.**

AP-2 proteins have a well conserved transactivation domain in the N-terminus region. The less conserved C-terminal region has a helix-span-helix motif which functions as a dimerization domain. The basic domain along with the dimerization domain make up the DNA binding domain.



Protein	Description	Domain	Function
APC	Tumor suppressor	Basic	Inhibition of transcription
CITED2	Coactivator	Dimerization	Transcriptional activation
CITED4	Coactivator	ND	Transcriptional activation
E1A	Adenovirus transforming protein	DNA binding, Dimerization	Repression of AP-2 targets
c-Myc	Onco-protein	C-terminus	Disruption of Myc/Max DNA binding
PARP	DNA repair protein	C-terminus	Transcriptional activation
PAX-6	Transcription factor	ND	Gelatinase B transcriptional activation
P300/CBP	Coactivator	N-terminus	Transcriptional activation
p53	Tumor suppressor	ND	Activation of p53 dependent transcription
Rb	Tumor suppressor	N-terminus	Transcriptional activation of E-cadherin
SP1	Transcription factor	Basic	Transcriptional activation of CYP1 IA1
UBC9	E2 conjugating enzyme	DNA binding, Dimerization	Sumoylation
WWOX	Tumor suppressor	PY motif	Cytoplasmic translocation of AP-2
YB-1	Transcription factor	ND	Activation of gelatinase A transcription

**Table 1.2 Interacting partners of AP-2 transcription factors**

<b>AP-2 family member</b>	<b>Knockout Phenotype</b>
AP-2 $\alpha$	Die perinatally with craniofacial defects and severe skeletal defects in head and trunk region
AP-2 $\beta$	Die shortly after birth due to polycystic kidney disease and terminal renal failure
AP-2 $\gamma$	Lethal during early embryogenic development directly after implantation during gastrulation
AP-2 $\delta$	Defects in midbrain development
AP-2 $\epsilon$	Defects in olfactory bulb formation

**Table 1.3 Phenotypes of AP-2 knockout mice**

(PKA) both *in vitro* and *in vivo*. PKA phosphorylates AP-2 at S239. It has also been shown that cAMP and activated PKA do not affect the basal expression of AP-2 mRNA<sup>112</sup>. However, PKA does increase the transcriptional activity of AP-2 on the promoter of target genes both *in vivo* and *in vitro*<sup>108</sup>. Sumoylation of AP-2 has been shown to suppress its transactivation potential in MDA-MB-436 cells<sup>109</sup>. A study by Bogachek *et al.*<sup>110</sup> indicates that sumoylation of AP-2 is required to maintain the luminal subtype of breast cancer and inhibition of sumoylation leads to luminal to basal transition<sup>110</sup>. Another study shows that inhibition of AP-2 sumoylation leads to the suppression of the cancer stem cell population in breast and colorectal cancer<sup>113</sup>. Both retinoic acid and cAMP induce AP-2 activity<sup>114</sup>. The induction of AP-2 expression by retinoic acid is transient, peaking at 72 h, and is at the transcription level. cAMP, on the other hand, does not change AP-2 RNA levels but only increases the activity of AP-2. AP-2 regulates the transcription of genes with retinoic acid response elements (RARE) and cAMP response elements in their promoters<sup>115</sup>.

### **1.3.2 AP-2 in embryonic development and AP-2 knockout mice**

The tissue distribution pattern and developmental roles of AP-2s have been studied in different species<sup>96</sup>. Spatial and temporal expression patterns of AP-2s have been examined during early embryonic development in various tissues. Overlapping and diverging AP-2 expression patterns suggest redundant and non-redundant roles for AP-2 family members. In mice, AP-2 $\alpha$ , AP-2 $\beta$  and AP-2 $\gamma$  are co-expressed in neural crest cell lineages<sup>116-119</sup>, the peripheral nervous system, facial and limb mesenchyme, as well as in the epithelia of the developing embryo and extraembryonic trophoderm<sup>120</sup>. AP-2 $\delta$  is expressed in developing heart and CNS<sup>93, 121</sup> and AP-2 $\epsilon$  expression is primarily

detected in the olfactory bulb<sup>122</sup>. Despite overlapping expression patterns, inactivation of individual AP-2 genes reveals non-redundant roles during early development.

AP-2 knockout mice have shed light into the diverse roles of AP-2 family members in early embryonic development (Table 1.3). *AP-2 $\alpha$* <sup>-/-</sup> mice die perinatally with craniofacial defects and severe skeletal defects in the head and trunk region<sup>123-125</sup>. *AP-2 $\beta$* <sup>-/-</sup> mice die postnatally due to polycystic kidney disease and terminal renal failure<sup>126, 127</sup>. *AP-2 $\gamma$* <sup>-/-</sup> offspring are not viable and die directly after implantation during gastrulation<sup>128, 129</sup>. Mice lacking *AP-2 $\delta$*  and *AP-2 $\epsilon$*  show defects in midbrain development and olfactory bulb formation, respectively<sup>130, 131</sup>. Mutations in *AP-2 $\alpha$*  have been identified in patients with Branchio-Oculo-Facial Syndrome (BOFS)<sup>132</sup>. Moreover, mutant AP-2 $\alpha$  has a cytoplasmic localization compared to wild-type AP-2 $\alpha$ , which is predominantly localized to the nucleus. Mutations in *AP-2 $\beta$*  cause Char syndrome, an autosomal dominant trait characterized by facial dysmorphism and hand anomalies<sup>133</sup>.

AP-2 transcription factors play a significant role in eye development<sup>134, 135</sup>, with all five AP-2s expressed in developing retina<sup>134, 136, 137</sup>. In chick retina, *AP-2 $\alpha$*  is expressed in amacrine cells<sup>136</sup>, *AP-2 $\beta$*  is expressed in both amacrine and horizontal cells<sup>136</sup>, whereas *AP-2 $\delta$*  is expressed in a subset of ganglion cells<sup>137</sup>. Similar expression patterns have been reported for AP-2 $\alpha$  and AP-2 $\beta$  in mouse retina<sup>135</sup>. Conditional (retina-specific) *AP-2 $\alpha$*  and *AP-2 $\beta$*  knockout mice show horizontal and amacrine cell defects that were not detected upon deletion of either one of the family members alone<sup>134</sup>, with a more recent study showing that combined deletion of *AP-2 $\alpha$*  and *AP-2 $\beta$*  does not change the number of amacrine cells but results in aberrant mosaic formation<sup>138</sup>. These combined studies suggest redundant roles for AP-2 $\alpha$  and AP-2 $\beta$  in amacrine and horizontal cell

development. *AP-2δ* is expressed in a subset of ganglion cells in chick retina<sup>137</sup>. Using chick retina as a model system, our lab has demonstrated that *AP-2δ* plays a significant role in axonal trafficking by regulating polysialylated neuronal cell adhesion molecule (PSA-NCAM)<sup>139</sup>. *AP-2δ* knockout mice have reduced numbers of ganglion cells and reduced axonal projections to the superior colliculus, a visual center in the brain<sup>140</sup>.

#### **1.4 Role of AP-2 in cancer**

*AP-2* plays an important role in regulating the expression of genes associated with tumour growth and metastasis. *AP-2* regulates genes involved in proliferation, cell cycle progression<sup>141</sup>, apoptosis (c-KIT, BCL2)<sup>142, 143</sup>, cell adhesion (MCAM/MUC18, E-cadherin)<sup>144</sup> and invasion/angiogenesis (MMP2, VEGF)<sup>99, 145</sup>. Regulation of target genes by *AP-2* is complex and cell type-specific. Our previous studies showed that transfection of *AP-2α* and/or *AP-2β* expression constructs into retinoblastoma cells induces apoptosis and inhibits proliferation<sup>146</sup>. Others have shown that overexpression of *AP-2α* or *AP-2γ* in mouse mammary epithelial cells induces hyper-proliferation<sup>147, 148</sup>. Furthermore, both *AP-2α* and *AP-2γ* increase cell migration and colony formation in soft agar and promote xenograft outgrowth<sup>149</sup>. Moreover, *AP-2γ* down-regulates the transcription of the cell cycle inhibitor p21<sup>cip</sup>, and plays a role in hormone-responsive breast cancer, acting as a novel collaborative factor in ERα-mediated transcription<sup>150</sup>. Some studies have also reported genomic and epigenetic alterations of *AP-2ε* in human cancers<sup>151-153</sup>.

### **1.4.1 AP-2 aberrant expression and subcellular localization**

Aberrant expression and subcellular localization of AP-2 can lead to malignant transformation<sup>154-157</sup>. Central to their role as transcription factors, AP-2 proteins are primarily localized in the nucleus. Interestingly, cytoplasmic AP-2 localization has been observed in various cancers<sup>154-156, 158, 159</sup>. For example, loss of AP-2 $\alpha$  expression in melanoma, resulting in over-expression of the cell adhesion molecule MCAM/MUC18 and protease-activated receptor I (PAR-I), is a crucial event in tumour progression<sup>143, 144, 160, 161</sup>. Furthermore, clinical data suggest that reduced levels of nuclear AP-2 in melanoma is associated with shorter recurrence-free survival and aggressive clinicopathological features<sup>154</sup>. In ovarian cancer, elevated AP-2 $\alpha$  in the nucleus and reduced cytoplasmic expression of AP-2 $\alpha$  is associated with poor survival<sup>155</sup>. In ovarian cancer cell lines, AP-2 $\alpha$  suppresses cell proliferation and invasion mediated by decreased phosphorylation of Akt and ERK signaling pathways<sup>162</sup>. Pro-MMP2 levels are reduced whereas E-cadherin expression is induced in AP-2 $\alpha$ -depleted ovarian cancer cells<sup>162</sup>.

AP-2 $\alpha$ , AP-2 $\beta$  and AP-2 $\gamma$  are expressed in breast tissue where they play essential roles in normal breast development<sup>147</sup> by regulating key genes, such as human epidermal growth factor receptor-2 (HER2)<sup>163</sup> and estrogen receptor (ER). Levels of nuclear AP-2 $\alpha$  are significantly reduced in invasive breast carcinomas and are associated with adverse clinicopathological factors<sup>164, 165</sup>. Controversial results have been obtained for AP-2 $\gamma$ , with both upregulation and downregulation of nuclear AP-2 $\gamma$  reported in breast cancer<sup>166, 167</sup>. Thus, while AP-2 $\alpha$  appears to be a tumour suppressor in breast tissue, the role of other AP-2 family members remains inconclusive.

### **1.4.2 AP-2 in glioblastoma**

A study by Heimberger *et al.*<sup>168</sup> described the association between the loss of nuclear AP-2 $\alpha$  and increasing grade in GBM. In this study, the authors examined a tissue microarray made up of 72 GBM tissue samples, 49 anaplastic astrocytomas, 9 low-grade astrocytomas and normal brain tissue. The results showed loss of nuclear AP-2 $\alpha$  in 71 out of 72 GBM tumours in comparison to low grade and normal brain, which showed nuclear AP-2 $\alpha$  expression in 100% of the samples<sup>168</sup>. This inverse correlation of nuclear AP-2 expression with astrocytoma grade suggests a possible role for AP-2 subcellular localization in GBM malignancy. Similar data were reported in an independent study which showed that AP-2 $\alpha$  was localized to the cytoplasm in high-grade astrocytomas<sup>169</sup>. A statistically significant association was observed between loss of nuclear AP-2 $\alpha$  expression and over-expression of AP-2 target genes *MMP2* and *VEGF* in GBM<sup>168</sup>. AP-2 $\alpha$  has also been shown to downregulate *MMP2* in melanoma cell lines and *VEGF* in prostate cancer cell lines<sup>170</sup>. Transfer of AP-2 from the nucleus to the cytoplasm as a function of increased malignancy suggests the need for reduced nuclear AP-2 in cancer. In keeping with this idea, overexpression of AP-2 $\alpha$  in GBM cell lines results in reduced cell proliferation and migration<sup>171</sup>. Given the complex role of AP-2 proteins in gene regulation, further studies are needed to understand the role of AP-2 in carcinogenesis.

## 1.5 Transcription factor Nuclear Factor I

NFI is a family of transcription factors first described as a protein required for initiation of adenoviral DNA replication<sup>172, 173</sup>. The NFI family consists of four members: NFIA, NFIB, NFIC and NFIX<sup>174</sup>. These transcription factors play important roles during development by regulating key genes involved in cell proliferation and differentiation<sup>175</sup>. NFIs bind to the palindromic sequence TTGGC(N5)GCCAA as either homodimers or heterodimers and can either activate or repress genes based on cellular context<sup>176, 177</sup>.

### 1.5.1 Structure and function

NFI proteins have a well-conserved DNA binding and dimerization domain at the N-terminus and a divergent transactivation domain at the C-terminus (Figure 1.8)<sup>175</sup>. The high level of conservation in the amino acid sequences of the four NFI DNA binding and dimerization domains suggests that all four NFIs can bind to the same target sequences. The variability in the transactivation domain suggests that the different members of the NFI family can bind to different co-factors. Additional diversity in the NFI protein family comes from the presence of multiple splice variants primarily in 3' half of the gene encoding the transactivation domain<sup>178, 179</sup>. The different isoforms resulting from alternative splicing have different functions; e.g., NFI-X3 induces *GFAP* expression leading to differentiation of astrocytes from neural progenitors; however, NFI-X1 which skips exon 9, cannot induce *GFAP* expression<sup>180</sup>. Complete loss of either DNA binding domain or transactivation domain in some isoforms results in loss of function and may explain the opposite roles of NFI proteins observed in some cancers<sup>178</sup>. The divergent

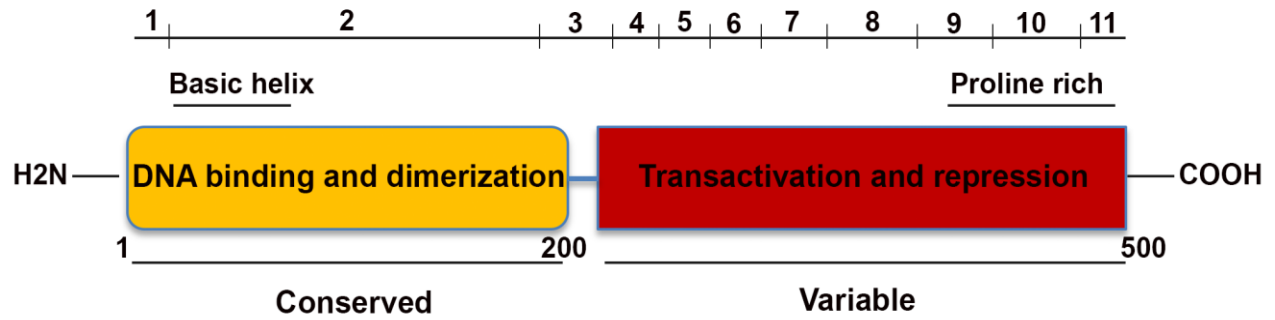


**Figure 1.8 Structural organization of NFI protein.**

NFI proteins have a well-conserved DNA binding and dimerization domain located in the N-terminus region and a variable transactivation domain located in the C-terminal region. Exons are indicated by the lines and numbers at the top of the diagram. This figure has been adapted with permission from Elsevier (Gene) (Gronostajski et. al.)<sup>175</sup>

nature of the C-terminus of NFIs is further complemented by post-translational modifications. Different types of post-translational modifications have been reported for NFIs and have been associated with different NFI functions. For example, phosphorylation of NFI is important for its activity, with differential phosphorylation of NFI shown to regulate the expression of *B-FABP* and *GFAP*, markers of radial glial cells and astrocytes, respectively<sup>181, 182</sup>. Similarly, glycosylation of NFI is important for transcriptional activation of Whey Acidic Protein and the recruitment of co-activators and repressors during development of mammary glands<sup>179</sup>. Other post translational modifications like sumoylation and acetylation have also been reported but their exact role in determining NFI activity is still unknown<sup>183, 184</sup>.

### **1.5.2 Role of NFI in gliogenesis**

Overlapping expression patterns of *Nfia*, *Nfib* and *Nfix* in developing and postnatal mouse brain, combined with knockout mouse models support a role for NFIs in developing brain<sup>185-188</sup>. In the developing central nervous system, NFIA, NFIB and NFIX are expressed in neocortex region of telencephalon, ependymal cells of the neural tube as well as some parts of the ventricular zone<sup>189</sup>. Expression of NFIC is very low in developing CNS, with some positive cells detected in the developing telencephalon<sup>189</sup>. NFIs are involved in the regulation of several important processes in brain development including axon guidance and maturation, differentiation of glial and neuronal cells and neuronal migration<sup>175, 190</sup>.

*Nfia*<sup>-/-</sup>, *Nfib*<sup>-/-</sup>, and *Nfix*<sup>-/-</sup> mice demonstrate a role for NFIs in brain development<sup>191-193</sup>. *Nfia*<sup>-/-</sup> mice die perinatally due to renal developmental problems<sup>194</sup>, while *Nfib*<sup>-/-</sup>

mice die at birth due to lung hyperplasia<sup>188</sup>. *Nfic*<sup>-/-</sup> mice are viable with defects in tooth development<sup>195</sup> while *Nfix*<sup>-/-</sup> display postnatal lethality<sup>196</sup>. *Nfia*<sup>-/-</sup> and *Nfib*<sup>-/-</sup> mice show defects in developing brain, including agenesis of the corpus callosum, enlargement of ventricles, disruption of midline glial structures, defects in hippocampus formation and delayed differentiation of neuronal and glial lineages<sup>187, 188</sup>. *Nfic*<sup>-/-</sup> mice do not show any brain abnormalities. *Nfix*<sup>-/-</sup> mice do not display agenesis of the corpus callosum but have enlarged ventricles. *Nfia*<sup>-/-</sup>, *Nfib*<sup>-/-</sup>, and *Nfix*<sup>-/-</sup> mice all show delay in neuronal and glial maturation<sup>185-187, 197</sup>.

In the developing spinal cord, NFIA and NFIB play important roles in the onset of gliogenesis and later on, in astrocyte maturation<sup>198</sup>. During development of the spinal cord, neurons are generated first followed by glia, a process known as gliogenic switch. There are two steps in the gliogenic switch: inhibition of neurogenesis and activation of gliogenesis. Both NFIA and NFIB, expressed in ventricular zone progenitor cells, are important for the onset of gliogenesis<sup>198</sup>. NFIA induction during gliogenesis is mediated by Sox9 and NFIA/Sox9 co-regulate the expression of a set of genes including *Apccd1* and *Mmd2* (important for migratory and metabolic roles) during gliogenesis and astrocyte precursor migration<sup>199</sup>. NFIA is required for the expression of NFIB, with both NFIA and NFIB needed for the induction of glial-specific genes such as *GLAST*, *FGFR3* and *OLIG2*<sup>198</sup>.

NFIA contributes to the inhibition of neurogenesis by regulating the Notch effector HES5<sup>198</sup>. Notch signaling has been shown to induce NFIA expression in the neural progenitors of the developing telencephalon, in turn inducing gliogenesis through demethylation of the STAT3 binding site in the *GFAP* promoter<sup>200</sup>. Moreover, NFI directly

binds to and regulates *GFAP* transcription in differentiating astrocytes<sup>201</sup>. Interestingly, NFIA has also been shown to inhibit Notch signaling via the repression of Notch effector *Hes1*, suggesting the presence of a Notch signaling/NFIA regulatory loop<sup>186</sup>. NFIX is also involved in the regulation of astrocytic genes, with *Nfix*<sup>-/-</sup> mice showing a delay in gliogenesis in the developing forebrain and cerebellum<sup>185</sup>. In the developing spinal cord, NFIX is expressed in the ventricular zone progenitor cells post-gliogenic switch, after the expression of NFIA and NFIB. NFIX expression is transcriptionally regulated by NFIB and is required for late astrocytic maturation<sup>202</sup>. These studies show hierarchical roles for three members of the NFI family in regulation of gliogenesis during CNS development.

NFI has also been shown to regulate the differentiation of radial glial cells into astrocytes not only through activation of astrocytic genes but also by repressing neural stem cell maintenance genes<sup>203</sup>. NFIB and NFIX repress the expression of self-renewal genes *Ezh2* and *Sox9*<sup>185, 187</sup>. Similarly, NFIA and NFIB repress the Notch effector family genes *Hes1* and *Hes5* which are involved in stem cell self-renewal<sup>201</sup>.

In adult brain, NFIs play a rather opposite role to that observed in developing brain. NFIs are expressed in the adult neural stem cell populations and promote quiescence/maintenance of stem cells and not their differentiation<sup>204</sup>. Epigenomic profiling of an *in vitro* model of neural stem cells indicates that enhancers of genes actively required for neural stem cell quiescence/maintenance are occupied by NFI transcription factors. In the adult, NFIX rather than NFIA and NFIB is the master regulator of quiescence of neural stem cells<sup>203, 204</sup>.

### **1.5.3 NFI in glioblastoma**

NFIA, NFIB and NFIX have all been implicated in astrocytomas. *NFIA* levels are inversely correlated with astrocytoma tumour grade, with elevated expression observed in the majority of cells in low grade astrocytomas (91%, and 77% of cells in grades I and II, respectively) compared to high grade astrocytomas (48% and 37% graded III and IV, respectively)<sup>205</sup>. Furthermore, high levels of *NFIA* RNA in GBM are associated with better survival and correlate with better clinical outcome<sup>205</sup>. These results suggest that *NFIA* inhibits rather than promotes malignant properties. However, a few studies implicate *NFIA* as an oncogenic agent in GBM. For example, Lee *et al.* showed that *NFIA* promotes tumour growth, proliferation and migration through transcriptional repression of tumour suppressors p53, p21 and PAI1<sup>206</sup>. Another study by Glasgow *et al.* showed that mir-223 inhibits GBM cell proliferation by repressing *NFIA*, with *NFIA* overexpression rescuing this effect<sup>207</sup>. These authors further showed that *NFIA* was required for tumour growth in a GBM mouse model. *NFIA* has also been implicated in the determination of glioma type specificity. Expression of *NFIA* in oligodendrogliomas (<5%) is very low compared to astrocytomas. When *NFIA* is overexpressed in oligodendroglioma mouse models, the tumours take on the properties of astrocytomas<sup>208</sup>.

Similar to *NFIA*, there is an inverse correlation between *NFIB* mRNA levels and astrocytoma tumour grade, with elevated levels of *NFIB* associated with improved survival<sup>209</sup>. Expression of *NFIB* is also subtype-specific in GBM with highest levels in proneural GBM and lowest levels in mesenchymal GBM. Ectopic expression of *NFIB* inhibits tumour growth in intracranial xenograft mouse models of human mesenchymal but not proneural GBM. Notably, *NFIB* promotes tumour growth in neural GBM,

suggesting an oncogenic role in this subtype. These results demonstrate that NFIB can act as tumour suppressor or oncogene depending on the genetic context. The effect of NFIB in mesenchymal GBM is mediated through STAT3 signaling<sup>209</sup>.

STAT3 has previously been shown to be important for astrocytic differentiation. Like NFIA and NFIB, STAT3 activates *GFAP* transcription by binding to its promoter. NFIA has been shown to facilitate binding of STAT3 to the *GFAP* promoter<sup>200</sup>. Interestingly, isoform NFIX-3 regulates migration and invasion of GBM cells in conjunction with STAT3. The NFIX-3/STAT3 complex binds to the promoter of inflammation-associated *YKL-40* and activates its transcription, thereby promoting cell migration in GBM<sup>180</sup>.

Studies from our lab and other labs have shown that, in GBM cells, NFI family members regulate several key genes including *GFAP* and *B-FABP* that contribute to GBM pathogenesis<sup>181, 182</sup>. *GFAP* is a marker of astrocytes whereas *B-FABP* is neural stem cell marker expressed in radial glial cells. *B-FABP* and *GFAP* are often co-expressed in GBM cell lines. Expression of *B-FABP* in GBM cells promotes cell migration<sup>210</sup>. Based on immunostaining analysis, NFIA and *B-FABP* have similar distribution patterns, showing preferential expression in the perivascular niche associated with more migratory cells<sup>205, 210</sup>.

## 1.6 HEY1: A Notch effector

### 1.6.1 HEY family

HEY (hairy/E(spl)-related with YPRW motif) proteins belong to the basic helix-loop-helix family of transcription factors and consists of three proteins: HEY1-1, HEY1-2 and HEY1L<sup>211-214</sup>. HEY proteins are closely related to the bHLH HES (hairy and enhancer of split) family of transcription factors<sup>211-213</sup>. HEY and HES proteins are targets of the Notch signaling pathway, a classic pathway implicated in several developmental processes and which act as tumour suppressors<sup>215</sup>. HEY and HES proteins have three domains, a basic domain, followed by an HLH domain and an Orange domain, as well as two conserved motifs at the C-terminus. The basic domain is the DNA binding domain which recognizes E-box sequence CACGTGCACGCG<sup>216</sup>. The HLH domain acts as a dimerization domain and accounts for homodimerization and heterodimerization between HEY and HES proteins and for other protein-protein interactions<sup>217, 218</sup>. The Orange domain along with the HLH domain further promotes interaction with co-factors<sup>219</sup>. The function of the two conserved C-terminal motifs (YRPW and GTE) is still unknown.

The activation of HEY proteins is mediated by ligand binding (Jagged or Delta-like ligands) to the Notch receptors via their extracellular domains. This ligand-receptor interaction results in cleavage of the Notch intracellular domain, NICD, and its translocation to the nucleus. Upon reaching the nucleus, NICD interacts with a DNA binding protein Rbp-Jk and replaces its corepressors by its co-activators resulting in the conversion of Rbp-Jk complex from repressor to activator<sup>220</sup>. Binding of Rbp-Jk protein to the *HEY1* promoter in the presence of activators results in *HEY1* transcription activation<sup>221-223</sup>. In addition to the Notch signaling pathway, HEY1 expression is regulated

by crosstalk between Notch signaling and the Jak2-Stat3 pathway which has been shown to further enhance Notch activity<sup>224</sup>. FoxC proteins, Foxc1 and Foxc2 induce HEY2 expression by binding to the *HEY1* promoter through interaction with NICD<sup>225</sup>.

In addition to Notch signaling, HEY1 expression is also regulated by TGF $\beta$ /Smad signaling<sup>226</sup>. Bone morphogenetic proteins (BMPs) activate Smad proteins, which in turn directly bind to the *HEY1* promoter and activate its transcription, independent of Notch. Interaction of Smad1/3 and 5 with NICD appears to enhance this activation<sup>227</sup>.

### **1.6.2 HEY in brain development**

The Notch signaling pathway plays a key role in regulating differentiation during development<sup>200, 228</sup>. bHLH transcription factors including the HES and the HEY families are Notch signaling effectors that have a broad expression pattern. These transcription factors regulate a plethora of target genes during development and have been implicated in various developmental processes including heart development, vascular development, myogenesis, bone development, homeostasis and development of the nervous system<sup>217, 226, 229-231</sup>. In the developing retina, overexpression of HEY2 plays an important role in gliogenesis and promotes Müller glia formation, a function similar to that of HES genes<sup>232</sup>.

A balance between different bHLH family members is required to regulate neural progenitor maintenance, gliogenesis and neurogenesis<sup>233</sup>. HES1 and HES2 promote the maintenance of neural precursor cells during early embryonic development and the differentiation of glial cells at late stages of embryonic development<sup>233</sup>. In contrast, neuronal bHLH genes such as *MAS1*, *MATH3* and *Neurogenin* promote neurogenesis.

In the developing mouse neural tube, both *Hey1* and *Hey2* are expressed in the ventricular zone. *Hey1* is expressed ubiquitously in developing brain at embryonic day 12, whereas *Hey2* expression is limited to the mediodorsal region of the brain<sup>233</sup>. Expression of *Hey1* and *Hey2* is also observed in the ventricular region of the developing spinal cord. Like HES1 and HES2, HEY1 and HEY2 maintain neural precursor cells and regulate gliogenesis. Increased levels of HEY1 are observed in human astrocytes compared to neural stem cells<sup>234</sup>. Ectopic expression of HEY1 and HEY2 at early stages of brain development promotes maintenance of neural precursors, whereas ectopic expression at later stages results in induction of gliogenesis and inhibition of neurogenesis through inhibition of neuronal bHLH genes *Mash*, *Math3* and *Neurogenin* transcription<sup>233</sup>.

HEYL, a third member of HEY family, along with HEY2 are expressed in neural crest cells and in dorsal root ganglia<sup>235</sup>. *HeyL*<sup>-/-</sup> mice show reduction of TrkC-positive neurons in dorsal root ganglia, in contrast to *Hey1*<sup>-/-</sup> mice which show increases in the numbers of these neurons<sup>236</sup>. In keeping with HEYL and HEY1/HEY2 having opposite roles, HEYL promotes neuronal differentiation in neural progenitor cells and activates transcription of neural bHLH gene *Neurogenin*<sup>237</sup>. These results show that coordinated expression of Hey family members is required for key processes during brain development.

### **1.6.3 HEY1 in glioblastoma**

Several studies have shown that HEY proteins are associated with various tumours and play a key role in tumorigenesis. Hey protein levels are elevated in several

cancers including osteosarcoma, colorectal cancer, squamous cell carcinoma, pancreatic cancer, and is associated with poor prognosis, decreased overall survival and chemoresistance in these tumours<sup>238-242</sup>. The role of HEY1 in cancer is mediated through a variety of mechanisms. For example, HEY1 promotes cancer metastasis in osteosarcoma by activating *MMP9* transcription<sup>243</sup>. HEY proteins have also been associated with induction of EMT or MET depending on the signaling pathway governing its expression<sup>244</sup>. HEY1 interacts with SMAD3 to repress transcription of epithelial factor E-cadherin directly or by interacting with Snail1<sup>244, 245</sup>. Induction of HEY1 by TGF $\beta$  results in induction of EMT, whereas HEY1 induction by Notch can lead to either EMT or MET<sup>246</sup>.

HEY proteins regulate cellular differentiation, proliferation and self-renewal of cancer cells. High levels of HEY1 are observed in cancer stem cells, with depletion of HEY1 resulting in reduced sphere formation and tumour growth<sup>247</sup>. In hepatocellular carcinoma, HEY1 and HEY2 overexpression have been implicated in increased formation of spheres, increased cell proliferation and increased cell viability<sup>248</sup>. In breast carcinoma, HEYL promotes breast cancer initiation mediated by the TGF $\beta$ /Smad pathway<sup>246</sup>. Moreover, the balance between HEY proteins is important for neovasculature formation in cancer<sup>249</sup>. HEY1/HEY2 induce *VEGFR2* expression downstream of DLL4 (Delta like 4) and thus induce vessel formation. The Notch-HEY1 signaling pathway is hyperactivated in breast cancer cell lines, with Notch inhibition of this pathway resulting in downregulation of HEY and accompanying decreased cell migration and invasion<sup>250</sup>.

Several studies have addressed the role of Notch signaling in gliomas<sup>238</sup>. High levels of Notch1, Notch3 and Notch4 have been shown to be associated with increasing tumour grade in astrocytomas<sup>251</sup>, although one report indicates that Notch1 expression

and activity are elevated in grade II and III astrocytomas compared to GBM<sup>252</sup>. Dysregulation of two main Notch ligands, DLL1 and Jagged-1 (JAG-1), has been reported in GBM<sup>253</sup>. Increased expression of DLL1 is associated with low grade gliomas and secondary GBMs, while levels of Jagged-1 are higher in GBM compared to lower grade astrocytomas<sup>253</sup>. Depletion of Notch1 using siRNAs results in decreased cell proliferation and increased cell death in GBM cells, and increased survival in an orthotopic GBM tumour model compared to control mice<sup>253</sup>. Several Notch signaling target genes are upregulated in GBM, including GFAP, Nestin, TNC and HES1 and HEY1.

Like Notch, HEY1 is upregulated in glioma<sup>254</sup>, with high levels of *HEY1* mRNA correlating with higher grade gliomas and lower disease-free survival. In GBM cell lines and xenograft models, depletion of HEY1 by siRNA results in decreased cell proliferation and migration<sup>254</sup>. The *HEY1* promoter is hyper-methylated in normal brain compared to GBM, indicating that the methylation status of *HEY1* contributes to GBM pathogenesis<sup>255</sup>.

## 1.7 Research objectives

### 1.7.1 Chapter 2: *AP-2 $\epsilon$ expression in developing retina*

AP-2 transcription factors play important roles in the regulation of gene expression during development. Four of the five members of the AP-2 family (AP-2 $\alpha$ , AP-2 $\beta$ , AP-2 $\gamma$  and AP-2 $\delta$ ) have previously been shown to be expressed in developing retina. Mouse knockouts have revealed roles for AP-2 $\alpha$ , AP-2 $\beta$  and AP-2 $\delta$  in retinal cell specification and function. In chapter 2 we show that the fifth member of the AP-2 family, AP-2 $\epsilon$ , is also expressed in amacrine cells in developing mammalian and chicken retina. Our data indicate that there are considerably fewer AP-2 $\epsilon$ -positive cells in the developing mouse retina compared to AP-2 $\alpha$ , AP-2 $\beta$  and AP-2 $\gamma$ -positive cells, suggesting a specialized role for AP-2 $\epsilon$  in a subset of amacrine cells. AP-2 $\epsilon$ , which is restricted to the GABAergic amacrine lineage, is most commonly co-expressed with AP-2 $\alpha$  and AP-2 $\beta$ , especially at early stages of retinal development. Co-expression of AP-2 $\epsilon$  and AP-2 $\gamma$  increases with differentiation. Analysis of previously published Drop-seq data from single retinal cells supports co-expression of multiple AP-2s in the same cell. Since AP-2s bind to their target sequences as either homodimers or heterodimers, our work suggests spatially- and temporally-coordinated roles for combinations of AP-2 transcription factors in amacrine cells during retinal development.

### **1.7.2 Chapter 3: NFI represses Notch effector HEY1 in glioblastoma**

Glioblastomas (GBM) are highly aggressive brain tumors with a dismal prognosis. Nuclear factor I (NFI) is a family of transcription factors that controls glial cell differentiation in the developing central nervous system. NFIs have previously been shown to regulate the expression of astrocyte markers such as glial fibrillary acidic protein (*GFAP*) in both normal brain and GBM cells. We used ChIP-on-chip to identify additional NFI targets in GBM cells. Analysis of our ChIP data revealed ~400 putative NFI target genes including an effector of the Notch signaling pathway, *HEY1*, implicated in the maintenance of neural stem cells. All four NFIs (NFIA, NFIB, NFIC and NFIX) bind to NFI recognition sites located within 1 kb upstream of the *HEY1* transcription site. We further showed that NFI negatively regulates *HEY1* expression, with knockdown of all four NFIs in GBM cells resulting in increased *HEY1* RNA levels. *HEY1* knockdown in GBM cells decreased cell proliferation and increased cell migration. Finally, we found a general correlation between elevated levels of *HEY1* and expression of the brain neural stem/progenitor cell marker *B-FABP* in GBM cell lines, with knockdown of *HEY1* resulting in an increase in the levels of the glial fibrillary acidic protein (*GFAP*) astrocyte marker. Overall, our data indicate that *HEY1* is negatively regulated by NFI family members, and is associated with increased proliferation, expression of neural stem markers and decreased migration in GBM cells.

### **1.7.3 Chapter 4: Role of AP-2 $\beta$ in stem cell maintenance in glioblastoma**

AP-2 transcription factors are involved in the regulation of genes responsible for early development, cellular growth and differentiation. Aberrant regulation of AP-2 proteins has been associated with several cancers. The subcellular localization of AP-2 $\alpha$  has been shown to correlate with astrocytoma tumour grade. In low-grade astrocytoma, AP-2 $\alpha$  is primarily found in the nucleus, whereas in GBM, it has a cytoplasmic pattern. Our immunofluorescence and nuclear-cytoplasmic fractionation analyses indicate that AP-2 $\beta$  localizes to the cytoplasm of GBM cells.

We are particularly interested in AP-2 $\beta$  as its expression correlates with poor survival in gliomas. To address AP-2 $\beta$ 's role in glioblastoma, we are using patient-derived tumour neurospheres as well as glioblastoma cell lines cultured under standard conditions (i.e., with fetal calf serum). We show that AP-2 $\beta$  is more highly expressed when cells are cultured under neurosphere conditions compared to standard conditions. Interestingly, whereas AP-2 $\beta$  is primarily found in the nucleus of glioblastoma cultured under standard conditions, it primarily localizes to the nucleus of neurosphere cultures. Knockdown of AP-2 $\beta$  in glioblastoma cells cultured under neurosphere conditions results in decreased expression of stem cell markers Nestin and SOX2, as well as decreased cell migration. Stem cell maintenance and mesenchymal characteristics are associated with hypoxia in GBM. We observed an increase in AP-2 $\beta$  levels in GBM neurospheres cultured under hypoxia (0.5% oxygen). Knockdown of AP-2 $\beta$  in GBM neurosphere cultures under hypoxic conditions results in reduction of stem cell and mesenchymal markers. These combined data suggest that AP-2 $\beta$  may regulate stem cell maintenance and migration in GBM.

## **Chapter 2 AP-2 $\epsilon$ Expression in Developing Retina**

## 2.1 Introduction

The vertebrate retina consists of diverse neuronal cell types which coordinate the reception, processing and transfer of the visual signal to the optic centers in the brain. There are six major neuronal cell types (rod and cone photoreceptors, horizontal cells, bipolar cells, amacrine cells and ganglion cells) in the retina. Retinal progenitor cells give rise to these different neuronal cell types as well as Müller glial cells in a highly-coordinated manner governed by both extrinsic and intrinsic factors<sup>2, 256</sup>. Retinal development can be broadly divided into three phases: cell proliferation, migration (exit from the cell cycle/lineage commitment), and differentiation. Transcription factors play important roles in all aspects of retinal development<sup>1</sup>.

AP-2 is a family of transcription factors involved in the regulation of genes responsible for cellular growth and differentiation during early development<sup>96, 116, 257</sup>. Overlapping and divergent AP-2 expression patterns suggest both redundant and non-redundant roles for AP-2 family members. In mice, AP-2 $\alpha$ , AP-2 $\beta$  and AP-2 $\gamma$  are expressed in neural crest cell lineages, the peripheral nervous system, facial and limb mesenchyme, the epithelia of the developing embryo and/or extraembryonic trophoctoderm<sup>120, 128, 258</sup>. AP-2 $\delta$  is expressed in developing heart and CNS<sup>121</sup> and AP-2 $\epsilon$  expression was first reported in the olfactory bulb<sup>94, 122</sup> and keratinocytes<sup>259</sup>. AP-2 $\alpha$  knockout mice die perinatally with craniofacial defects and severe skeletal defects in head and trunk regions<sup>124, 125</sup>. AP-2 $\beta$  knockout mice die shortly after birth due to polycystic kidney disease and terminal renal failure<sup>126, 127</sup>. AP-2 $\gamma$  knockout mice die during early embryonic development immediately after implantation<sup>128, 129</sup>. Both AP-2 $\delta$  and AP-2 $\epsilon$  knockout mice are viable, with defects in midbrain development<sup>130, 260</sup> and olfactory bulb

formation<sup>131</sup>, respectively.

AP-2 transcription factors play a significant role in eye development<sup>261-264</sup>, with four AP-2s ( $\alpha$ ,  $\beta$ ,  $\gamma$  and  $\delta$ ) expressed in developing retina<sup>134-136, 264, 265</sup>. *AP-2 $\alpha$*  and *AP-2 $\beta$*  are restricted to amacrine cells and horizontal cells<sup>136, 265</sup>. *AP-2 $\gamma$*  is also expressed in amacrine cells, but in a population that is distinct from that of *AP-2 $\alpha$*  and *AP-2 $\beta$* <sup>134</sup>, whereas *AP-2 $\delta$*  is found in a subset of ganglion cells<sup>137</sup>. Conditional (retina-specific) *AP-2 $\alpha$*  and *AP-2 $\beta$*  knockout mice show horizontal and amacrine cell defects that were not observed upon deletion of *AP-2 $\alpha$*  alone<sup>134, 135</sup>. This suggests redundant roles for *AP-2 $\alpha$*  and *AP-2 $\beta$*  in amacrine and horizontal cell differentiation. In addition to midbrain defects, *AP-2 $\delta$*  knockout mice also show reduced ganglion cell numbers as well as reduced axonal projections to the superior colliculus, a major visual center in the brain<sup>260</sup>. In chick retina, overexpression of *AP-2 $\delta$*  results in axonal misrouting<sup>266</sup>.

Amacrine cells, distributed in the innermost part of the inner nuclear layer of the retina, are interneurons that form synapses with ganglion and/or bipolar cells, with key roles in the processing of visual signals<sup>47, 267</sup>. Amacrine cells are the most diverse type of cells in the retina with >30 subtypes characterized to date<sup>43, 267</sup>. Here, we report that *AP-2 $\epsilon$*  is expressed in amacrine cells in chicken, mouse and human fetal retina. Immunofluorescence analysis reveals co-localization of *AP-2 $\epsilon$*  with the other members of the AP-2 family, but only in subsets of cells and at specific developmental stages. Our results indicate highly specific and cell-restricted roles in the retina for this latest member of the AP-2 family. Since AP-2s can function as either homodimers or heterodimers, expression of four AP-2s in subsets of amacrine cells has implications for finely-tuned regulation of AP-2 target genes.

## **2.2 Material and Methods**

### **2.2.1 Ethics statement**

Ethics approval for the collection of human fetal retina was obtained from the Health Research Ethics Board of Alberta – protocol 17561. In the case of the human fetal retina (collected more than 20 years ago), the need for consent was waived as the tissue was collected under a general protocol that did not require any information regarding the patient. Ethics approval for collection of mouse retina was obtained from the Cross Cancer Institute Animal Care Committee – protocol AC 16226. All methods used for collection of retinal tissue were carried out in accordance with human ethics and Canadian Council on Animal Care (CCAC) Guidelines and Policies. Retinal tissue from mouse was collected from euthanized animals. Chick retinal tissue was collected from euthanized animals as part of previous studies<sup>136, 268</sup>

### **2.2.2 Semi-quantitative and quantitative RT-PCR**

RNA was purified from at least two different batches of chick retina [embryonic day E5, E7, E10 and E15] and mouse retina [E16.5, post-natal (P)1, P14 and adult]. RNA was reverse transcribed using oligo(dT) and Superscript reverse transcriptase II (Invitrogen). The following primers were used for semi-quantitative RT-PCR analysis of mouse and chicken retina: mouse AP-2 $\epsilon$  (forward primer: 5'-GTTGCTCAGCTCAACATCCA-3'; reverse primer: 5'-CTGAGCCATCAAGTCTGCAA-3'), and chicken AP-2 $\epsilon$  (forward primer: 5'-GCTCCACACCAGGAAGAACATG-3'; reverse primer: 5'-CAT CAA ACT GGC TCA TTT TC-3).

Y79 and WERI-Rb1 retinoblastoma cell lines were obtained from the American

Type Culture Collection. RB522A, RB778, RB893, RB894, RB898, RB1021, RB544 cell lines were established by Dr. Brenda Gallie, Department of Medical Genetics, University of Toronto, Canada. RB(E)-2, RB(E)-3, RB(E)-6 and RB(E)-8 cell lines, as well as RNA preparation, have been previously described<sup>146</sup>. The following primers were used for RT-PCR analysis of retinoblastoma cells: human AP-2 $\epsilon$  (forward primer: 5'-CAATGTGACGCTGCTGACTT-3'; reverse primer: CACTGCCCACACTGCTTAG-3'), and human AP-2 $\gamma$  (forward primer: 5'-AAAGCCGCTCATGTGACTCT-3'; reverse primer: TGGTCTCCAGGGTTCATGT-3'). Quantitative RT-PCR was carried out using the SYBR green based qPCR system (Applied Biological Materials Inc. Canada) and analyzed on an ABI 7900HT PCR system, with primers designed to amplify a 150 bp region of AP-2 $\epsilon$  (forward primer: 5'-ATTGCAGGCGATAGATGACC-3'; reverse primer: 5'-GAGCAGAAGACCTCACTGG-3').

### **2.2.3 *In situ* hybridization**

Tissue sections (7-8  $\mu$ m) were prepared from E16.5, P1, P7, P15.5 mouse retina, as well as E10 chick retina. Tissue sections were fixed in 4% paraformaldehyde, and incubated with DIG-labelled probes overnight at 55°C, as previously described<sup>269</sup>. Tissue sections were then washed and digested with ribonuclease A. The signal was detected with anti-DIG antibody using NBT and BCIP as substrates<sup>263</sup>. For *in situ* hybridization probes, we PCR amplified a 700 bp mouse AP-2 $\epsilon$  cDNA fragment and a 560 bp chicken AP-2 $\epsilon$  cDNA fragment. cDNAs were cloned into the pBluescript vector and pGEM-T Easy vector, respectively. The constructs were linearized and electrophoresed in a polyacrylamide gel. Bands were cut out, electrophoresed out of the gel and the DNA

extracted with phenol and chloroform. Probes were generated using T3 and T7 RNA polymerases and digoxigenin (DIG)-labeling mix, as specified by the manufacturer (Roche). The probes were quantified by comparing labeling intensity to a control probe supplied by manufacturer. Image acquisitions were made using a Zeiss Axioskop2 Plus microscope and AxioVision 4.7.1 software.

#### **2.2.4 Immunostaining**

Immunohistochemistry and immunofluorescence analyses were carried out as previously described<sup>146, 270</sup>. Mouse P1 (from 2 pups), P7 (from 3 pups) and P14 (from 2 pups) retinas and human fetal retina tissue at 17 weeks gestation were fixed in formalin and paraffin-embedded. Note that mouse retina tissue at P14 -16 is roughly equivalent, with most cells in the retina being fully differentiated by P11<sup>6</sup>. Tissue sections were deparaffinized in xylene, rehydrated and microwaved in a pressure cooker for 20 min for antigen retrieval. The rabbit anti-AP-2 $\epsilon$  antibody (1:1,500, generated by Dr. Markus Moser, Max Plank Institute of Biochemistry) was used for immunohistochemistry. The following antibodies were used for immunofluorescence analysis: anti-AP-2 $\alpha$ , mouse monoclonal antibody (1:400, 3B5, Developmental Studies Hybridoma Bank developed under the auspices of the NICHD and maintained by the University of Iowa)<sup>134</sup>, anti-AP-2 $\beta$ , rabbit polyclonal antibody (1:1,000, #2509, Cell Signaling Technology)<sup>134</sup>, anti-AP-2 $\gamma$ , mouse monoclonal antibody (1:200, 6E4/4, Santa Cruz Biotechnology)<sup>134</sup>, and anti-AP-2 $\epsilon$ , rabbit polyclonal antibody (1:1,500, described above). GABAergic amacrine cells were immunostained with anti-GAD67, mouse monoclonal antibody (1:3000, MAB5406, Chemicon International). Glycinergic amacrine cells were immunostained with anti-

GLYT1, goat polyclonal antibody (1:6000, AB1770, Millipore).

For co-immunofluorescence of same species anti-AP-2 $\beta$  and anti-AP-2 $\epsilon$  rabbit antibodies, we used the Tyramide Signal Amplification (TSA) kit (PerkinElmer). Tissue sections were first immunostained with anti-AP-2 $\epsilon$  antibody followed by goat anti-rabbit HRP-conjugated secondary antibody (DAKO). Cy3-conjugated tyramide was then applied, resulting in a tyramide-protein-antibody complex, with HRP activating bound tyramide. The protein-antibody complex was then heat-denatured in sodium citrate, leaving the Cy3-conjugated tyramide intact. Next, tissue sections were immunostained with AP-2 $\beta$  primary antibody followed by Alexa 488-conjugated secondary antibody. Immunofluorescence images were captured on a Zeiss LSM710 confocal laser scanning microscope with a plan-Apochromat 20X lens using ZEN software.

To ensure AP-2 antibody specificity, HeLa cells were transfected with each of the five AP-2 expression constructs in p3xFLAG-CMV vector. Cells were harvested, and total cell lysates were prepared using RIPA buffer. Lysates were electrophoresed through a 10% SDS-PAGE gel and western blot analysis carried out using antibodies to each of the five AP-2s.

### **2.2.5 Analysis of AP-2 expression in mouse retinal cells**

We utilized the merged expression data set generated by Drop-seq of single P14 mouse retinal cells (GEO accession viewer GSE63472)<sup>49</sup>. Individual cells were grouped as per the 39 clusters defined by Macosko *et al.*<sup>49</sup>, and further analysis was performed on those clusters identified as amacrine cell types (clusters 3 to 23, comprising a total of 3,711 individual cells). These cells were then scored as positive or negative for

expression of AP-2 $\alpha$ , AP-2 $\beta$ , AP-2 $\gamma$  or AP-2 $\epsilon$ . A more detailed analysis of AP-2 $\epsilon$  was performed with cell clusters containing >30% AP-2 $\epsilon$ -positive cells (high expression or HE, clusters 5 and 9: 343 cells), >10% AP-2 $\epsilon$ - positive cells (mid-level expression or ME, clusters 8 and 15: 182 cells), with the remaining cell clusters labelled as low or no expression (NE, 3,186 cells).

### **2.2.6 Data availability statement**

The datasets analyzed in the current study are from a published study by Macosko *et al.*<sup>49</sup>. These datasets are publicly available through GEO accession viewer repository GSE63472.

## 2.3 Results

### 2.3.1 *AP-2 $\epsilon$ is expressed in amacrine cells*

Expression of four members of AP-2 family has previously been documented in the developing retina, with AP-2 $\alpha$ , AP-2 $\beta$  and AP-2 $\gamma$  all expressed in amacrine cells. We examined whether AP-2 $\epsilon$  might also be expressed in the retina by carrying out *in situ* hybridization of mouse retinal tissue sections at E16.5 (mostly proliferative cells), P1 (early stage of differentiation), P7 (intermediate stage of differentiation) and P15.5 (late stage of differentiation). Only background staining was observed at E16.5, indicating that AP-2 $\epsilon$  is not expressed in proliferating cells (Figure 2.1A). By P1, AP-2 $\epsilon$  RNA was detected in the inner part of the inner neuroblastic layer where amacrine cells are located. At P7 and P15.5, there were AP-2 $\epsilon$ -positive cells throughout the inner part of the inner nuclear layer, along with a few positive cells in the ganglion cell layer of P7 retina. The AP-2 $\epsilon$  distribution patterns at P1, P7 and P15.5 are consistent with expression in amacrine cells, as displaced amacrine cells are also found in the ganglion cell layer.

We then examined whether AP-2 $\epsilon$  expression in amacrine cells is evolutionarily conserved. *In situ* hybridization of chick retina tissue sections was carried out at E10 which is roughly equivalent to mouse P7 retina<sup>6, 271</sup>. Similar to mouse, AP-2 $\epsilon$  RNA in chick retina was found in the amacrine cells located in the inner part of the inner nuclear layer (indicated by arrowheads in Figure 2.1B). No signal was observed in the ganglion cell layer, likely reflecting the reduced numbers of displaced amacrine cells in the ganglion cell layer of chick retina compared to mouse retina<sup>272, 273</sup>. However, there was a layer of AP-2 $\epsilon$ -positive cells in the outer part of the inner nuclear layer where horizontal cells are located (indicated by arrow in Figure 2.1B).

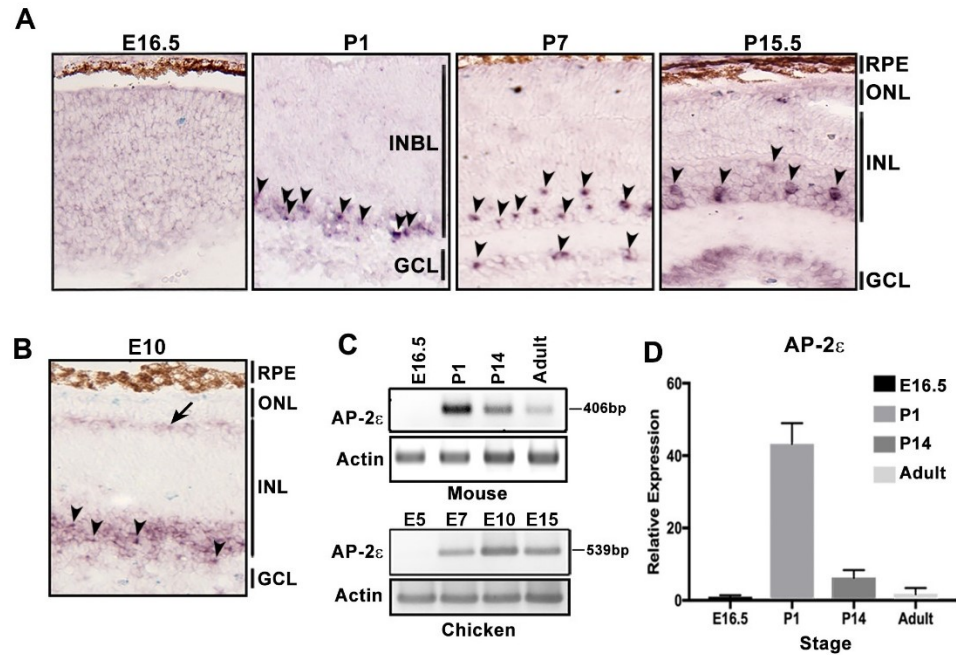


**Figure 2.1** *AP-2ε* RNA is expressed in mouse and chick retina.

**(A)** *In situ* hybridization showing expression of *AP-2ε* at E16.5, P1, P7 and P15.5 in mouse retina. **(B)** *In situ* hybridization showing expression of *AP-2ε* in E10 chick retina. **(C)** RT-PCR analysis of *AP-2ε* in mouse retina at E16.5, P1, P14 and adult (top), and in chick retina at E5, E7, E10 and E15 (bottom). Sizes of RT-PCR products are indicated on the right. **(D)** qPCR analysis showing relative expression of *AP-2ε* in mouse retina at E16.5, P1, P14 and adult. The error bars are calculated using standard deviation. Arrowheads point to positive amacrine cells. The arrow points to the horizontal cell layer. Abbreviations: RPE, retinal pigmented epithelium; INL, inner nuclear layer; ONL, outer nuclear layer; GCL, ganglion cell layer; INBL, inner neuroblastic layer.

To confirm our findings that AP-2 $\epsilon$  is expressed in both mouse and chicken retina, we carried out RT-PCR analysis at different stages of development. In mouse retina, no signal was detected at E16.5, in agreement with the *in situ* hybridization data (Figure 2.1C). A strong signal was obtained in P1 retina, with progressively weaker signals in P14 and adult retina. These semi-quantitative data were verified by quantitative RT-PCR (Figure 2.1D). In chick retina, no signal was detected in the relatively undifferentiated E5 retina, with a peak signal observed in E10 retina (Figure 2.1C).

Next, we carried out immunohistochemical analysis to examine the distribution of AP-2 $\epsilon$  protein in retina. We first tested the specificity of our AP-2 antibodies by western blot analysis of HeLa cells transfected with different AP-2 expression constructs. Based on western blotting, the AP-2 $\alpha$ , AP-2 $\beta$ , AP-2 $\gamma$  and AP-2 $\epsilon$  antibodies are highly specific (Figure 2.2A). The presence of doublet bands suggests post-translational modification of AP-2 proteins. We then used the AP-2 $\epsilon$  antibody to immunostain mouse retina. In P7 mouse retina, AP-2 $\epsilon$ -positive cells were observed in the inner nuclear layer (arrowheads point to positive cells) (Figure 2.2B). We also examined the distribution of AP-2 $\epsilon$  in human fetal retina at 17 weeks gestation, a stage when amacrine cells are differentiated<sup>274</sup>. Similar to what we observed in mouse retina, AP-2 $\epsilon$ -positive cells in human retina were mostly confined to the inner part of the inner nuclear layer where amacrine cells are located (Figure 2.2C). A few AP-2 $\epsilon$ -positive cells were also found in the ganglion cell layer, likely displaced amacrine cells.

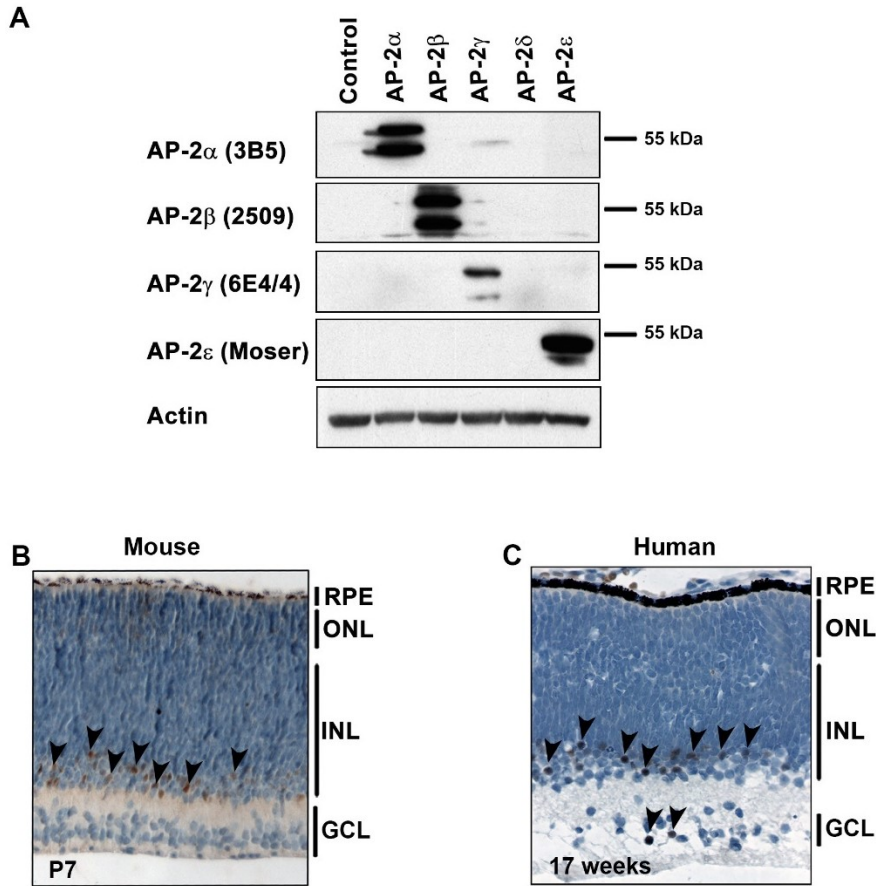


**Figure 2.2 Immunohistochemical analysis of AP-2 $\epsilon$  in retina**

**(A)** Western blot analysis of AP-2 antibodies. HeLa cells were transfected with vector control, AP-2 $\alpha$ , AP-2 $\beta$ , AP-2 $\gamma$ , AP-2 $\delta$  or AP-2 $\epsilon$  expression constructs. Blots were immunostained with antibodies to AP-2 $\alpha$ , AP-2 $\beta$ , AP-2 $\gamma$  or AP-2 $\epsilon$ . **(B)** P7 mouse retina and **(C)** human fetal retina at 17 weeks gestation were immunostained with the anti-AP-2 $\epsilon$  antibody. Positive cells are indicated by arrowheads. Abbreviations: RPE, retinal pigmented epithelium; INL, inner nuclear layer; ONL, outer nuclear layer; GCL, ganglion cell layer.

### **2.3.2 Co-expression of AP-2 $\epsilon$ and other AP-2 family members in retina**

Immunofluorescence analysis was carried out to determine whether AP-2 $\epsilon$  is co-expressed with other AP-2 family members at P1 (2 pups), P7 (3 pups) and P14 (2 pups) in mouse retina. Sections from P1, P7 and P14 mouse eyes were first co-immunostained with antibodies to AP-2 $\alpha$  and AP-2 $\epsilon$ . Considerably fewer AP-2 $\epsilon$ -positive cells were observed compared to AP-2 $\alpha$ -positive cells (Figure 2.3). The majority of AP-2 $\epsilon$ -positive cells co-expressed AP-2 $\alpha$  (54.8% at P1; 74.4% at P7; 72.9% at P14) (Figures 2.3, 2.4A). Similar results were obtained with AP-2 $\beta$  (41.2% at P1; 73.5% at P7; 82.5% at P14) (Figures 2.5, 2.4B). Thus, retinal differentiation is accompanied by increased co-expression of AP-2 $\epsilon$  with AP-2 $\alpha$  and AP-2 $\beta$ .

AP-2 $\gamma$  and AP-2 $\epsilon$  co-immunostaining revealed expression patterns different from that described for AP-2 $\alpha$  and AP-2 $\beta$ , with little co-expression observed at early developmental stages. At P1, only 3.9% AP-2 $\epsilon$ -positive cells co-expressed AP-2 $\gamma$ . At P7, 23.5% AP-2 $\epsilon$ -positive cells co-expressed AP-2 $\gamma$ . At P14, 41.7% AP-2 $\epsilon$ -positive cells co-expressed AP-2 $\gamma$  (Figures 2.6, 4C). The relatively high percentages of AP-2 $\epsilon$ -positive cells co-expressing AP-2 $\alpha$  (72.9%), AP-2 $\beta$  (82.5%) and AP-2 $\gamma$  (41.7%) at P14 suggest that a significant proportion of AP-2 $\epsilon$ -positive amacrine cells co-express three or more AP-2's.

As we observed a few AP-2 $\epsilon$ -positive cells in the ganglion cell layer, we co-immunostained mouse tissue sections with anti-AP-2 $\delta$  (ganglion cell-specific) and anti-AP-2 $\epsilon$  antibodies. There was no co-localization of AP-2 $\delta$  and anti-AP-2 $\epsilon$  at any of the

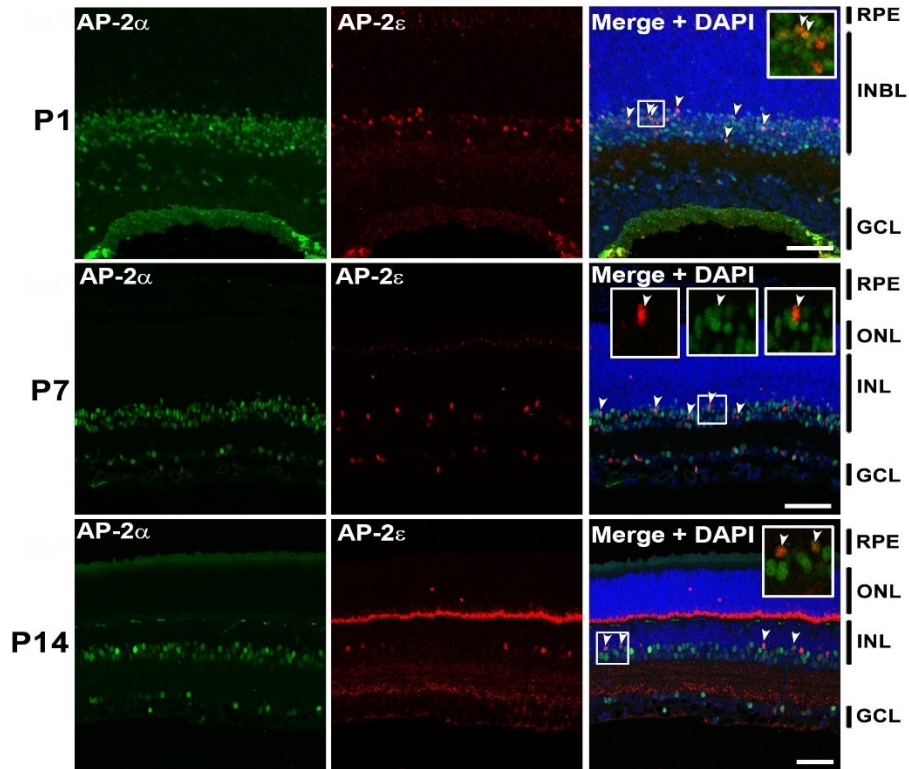


**Figure 2.3 Co-immunostaining of AP-2 $\alpha$  and AP-2 $\epsilon$  in P1, P7 and P14 mouse retina.**

Tissues were co-immunostained with rabbit anti-AP-2 $\epsilon$  (red) and mouse anti-AP-2 $\alpha$  (green). DAPI was used to stain nuclei. Merged images show co-localization of AP-2 $\alpha$  and AP-2 $\epsilon$  (yellow/orange color). Arrowheads point to cells co-expressing AP-2 $\alpha$  and AP-2 $\epsilon$ . Insets show a magnified view of designated areas. In P7, the arrowhead in the three insets points to the same cell co-expressing AP-2 $\alpha$  and AP-2 $\epsilon$  in the red, green and combined red/green channels. Abbreviations: RPE, retinal pigmented epithelium; INL, inner nuclear layer; ONL, outer nuclear layer; INBL, inner neuroblastic layer; GCL, ganglion cell layer. Scale bars = 50  $\mu$ m.

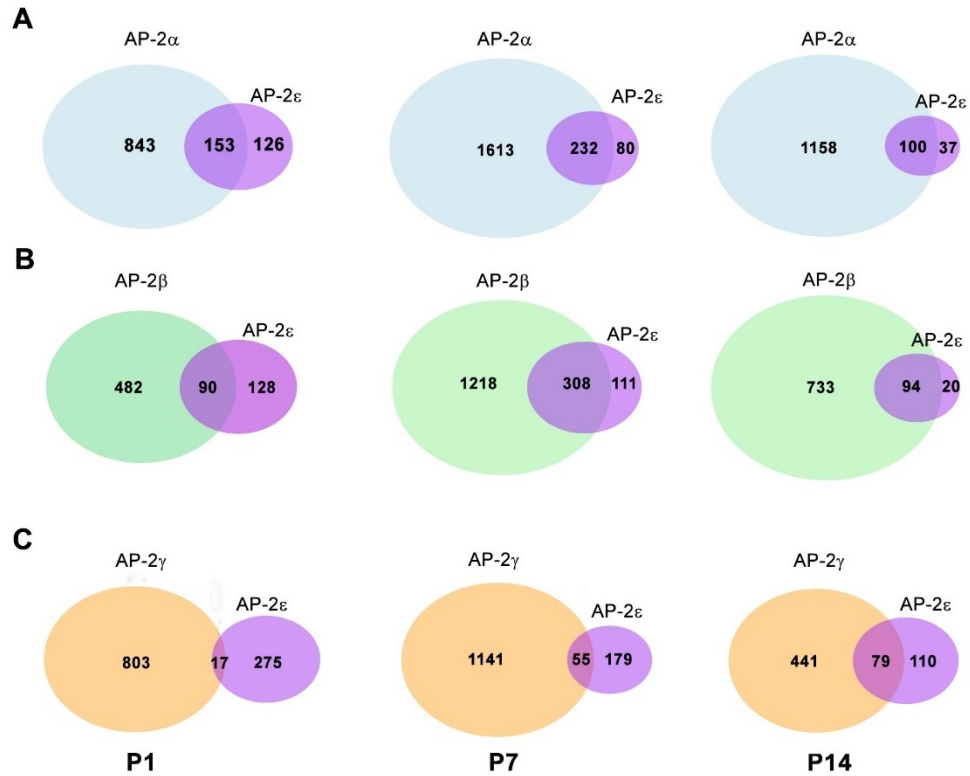


**Figure 2.4 Quantification of AP-2 expression data obtained from co-immunofluorescence analysis.**

Venn diagrams depict number of cells expressing a particular AP-2 with overlapping areas indicating the number of cells that express both AP-2s. **(A)** Cells expressing AP-2 $\alpha$ , AP-2 $\epsilon$ , and both AP-2 $\alpha$  and AP-2 $\epsilon$ . **(B)** Cells expressing AP-2 $\beta$ , AP-2 $\epsilon$ , and both AP-2 $\beta$  and AP-2 $\epsilon$ . **(C)** Cells expressing AP-2 $\gamma$ , AP-2 $\epsilon$ , and both AP-2 $\gamma$  and AP-2 $\epsilon$ . Counts were obtained from 2 eyes at P1 and P14 and 3 eyes at P7. The size of each oval is representative of the number of cells. RStudio software was used to plot Venn diagrams.

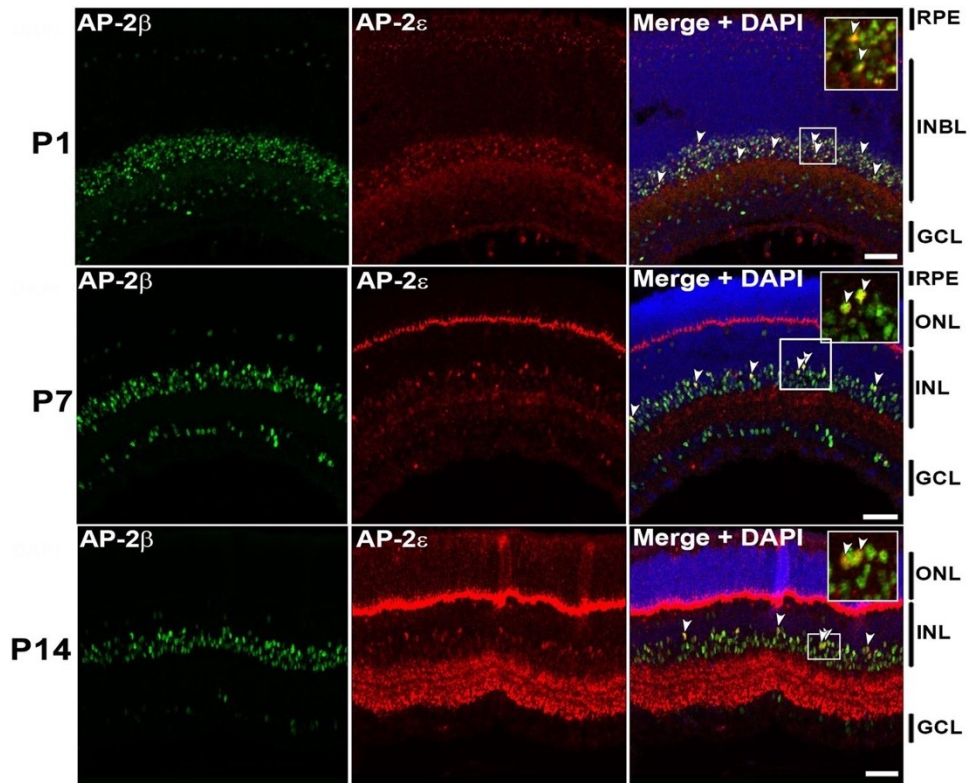


**Figure 2.5 Co-immunostaining of AP-2 $\beta$  and AP-2 $\epsilon$  in P1, P7 and P14 mouse retina.**

Tissues were immunostained sequentially with rabbit anti-AP-2 $\epsilon$  (red) and rabbit anti-AP-2 $\beta$  (green). Tyramide signal amplification (TSA) with multiplex capability allowed co-detection of AP-2 $\epsilon$  and AP-2 $\beta$  (the procedure is explained in Materials and Methods). DAPI was used to stain nuclei. Merged images show co-localization of AP-2 $\beta$  and AP-2 $\epsilon$  (yellow). Arrowheads point to cells co-expressing AP-2 $\beta$  and AP-2 $\epsilon$ . Insets show a magnified view of designated areas. Abbreviations: RPE, retinal pigmented epithelium; INL, inner nuclear layer; ONL, outer nuclear layer; INBL, inner neuroblastic layer; GCL, ganglion cell layer. Scale bars = 50  $\mu$ m. epithelium; INBL, inner neuroblastic layer; ONL, outer nuclear layer; INL, inner nuclear layer; GCL, ganglion cell layer. Scale bars = 50  $\mu$ m

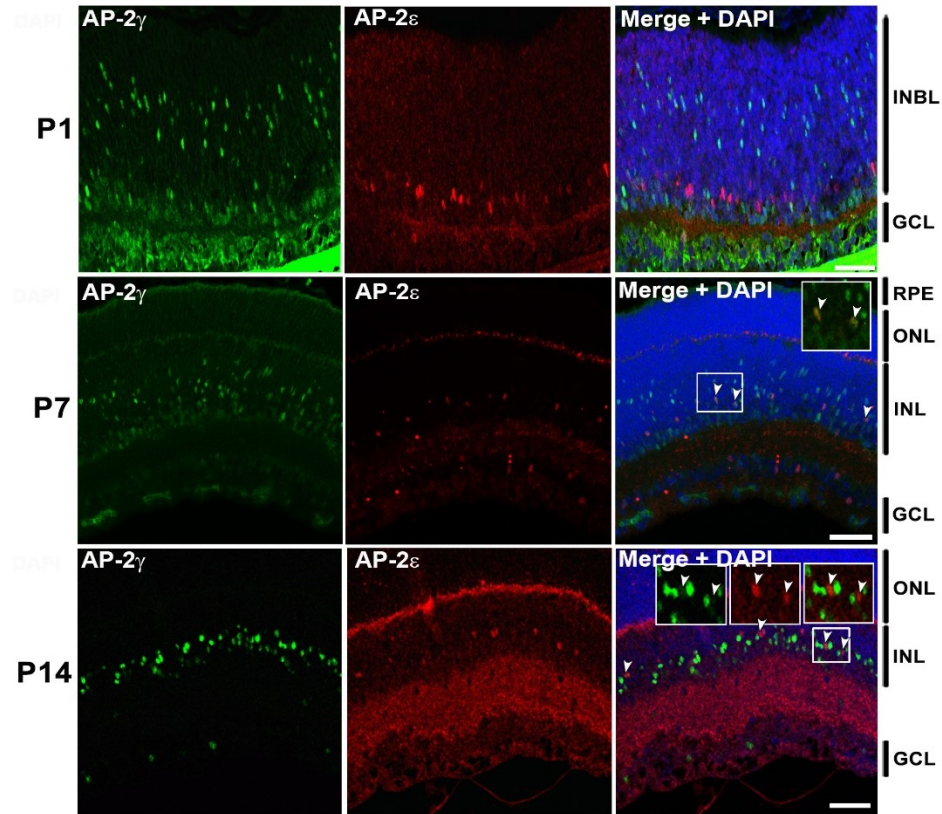


**Figure 2.6 Co-immunostaining of AP-2 $\gamma$  and AP-2 $\epsilon$  at P1, P7 and P14 in mouse retina.**

Tissues were immunostained sequentially with rabbit anti-AP-2 $\epsilon$  (red) and mouse anti-AP-2 $\gamma$  (green). DAPI was used as a nuclear stain. Merged images show co-localization of AP-2 $\gamma$  and AP-2 $\epsilon$  (yellow/orange). Arrowheads point to cells co-expressing AP-2 $\gamma$  and AP-2 $\epsilon$ . Insets show a magnified view of designated areas. In P14, the two arrowheads in the three insets point to the same two cells co-expressing AP-2 $\gamma$  and AP-2 $\epsilon$  in the red, green and combined red/green channels. Abbreviations: RPE, retinal pigmented

stages analyzed (P1, P7 and P14) (data not shown). These combined data demonstrate complex spatial relationships between AP-2 $\epsilon$  and AP-2 $\alpha$ ,  $\beta$ ,  $\gamma$  in the developing retina, with strongest associations observed with AP-2 $\alpha$  and AP-2 $\beta$  at P7 and P14. The limited overlap in AP-2 $\epsilon$  and AP-2 $\gamma$  co-expression at P1 suggests that there is little need for AP-2 $\gamma$ /AP-2 $\epsilon$ -positive amacrine cells at early stages of retinal development.

### **2.3.3 AP-2 $\epsilon$ is expressed in GABAergic amacrine cells**

There are two major categories of amacrine cells based on the neurotransmitter used to transmit signals across the retina: glycinergic and GABAergic<sup>48, 275</sup>. Previous studies have shown that AP-2 $\alpha$  and AP-2 $\beta$ -positive cells can be either glycinergic or GABAergic<sup>134</sup>. We carried out immunofluorescence studies to determine whether AP-2 $\epsilon$  is preferentially expressed in glycinergic or GABAergic amacrine cells. Anti-GLYT1 (glycinergic) and anti-GAD67 (a biosynthetic enzyme for GABA) antibodies were used to identify the two different categories of amacrine cells. Examination of P14 mouse retina tissue sections revealed no co-expression of AP-2 $\epsilon$  with GLYT1 (Figure 2.7A). On the other hand, virtually every AP-2 $\epsilon$ -positive cell expressed GAD67, although AP-2 $\epsilon$ -positive cells represented a small fraction of GAD67-positive cells (~10%) (Figure 2.7B). These results indicate that the amacrine cells that express AP-2 $\epsilon$  are GABAergic.

We also examined AP-2 $\epsilon$ /GAD67 co-immunostaining in the ganglion cell layer. The observed co-immunostaining of AP-2 $\epsilon$  and GAD67 confirmed that the few AP-2 $\epsilon$ -positive cells in the ganglion cell layer are indeed displaced amacrine cells (Figure 2.10)

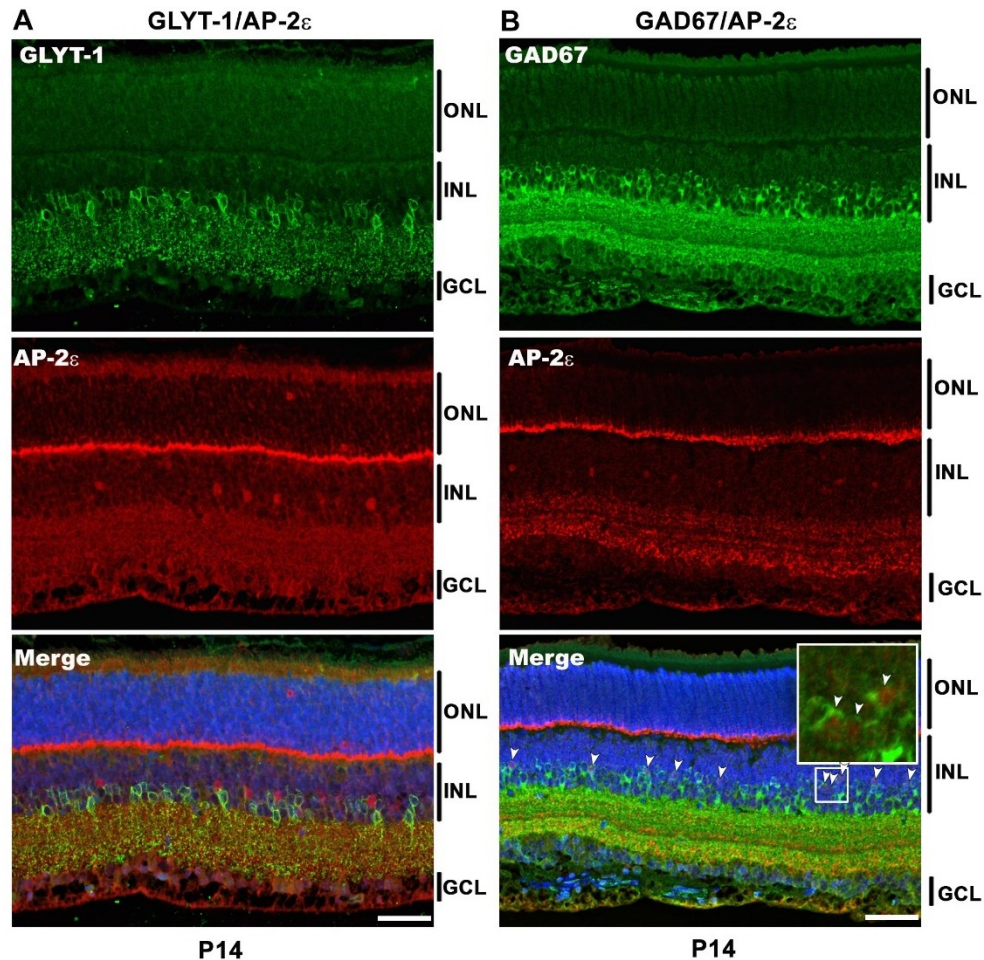


**Figure 2.7 Co-immunofluorescence showing AP-2 $\epsilon$  expression in glycinergic and GABAergic amacrine cells.**

**(A)** P14 mouse retina tissue sections were co-immunostained with anti-AP-2 $\epsilon$  antibody (red) and anti-GLYT-1 antibody (glycinergic amacrine cell marker; green). Little, if any, co-immunostaining was observed with the anti-GLYT-1 antibody. **(B)** P14 mouse retina tissue sections were co-immunostained with anti-AP-2 $\epsilon$  antibody (red) and anti-GAD67 antibody (GABAergic amacrine cell marker; green). As observed in the merged diagram (bottom panel), most of the AP-2 $\epsilon$  positive cells are GAD67 positive. The inset shows a magnified view of the designated area. DAPI was used to stain nuclei. Abbreviations: ONL, outer nuclear layer; INL, inner nuclear layer; GCL, ganglion cell layer. Size bars = 50  $\mu$ m.

### 2.3.4 Co-expression analysis of AP-2 transcription factors using single cell RNA sequencing data

Macosko *et al.*<sup>49</sup> carried out single-cell Drop-seq analysis of 44,808 cells isolated from P14 mouse retina and obtained 39 transcriptionally distinct clusters ranging in size from 50 to 29,400 cells. Ganglion cells, cones, rods, horizontal, Müller glia and astrocytic cells were each placed in a single cluster, and bipolar cells in 8 clusters. Amacrine cells were placed in 21 clusters (clusters 3 to 23): 12 GABAergic, 5 glycinergic, 1 excitatory based on glutamate transporter *Slc17a8* expression and 3 with low levels of GABAergic, glycinergic and glutamatergic markers. Subgrouping of the GABAergic and glycinergic clusters was based on differential expression of known amacrine markers. Approximately 10% of sequenced single cells (~4,400 of 44,808 cells) were classified as amacrine cells.

We examined 3,711 cells with complete sequencing data for expression of AP-2 family members. *AP-2 $\epsilon$*  RNA sequences were found in 133 cells, 108 of which belonged to two clusters: cluster 5 (21/68 cells) and 9 (87/275 cells) (Table 2.1). Of the remaining 25 AP-2 $\epsilon$ -positive cells, 24 belonged to three clusters: cluster 8 (14/125 cells), cluster 12 (3/224 cells) and cluster 15 (7/57 cells). Next, we examined co-expression of *AP-2 $\epsilon$*  RNA with that of the other AP-2s in the same cluster. In cluster 5, 58.8% (40/68), 5.88% (4/68) and 20.59% (14/68) of amacrine cells were positive for AP-2 $\alpha$ , AP-2 $\beta$  and AP-2 $\gamma$ , respectively, suggesting the possibility of significant overlap in AP-2 $\alpha$  and AP-2 $\epsilon$  expression for this particular subset of amacrine cells. For cluster 9, 68.7% (189/275) of cells were positive for AP-2 $\alpha$ , 84% (231/275) for AP-2 $\beta$ , and 17.5% (48/275) for AP-2 $\gamma$  indicating at least some overlap with AP-2 $\beta$ , and likely overlap with AP-2 $\alpha$  in this cluster (Table 2.1).

Cluster	Count	AP-2 $\alpha$	%	AP-2 $\beta$	%	AP-2 $\gamma$	%	AP-2 $\epsilon$	%	Co-expression
3	233	77	33.05	179	76.82	0	0	0	0	AP-2 $\alpha/\beta$
4	67	6	8.96	1	1.49	0	0	0	0	-
5	68	40	58.82	4	5.88	14	20.59	21	30.88	AP-2 $\alpha/\epsilon$
6	182	95	52.2	58	31.87	65	35.71	1	0.55	AP-2 $\alpha/\beta/\gamma$
7	257	55	21.4	38	14.79	148	57.59	0	0	AP-2 $\gamma$
8	125	58	46.4	82	65.6	14	11.2	14	11.2	AP-2 $\alpha/\beta$
9	275	189	68.73	231	84	48	17.45	87	31.64	AP-2 $\alpha/\beta/\epsilon$
10	166	78	46.99	135	81.33	11	6.63	0	0	AP-2 $\alpha/\beta$
11	189	42	22.22	136	71.96	5	2.65	0	0	AP-2 $\beta$
12	224	57	25.45	157	70.09	5	2.23	3	1.34	AP-2 $\beta$
13	41	31	75.61	39	95.12	0	0	0	0	AP-2 $\alpha/\beta$
14	95	62	65.26	92	96.84	0	0	0	0	AP-2 $\alpha/\beta$
15	57	32	56.14	50	87.72	2	3.51	7	12.28	AP-2 $\alpha/\beta$
16	211	35	16.59	198	93.84	2	0.95	0	0	AP-2 $\beta$
17	328	0	0	10	3.05	200	60.98	0	0	AP-2 $\gamma$
18	75	1	1.33	4	5.33	41	54.67	0	0	AP-2 $\gamma$
19	115	9	7.83	5	4.35	3	2.61	0	0	-
20	342	1	0.29	6	1.75	0	0	0	0	-
21	224	0	0	8	3.57	1	0.45	0	0	-
22	228	57	25	188	82.46	0	0	0	0	AP-2 $\beta$
23	209	82	39.23	192	91.87	2	0.96	0	0	AP-2 $\alpha/\beta$

**Table 2.1 Analysis of 21 clusters of amacrine cells.**

Twenty-one previously defined clusters of amacrine cells numbered 3 to 23 were analyzed for expression of AP-2 family members. The table shows numbers of cells in each cluster and the number and percentage of cells expressing AP-2 $\alpha$ , AP-2 $\beta$ , AP-2 $\gamma$  or AP-2 $\epsilon$ . The clusters which have >30% cells for a particular AP-2 are highlighted in red. The last column indicates possible combinations of AP-2s expressed in each cluster based on percentage of cells (30% cut-off) expressing specific AP-2s.

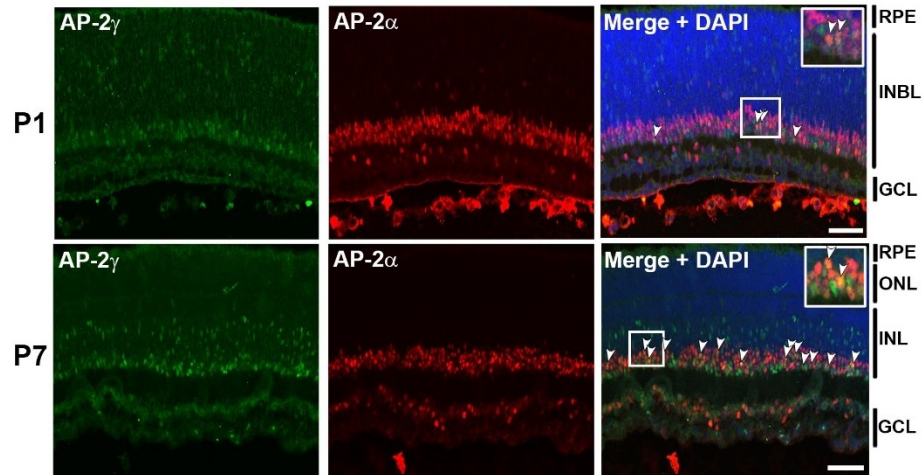


**Figure 2.8 Co-immunostaining of AP-2 $\alpha$  and AP-2 $\gamma$  in P1 and P7 mouse retina.**

Tissues were co-immunostained with mouse anti-AP-2 $\alpha$  (red) and mouse anti-AP-2 $\gamma$  (green) antibodies. Tyramide signal amplification (TSA) with multiplex capability allowed co-detection of AP-2 $\alpha$  and AP-2 $\gamma$  (the procedure is explained in Materials and Methods). DAPI was used to stain the nuclei. Merged images show co-localization of AP-2 $\alpha$  and AP-2 $\gamma$  (yellow/orange; indicated by arrowheads). The insets show magnified views of the designated areas. DAPI was used to stain nuclei. Abbreviations: RPE, retinal pigmented epithelium; INL, inner nuclear layer; ONL, outer nuclear layer; INBL, inner neuroblastic layer; GCL, ganglion cell layer. Scale bars = 50  $\mu$ m.

In keeping with previously reported data on AP-2 expression in mouse retina<sup>134</sup>, there were clusters (e.g. cluster 6) with elevated levels of AP-2 $\alpha$ , AP-2 $\beta$  and AP-2 $\gamma$  sequences. As co-expression of AP-2 $\alpha$  and AP-2 $\gamma$  has not previously been reported in the literature, we tested this *in silico* finding by co-immunofluorescence analysis using anti-AP-2 $\gamma$  and AP-2 $\alpha$  antibodies. Our analysis revealed only a few AP-2 $\alpha$ /AP-2 $\gamma$  co-expressing cells in P1 mouse retina, with the number of AP-2 $\alpha$ /AP-2 $\gamma$ -co-expressing cells increasing at P7 compared to P1 (Figure 2.8). Notably, AP-2 $\gamma$ -positive cells located in the middle of the inner nuclear layer, presumably migrating amacrine cells, were exclusively negative for AP-2 $\alpha$  (Figure 2.8). The pattern of expression of AP-2 $\gamma$  compared to AP-2 $\alpha$  suggests that AP-2 $\gamma$  is expressed in migrating cells committed to the amacrine lineage as well as differentiated amacrine cells, and that AP-2 $\gamma$ -expressing amacrine cells differentiate later than AP-2 $\alpha$ -expressing amacrine cells. This interpretation of our results is in agreement with Drop-seq data showing amacrine clusters that were positive for AP-2 $\gamma$ , with no or very little AP-2 $\alpha$  or AP-2 $\beta$  (clusters 17 and 18). Thus, the Drop-seq data for the different members of the AP-2 family suggest overlapping expression patterns that are aligned with co-immunofluorescence data obtained by us and others.

### **2.3.5 AP-2 $\epsilon$ RNA is expressed in retinoblastoma cell lines**

We have previously shown that AP-2 $\alpha$  RNA is expressed in retinoblastoma cell lines<sup>146</sup>. However, retinoblastoma cells do not express AP-2 $\beta$  RNA<sup>146</sup>. To further investigate expression of amacrine lineage-specific AP-2s in retinoblastoma cells, we examined the expression of AP-2 $\gamma$  and AP-2 $\epsilon$  RNA in 13 retinoblastoma cell lines. Semi-

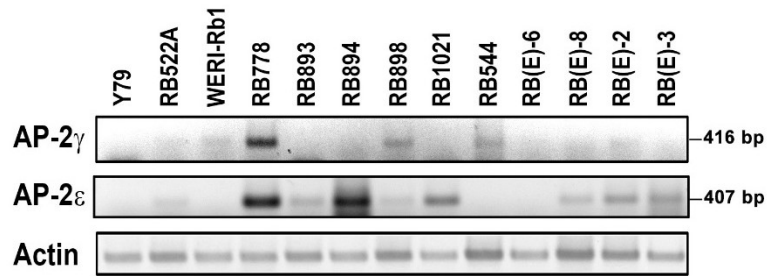


**Figure 2.9 Semi-quantitative RT-PCR showing expression of *AP-2 $\gamma$*  and *AP-2 $\epsilon$*  in RB cells.**

RT-PCR was carried out using cDNAs obtained from 13 RB cell lines. Sizes of RT-PCR products are indicated on the right. Actin was used as the loading control.

quantitative RT-PCR analysis revealed expression of *AP-2 $\gamma$*  and *AP-2 $\epsilon$*  in subsets of retinoblastoma lines (Figure 2.9). With the exception of RB778 cells which were positive for both *AP-2 $\gamma$*  and *AP-2 $\epsilon$* , there was a trend towards mutual exclusion for these two AP-2s. These results provide further support for a link between RB and amacrine cells and suggest that AP-2 expression patterns in retinoblastoma cell lines mimic developmentally-regulated amacrine cell differentiation patterns.

## 2.4 Discussion

Four members of the AP-2 family ( $\alpha$ ,  $\beta$ ,  $\gamma$  and  $\delta$ ) have previously been shown to be expressed in subsets of cells in the retina. In this study, we demonstrate that the fifth member of the AP-2 family, AP-2 $\epsilon$ , is also expressed in vertebrate retina. Like AP-2 $\alpha$ , AP-2 $\beta$  and AP-2 $\gamma$ , AP-2 $\epsilon$  is specifically expressed in a subset of amacrine cells. The AP-2 $\epsilon$  expression pattern is similar in chicken, mouse and human, although peak expression is observed at an earlier developmental stage in mouse (P1) compared to chicken (E10).

AP-2 $\epsilon$  has previously been shown to have a limited expression pattern during mouse embryogenesis compared to AP-2 $\alpha$ , AP-2 $\beta$  and AP-2 $\gamma$ . AP-2 $\epsilon$  is mainly expressed in developing brain and spinal cord in mouse, with highest levels in the olfactory bulb<sup>11</sup>. AP-2 $\epsilon$  is no longer detected in the olfactory bulb by P14<sup>11</sup>. AP-2 $\epsilon$ -knockout mice have an abnormal olfactory bulb architecture<sup>21</sup>, with defects in lamination of projection neurons and their associated axons. Surprisingly, AP-2 $\epsilon$ <sup>-/-</sup> mice can still sense odors, suggesting that other members of the AP-2 family may be compensating for loss of AP-2 $\epsilon$  in the olfactory bulb<sup>21</sup>.

The expression pattern of AP-2 $\epsilon$  in amacrine cells is more restricted than that of the other AP-2s. For example, both AP-2 $\alpha$  and AP-2 $\beta$  are widely distributed in amacrine cells, with AP-2 $\alpha$ /AP-2 $\beta$  co-expression observed in a high percentage of cells<sup>27</sup>. AP-2 $\gamma$  is primarily found in a subset of amacrine cells distinct from those expressing AP-2 $\alpha$  and AP-2 $\beta$  (AP-2 $\beta$ /AP-2 $\gamma$  co-localization is described in Bassett *et al.*<sup>26</sup>; AP-2 $\alpha$ /AP-2 $\gamma$  co-localization is shown in Figure 2.8). Although ocular abnormalities have not yet been reported for AP-2 $\epsilon$ <sup>-/-</sup> mice, this may be due to the relatively small number of cells expressing AP-2 $\epsilon$  in the retina. As a case in point, it was only upon detailed analysis of

the retina and visual centers of the brain that an ocular phenotype was identified in *AP-2 $\delta$*  knockout mice<sup>44</sup>. Furthermore, as described for *AP-2 $\alpha$*  and *AP-2 $\beta$* <sup>26</sup>, other members of the AP-2 family may compensate for loss of *AP-2 $\epsilon$*  expression.

Structurally, AP-2 proteins have a helix-span-helix dimerization domain at the carboxy terminal region preceded by a basic region. The helix-span-helix motif along with the central basic region constitute the DNA binding domain<sup>45,46</sup>. The DNA binding domain of *AP-2 $\epsilon$*  is evolutionary conserved and is highly similar to that of the other AP-2s suggesting that these transcription factors bind to similar AP-2 recognition elements. In agreement with this, *AP-2 $\epsilon$*  binds to the consensus AP-2 recognition element GCCNNNGGC as either a homodimer or heterodimer with other members of the AP-2 family<sup>47,48</sup>. The N-terminus contains the activation domain which is generally less conserved between different AP-2 proteins except for a proline-rich region found in all AP-2s except *AP-2 $\delta$* <sup>45-48</sup>. These similarities and differences in the structure of AP-2 proteins may affect protein-protein and protein-DNA interactions, thereby determining AP-2 target gene specificity. For example, *AP-2 $\alpha$* , *AP-2 $\beta$*  and *AP-2 $\gamma$*  can all bind as either homodimers or heterodimers to an AP-2 recognition site in the *c-erbB2* promoter; however, *AP-2 $\alpha$*  and *AP-2 $\gamma$*  are four times more active than *AP-2 $\beta$*  at activating a *c-erbB2*-driven reporter construct<sup>49</sup>. Considering that: (i) there are four members of the AP-2 family expressed in amacrine cells with distinct and overlapping patterns, (ii) AP-2 can function as either homodimers or heterodimers, and (iii) there are at least 33 amacrine subtypes in mammalian retina<sup>32,33</sup>, AP-2s could play key roles in the determination of amacrine subtype-specific functions in the retina.

Only a few genes have been identified as *AP-2 $\epsilon$*  target genes in mammals,

including *ITGA10* encoding integrin  $\alpha 10$  (important for chondrocyte differentiation)<sup>50</sup>, *COL2A1* (involved in modulation of cartilage development)<sup>51</sup>, *DKK4* (associated with resistance to chemotherapy in colon cancer)<sup>52</sup>, and *CDKNA1* encoding p21WAF1 (identified in neuroblastoma cells)<sup>53</sup>. The *Mmp13* gene has also been shown to be upregulated in adult *AP-2 $\epsilon$* <sup>-/-</sup> mice, although it's not known whether *Mmp13* is a direct target of AP-2 $\epsilon$ <sup>54</sup>. Similarly, *Xenopus* AP-2 $\epsilon$  activates neural crest-specific genes *Snail2* and *SOX10*<sup>55</sup>, and zebrafish AP-2 $\epsilon$  activates *kita* expression in melanophores and helps promote melanophore differentiation<sup>56</sup>. Additional putative AP-2 $\epsilon$  target genes come from cDNA microarray analysis of colorectal cancer cells that either express or don't express AP-2 $\epsilon$ <sup>52</sup>. Of the top 50 genes identified in this cDNA microarray, one was previously shown to be expressed in amacrine cells in chick retina: Tenascin C (*TNC*)<sup>57</sup>. Cluster analysis of Drop-seq data, dividing amacrine cells into 3 clusters [group 1 including clusters 5 and 9 (>30% AP-2 $\epsilon$ -positive cells), group 2 including clusters 8 and 15 (10-15% AP-2 $\epsilon$ -positive cells), group 3 including the remaining clusters with few or no AP-2 $\epsilon$ -positive cells], revealed no correlation with any of the putative AP-2 $\epsilon$  target genes mentioned above. A next step would be to compare gene expression in wild-type versus *AP-2 $\epsilon$* <sup>-/-</sup> retina in an attempt to identify AP-2 $\epsilon$  target genes.

Amacrine cells are broadly defined on the basis of the neurotransmitter that they use to transmit signal. There are two main categories of neurotransmitters in amacrine cells: GABAergic (GAT1 positive) and glycinergic (GLYT1 positive)<sup>40,41</sup>. GABAergic amacrine cells are further divided based on whether they express cholinergic (*VACHT* positive) or tachykinin (*Tac1* positive) neurotransmitters. AP-2 $\alpha$ , AP-2 $\beta$  and AP-2 $\gamma$  are found in both GABAergic and glycinergic amacrine cells. In contrast, AP-2 $\epsilon$  is exclusively

found in GABAergic amacrine cells, a result that is in agreement with the Drop-seq data<sup>42</sup>. Thus, AP-2 $\epsilon$  may play a specialized role in the regulation of genes involved in fate determination of GABAergic amacrine cells.

A previous study showed that AP-2 $\alpha$  RNA is expressed in retinoblastoma cells<sup>43</sup>. Transfection of either AP-2 $\alpha$  or AP-2 $\beta$  expression constructs in retinoblastoma cells induced apoptosis, suggesting incompatibility with expression of AP-2 amacrine cell differentiation markers and survival in retinoblastoma cells<sup>43</sup>. Our results demonstrating AP-2 $\gamma$  and AP-2 $\epsilon$  expression in retinoblastoma cells further support an amacrine cell lineage for retinoblastoma tumors. The trend towards mutual exclusion of AP-2 $\epsilon$  and AP-2 $\gamma$  RNAs in different retinoblastoma cell lines also supports the idea that retinoblastoma tumors are derived from different amacrine subtypes, in keeping with the low level of overlap between AP-2 $\epsilon$ - and AP-2 $\gamma$ -expressing amacrine cells at early stage of retinal differentiation in mouse.

In conclusion, we show that AP-2 $\epsilon$  is expressed in a subset of amacrine cells in developing vertebrate retina with peak expression at P1 in mouse and E10 in chick. AP-2 $\epsilon$  expression overlaps with the other three AP-2s previously shown to be expressed in amacrine cells, with extensive overlap with AP-2 $\alpha$  and AP-2 $\beta$  at all stages tested. Our immunostaining data are in agreement with previously reported sequencing data obtained from single amacrine retinal cells by Drop-seq. Expression of four AP-2s in amacrine cells suggests complex and cell-specific roles for this family of transcription factors in determining the identity and/or function of amacrine cell subtypes.

## **Chapter 3 Nuclear Factor I represses Notch effector HEY1 in glioblastoma**

### 3.1 Introduction

Glioblastomas (GBM) (or grade IV astrocytomas) are the most common brain tumours in adults<sup>62, 276</sup>. Despite aggressive treatment involving surgical resection, radiotherapy, and adjuvant chemotherapy with temozolomide, the median survival for GBM patients is approximately 15 months<sup>68, 277, 278</sup>. These tumours are highly infiltrative, resulting in high rates of recurrence and treatment failure<sup>279</sup>.

The Nuclear Factor I (NFI) family of transcription factors regulates the expression of the brain fatty acid-binding protein (*B-FABP* or *FABP7*) and glial fibrillary acidic protein (*GFAP*) genes in GBM<sup>181</sup>. The four members of the NFI family (NFIA, B, C and X) bind to the consensus NFI recognition element 5'-TTGGCA(N<sub>5</sub>)GCCAA-3' as homodimers or heterodimers<sup>176, 280, 281</sup>. The N-terminal DNA binding and dimerization domain of all 4 NFI family members is highly conserved; however, the C-terminal domain is more divergent, resulting in variation in transactivation potential<sup>282</sup>. NFIs can both activate or repress transcription, with regulation of transcription being dependent on both promoter context and type of cell or tissue in which the NFIs are expressed<sup>175</sup>.

NFI recognition sites are enriched in many brain-specific promoters<sup>283</sup> and NFIs are important regulators of gliogenesis and astrocyte differentiation in the developing central nervous system<sup>174, 198, 200</sup>. In particular, NFIA and NFIB are necessary for the onset of gliogenesis downstream of Notch signaling<sup>186, 200</sup>. Following glial fate specification, these two NFIs along with NFIX, further promote astrocyte differentiation<sup>174, 198, 199, 202, 208</sup>. *Nfia*<sup>-/-</sup>, *Nfib*<sup>-/-</sup> and *Nfix*<sup>-/-</sup> mice all display delayed neuronal and glial cell differentiation in the brain<sup>185, 188, 191-193, 284, 285</sup>.

Reduced *NFIA* mRNA levels are associated with high-grade astrocytomas, with 91%, 77%, 48% and 37% of cells expressing *NFIA* in grades I, II, III and IV astrocytomas,

respectively<sup>205, 206</sup>. NFIA is enriched in astrocytomas compared to other tumours, with fewer than 5% of cells expressing NFIA in oligodendrogliomas<sup>205</sup>. Furthermore, ectopic expression of NFIA in an oligodendroglioma model promotes conversion to an astrocytoma-like phenotype<sup>208</sup>. Low *NFIB* mRNA levels are also associated with high-grade astrocytomas, with elevated levels of *NFIB* RNA correlating with better overall and recurrence free survival in GBM<sup>209</sup>. *NFIB* overexpression induces cell differentiation and inhibits GBM tumour growth<sup>209</sup>.

To gain insight into the role of NFI in GBM, we carried out chromatin immunoprecipitation (ChIP)-on-chip using a pan-specific NFI antibody to immunoprecipitate NFIs bound to their target genes in U251 GBM cells. A total of 403 NFI target genes were identified, including *HEY1*, a Notch effector gene. Notch signaling has previously been implicated in regulation of tumour progression in GBM<sup>72, 286, 287</sup>. *HEY1* is a member of the Hairy/Enhancer of split (E/(spl) family of basic helix-loop-helix transcription factors and is important for maintenance of neural precursor cells downstream of Notch<sup>233</sup>. *HEY1* expression increases with increasing astrocytoma tumour grade and correlates with decreased overall survival and disease free survival<sup>254</sup>. Here, we show that NFI binds to three NFI recognition elements in the *HEY1* promoter and negatively regulates *HEY1* in GBM cells. Depletion of *HEY1* in adherent and neurosphere GBM cultures results in decreased cell proliferation and increased migration. These results suggest a fine balance between levels of NFI transcription factors and the Notch effector *HEY1* in GBM, thereby allowing these tumours to express some astrocytic properties while retaining neural stem cell characteristics.

## 3.2 Material and Methods

### 3.2.1 Cell lines, constructs, siRNAs, and transfections

The established human GBM cell lines used in this study have been previously described<sup>182, 288</sup>. Cells were cultured in Dulbecco's modification of Eagle's minimum essential medium (DMEM) supplemented with 10% fetal calf serum, penicillin (50 U/mL) and streptomycin (50 µg/mL). The primary GBM cultures (A4-004, A4-007, ED512) were prepared by enzymatic dissociation of GBM biopsies obtained with patient consent prior to surgery. A4-004 and A4-007 adherent lines were generated by culturing cells directly in DMEM supplemented with 10% fetal calf serum (defined throughout the chapter as "adherent"). GBM tumour neurosphere cultures were generated by plating cells directly in DMEM/F12, supplemented with B27, epidermal growth factor (EGF) and fibroblast growth factor (FGF) (defined throughout the chapter as "neurospheres" or "neurosphere conditions" or "neurosphere cultures"). Please note that A4-004 cells cultured in neurosphere medium grow as adherent cells unless plated in low attachment plates. All procedures involving tumour biopsies were approved by the Health Research Ethics Board of Alberta Cancer Committee Protocol #HREBA.CC-14-0070.

The pCH-NFI expression vectors pCH, pCH-NFIA, pCH-NFIB, pCH-NFIC and pCH-NFIX were obtained from Dr. R. Gronostajski (State University of New York at Buffalo). The luciferase reporter gene construct was prepared by inserting the 5' *HEY1* flanking DNA from -913 bp to +15 bp into the pGL3-Basic vector (Promega). Stealth siRNAs (Life Technologies) were used to knockdown NFIA, NFIB, NFIC, NFIX, and HEY1: NM\_005595\_stealth\_919 targeting 5'-GAAAGUUCUUCAUACUACAG-CAUGA-3'(NFIA); NM\_005596\_stealth\_1020 targeting 5'-AAGCCACAAUGA-

UCCUGCCAAGAAU-3' (NFIB); NM\_005597\_stealth\_1045 targeting 5'-CAGAGAU-GGACAAGUCACCAUUC-3' (NFIC); NM\_002501\_stealth\_752 targeting 5'-GAGAGUAUCACAGACUCCUGUUGCA-3' (NFI); NM\_012258.3\_stealth\_284 targeting 5'-UAGAGCCGAACUCAAGUUUCCAUUC-3' (HEY siRNA 1) and NM\_012258.3\_stealth\_652 targeting 5'-UUGAGAUGCGAAACCAGUCGAACUC-3' (HEY1 siRNA 2). Scrambled siRNAs (Cat. Nos. 12935-200 and 12935-300) were used as negative controls. The Stealth siRNAs selected for NFI knockdown have been previously characterized<sup>182</sup>.

U251 GBM cells were transfected with plasmid DNA constructs using polyethylenimine (PEI) (Polysciences Inc. For knockdown experiments, cells were transfected with 10 nM siRNAs using RNAiMAX-Lipofectamine (Life Technologies). For co-transfection experiments, cells were transfected first with siRNA, followed by plasmid transfection 24 h later. Cells were harvested 60 h after the last transfection. For 2X transfections with siRNAs, cells were transfected, grown to confluency, re-plated at 1/7 dilution, and transfected again.

### **3.2.2 Chromatin immunoprecipitation-on-chip (ChIP-on-chip) and ChIP-PCR**

Chromatin immunoprecipitation (ChIP) to isolate NFI-bound DNA was carried out following Agilent's mammalian ChIP-on-chip protocol version 10.0. Briefly,  $\sim 8 \times 10^8$  U251 GBM cells were crosslinked with 1% formaldehyde for 12 min at room temperature, followed by addition of glycine to 0.125 M to terminate the crosslinking reaction. After cell lysis, nuclei were sonicated 30 x 30 s at 30% output (model 300VT, Ultrasonic Homogenizer, BioLogics, Inc), and Triton X-100 added to a final concentration of 1%. Cellular debris was removed by centrifugation and 50  $\mu$ L of the lysate frozen at -20°C for

input DNA (non-enriched control). The remaining lysate was precleared with Protein-A Sepharose beads (GE Healthcare). The precleared lysate was incubated with 3  $\mu$ g anti-NFI antibody (N-20 Santa Cruz Biotechnology) and incubated at 4°C for 16 h. Protein-A Sepharose beads were added and incubated for 2 h at 4°C. Beads were washed 7X in wash buffer (50 mM Hepes-KOH, 500 mM LiCl, 1 mM EDTA, 1% Nonidet-P40, 0.7% sodium deoxycholate), and 1X in TE with 50 mM NaCl at 4°C. Protein-DNA complexes were eluted in elution buffer (50 mM Tris-HCl pH 8.0, 10 mM EDTA, 1% SDS) at 65°C for 15 min.

Linkers (5'-GCGGTGACCCGGGAGATCTGAATTC-3', and 5'-GAATTCAGATC-3') were prepared by annealing at 70°C for 1 min, and cooling slowly to 4°C. Input and ChIP DNAs were amplified by LM-PCR. PCR reactions containing input or ChIP DNAs, 1X Thermopol buffer (NEB), 250  $\mu$ M dNTPs, 1  $\mu$ M LM-PCR primer 5'-GCGGTGACCCGGGAGATCTGAATTC-3', and 0.25 U Taq polymerase were carried out as follows: 55°C/4 min, 72°C/3 min, 95°C/2 min, (95°C/30 s, 60°C/30 s, 72°C/1 min) X 15, 72°C/5 min. One hundredth of the resulting PCR products was used in a second round of PCR amplification as described above for 25 cycles. The PCR products were precipitated with ethanol, resuspended in sterile H<sub>2</sub>O, and diluted to 100 ng/ $\mu$ L.

Input and ChIP DNAs were fluorescently labeled with Agilent Genomic DNA Labeling Kit PLUS (Agilent Technologies). For each reaction, 2  $\mu$ g input or ChIP DNA were incubated with 5  $\mu$ L random primers, 1X buffer, 1X dNTPs, 3  $\mu$ L 1.0 mM Cyanine 3-dUTP (Cy3) (input DNA) or 3  $\mu$ L 1.0 mM Cyanine 5-dUTP (Cy5) (ChIP DNA), and 1  $\mu$ L Exo-Klenow DNA polymerase fragment in a final volume of 50  $\mu$ L, and incubated at 37°C for 2 h, followed by 10 min incubation at 65°C to inactivate the enzyme. For hybridization,

5  $\mu$ g Cy3-labeled DNA, 5  $\mu$ g Cy5-labeled DNA, 50  $\mu$ g Human Cot1, 1X Agilent blocking agent, and 1X Agilent hybridization buffer per slide were heated for 3 min at 95°C, followed by incubation at 37°C for 30 min, then applied to the Agilent Human Promoter 1 ChIP-on-chip 244K 014706 and 014797 (Agilent Technologies) in duplicate (4 slides total). Slides were hybridized with shaking (20 RPM) in a hybridization oven at 65°C for 40 h. The slides were then washed 1X with Oligo aCGH/ChIP-on-chip wash buffer (Agilent Technologies) at room temperature and 1X with Oligo aCGH/ChIP-on-chip wash buffer at 31°C. Slides were scanned on a GenePix 4000B scanner, and data extracted using Agilent Feature Extraction Software (Agilent Technologies). Data were analyzed using Agilent Genomic Workbench (Agilent Technologies).

ChIP-PCR analysis was carried out as previously described<sup>289</sup>. Briefly, U251 cells crosslinked with 1% formaldehyde were resuspended in lysis buffer and sonicated to shear the DNA. Pre-cleared lysates were incubated with either 2  $\mu$ g IgG or 2  $\mu$ g anti-NFI antibody (N-20 Santa Cruz Biotechnology), followed by incubation with Protein A-Sepharose beads. Protein-DNA complexes were eluted and the DNA was amplified using primers flanking putative NFI binding sites located upstream of the *HEY1* transcription start site (+1). Primer sequences flanking the -488 to -216 bp region contained two putative NFI binding sites, at -332 to -317 bp and -411 to -396 bp and primers flanking the -822 to -628 bp region contained one putative NFI binding site, at -794 to -779 bp. The *GAPDH* promoter was used as the negative control. Input DNA was obtained from cells lysed after the sonication step.

### 3.2.3 Electrophoretic mobility shift assay (EMSA)

EMSAs were carried out as previously described<sup>290</sup>. Putative NFI binding sequences in the *HEY1* promoter are listed in Figure 3.1A. Complementary oligonucleotides (Figure 3.2B) were annealed and radiolabeled by Klenow polymerase in the presence of  $\alpha^{32}\text{P}$ -deoxycytidine triphosphate. Oligonucleotides containing mutated NFI binding sites were generated by substituting AA for the conserved GG at positions 3 and 4 of the NFI consensus binding site (Figure 3.2A). Nuclear extracts were prepared from untransfected U251 GBM cells as described previously<sup>291</sup>, and nuclear extracts from U251 GBM cells transfected with pCH, pCH-NFIA, pCH-NFIB, pCH-NFIC, and pCH-NFIX were prepared using the Thermo Scientific NE-PER Nuclear and Cytoplasmic Extraction Kit (Life Technologies). Nuclear extracts (3  $\mu\text{g}$  for untransfected U251 GBM cells, 2  $\mu\text{g}$  for pCH-transfected cells, 3  $\mu\text{g}$  for pCH-NFIA-transfected cells, 4  $\mu\text{g}$  for pCH-NFIB-transfected cells, 1  $\mu\text{g}$  for pCH-NFIC-transfected cells, and 2  $\mu\text{g}$  for pCH-NFIX-transfected cells) were preincubated in binding buffer (20 mM Hepes pH 7.9, 20 mM KCl, 1 mM spermidine, 10 mM dithiothreitol, 10% glycerol, 0.1% Nonidet P-40) in the presence of 1.25  $\mu\text{g}$  poly(dI-dC) for 10 min at room temperature. Where indicated, a 100X molar excess of competitor oligonucleotide was included during preincubation. Radiolabeled oligonucleotides were added to the reaction mixture and incubated 20 min at room temperature. For supershift experiments, 1  $\mu\text{L}$  anti-NFI antibody (a gift from Dr. N. Tanese, New York University Medical Center), 1  $\mu\text{L}$  anti-AP-2 antibody (negative control) (Santa Cruz Biotechnology) or 1  $\mu\text{L}$  anti-Pax6 (negative control) (Developmental Studies Hybridoma Bank) was added with the radiolabeled oligonucleotides. DNA-protein

complexes were electrophoresed in 6% native polyacrylamide gels in 0.5X TBE buffer, and exposed to film.

### 3.2.4 **Western blot analysis**

Nuclear extracts were prepared using Thermo-Scientific NE-PER Nuclear and Cytoplasmic Extraction Kit (Life Technologies). Protein extracts were electrophoresed in 8% polyacrylamide-SDS gel and transferred to PVDF (polyvinylidene fluoride) membrane. The membrane was immunostained with mouse anti-HA antibody (Sigma) (1:10 000) and rabbit anti-DDX1 antibody (1:5000)<sup>292</sup>. Primary antibodies were detected with horseradish-peroxidase-conjugated secondary antibodies (Jackson ImmunoResearch Biotech) using Immobilon (EMD Millipore).

### 3.2.5 **Quantitative real time-PCR (qPCR)**

Total RNA was isolated from GBM cells using the RNeasy Plus Kit (Qiagen), and cDNA synthesized with Superscript II reverse transcriptase (Life Technologies). qPCR was carried out using an ABI 7900HT Fast Real-Time PCR System, with gene-specific oligonucleotides labeled at the 5' end with the fluorescent reporter dye FAM (NFIA, Hs00325656\_m1; NFIB, Hs00232149\_m1; NFIC, Hs00907819\_m1; NFIX, Hs00958849\_m1; GFAP, Hs00157674\_m1; B-FABP, Hs00361426\_m1; NES, Hs04187831\_g1; HEY1, Hs01114113\_m1; GAPDH, Hs99999905\_m1) and Taqman Fast Master Mix (Life Technologies). All samples were assayed in triplicate, and gene expression normalized to *GAPDH*.

### 3.2.6 **Reporter gene assay**

U251 GBM cells were cultured in 12-well cell culture plates. Following transfection, cells were harvested in 250  $\mu$ L of 1X Luciferase Cell Culture Lysis Buffer (Promega) and stored at  $-80^{\circ}\text{C}$ . Luciferase activity was measured in 20  $\mu$ L aliquots of lysate following automatic injection of 100  $\mu$ L of Luciferase Assay Reagent (Promega) using a FLUOstar Optima microplate reader (BMG Labtech).

### 3.2.7 **Cell proliferation assay**

U251 GBM cells cultured under standard conditions (DMEM supplemented with 10% FCS) and A4-004 GBM cells cultured under neurosphere conditions were transfected with scrambled or HEY1 siRNAs. Forth-eight hours later, transfected cells were seeded in triplicate (30,000 cells per well) in a 12-well plate. Cell growth was measured by counting the cells in triplicate wells every 24 h for a period of 96 h using a Coulter Particle and Size Analyzer (Coulter Corporation). Cell counts in the triplicate wells were averaged and plotted on a semi-log graph.

### 3.2.8 **Scratch assay**

U251 and A4-004 cells were cultured and transfected with either scrambled or HEY1 siRNAs as described for the cell proliferation assay. Cells were seeded in triplicate in 12-well plates 48 h post-transfection. Cells were allowed to form a monolayer, at which time a scratch was made in the center of the wells using a P20 pipette tip. Cells were cultured for an additional 24 h (A4-004) or 30 h (U251). Digital imaging microscopy (Axiovert 200M, Zeiss) was used to image the cells at 2 separate positions in each well using a phase contrast lens at 10X magnification (6 positions in total for triplicate wells). Metamorph imaging software (Version 7.8.8.0, Molecular Devices) was used to capture

a total of 97 images at each position at 15-minute intervals over a period of 24 h or 30 h. TScratch software was used to analyze the images. The percentage open area of the scratch at different time points was measured. The open area of each scratch at 0 h was normalized to 100% to nullify the effects of minor differences of the scratch size in different wells. The open area at subsequent time points is represented relative to their respective 0 h time point.

### **3.2.9 Transwell migration assay**

U251 and A4-004 cells were cultured and transfected with either scrambled or HEY1 siRNAs as described for the cell proliferation assay. Directional cell migration was measured using the Transwell cell migration assay. Twenty-five thousand cells in DMEM medium containing 1% fetal calf serum were seeded in the top chambers of 24-well cell culture Transwell inserts (Falcon™ Cell Culture Inserts). Cells were allowed to migrate through an 8µm polyethylene terephthalate (PET) membrane towards a chemoattractant (DMEM+10% fetal calf serum) in the bottom chamber for 20 h. Cells were then fixed with 100% cold methanol for 20 minutes and stained with 1% crystal violet in 20% methanol for 30 minutes at room temperature. Migrated cells were imaged using a Zeiss Axioskop2 plus microscope by capturing different fields of view. Cell counting was carried out using Meta express imaging software.

### **3.2.10 Neurosphere formation assay**

Either 200 or 1000 cells were seeded in triplicate in a 24-well low attachment plate (Corning). Cells were allowed to form spheres for a period of 10 days. Digital imaging microscopy (Axiovert 200M, Zeiss) was used to image the spheres using a phase contrast

lens at 5X magnification. Total area of all the spheres in each well was calculated for each treatment using Meta express imaging software.

### **3.2.11 Statistical analysis**

ChIP-on-chip results from 2 arrays were analyzed using ChIP analytics software (Agilent Technologies). Identification of putative NFI targets was based on the following parameters: enriched binding to NFI (compared to IgG control) based on a cutoff of Log<sub>2</sub> ratio >0.86 (enrichment of 1.8X) ( $p < 0.01$ ). All other experiments were done in triplicate (technical replicated) and were repeated three times (biological replicates). The data shown in the graphs is a summary of all three independent experiments unless otherwise stated. The statistical significance between two treatments was calculated using an unpaired t-test.

### 3.3 Results

#### 3.3.2 Chromatin immunoprecipitation (ChIP)-on-chip of NFI binding regions in GBM cells

To identify NFI target genes in GBM cells, U251 cells were treated with 1% formaldehyde to crosslink DNA to proteins. Cell lysates were prepared and sonicated to shear the DNA into fragments of ~500 bp. A pan-specific NFI antibody was used to pull down NFIs bound to DNA. This NFI-bound DNA was hybridized to two Agilent Human Promoter 1 arrays (Agilent Technologies) containing probes from -5.5 kb upstream to +2.5 kb downstream from the transcription start site of ~17,000 RefSeq genes. The data were analyzed with ChIP Analytics software (Agilent Technologies) resulting in the identification of 403 genes with enriched NFI binding based on a cut-off of log (2) ratio >0.85 (enrichment of >1.8 fold) (p<0.01) (Table 3.1). The list includes previously identified NFI target genes including *GFAP*<sup>182, 201, 293</sup>, *CDKN1A*<sup>206, 294</sup>, and *NEFL* (neurofilament light)<sup>283</sup>.

Gene ontology (GO) enrichment analysis (GO biological process complete annotation data set, 27,378 terms) of NFI putative target genes revealed enrichment in several developmental processes, including system development, organ morphogenesis, differentiation, and specifically cardiovascular, skeletal, and neuronal development<sup>295, 296</sup>. NFI target genes were also enriched in the category of genes involved in regulation of gene expression, both positive and negative, and transcription from RNA pol II promoters, suggesting that NFI itself may regulate other transcription factors. In addition, GO enrichment analysis using the PANTHER GO-slim Biological Process annotation data

set, which contains 257 biological process terms, clearly highlights enrichment in development, specifically nervous system development (Table 3.2)<sup>297</sup>.

**Table 3.1 Putative NFI target genes identified by ChIP-on-chip**

Gene	Chr	Start	Location	Log Ratio 1	Log Ratio 2
A2M	12	9113245	Inside	2.3449	2.13
ABCD3	1	94655702	Promoter	0.8391	0.8578
ABL1	9	132699679	Promoter	1.9824	2.8428
ABLIM1	10	116434625	Promoter		1.2935
ACTA2	10	90700226	Inside	1.2636	1.5899
ADAM12	10	128065860	Inside	1.3293	1.0154
ADIPOR2	12	1669620	Promoter	1.6344	1.0305
AKAP12	6	151604981	Inside	1.0677	0.5923
AP3S2	15	88238623	Promoter	2.3766	4.452
AP4S1	14	30605761	Inside	4.1749	2.6825
ARAP2	4	35922189	Inside	0.883	0.9511
ARFGEF2	20	46973980	Inside	1.0145	1.6826
ARID3A	19	873094	Promoter	1.3973	2.8587
ARID5A	2	96561634	Promoter	1.3574	1.4605
ARNTL2	12	27378226	Inside	2.9563	1.4642
ASPH	8	62788839	Inside	1.3963	0.9914
ASXL1	20	30408852	Promoter	1.8043	1.819
AZI2	3	28365132	Inside	0.8752	0.9516
B3GAT2	6	71723193	Inside	0.5558	1.0723
BARD1	2	215383130	Promoter	0.8541	0.8832
BARX1	9	95757258	Inside	0.9012	0.9674
BBS4	15	70766186	Inside	0.9716	0.883
BCOR	X	39844258	Promoter	1.123	0.9873
BHLHE40	3	4997058	Inside	1.9107	1.9376
BIVM	13	102250488	Inside	1.5475	1.7952
BMPR1A	10	88623573	Inside	2.0163	1.427
BOK	2	242146996	Inside	2.8644	
C12orf50	12	86945053	Inside		1.3029
C14orf93	14	22548858	Inside	2.1231	0.6826
C4orf46	4	159811801	Inside	0.8529	0.795
C6orf226	6	42966730	Promoter	0.9194	0.8339
C6orf48	6	31902882	Promoter	2.9354	1.9704
CAB39L	13	48871772	Inside		2.7623
CALD1	7	134221728	Promoter	1.043	0.8438
CALU	7	128168470	Inside	1.0949	1.0157
CAMK1	3	9787282	Promoter	0.7474	1.2159
CAPS2	12	74070664	Inside	1.5286	0.6155
CASD1	7	93978527	Inside	0.9683	0.7883
CAST	5	96080515	Inside	0.7114	0.86
CBLN3	14	23964730	Downstream	2.1749	1.75

Gene	Chr	Start	Location	Log Ratio 1	Log Ratio 2
CCBE1	18	55519524	Promoter	1.0248	1.228
CCDC150	2	197212889	Inside	1.0609	0.7303
CCDC18	1	93417823	Promoter	1.6742	2.8547
CCDC63	12	109767259	Promoter	1.3922	2.3241
CCDC89	11	85075244	Promoter	0.7093	0.9903
CCL2	17	29605928	Promoter	1.4862	1.5466
CCM2	7	45005877	Promoter	0.8848	0.8779
CCNA1	13	35900528	Promoter	2.7599	5.2676
CCNL1	3	158360010	Inside	0.9441	0.8409
CCNT2	2	135393397	Inside	0.931	0.7432
CCNYL1	2	208284923	Inside	0.9386	0.7282
CCRN4L	4	140156163	Promoter	0.9815	1.0638
CCT4	2	61968894	Inside	1.0762	1.4236
CD274	9	5440826	Inside	1.3285	2.3594
CD55	1	205561713	Inside	0.8691	0.8141
CDH26	20	58001523	Promoter	1.9592	0.7257
CDK1	10	62209644	Promoter	1.8754	0.6561
CDKL1	14	49936425	Promoter	1.1446	1.6956
CDKN1A	6	36756502	Inside	0.881	0.6717
CDR2	16	22291327	Inside	2.3448	2.1586
CEP170-SDCCAG8	1	241485512	Divergent promoter	1.941	2.2168
CEP85	1	26474887	Inside	0.8501	0.6725
CHL1	3	215054	Inside	0.9341	0.9227
CHST12	7	2406240	Promoter	1.479	1.446
CLEC18C	17	3238495	Inside	0.7295	1.1596
CLEC2D	12	9714034	Inside	3.1749	
CNNM3	2	96845754	Inside	0.8178	0.8617
COL12A1	6	75970048	Inside	0.7777	1.3099
COQ4	9	130124836	Inside	5.9865	
CORO1C	12	107647973	Inside	1.3954	0.9799
CSF1R	5	149472454	Inside	1.5463	1.2047
CSRP3	11	19178852	Inside	1.6173	1.7579
CTGF	6	132317596	Promoter	1.1817	0.9029
CTHRC1	8	104453722	Inside	1.5791	1.3662
CTNNA1	5	138118093	Inside	1.1389	1.0538
CTNND2	5	11957555	Promoter	1.0407	0.9424
CTR9	11	10728883	Promoter		2.6155
CUL1	7	148026670	Promoter	0.8901	0.9048
CXCL9	4	77152060	Promoter	0.9205	0.9392
CXXC5	5	139008561	Promoter	0.9512	0.9865
CYBRD1	2	172087903	Inside	0.8191	0.9964

Gene	Chr	Start	Location	Log Ratio 1	Log Ratio 2
DALRD3	3	49030738	Inside	0.7058	0.8781
DCAF6	1	166173189	Inside	1.3486	0.5098
DCBLD2	3	100107833	Promoter	1.4793	1.5552
DDB2	11	47194632	Inside	0.9606	1.1489
DEFB118	20	29420503	Inside		2.867
DEPTOR	8	120955481	Inside	1.1023	0.8643
DLAT	11	111398703	Promoter	1.7599	3.5086
DNAH5	5	13998104	Promoter	1.0857	0.9746
DNAJB6	7	156824418	Inside	1.5893	1.8169
DNMBP	10	101727078	Promoter		1.9456
DTWD1	15	47700817	Inside		1.9236
DUSP14	17	32922698	Promoter	1.0192	1.0282
DUSP22	6	236964	Promoter	1.0673	1.414
DYRK3	1	204876002	Inside	1.046	1.1218
E2F5	8	86320350	Downstream	1.5241	1.2968
EFCAB2	1	243201339	Inside	1.4662	1.2058
EIF4A2	3	187983486	Promoter	1.0448	1.5373
ELL3	15	41856955	Promoter	4.2047	1.9385
EMP1	12	13237614	Promoter	1.2064	1.9012
ENAH	1	223910311	Promoter	1.1427	1.0571
ENO1	1	8862939	Promoter		3.1611
EPAS1	2	46380123	Inside	0.6408	0.9732
EPB41L3	18	5538249	Promoter		2.1301
ERLIN2	8	37713231	Promoter	4.0235	1.1796
ERRFI1	1	8008978	Promoter	0.7638	0.883
ETV1	7	13998960	Promoter	2.4876	2.8207
F12	5	176763982	Inside	1.4547	1.3798
FAM133A	X	92820651	Inside	2.1749	1.3386
FAM150B	2	278156	Inside	1.0176	1.0877
FAM160A2	11	6210731	Inside	1.3302	2.3487
FAM184A	6	119442219	Promoter	2.467	
FAM198B	4	159310123	Inside	1.6559	0.8468
FAM212B	1	112084649	Promoter	1.2915	1.2984
FAM26D	6	116986039	Inside	0.9273	1.1093
FAM43B	1	20752757	Inside	0.7069	0.903
FAM46A	6	82518382	Inside	0.7327	0.9501
FAM5C	1	188714347	Promoter	1.1799	1.1724
FAM63B	15	56850025	Promoter	1.4249	1.9441
FAM76B	11	95160902	Inside		3.3524
FAM83D	20	36989268	Inside	2.068	1.3931
FAS	10	90738240	Promoter	1.4337	0.8922

Gene	Chr	Start	Location	Log Ratio 1	Log Ratio 2
FBXL5	4	15265780	Inside	0.8179	0.8869
FGF9	13	21143410	Promoter	0.6079	1.0686
FLJ38984	1	35956513	Inside	1.2656	1.0383
FNTA	8	43030356	Promoter	0.9929	0.9401
FOXJ2	12	8073435	Promoter	1.6774	2.2678
FZD7	2	202605768	Promoter	1.1294	1.2073
GABPB2	15	48434824	Promoter	0.8781	1.1448
GALNT7	4	174327101	Inside	1.2428	1.0712
GBE1	3	81892929	Inside	0.9443	0.7074
GBP5	1	89509960	Inside	0.8174	0.9367
GCLM	1	94146101	Inside	1.7484	1.9013
GFAP	17	40348396	Promoter	1.471	1.6689
GGNBP2	17	31972190	Promoter		2.1301
GIN1	5	102483328	Inside	1.096	1.3189
GLI3	7	42232735	Inside	2.2832	
GLIPR1	12	74158401	Promoter		1.1139
GLIPR2	9	36122089	Promoter	1.08	1.0909
GNAI3	1	109892505	Promoter	0.9276	1.1387
GORAB	1	168768031	Inside	0.9291	0.6116
GPCPD1	20	5541103	Promoter	1.4644	1.9307
GSX2	4	54660676	Promoter	2.0596	2.6342
GUK1	1	226394685	Inside	0.9175	0.8924
HBP1	7	106596263	Promoter	1.3612	1.1513
HDGF	1	154987886	Inside	0.9429	0.9364
HELZ	17	62669404	Inside	0.9055	0.6826
HEXIM1	17	40581111	Inside	1.853	1.046
HEY1	8	80843258	Promoter	0.9866	0.9256
HIST1H2BJ	6	27207844	Downstream	2.6994	3.298
HMG20A	15	75499939	Promoter	0.7708	1.1065
HNRPDL	4	83569798	Inside	0.5667	0.9533
HSF2BP	21	43901045	Inside	1.512	1.3931
ICMT-HES3	1	6224841	Divergent promoter	1.006	1.0496
ID3	1	23757574	Inside	1.883	
IER5L	9	130979866	Inside	0.8672	0.7791
IFIT1	10	91140690	Promoter	1.8876	3.3931
IFRD2	3	50304903	Promoter	0.9265	
IFT88	13	20039819	Inside	6.0329	4.6661
IL1RAPL2	X	103790321	Inside		2.8081
INA	10	105023095	Promoter	0.847	0.8954
ING2	4	184663304	Inside	1.0897	1.0266

Gene	Chr	Start	Location	Log Ratio 1	Log Ratio 2
INTS12-GSTCD	4	106849357	Divergent promoter	1.1416	
IRF2BP2	1	232814979	Promoter	1.7022	1.6503
IRS2	13	109242223	Promoter	0.7599	1.1618
ITGBL1	13	100900982	Promoter	0.9854	0.6561
JAG1	20	10600976	Inside	1.465	1.4926
KANK1	9	494998	Inside	1.0107	0.9323
KCNH2	7	150286133	Promoter	1.0967	1.0681
KCNK10	14	87863177	Promoter	2.2983	1.3151
KCTD13	16	29843124	Inside		3.5086
KDM3A	2	86521682	Promoter	2.1711	
KIF18A	11	28085526	Inside	1.8057	2.6826
KLF9	9	72217435	Inside	0.9515	0.7306
KLRF1	12	9873240	Inside	2.6344	
KRT10	17	36236502	Promoter	1.0267	0.9381
KRT13	17	36914588	Inside	0.9703	1.1909
KRT37	17	36838500	Promoter	0.9259	1.04876
KRTAP19-5	21	30797152	Promoter		1.7821
KRTAP23-1	21	30643668	Promoter	1.2097	5.5985
KRTAP4-2	17	36591407	Promoter	1.3448	
KTN1	14	55115205	Promoter	0.7037	0.9873
L3MBTL4	18	6299434	Inside	1.9317	2.5895
LARP6	15	68931809	Inside	0.9787	0.9348
LEMD3	12	63849245	Promoter	1.1687	1.2232
LHX1	17	32363515	Promoter	1.2987	1.4615
LIN7B	19	54305925	Promoter	1.3844	1.0712
LINC00173	12	115456450	Inside		3.715
LIX1L	1	144189562	Inside	3.1479	1.7586
LMBR1	7	156378711	Promoter	1.1167	0.8903
LNX2	13	27091478	Inside	0.863	1.0914
LOXL2	8	23321325	Promoter	1.6795	1.5987
LPGAT1	1	210070651	Inside	0.9113	0.6642
LRIG3	12	57601195	Promoter	3.0818	0.6312
LRP11	6	150226326	Inside	0.844	0.9151
LUC7L3	17	46153029	Inside	0.7599	2.0008
LYST	1	234113659	Promoter	1.0678	1.0687
MAB21L1	13	34949195	Promoter	2.0246	1.4995
MAGEB3	X	30165456	Inside	Infinity	1.2676
MARCKS	6	114287069	Inside	0.8813	1.4392
MBNL1	3	153499615	Promoter	1.281	0.8607

Gene	Chr	Start	Location	Log Ratio 1	Log Ratio 2
MCU	10	74123406	Inside	1.7932	1.8959
MED20	6	41996698	Inside	2.6175	0.8524
MEF2C	5	88213383	Inside	1.1965	1.7183
MEIS2	15	35179607	Promoter		1.4909
METAP2	12	94393160	Inside	0.9339	1.5737
METTL23	17	72234989	Inside	1.3492	1.2214
METTL7A	12	49604807	Inside	3.6344	4.9723
MGP	12	14930159	Promoter	1.2727	1.3211
MGST1	12	16393324	Promoter	1.3499	1.657
MIR125B2	21	16880927	Promoter	1.0955	2.452
MIR149	2	241040806	Promoter	0.8737	0.8394
MIR181A1	1	197094961	Promoter	0.8738	1.2512
MIR205	1	207673444	Downstream	1.1632	0.8121
MIR216A	2	56073153	Promoter	1.0836	0.9672
MIR548B	6	119441594	Promoter	1.1045	1.6763
MIR99A	21	16828801	Promoter	1.0363	1.1253
MIRLET7I	12	61287764	Downstream		1.13
MPPED2	11	30558664	Promoter	2.5534	1.408
MPZL3	11	117628311	Promoter	1.0034	1.0256
MRPL1	4	78999542	Promoter	1.094	0.9655
MTFMT	15	63113497	Promoter		2.0176
MTPN	7	135312739	Promoter	0.7316	1.1827
MUTYH	1	45578374	Promoter	0.7639	1.1403
NAA50	3	114947510	Inside	1.187	0.9951
NARG2	15	58556607	Inside	1.7599	
NCAM2	21	21287395	Promoter	2.5672	1.6706
NCAPH	2	96360052	Promoter	0.9675	0.9379
NDUFA4	7	10946379	Promoter	1.1701	1.2548
NEDD4	15	53997292	Promoter	1.1285	1.9057
NEFL	8	24875334	Promoter	1.1197	1.0298
NEK6	9	126061540	Inside	1.0058	2.3111
NFIA	1	61318395	Promoter	1.7578	1.5734
NHS	X	17662326	Inside		3.666
NPR3	5	32821654	Inside	0.8681	0.7434
NR2F1	5	92944603	Promoter	1.724	1.6766
NRXN3	14	78185282	Inside		3.8956
NSUN4	1	46578948	Promoter	0.3593	2.1549
NUP153	6	17815540	Promoter	1.3413	1.339
NUSAP1	15	39412952	Inside	0.7062	0.9863
OR4K5	14	19457562	Promoter	1.1584	0.5645
OR5B2	11	57949404	Promoter		2.2411

Gene	Chr	Start	Location	Log Ratio 1	Log Ratio 2
OR8K1	11	55867174	Promoter	4.2624	0.7744
OSGIN2	8	90983730	Inside	0.9755	0.8275
OSMR	5	38881767	Promoter	2.2867	3.6053
OSTM1	6	108502607	Inside	0.8983	0.7542
OTOF	2	26639471	Promoter	1.4405	1.4627
PAICS	4	56996755	Promoter	1.4424	1.3502
PAK3	X	110253345	Inside		2.5086
PAN2-IL23A	12	55014286	Divergent Promoter	1.1135	2.978
PAPSS2	10	89407139	Promoter	1.3973	
PARPBP	12	101114267	Inside	0.8564	0.7389
PCDH11Y	Y	4982161	Promoter	1.4969	3.5086
PCDH20	13	60887639	Promoter	2.0018	2.5372
PCDHGC3	5	140835207	Promoter	0.5412	1.0438
PCYOX1L	5	148717764	Promoter	0.806	0.8943
PDCD5	19	37764645	Inside	1.5551	0.984
PDE1C	7	32075349	Inside	0.9477	1.213
PHEX	X	21961908	Inside	1.3092	0.8861
PHIP	6	79844705	Promoter	0.8298	0.9198
PHKB	16	46056443	Inside	Infinity	3.7467
PHKG2	16	30662879	Promoter	1.9475	0.5451
PIGW	17	31968591	Inside	2.4229	1.6237
PLA2G6	22	36907952	Promoter	0.8237	1.0237
PLAG1-CHCHD7	8	57286601	Divergent promoter	1.0339	1.0007
PLEKHA1	10	124125339	Inside		3.2676
PLEKHF2	8	96215015	Promoter	0.8497	0.8805
PLEKHG7	12	91650086	Promoter	1.4745	2.1036
PLSCR4	3	147451761	Promoter	1.4499	1.3556
PLXND1	3	130807793	Inside	1.2362	1.2639
PMCH	12	101114699	Inside	1.8754	1.9236
POLR2M	15	55786150	Promoter	1.376	1.4702
POP7	7	100142485	Inside	1.163	1.2064
PPIB	15	62247347	Promoter	0.7599	1.2588
PPM1D	17	56033871	Inside	0.9405	0.957
PPRC1	10	103882474	Promoter	1.5316	1.893
PREP	6	105957405	Inside	0.8652	0.9023
PRKCZ	1	1971786	Inside	1.0996	1.2305
PRR11	17	54598116	Inside	1.1638	1.1606
PSMD5	9	122645227	Promoter		1.752
PTCH1	9	97309577	Promoter	4.667	2.5832
PTHLH	12	28012193	Inside	1.916	4.3931

Gene	Chr	Start	Location	Log Ratio 1	Log Ratio 2
PVRL3	3	112273071	Promoter	1.1668	0.8705
QKI	6	163755950	Inside	0.8161	0.9088
QSOX1	1	178387365	Promoter	1.3136	1.2724
RAB13	1	152225381	Inside	0.8856	0.5711
RAB27A	15	53369884	Promoter	1.8754	1.7257
RAB32	6	146906540	Inside	0.9266	0.9193
RAB3GAP2	1	218512608	Promoter	1.6686	2.1385
RAB4A	1	227472130	Promoter	1.5611	1.1593
RARB	3	25444505	Promoter	1.5131	1.1602
RASL10B	17	31077950	Promoter	1.4961	1.5103
RBM8A	1	144219300	Inside	0.8511	0.6152
RCBTB1	13	49058882	Promoter	2.005	1.715
RGS12	4	3341510	Inside	1.1184	0.9916
RNF219	13	78131510	Promoter	2.0182	1.1107
RNF43	17	53850241	Promoter	1.3202	1.1636
RPA3	7	7725436	Promoter	0.9336	1.1595
RPL35- ARPC5L	9	126671430	Inside	0.8536	0.7386
RPL7- RDH10	8	74368863	Divergent promoter	2.142	
RPS14	5	149809356	Inside	0.9447	0.7391
RPS26P25	12	54722045	Promoter	2.0229	1.2747
RPS6KA5	14	90594136	Inside	0.8299	1.1171
RUNX1	21	35187762	Promoter		1.8081
RXRA	9	136466823	Inside	1.4666	1.1116
S100A10	1	150234089	Promoter	1.7226	1.3661
S100A2	1	151805208	Promoter	0.7175	0.8918
SAAL1	11	18084458	Promoter	0.9111	0.8292
SALL1	16	49742667	Promoter	0.8851	0.9548
SAP30BP	17	71176036	Inside	0.7296	0.9472
SATB2	2	200028516	Inside	1.4823	1.1501
SEC22B	1	143804069	Promoter	1.8402	1.6841
SEC63	6	108386153	Promoter	1.2092	0.8009
SEMA3C	7	80384831	Inside	2.0581	2.2209
SENP2	3	186784484	Promoter	0.8401	0.8536
SERPINA12	14	94054227	Promoter	0.9043	1.0203
SERPINE1	7	100556642	Promoter	1.281	1.0997
SERPINE2	2	224615283	Promoter	1.7994	1.8375
SFR1	10	105867828	Promoter	1.5961	1.5375
SGPP2	2	222997476	Promoter	0.832	0.8975
SH3GLB1	1	86942572	Promoter	1.0742	0.7759
SLC1A3	5	36641944	Promoter	1.9592	1.9216

Gene	Chr	Start	Location	Log Ratio 1	Log Ratio 2
SLC25A24	1	108544889	Promoter	1.2235	1.0073
SLC25A38	3	39400641	Inside	0.9268	0.6487
SLC2A8	9	129199290	Inside	0.8095	0.9206
SLC34A2	4	25266397	Promoter	0.6397	0.9394
SLC35A1	6	88234292	Promoter	0.9993	0.9899
SLC39A1	1	152202903	Inside	1.2398	1.2455
SLC4A2	7	150388856	Inside	1.2223	1.12
SNAP91	6	84475571	Promoter	0.6865	0.8948
SNORD61	X	135789798	Promoter	0.9994	0.923
SNX18	5	53847891	Promoter	1.4868	1.8669
SOS2	14	49766863	Inside	1.2745	1.2881
SOX21	13	94164394	Promoter	1.4906	1.6101
SPATA31E1	9	89683959	Promoter	3.3902	1.7178
SPATA7	14	87918342	Promoter	0.9405	1.5419
SREBF2	22	40558801	Promoter	1.0166	1.0877
SRRT	7	100310524	Promoter	1.2548	1.0389
ST5	11	8884780	Inside		2.8081
STAMPB	2	73911856	Inside	1.2324	1.2124
STC1	8	23767712	Inside	1.7308	1.8818
SWAP70	11	9643126	Inside	1.2258	1.3621
SYTL2	11	85114675	Promoter	2.3124	0.5451
TANK	2	161700020	Promoter	1.8117	1.5764
TBC1D4	13	74958764	Promoter	2.1749	1.1077
TBC1D9	4	141897691	Promoter	1.3521	1.2753
TCF12	15	55295998	Promoter	Infinity	2.0305
TEKT2	1	36322390	Inside	1.2207	0.8003
TGFB1	5	135392598	Inside	0.9168	0.7522
TGFB2	1	216585830	Promoter	0.8472	0.8786
TIA1	2	70328493	Inside	1.2478	1.2808
TIPARP	3	157875103	Inside	0.9606	0.9971
TLE3	15	68180782	Promoter	1.4118	1.5755
TLN2	15	60727365	Inside		3.5086
TMEM106B	7	12218056	Inside	1.4318	1.2735
TMEM117	12	42517112	Inside	2.4969	0.8081
TMEM165	4	55957822	Inside	0.8309	1.5276
TMEM18	2	667475	Promoter	0.8736	1.0234
TMEM5	12	62458480	Promoter	1.0193	1.5086
TMEM68	8	56848373	Inside	1.4128	1.0885
TNC	9	116920425	Promoter	1.0671	1.1067
TNK2	3	197108216	Promoter	1.424	1.4345
TNRC6B	22	38769059	Promoter	Infinity	1.8849

Gene	Chr	Start	Location	Log Ratio 1	Log Ratio 2
TOP2B	3	25681044	Promoter	1.091	1.1184
TPM1	15	61130006	Inside	1.3379	1.0357
TRAPPC6B	14	38706756	Inside	3.8188	
TRIM24	7	137796161	Inside	0.9419	0.8926
TRIM27	6	28999877	Promoter	0.4587	1.0425
TRIM39	6	30401356	Promoter	0.9795	0.7046
TRIM68	11	4588395	Promoter	0.8437	1.978
TRIM7	5	180566074	Promoter	1.2226	1.5655
TRMT13	1	100371465	Inside	1.2459	0.872
TRMT5	14	60514612	Inside	2.1618	
TSC22D1	13	43908581	Inside	1.3124	1.8273
TSHZ1	18	71054967	Inside	1.1078	1.7696
TSPAN1	1	46421794	Inside	1.6963	0.4872
UBP1	3	33456791	Promoter		0.9941
UBQLNL	11	5494712	Promoter	3.8188	
UBTF	17	39656567	Promoter	2.232	2.261
UGT1A6	2	234263596	Promoter	1.0837	0.68
UPP1	7	48091159	Promoter	1.8999	1.868
UTRN	6	144650122	Promoter	1.6635	1.4185
UTS2D	3	192483245	Promoter	0.7589	1.1478
VWCE	11	60821797	Promoter	1.0582	1.1159
WAC	10	28862027	Promoter	0.9559	0.9373
WBSCR17	7	70232063	Promoter	1.4624	1.4046
WHSC1	4	1842782	Promoter	1.0058	0.7851
WNT2B	1	112810639	Promoter	1.2258	0.6594
WNT5A	3	55500570	Promoter	0.9735	0.7655
WNT9A	1	226202113	Inside	1.1542	1.2018
ZBTB8OS- RBBP4	1	32889059	Divergent promoter	1.1693	0.9177
ZFAND3	6	37894564	Promoter	1.2631	1.2166
ZIM2	19	62044765	Promoter		1.37
ZKSCAN8	6	28212586	Promoter	1.8771	1.3735
ZMYND11	10	171940	Inside	0.8085	0.8826
ZMYND8	20	45422915	Promoter	0.9489	1.1383
ZNF24	18	31179965	Promoter	1.3257	0.7557
ZNF426	19	9510687	Promoter	0.7344	0.9575
ZNF615	19	57201227	Inside	1.3593	0.8723
ZNF703	8	37668165	Promoter	1.2573	1.3695
ZNF706	8	102287188	Promoter	0.8385	0.8897
ZNF76	6	35335395	Promoter	2.258	2.4167

**Table 3.2 PANTHER enrichment analysis of putative NFI target genes identified by ChIP-on-chip.**

<b>Gene Ontology Term</b>	<b>Sample Frequency</b>	<b>Expected Frequency</b>	<b>Fold Enrichment</b>	<b>P value</b>
<b>developmental process</b>	85	49.6	1.71	9.02E-05
<b>cellular process</b>	144	103.73	1.39	9.56E-04
<b>regulation of biological process</b>	65	37.91	1.71	2.75E-03
<b>system development</b>	51	28.67	1.78	1.07E-02
<b>biological regulation</b>	84	56.68	1.48	2.55E-02
<b>nervous system development</b>	34	17.57	1.94	4.70E-02

### 3.3.3 NFI binds to the HEY1 promoter in vivo

Of the 403 putative NFI binding regions identified by ChIP-on-chip, 221 were in the promoter regions of genes. One of the putative NFI target genes, *HEY1*, was of particular interest because of its role as a Notch effector gene<sup>215</sup>. *HEY1* has previously been shown to be important for maintenance of neural precursor cells<sup>233</sup> and is highly expressed in GBM tumours compared to normal brain<sup>254</sup>.

ChIP analysis showed enriched binding of NFI to a microchip probe corresponding to the region upstream of the *HEY1* transcription start site. Sequence analysis of the *HEY1* promoter region from -1100 bp to +1 revealed four putative NFI binding sites, located at -32 to -17 bp, -332 to -317 bp, -411 to -396 bp and -794 to -779 bp (Figure 3.1A). Of note, the region spanning -30 to -247 bp upstream of the mouse *Hey1* transcription start site has previously been reported to be essential for basal *Hey1* transcription, with additional regulatory sequences located between -247 to -647 bp in mouse (with -647 bp corresponding to -680 bp in human)<sup>222</sup>.

To confirm the ChIP-on-chip results, we carried out ChIP analysis in U251 GBM cells using primers corresponding to two regions of the *HEY1* promoter: -216 to -488 bp containing two putative NFI binding sites and -628 to -822 bp containing one putative NFI binding site. DNA cross-linked to NFI in U251 cells was immunoprecipitated with a pan-specific NFI antibody and amplified by PCR. Rabbit IgG and primers to the *GAPDH* promoter were used as negative controls for the ChIP experiments. Bands corresponding to the *HEY1* promoter between -488 to -216 bp, and -822 to -628 bp, were clearly detected and enriched following immunoprecipitation with an NFI antibody compared to rabbit IgG

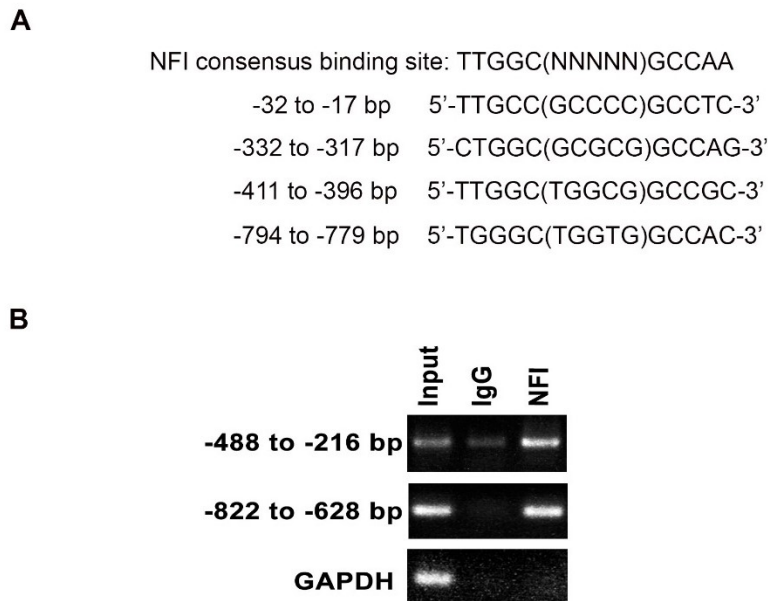


**Figure 3.1 NFI binds to the *HEY1* promoter *in vivo*.**

**(A)** Location of consensus NFI binding sites, and putative NFI binding sequences identified upstream of the *HEY1* transcription start site (+1). **(B)** Chromatin immunoprecipitation analysis showing NFI binding to the *HEY1* promoter. DNA crosslinked to protein in U251 cells was immunoprecipitated with a pan-specific NFI antibody followed by PCR amplification. Rabbit IgG antibody and GAPDH primers were used as negative controls.

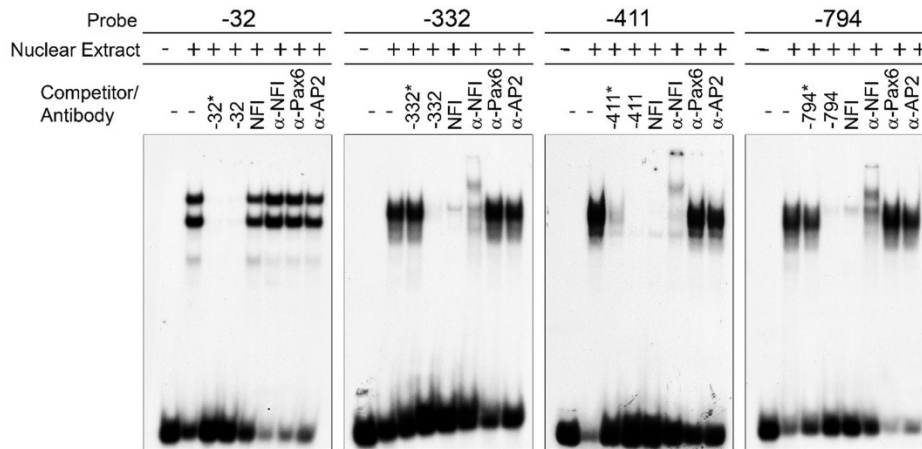
(Figure 3.1B). No bands were detected in either the IgG or NFI IP lanes when primers to the *GAPDH* promoter were used.

#### **3.3.4 NFI binds to NFI recognition sequences in the *HEY1* promoter**

We used the electrophoretic mobility shift assay (EMSA) to examine NFI binding to the four putative NFI recognition sites (at -32 bp, -332 bp, -411 bp and -794 bp) located upstream of the *HEY* gene. Double-stranded oligonucleotides (Figure 3.2A) corresponding to each putative recognition site were radiolabeled and incubated with nuclear extracts prepared from U251 GBM cells. To address specificity of binding, a 100X fold molar excess of unlabeled oligonucleotides was used as a competitor. Competitor oligonucleotides included wild-type -32 bp, -332 bp, -411 bp, -794 bp, and mutated -32\* bp, -332\* bp, -411\* bp, -794\* bp NFI recognition sites, and the NFI consensus recognition site (Figure 3.2A).

**A**

Probes				Competitors			
-32	5'	CTG GAG <b>TTG CCG CCC CGC CTC TC</b>	3'	-32*	5'	CTG GAG <b>Taa CCG CCC CGC CTC TC</b>	3'
	3'	<b>C AAC GGC GGG GCGGAG AGG C</b>	5'		3'	<b>C Att GGC GGG GCG GAG AGG C</b>	5'
-332	5'	CGG CCC <b>TGG CGC GCG GCC AGG C</b>	3'	-332*	5'	CGG CCC <b>Taa CGC GCG GCC AGG C</b>	3'
	3'	<b>GG ACC GCG CGC CGG TCC G GTTA</b>	5'		3'	<b>GG Att GCG CGC CGG TCC G GTTA</b>	5'
-411	5'	CCG GAT <b>TGG CTG GCG GCC GCG</b>	3'	-411*	5'	CCG GAT <b>Taa CTG GCG GCC GCG</b>	3'
	3'	<b>CTA ACC GAC CGC CGG CGC CGC G</b>	5'		3'	<b>CTA Att GAC CGC CGG CGC CGC G</b>	5'
-794	5'	GCC CCT <b>GGG CTG GTG GCC A</b>	3'	-794*	5'	GCC CCT <b>aaG CTG GTG GCC A</b>	3'
	3'	<b>GGA CCC GAC CAC CGG TGA CAC</b>	5'		3'	<b>GGA ttC GAC CAC CGG TGA CAC</b>	5'
				NFI	5'	ATT TTG GCT TGA AGC CAA TAT G	3'
					3'	TAA AAC CGA ACT TCG GTT ATAC	5'

**B**

**Figure 3.2 Binding of NFI to putative NFI binding sequences in the *HEY1* promoter.**

**(A)** Primers used to generate oligonucleotides for the electrophoretic mobility shift assay, with putative NFI binding sequences in bold. The third and fourth residues in the NFI binding sequences were mutated from GG→AA. These residues are critical for NFI binding. **(B)** Electrophoretic mobility shift assays were carried out by incubating radiolabeled probes -32 bp, -332 bp, -411 bp, and -794 bp, with 3  $\mu$ g U251 GBM nuclear extracts. DNA-protein complexes were electrophoresed through a 6% polyacrylamide gel buffered in 0.5X TBE. Where indicated, a 100X molar excess of competitors (\* denotes mutated NFI binding site) were added to the binding reaction. Where indicated, antibodies (1  $\mu$ L) to NFI ( $\alpha$ -NFI), Pax6 ( $\alpha$ -Pax6) or AP-2 ( $\alpha$ -AP-2) were added immediately before the radiolabeled probes.

Two strong and one weak DNA-protein complexes were observed when the -32 bp probe was incubated with nuclear extracts from U251 GBM cells, and one major DNA-protein complex was observed upon incubation of these nuclear extracts with the -332 bp, -411 bp, and -794 bp probes (Figure 3.2B). Incubation with excess mutated -32\* bp oligonucleotide (two key NFI binding residues mutated) resulted in complete loss of shifted bands, indicating that the DNA-protein complexes observed with the -32 bp probe do not involve NFI binding. These data are further supported by the inability of excess NFI consensus binding site oligonucleotide to serve as competitor for the three DNA-protein complexes observed with the -32 bp probe.

In contrast to the -32 bp probe, addition of excess wild-type competitor oligonucleotides abolished binding to the -332 bp, -411 bp and -794 bp probes, while addition of excess NFI consensus oligonucleotide significantly reduced the signal intensity of the DNA-protein complexes (Figure 3.2B). Addition of excess -332\* bp oligonucleotide did not significantly affect binding to the radiolabeled -332 bp probe, whereas addition of excess -411\* bp and -794\* bp oligonucleotides resulted in significant and slight reductions in binding, respectively.

To determine if the observed DNA-protein complexes contain NFI, we incubated the radiolabeled probes with nuclear extracts from U251 GBM cells and an anti-NFI antibody that has previously been shown to supershift NFI-DNA complexes<sup>181, 182</sup>. Addition of the anti-NFI antibody resulted in a supershifted band for the -332 bp, -411 bp and -794 bp probes, but not the -32 bp probe (Figure 3.2B). The relatively weak intensity of the supershifted bands observed with the anti-NFI antibody, combined with the significant decrease in intensity of the DNA-protein complexes, suggests that the anti-NFI

antibody impedes binding of NFI to these probes. Anti-Pax6 and anti-AP-2 antibodies had no effect on the protein-DNA complexes regardless of the probe used.

As there are four NFIs, we next asked whether specific members of the NFI family can preferentially bind to the NFI recognition motifs upstream of the *HEY1* transcription start site. To do this experiment, U251 GBM cells were transfected with pCH (empty vector), HA-tagged NFIA, HA-NFIB, HA-NFIC, or HA-NFIX expression constructs. Nuclear extracts were prepared, and expression of NFIs analyzed by western blot. NFIC levels were the highest in the transfected cells, followed by NFIX, NFIA and NFIB (Figure 3.3A). To correct for differences in expression levels, we incubated 1  $\mu$ g of NFIC nuclear extract, 2  $\mu$ g NFIX nuclear extract, 3  $\mu$ g NFIA nuclear extract, and 4  $\mu$ g of NFIB nuclear extract with radiolabeled -32 bp, -332 bp, -411 bp, and -794 bp oligonucleotides. As expected, no DNA-protein complexes were observed with the -32 bp oligonucleotide, indicating that NFIs do not binding to this region.

NFIA, NFIB, NFIC, and NFIX all formed complexes with the -332 bp, -411 bp, and -794 bp oligonucleotides (Figure 3.3B). Bands of similar intensities were observed when nuclear extracts prepared from each of the four HA-NFI transfected cells were incubated with the -332 bp probe. Similar results were obtained with the -794 bp probe except that band intensities were reduced in the NFIA and NFIB lanes compared to NFIC and NFIX (Figure 3.3B). In contrast, the only nuclear extract that generated a strong signal when incubated with the -411 bp probe was from HA-NFIX-transfected cells, with only weak bands observed with HA-NFIA and HA-NFIB-transfected cells. Taken together, these results indicate that all four NFIs can bind, albeit with different affinities, to the -332 bp, -411 bp and -794 bp probes, with NFIA and NFIB showing a relative preference for the –

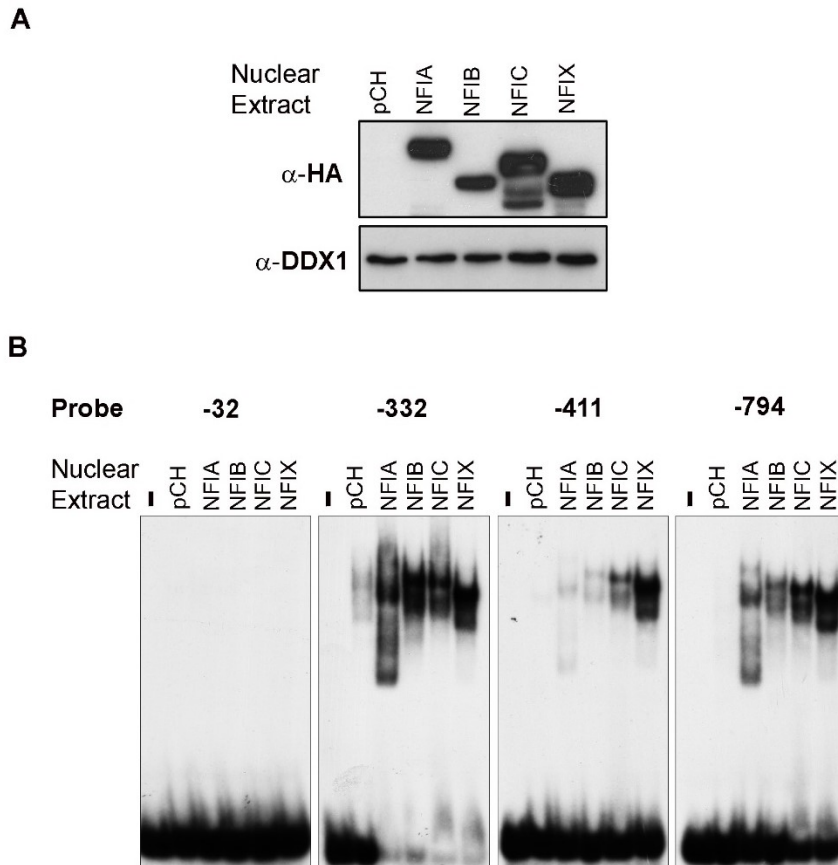


**Figure 3.3 Binding of NFIA, NFIB, NFIC, and NFIX to NF1 binding sites in the *HEY1* promoter.**

Nuclear extracts were prepared from U251 GBM cells transfected with control (pCH), NFIA (pCH-NFIA), NFIB (pCH-NFIB), NFIC (pCH-NFIC), or NFIX (pCH-NFIX) expression constructs. **(A)** Western blot analysis of transfected cells. Nuclear extracts (20  $\mu$ g) were electrophoresed through an 8% polyacrylamide-SDS gel, electroblotted onto PVDF (polyvinylidene fluoride) membranes, and immunostained with  $\alpha$ -HA antibody or  $\alpha$ -DDX1 antibody. **(B)** Electrophoretic mobility shift assays were performed with the indicated radiolabeled probes: -32 bp, -332 bp, -411 bp and -794 bp. Probes were incubated with the indicated nuclear extracts (2  $\mu$ g pCH, 3  $\mu$ g NFIA, 4  $\mu$ g NFIB, 1  $\mu$ g NFIC, and 2  $\mu$ g NFIX). Amounts of protein were adjusted to compensate for differences in expression of transfected HA-NFIs. DNA-protein complexes were electrophoresed through a 6% polyacrylamide gel buffered in 0.5X TBE.

332 bp probe, NFIX showing no preference for any of the three probes and NFIC showing preference for the -332 bp and -794 bp probes.

### **3.3.5 NFI represses HEY1 expression and promoter activity**

Our combined CHIP and gel shift experiments indicate that NFIs bind to three distinct regions in the *HEY1* promoter, suggesting a role for NFIs in the regulation of *HEY1* expression. We therefore examined whether changes in NFI levels can affect endogenous *HEY1* mRNA levels. U251 GBM cells were transfected with control (scrambled) siRNAs, or siRNAs targeting specific NFIs, alone or in combination. Previously validated NFI siRNAs<sup>182</sup> were used for these analyses, resulting in 75-93% decreases in *NFIA*, *NFIB*, *NFIC*, and *NFIX* mRNA levels after one round of transfection (Figure 3.4A). Endogenous levels of *HEY1* mRNA were not significantly altered upon knockdown of single NFIs; however, when all four NFIs were depleted, we observed a 2.4-fold increase in *HEY1* mRNA levels (Figure 3.4B – top panel). Two rounds of NFI siRNA transfections resulted in an even greater increase (4.6-fold) in *HEY1* mRNA levels (Figure 3.4B – bottom panel). These data suggest that multiple members of the NFI family are involved in *HEY1* regulation, with NFIs repressing *HEY1* promoter activity.

Next, we used the luciferase reporter gene under the control of the *HEY1* promoter to investigate the effect of NFI on transcriptional activity. U251 GBM cells were transfected with siRNAs to knockdown single NFIs or a combination of all four NFIs, followed by transfection with the pGL3/*HEY1* construct containing -915 to +15 bp of the *HEY1* promoter upstream of the firefly luciferase reporter gene. Knockdown of *NFIA* did not affect *HEY1* transcriptional activity based on the luciferase assay (Figure 3.4C). However, transcriptional activity was significantly increased following knockdown

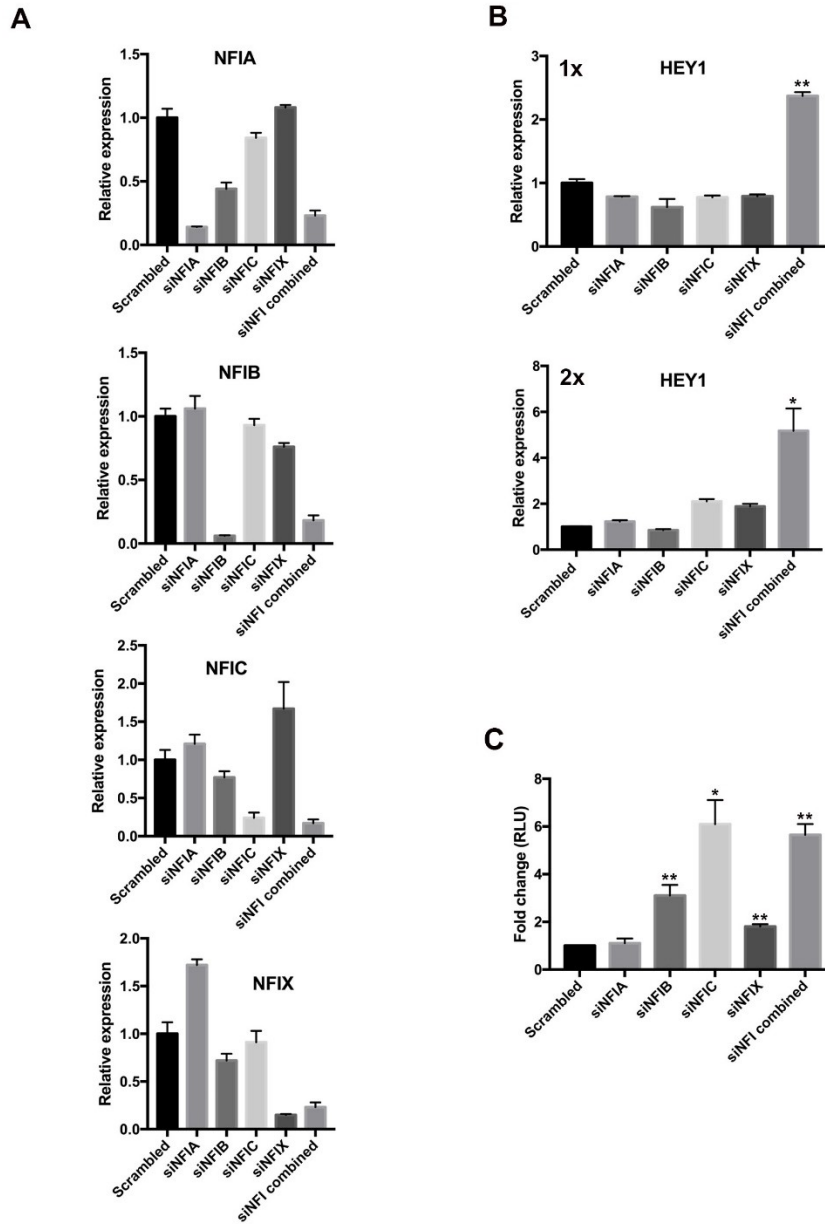


**Figure 3.4 Regulation of *HEY1* promoter activity by NFI.**

U251 GBM cells were transfected with 10 nM siRNAs, including control (scrambled), NFIA, NFIB, NFIC, NFIX, or combinations of NFI siRNAs. Where indicated (2x), cells underwent two rounds of siRNA transfection. (a) *NFIA*, *NFIB*, *NFIC*, *NFIX* and (b) *HEY1* mRNA expression was analyzed by qPCR. GAPDH was used as an endogenous control. Similar data were obtained in two separate experiments. (c) U251 GBM cells were transfected with 10 nM siRNAs, including control (scrambled), NFIA, NFIB, NFIC, NFIX, or combinations of NFI siRNAs, followed 24 h later by transfection with pGL3/*HEY1*. Cells were harvested 60 h later, and luciferase activity quantified. Changes in RLU (relative light units) are relative to RLU obtained in U251 GBM cells transfected with control (scrambled) siRNA and pGL3/*HEY1*. The data are from three experiments. SEM is indicated by error bars. Statistical significance, determined using the unpaired t-test, is indicated by \* ( $p < 0.05$ ) and \*\* ( $p < 0.01$ ).

of NFIB (3.1-fold), NFIC (6.1-fold) and NFIX (1.6-fold), suggesting that these three NFIs repress transcription from the *HEY1* promoter. Knockdown of all four NFIs increased transcriptional activity 5.6-fold compared to control (scrambled) siRNA. As the biggest increase in *HEY1* transcriptional activity was observed upon NFIC knockdown, with a similar effect seen upon knockdown of all four NFIs, these results suggest that NFIC is a key player in the repression of *HEY1* promoter activity, at least in the context of an extrachromosomal plasmid reporter gene assay. The combinatorial effect of NFIs on endogenous *HEY1* mRNA levels (Figure 3.4B) clearly indicate that multiple members of the NFI family are involved in endogenous *HEY1* regulation.

### **3.3.6 *HEY1* expression in GBM cells**

*HEY1* expression has previously been reported in the developing central nervous system and in GBM tumours<sup>233, 254</sup>. We carried out quantitative PCR analysis to measure relative *HEY1* mRNA levels in a panel of standard GBM cell lines (adherent; cultured in medium containing fetal calf serum), as well as GBM patient-derived adherent cell lines (cultured in medium containing fetal calf serum) and tumour neurosphere cultures (serum-free; medium supplemented with growth factors) (Figures 3.5A, B). Overall, there was a trend towards lower *HEY1* RNA levels in cell lines that expressed low levels of the neural stem cell marker, B-FABP<sup>210, 298-300</sup> (Figure 3.5A). High *HEY1* RNA levels were observed in all three GBM tumour neurosphere cell lines tested (A4-004, A4-007 and ED512) (Figure 3.5A). When we compared adherent cultures and tumour neurosphere cultures derived from the same patient, we observed considerably higher levels of *HEY1* RNA in the neurosphere cultures, in keeping with

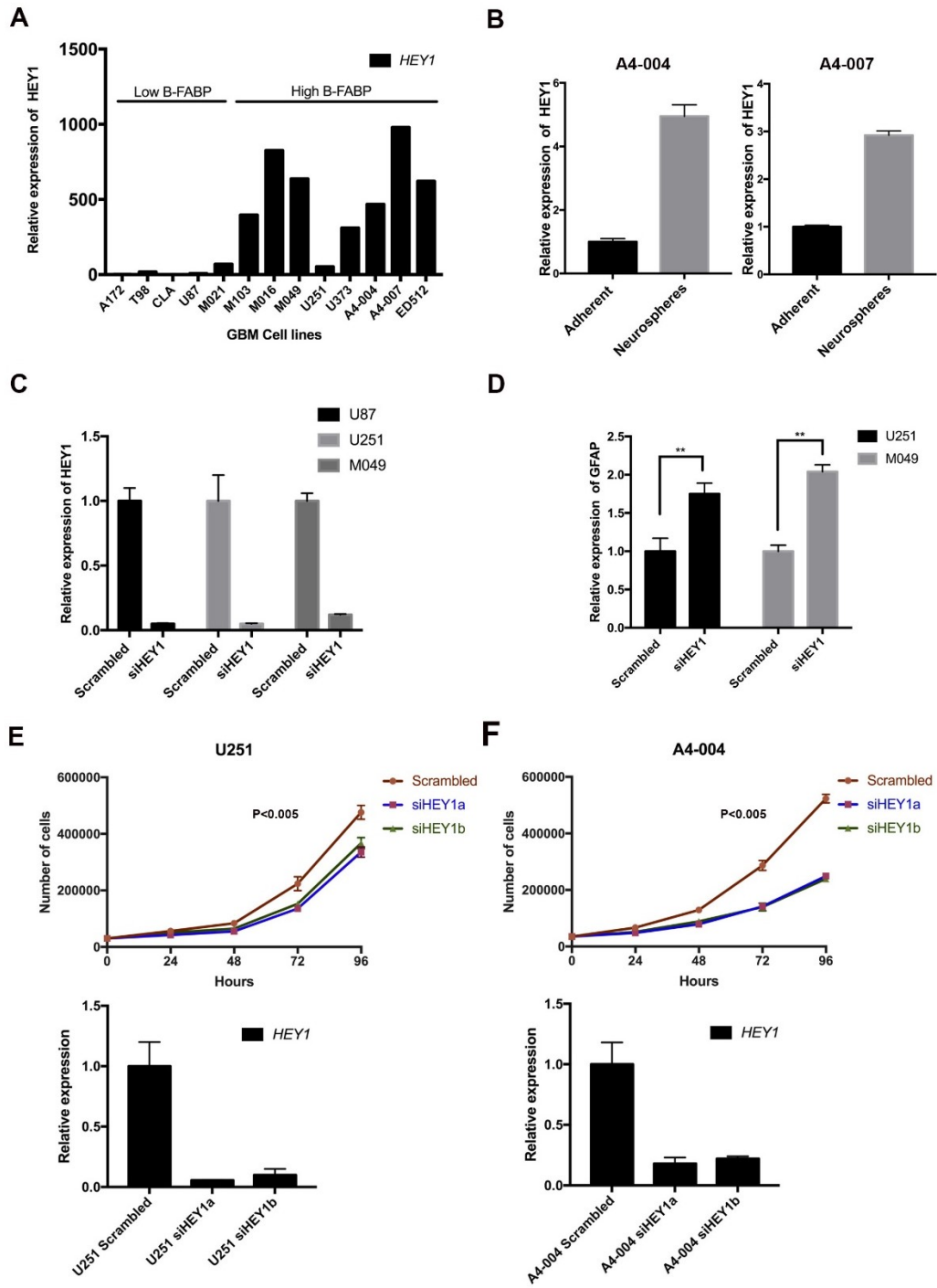


**Figure 3.5 HEY1 expression and effect of HEY1 knockdown on GFAP RNA levels and cell proliferation.**

**(A)** qPCR analysis showing *HEY1* mRNA levels in a panel of standard (adherent) and patient-derived GBM cell lines. The first five cell lines have no or low B-FABP expression and the rest of the cell lines express high levels of B-FABP. **(B)** qPCR analysis showing *HEY1* mRNA levels in A4-004 and A4-007 GBM cells cultured under standard (adherent) or neurosphere culture conditions. **(C, D)** U87, U251 and M049 GBM cells were transfected with 10 nM control (scrambled) siRNA, or siRNA targeting *HEY1*, and harvested 60 h later. Relative *HEY1* (C) and *GFAP* (D) mRNA levels were measured by qPCR. GAPDH served as an endogenous control. RNA levels are expressed as fold-change normalized to scrambled control. Similar data were obtained in a duplicate experiment. **(E, F)** U251 GBM and A4-004 (neurosphere) cells were transfected with either scrambled siRNA or siRNAs targeting *HEY1* (siHEY1a or siHEY1b). Cell proliferation was measured by counting cells every 24 h for a period of 96 h using a Coulter counter. Thirty thousand cells per well were seeded in triplicate. qRT-PCR was used to measure the efficiency of HEY1 knockdown. Experiments were repeated 3 times for each cell line. The unpaired t-test was used to measure statistical significance.

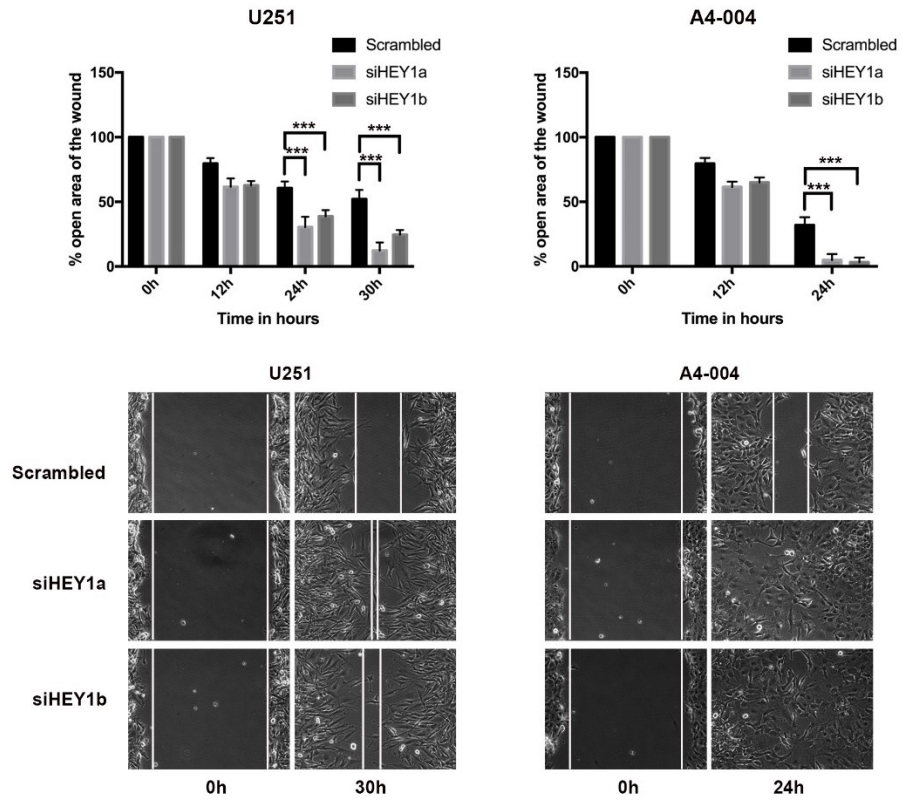
HEY1 being more highly expressed in tumour cells with neural stem cell properties (Figure 3.5B).

In the developing brain, HEY1 is required for the maintenance of neural precursor cells<sup>233</sup> whereas NFIA is required for initiation of gliogenesis and astrocyte differentiation<sup>198, 199</sup>. To address a possible role for HEY1 in the prevention of astrocyte differentiation, we transfected HEY1 siRNAs into three GBM cell lines: U87 (very low levels of *HEY1*; does not express astrocyte differentiation marker GFAP), U251 (low levels of *HEY1*; expresses GFAP) and M049 (high levels of HEY1; expresses GFAP). *HEY1* RNA levels were decreased by 85 to 94% in cells transfected with *HEY1* siRNA compared to control (scrambled) siRNA (Figure 3.5C). HEY1 knockdown had no effect on *GFAP* RNA levels in U87 cells, indicating that HEY1 depletion is not sufficient to induce *GFAP* expression in cells that don't express endogenous GFAP. However, there was a ~2X increase in *GFAP* RNA levels in U251 (1.8-fold) and M049 (2-fold) GBM cells (Figure 3.5D). These results suggest a role for HEY1 in the maintenance of neural stem cell properties that may involve inhibition of astrocyte differentiation.

### **3.3.7 *HEY1* depletion decreases cell proliferation and increases cell migration in GBM**

We transfected U251 GBM cells and A4-004 neurosphere cultures with *HEY1* siRNAs to examine the effect of HEY1 knockdown on cell proliferation and migration. Both *HEY1* siRNAs used for these experiments decreased *HEY1* RNA levels by >90% (U251)

**A**



**B**

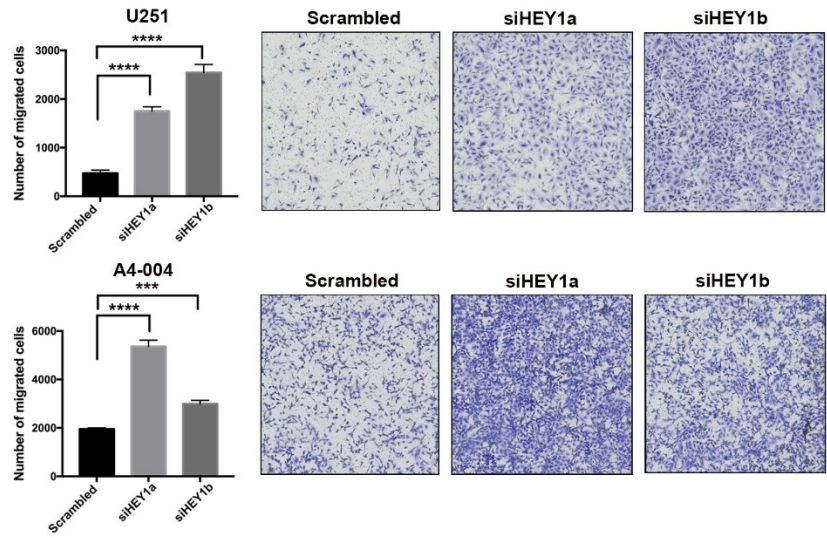
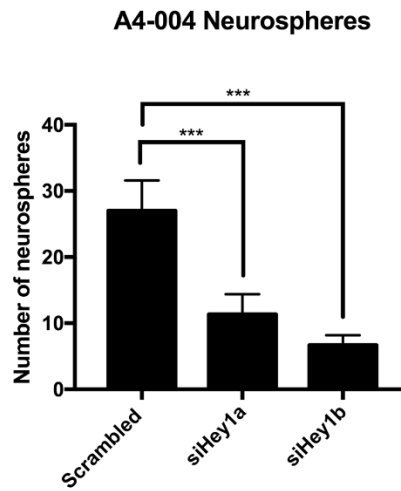


### Figure 3.6 HEY1 knockdown results in increased cell migration.

**(A)** U251 GBM and A4-004 (neurosphere) cells were transfected with either scrambled siRNAs or siRNAs against *HEY1* (siHEY1a or siHEY1b) and allowed to reach confluency. A scratch was made in the center of each well and cells were allowed to migrate over a period of 30 h (U251) or 24 h (A4-004) with live cell monitoring. Graphs represent percentage open area of the wound (scratch). Each experiment was carried out in triplicate with data obtained from 6 different positions for each time point. Experiments were repeated 3 times and the unpaired t-test was used to measure statistical significance. Images shown represent 0 h and 30 h (U251) or 24 h (A4-004) time points. **(B)** Transwell cell migration assay showing increased cell migration upon HEY1 knockdown. Twenty-five thousand cells were seeded in the upper chamber and allowed to migrate across a PET membrane towards medium containing 10% FCS over a period of 24 h. Migrated cells were fixed, stained and counted using Metamorph imaging software. The data shown in the graphs represent an average of two independent experiments. The unpaired t-test was used to measure statistical significance. \*\*\* represents  $p < 0.001$ ; \*\*\*\* represents  $p < 0.0001$ .

A



B

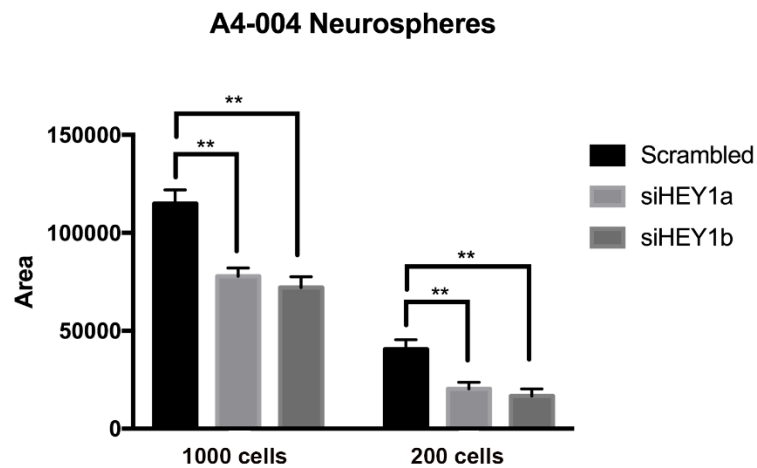


**Figure 3.7 HEY1 knockdown reduces neurosphere formation.**

Either 200 or 1000 A4-004 cells were seeded in triplicate in a 24 well low attachment plate and were allowed to form spheres for a period of 10 days. Sphere formation was analyzed either by counting the number of spheres (**A**) or by counting the total area of all the spheres in each well (**B**). The data shown in (A) is from one experiment and the data shown in (B) is obtained from three independent experiments. The unpaired t-test was used to measure statistical significance. \*\*\* represents  $p < 0.001$ ; \*\*\*\* represents  $p < 0.0001$ .

and ~80% (A4-004) (Figures 3.5E, F). HEY1 knockdown in both these cell lines resulted in decreased cell proliferation compared to cells transfected with control siRNAs (Figures 3.5E, F).

Next, we measured the cell motility of U251 and A4-004 cells transfected with either control or HEY1 siRNAs using the scratch assay. HEY1-depleted U251 and A4-004 cells both showed increased motility compared to control cells, closing the wound (scratch) significantly faster than cells transfected with control siRNAs (Figure 3.6A). In U251 cells, depletion of HEY1 by 2 different siRNAs (siHEY1a and siHEY1b) resulted in ~4.3-fold and ~2.2-fold increases in cell motility, respectively. In A4-004, HEY1 depletion resulted in 7 to 8-fold increases in cell motility. We also used the Transwell migration assay to measure the migration of HEY1-depleted cells compared to control cells. In keeping with the results obtained with the scratch assay, HEY1-depleted U251 and A4-004 GBM cells showed significantly higher migration rates compared to cells transfected with control siRNAs. Specifically, U251 cells transfected with 2 different siRNAs showed approximately 3.70 and 5.37-fold increases in migration compared to control transfectants (Figure 3.6B). HEY1-depleted A4-004 cells showed 2.57 and 1.53-fold increases in migration compared to cells transfected with scrambled (control) siRNAs.

### **3.3.8 *HEY1* depletion results in decrease neurosphere formation**

We transfected A4-004 cells with *HEY1* siRNAs to examine the effect of HEY1 knockdown on their ability to form neurospheres. Either 1000 or 200 cells were seeded in triplicate in low attachment 24-well plates and were allowed to form spheres for a period of 10 days. HEY1 depletion resulted in decreased numbers of neurospheres as well as smaller neurospheres. We therefore measured the total area covered by all the

neurospheres in each well. When 1000 cells were seeded, HEY1 depletion resulted in a significant decrease of ~33% and ~37% in total area covered by neurospheres, upon transfection with siHEY1a and siHEY1b, respectively. When 200 cells were seeded, the decrease in total area was ~50% and 58% for the two HEY1 siRNAs compared to control siRNAs (Figure 3.7).

### 3.4 Discussion

The NFI family is an important regulator of glial cell differentiation during development<sup>198</sup>, with a well-characterized role in the regulation of glial differentiation genes, including *GFAP*, in both normal brain and GBM cells<sup>182</sup>. We used a ChIP-on-chip approach to identify additional NFI target genes in GBM. DNA sequences from a total of 403 genes were found to be preferentially bound by NFI using a pan-specific anti-NFI antibody. Gene ontology analysis of putative NFI target genes identified enrichment of genes involved in multiple biological processes including gene expression, development and differentiation, and, of particular interest, genes involved in nervous system development.

One of the 403 genes identified by Chip-on-chip was the Notch effector gene *HEY1*. The HEY family consists of three basic helix-loop-helix (bHLH) proteins (*HEY1*, *HEY2*, and *HEYL*) closely related to the HES family of transcriptional repressors<sup>211</sup>. *HEY1* is normally expressed in undifferentiated cells of the developing mouse brain<sup>233</sup>. Ectopic expression of *HEY1* in the developing mouse brain inhibits neurogenesis and promotes maintenance of undifferentiated cells<sup>233</sup>. Promoter assays indicate that *HEY1* acts by inhibiting the neuronal bHLH genes *Ascl1* (also known as *Mash1*) and *Neurod4* (also known as *Math3*)<sup>233</sup>.

We identified four putative NFI binding sites within a 1000 bp region immediately upstream of the *HEY1* transcription start site. Gel shift assays revealed NFI binding to three of these four putative sites, at -794 bp, -411 bp, and -332 bp. Although multiple protein-DNA complexes were obtained with the putative NFI binding site at -32 bp, these complexes were competed out with excess cold oligonucleotide mutated at critical NFI

binding residues, and were not supershifted using anti-NFI antibody, indicating that proteins other than NFI bind to the -32 bp region. Combined data from gel shift and supershift experiments indicate that NFIs bind to the other three NFI recognition sites, at -332 bp, -411 bp and -794 bp. Gel shift experiments using nuclear extracts prepared from cells that ectopically express individual NFIs indicate differential NFI binding to these three sites, with the -411 bp site being the most discriminatory, as only NFIX binds effectively to this region.

Differential binding by different NFI family members *in vitro* has been previously reported<sup>179, 301</sup>. For example, the differential DNA binding specificities of NFI-A4, NFI-B2 and NFI-X1 for the CoRE response element located upstream of the *WAP* gene was shown to be dependent on other transcription factors binding to this region<sup>179</sup>. As all four NFIs have highly similar DNA binding domains, and bind DNA as either homodimers or heterodimers, binding site specificity may be due to NFI interacting partners, structural changes within NFI transcription factors caused alternative splicing or post-translational modifications, as well as the relative levels of the different members of the NFI family<sup>178, 301</sup>. Thus, differences in the sequences of the three NFI binding sites upstream of the *HEY1* gene may allow preferred binding to subsets of NFI recognition sites. In this regard, it is interesting to note that the main differences between the -411 bp NFI recognition sites and that of -332 bp and -794 bp are the last two nucleotides (GC in the case of -411 bp and AG and AC in the case of the -332 and -794 bp regions, respectively) (Figure 3.1A).

A requirement for knockdown of all four NFIs to detect an effect on endogenous *HEY1* RNA levels suggests complex regulation and cross-talk between NFI family members. There is considerable variability in the transactivation domain of NFI family

members<sup>175, 281</sup>, and the transactivation potential of heterodimers has previously been reported to be intermediate to that of NFI homodimers<sup>282</sup>. Thus, knockdown of single NFIs, with accompanying changes in NFI interactions, may alter the dynamics of NFI dimerization in the cell, but may still result in little to no effect on endogenous *HEY1* mRNA levels in the context of an intact cell. It is only when all four NFIs are depleted that their repressive effect on the *HEY1* promoter can be overcome. In contrast to the endogenous promoter, single knockdown of NFIB, NFIC, or NFIX, but not NFIA, was sufficient to induce exogenous *HEY1* promoter activity. Differences in regulation of NFI-dependent promoter activity in an endogenous (or chromosomal) context compared to an ectopic (or extrachromosomal) context has previously been reported for a number of promoters including *B-FABP*, *GFAP* and *MMTV*<sup>182, 302</sup>. This difference has been explained by a looser organization of the nucleosome structure in episomal DNA compared to chromosomal DNA, allowing easier access to transcription factors<sup>303</sup>.

*HEY1* expression in GBM correlates with increased tumour grade and decreased survival<sup>304</sup>. Similar to the results reported here, others have shown that *HEY1* knockdown decreases proliferation in U87, T98 and U373 GBM cell lines as well as GBM lines established from mouse xenografts<sup>254, 255</sup>. We extend these studies by demonstrating that *HEY1* is associated with higher levels of the neural stem cell marker *B-FABP* in GBM cells, in keeping with its proposed role in the brain<sup>233</sup>. Furthermore, *HEY1* depletion in GBM cells that already express the astrocyte differentiation marker *GFAP* results in increased *GFAP* mRNA levels. In contrast to a previous report indicating that *HEY1* knockdown resulted in decreased migration in GBM cell lines<sup>255</sup>, our results indicate a significant increase in migration upon *HEY1* depletion in GBM cells. This discrepancy

may stem from the fact that the pooled siRNAs used for HEY1 depletion by Tsung et al. resulted in increased apoptosis in GBM cell lines established from mouse xenografts<sup>255</sup>. Thus, our results support roles for NFIs and HEY1 in controlling fundamental pro-growth vs anti-growth properties of GBM, as well as support the 'go or grow' hypothesis whereby cells with reduced proliferation show increased migration and vice versa<sup>72</sup>.

In contrast to HEY1, high *NFIA* and *NFIB* mRNA levels correlate with improved patient survival in astrocytomas, with reduced expression of *NFIA* and *NFIB* associated with higher-grade astrocytomas<sup>205, 209</sup>. In the developing CNS, *NFIA* and *NFIB* drive the onset of gliogenesis (gliogenic switch)<sup>198-200, 208</sup>, with *NFIX* playing a role in the later stages of astrocyte differentiation<sup>202, 305</sup>. *Nfia*<sup>-/-</sup>, *Nfib*<sup>-/-</sup> and *Nfix*<sup>-/-</sup> null mice all show delays in the differentiation of glial cells in developing brain<sup>185, 188, 191-193, 284, 285</sup>. Although *NFIC* is widely expressed in the CNS, *Nfic* knockout in mice causes tooth pathologies rather than brain defects, suggesting that its roles in brain are redundant with other NFIs<sup>188, 306</sup>. Several studies have shown that NFIs, especially *NFIA* and *NFIB* positively regulate the expression of genes associated with glial cell differentiation (e.g., *GFAP*, *SPARCL1*, *APCDD1*, *MMD2*)<sup>199, 201, 293, 305</sup> while repressing genes associated with stem cell maintenance (*EZH2*, *HES1*)<sup>186, 187</sup>. As previously reported, the association between reduced levels of *NFIA/NFIB* and increased malignancy in astrocytoma is in agreement

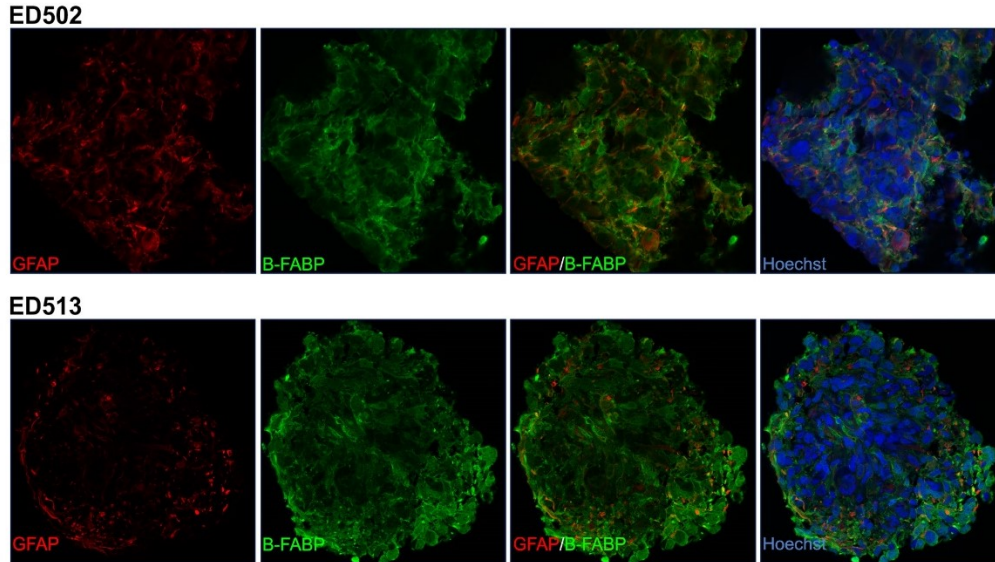


**Figure 3.8 Immunofluorescence analysis of MG tumour neurospheres.**

Neurospheres from two cultures were fixed in formalin and embedded in paraffin. Sections were cut and the tissue immunostained using anti-GFAP and anti-B-FABP antibodies. The signal was detected with secondary antibodies conjugated to Alexa 555 (red; GFAP) or Alexa 488 (green; B-FABP). Hoechst 33342 was used to label the nuclei. Heterogeneity in B-FABP and GFAP expression is observed in both neurosphere cultures.

with NFIs playing similar roles in gliogenesis and gliomagenesis; i.e., promotion of glial cell differentiation properties<sup>190, 307</sup>. Our results indicating that NFI knockdown upregulates *HEY1* expression adds to the repertoire of genes controlled by NFIs that determine stemness vs differentiation properties. It is a well-known fact that there is considerable heterogeneity in GBM tumours and the cell lines derived from these tumours. Thus, within a single tumour or cell line, there may be NFI-high cells associated with expression of astrocytic markers and less aggressive growth properties, and NFI-low cells associated with increased stemness and more aggressive growth properties. In support of this idea, examination of the astrocytic marker GFAP and neural stem/progenitor cell marker B-FABP in GBM neurosphere cultures reveals little overlap in the expression of these two markers (Figure 3.8).

In summary, we show that NFI transcription factors expressed in GBM cells bind to the promoters of multiple genes involved in many biological processes. We identify three NFI binding sites in the *HEY1* promoter and show that NFI represses *HEY1* promoter activity and expression in GBM cells. We demonstrate differential binding of the four members of the NFI family to the different NFI binding sites in the *HEY1* promoter. Our results indicate complex interactions between the different members of the NFI family and suggest that NFI dimerization, along with additional transcription factors, are involved in the regulation of the *HEY1* gene in GBM. The decrease in cell proliferation and increase in cell migration observed upon *HEY1* knockdown supports the 'go or grow' hypothesis validated for a number of tumour models. We propose that mutually exclusive cell migration and proliferation in GBM cells can be explained at least in part by relative levels of NFIs and *HEY1*.

## **Chapter 4 Role of AP-2 $\beta$ in GBM pathogenesis**

## 4.1 Introduction

Glioblastomas (GBM) are highly aggressive brain tumours<sup>64</sup>. Patients diagnosed with GBM have a median survival of only 14 months<sup>65, 66</sup>. Current treatment regimens involve surgery followed by radiotherapy and concurrent chemotherapy with temozolomide. Treatment failure is at least partly due to the highly invasive nature of GBM, with tumour cells infiltrating the surrounding normal tissue.

A subset of GBM tumour cells have the ability to self-renew and to differentiate into non-stem-like cells which form the bulk of the tumour. These self-renewing cells are called glioblastoma stem cells (GSCs) or brain tumour initiating cells<sup>76</sup>. Studies have shown that GSCs play key roles in tumour initiation, progression and resistance to radiation and chemotherapy<sup>72, 76</sup>. Although CD133 is a commonly used cell surface marker to identify GSCs, both CD133-positive and CD133-negative GBM cells have tumour stem cell-like properties<sup>308</sup>. Other commonly used GSC markers include SOX2, Nestin, ALDH1a, CD44 and CD15<sup>309, 310</sup>.

The AP-2 (TFAP2) family of transcription factors regulates the expression of genes associated with cell cycle and differentiation during early embryonic development<sup>96, 154-156, 257</sup>. Four of the five members of AP-2 family (AP-2 $\alpha$ , AP-2 $\beta$ , AP-2 $\gamma$ , AP-2 $\epsilon$ ) have been implicated in cancer<sup>154-156, 311</sup>. In normal breast tissue, AP-2 $\alpha$ , AP-2 $\beta$  and AP-2 $\gamma$  all play important roles in normal breast development<sup>311</sup>. Loss of nuclear AP-2 $\alpha$  is generally associated with a more invasive breast cancer phenotype, and increased levels of cytoplasmic AP-2 correlate with poor prognosis<sup>312</sup>. AP-2 $\alpha$  has also been shown to upregulate *HER2* expression in breast cancer<sup>163</sup>, and to downregulate *CCND1* (cyclin D1)<sup>313</sup>, thereby demonstrating both oncogenic and tumour suppressor properties<sup>163</sup>. Like AP-2 $\alpha$ , AP-2 $\gamma$  has been implicated in breast cancer, particularly as related to estrogen

response. AP-2 $\gamma$  positively regulates *ESR1*, the gene that encodes estrogen receptor alpha (ER $\alpha$ )<sup>150</sup>. AP-2 $\gamma$  RNA and protein levels are associated with a decreased rate of disease-free survival as well as overall survival in breast cancer<sup>314, 315</sup>. Interestingly, sumoylation of AP-2 $\alpha$  and AP-2 $\gamma$  has been shown to be a crucial factor in maintenance of the luminal subtype in breast cancer and inhibition of sumoylation leads to transition to the basal subtype<sup>110</sup>. A recent study showed that sumoylation of AP-2 is required for maintenance of stem cells in breast cancer as well as in colorectal cancer<sup>113</sup>. AP-2 $\beta$  is associated with poor prognosis in patients with lung adenocarcinoma and its overexpression results in increased tumour growth as a consequence of increased VEGF/PVDF signaling<sup>316</sup>. In contrast, low levels of AP-2 $\beta$  are associated with poor prognosis in endometrial cancer<sup>317</sup>.

In GBM cell lines, AP-2 $\alpha$  overexpression results in decreased cell proliferation and migration, suggesting a tumour suppressor role for AP-2 $\alpha$ <sup>318</sup>. In glioma tumours, loss of nuclear AP-2 $\alpha$  is associated with increased grade, with 71 out of 72 glioblastomas showing absence of nuclear AP-2 $\alpha$ , in contrast to 100% of low grade astrocytomas which have nuclear AP-2 $\alpha$  expression<sup>168</sup>. The absence of nuclear AP-2 $\alpha$  in GBM is also associated with increased MMP-2 and VEGF expression, suggesting that AP-2 $\alpha$  normally suppresses the expression of these two genes<sup>168</sup>. In a separate study, high levels of cytoplasmic AP-2 $\alpha$  were shown to correlate with increased glioma grade<sup>169</sup>. These findings suggest that the subcellular localization of AP-2 $\alpha$  plays an important role in GBM progression. AP-2 $\beta$  and AP-2 $\gamma$  have not been studied in GBM<sup>171</sup>.

Here, we characterize the expression of AP-2 family members in GBM cell lines and study their roles in regulating GBM cell growth properties. We show that AP-2 $\beta$  is

primarily found in the cytoplasm of adherent GBM cell cultures but localizes to the nucleus of GBM cells cultured in neurosphere medium. We show that elevated levels of *AP-2 $\beta$*  RNA are associated with the proneural GBM subtype and decreased patient survival. Furthermore, we found that AP-2 $\beta$  expression is induced under hypoxia and knockdown of AP-2 $\beta$  results in reduced Nestin and SOX2 expression. Our results suggest that AP-2 $\beta$  is important for stem cell maintenance in GBM.

## 4.2 Material and methods

### 4.2.1 Cell lines, siRNAs, and transfections

The established human GBM cell lines used in this study have been previously described <sup>182, 288</sup>. Cells were cultured in Dulbecco's modification of Eagle's minimum essential medium (DMEM) supplemented with 10% fetal calf serum, penicillin (50 U/mL) and streptomycin (50 µg/mL) (defined as standard conditions). The primary GBM cell cultures (A4-004, A4-007) were prepared by enzymatic dissociation of GBM biopsies obtained with patient consent prior to surgery. A4-004 and A4-007 adherent lines were generated by culturing cells directly in DMEM supplemented with 10% fetal calf serum (defined throughout the chapter as "adherent"). GBM tumour neurosphere cultures were generated by plating cells directly in DMEM/F12, supplemented with B27, epidermal growth factor (EGF) and fibroblast growth factor (FGF) (defined throughout the chapter as "neurospheres" or "neurosphere conditions" or "neurosphere cultures"). Please note that A4-004 cells cultured in neurosphere medium grow as adherent cells unless plated in low attachment plates. All procedures involving tumour biopsies were approved by the Health Research Ethics Board of Alberta Cancer Committee Protocol #HREBA.CC-14-0070.

Cells were transfected with 10 nM scrambled siRNA (Life Technologies; Cat. No#. 12935-200) or siRNAs targeting AP-2β (#195; CCATCATGCTCTGGAAGCTTGTGGA) or #720; CCAATAACAGCGGCATGAATCTATT) using the Lipofectamine RNAiMAX reagent (Life Technologies). The medium was replaced 16 h after transfection and cells harvested 48 h after transfection.

#### **4.2.2 Semi-quantitative and quantitative RT-PCR**

RNA was purified from a panel of adherent and patient-derived GBM cell lines. RNA was reverse transcribed using oligo(dT) and Superscript reverse transcriptase II (Invitrogen). Primers used for RT-PCR are shown in Table 4.1. Quantitative RT-PCR was carried out using SYBR Green-based qPCR (Applied Biological Materials Inc., Canada) and analyzed on an ABI 7900HT PCR system, with primers designed to amplify a 150 bp region of the respective targets. Primers used for qPCR are listed in Table 4.2. All samples were assayed in triplicate, and gene expression normalized to *GAPDH*.

#### **4.2.3 Western blot analysis**

Nuclear and cytoplasmic extracts were prepared using NE-PER Nuclear and Cytoplasmic Extraction Kit (Thermo Fisher Life Technologies). Protein extracts were electrophoresed in 10% polyacrylamide-SDS gels and transferred to PVDF (polyvinylidene fluoride) membranes. The following antibodies were used for analysis: anti-AP-2 $\alpha$ , mouse monoclonal antibody (1:400, 3B5, Developmental Studies Hybridoma Bank developed under the auspices of the NICHD and maintained by the University of Iowa); anti-AP-2 $\beta$ , rabbit polyclonal antibody (1:1,000, #2509, Cell Signaling Technology), anti-AP-2 $\gamma$ , mouse monoclonal antibody (1:200, 6E4/4, Santa Cruz Biotechnology). Primary antibodies were detected with horseradish-peroxidase-conjugated secondary antibodies (Jackson ImmunoResearch Biotech) using Immobilon (EMD Millipore). For AP-2 $\beta$  expression analysis in GBM patient tissues, lysates were prepared directly from tumours obtained from consented GBM patients (ethics protocol HREBA.CC-14-0070).

#### **4.2.4 Cell proliferation assay**

U251 GBM cells cultured under standard conditions (DMEM supplemented with 10% FCS) and A4-004 GBM cells cultured under neurosphere conditions were transfected with scrambled or AP-2 $\beta$  siRNAs. Forth-eight hours later, transfected cells were seeded in triplicate (30,000 cells per well) in a 12-well plate. Cell growth was measured by counting the cells in triplicate wells every 24 h for a period of 96 h using a Coulter Particle and Size Analyzer (Coulter Corporation). Cell counts in the triplicate wells were averaged and plotted on a semi-log graph.

#### **4.2.5 Scratch assay**

Cells were transfected with either scrambled or AP-2 $\beta$  siRNAs as described for the cell proliferation assay. Cells were seeded in triplicate in 12-well plates 48 h post-transfection. Cells were allowed to form a monolayer, at which time a scratch was made in the center of the wells using a P20 pipette tip. Cells were cultured for an additional 18 h. Digital imaging microscopy (Axiovert 200M, Zeiss) was used to image the cells at 2 separate positions in each well using a phase contrast lens at 10X magnification (6 positions in total for triplicate wells). Metamorph imaging software (Version 7.8.8.0, Molecular Devices) was used to capture a total of 97 images at each position at 15-minute intervals over a period of 18 h. TScratch software was used to analyze the images. The percentage open area of the scratch at different time points was measured. The open area of each scratch at 0 h was normalized to 100% to nullify the effects of minor differences of the scratch size in different wells. The open area at subsequent time points is represented relative to their respective 0 h time point.

AP-2 $\alpha$ Forward	5'- CTGGGCACTGTAGGTCAAT-3'
AP-2 $\alpha$ Reverse	5'-GAAGACTTCGTTGGGGTTC-3'
AP-2 $\beta$ Forward	5'-TACGATATCCACTCACCTCCTAGAGACC-3'
AP-2 $\beta$ Reverse	5'-TAGTCTAGATCATTTCTGTGTTTCTCCTC-3'
AP-2 $\gamma$ Forward	5'-AAAGCCGCTCATGTGACTCT-3
AP-2 $\gamma$ Reverse	5'-TGGTCTCCAGGGTTCATGT-3
AP-2 $\delta$ : Forward	5'-GACAAGCTTTCAACTACCTTTCCGGGAC-3'
AP-2 $\delta$ : Reverse	5'-CATAGATCTGTCTGTCTTTTCTGTTTTGCC-3'
AP-2 $\epsilon$ Forward	5'-CAATGTGACGCTGCTGACTT-3
AP-2 $\epsilon$ Reverse	5'-CACTGCCCACACTGCTTAG-3'
$\beta$ -actin Forward	5'-CTGGCACCCACACCTTCTAC-3
$\beta$ -actin Reverse	5'-CATACTCCTGCTTGCTGATC-3'

**Table 4.1 List of primer sequences used for RT-PCR analysis**

AP-2 $\alpha$ Forward	5'-GAGGTCCC GCATGTAGAA-3'
AP-2 $\alpha$ Reverse	5'-GAAGACTTCGTTGGGGTTCA-3'
AP-2 $\beta$ Forward	5'-CTCAATGCATCTCTCCTC-3'
AP-2 $\beta$ Reverse	5'-CAGCTTCTCCTTCCACCA-3'
AP-2 $\gamma$ Forward	5'-AAAGCCGCTCATGTGACT-3'
AP-2 $\gamma$ Reverse	5'-TGCCATCTCATTTCGTCC-3'
GAPDH Forward	5'-GAGATCCCTCCAAAATCAA-3'
GADPH Reverse	5'-CACACCCATGACGAACAT-3'
Nestin Forward	5'-AACAGCGACGGAGGTCT-3'
Nestin Reverse	5'-TCTCTTGTCCCGCAGAC-3'
CD133 Forward	5'-AATGACCCTCTGTGCTTGGT-3'
CD133 Reverse	5'-GTGGAAGCTGCCTCAGTTC-3'
SOX2 Forward	5'-CCGAGTGGAACTTTTGT-3'
SOX2 Reverse	5'-CAGCGTGTACTTATCCTTC
ALDH1A1 Forward	5'-TGTTAGCTGATGCCGACTTG-3'
ALDH1A1 Reverse	5'-TTCTTAGCCCGCTCAACACT-3'
ALDH1A2 Forward	5'-CTGGCAATAGTTCGGCTCTC-3'
ALDH1A2 Reverse	5'-TGATCCTGCAAACACTGCTC-3'
ALDH1A3 Forward	5'-TCTCGACAAAGCCCTGAAGT-3'
ALDH1A1 Reverse	5'-TATTCGGCCAAAGCGTATTC-3'

**Table 4.2 List of primer sequences used for quantitative RT-PCR analysis**

#### **4.2.6 Transwell migration assay**

Cells were cultured and transfected with either scrambled or AP-2 $\beta$  siRNAs as described for the cell proliferation assay. Directional cell migration was measured using the Transwell cell migration assay. Twenty-five thousand cells in DMEM medium containing 1% fetal calf serum were seeded in the top chambers of 24-well cell culture Transwell inserts (Falcon™ Cell Culture Inserts). Cells were allowed to migrate through an 8 $\mu$ m polyethylene terephthalate (PET) membrane towards a chemoattractant (DMEM+10% fetal calf serum) in the bottom chamber over a 20 h period. Cells were then fixed with 100% cold methanol for 20 minutes and stained with 1% crystal violet in 20% methanol for 30 minutes at room temperature. Migrated cells were imaged using a Zeiss Axioskop2 plus microscope by capturing different fields of view. Cell counting was carried out using Meta express imaging software.

#### **4.2.7 Immunostaining**

Immunohistochemistry and immunofluorescence analyses were carried out as previously described<sup>146, 270</sup>. Cells were fixed in formalin and paraffin-embedded. Tissue sections were deparaffinized in xylene, rehydrated and microwaved in a pressure cooker for 20 min for antigen retrieval. Rabbit anti-AP-2 $\beta$  antibody (1:1,500, generated by Dr. Markus Moser, Max Plank Institute of Biochemistry) was used for immunohistochemistry. The following antibodies were used for immunofluorescence analysis: anti-AP-2 $\alpha$ , mouse monoclonal antibody (1:400, 3B5, Developmental Studies Hybridoma Bank), anti-AP-2 $\beta$ , rabbit polyclonal antibody (1:1,000, #2509, Cell Signaling Technology), anti-AP-2 $\gamma$ , mouse monoclonal antibody (1:200, 6E4/4, Santa Cruz Biotechnology).

Immunofluorescence images were captured on a Zeiss LSM710 confocal laser scanning microscope with a plan-Apochromat 20X lens using ZEN software. To ensure AP-2 antibody specificity, HeLa cells were transfected with each of the five AP-2 expression constructs in p3xFLAG-CMV vector. Cells were harvested, and total cell lysates were prepared using RIPA buffer. Lysates were electrophoresed through a 10% SDS-PAGE gel and western blot analysis carried out using antibodies to each of the five AP-2s.

#### **4.2.8 Phosphatase and sumoylation assays**

For phosphatase experiments, cells were lysed in RIPA buffer. Forty  $\mu\text{g}$  lysates were incubated with phosphatase buffer,  $\text{MnCl}_2$  and 400 U lambda phosphatase (New England Biolabs) at  $30^\circ\text{C}$  for 1 h. Water was added to the control tubes instead of  $\lambda$  PPase. 5X SDS sample buffer was added to each treatment to terminate the phosphatase reaction. Results were analyzed by western blotting.

Detection of sumoylation was carried out by immunoprecipitation followed by western blot analysis. Cells U251 and A4-004 cells were transfected with a FLAG-tagged AP-2 $\beta$  or AP-2 $\gamma$  expression constructs. Cells were lysed in a RIPA buffer (50 mM Tris-HCl pH 7.5, 150 mM NaCl, 0.5% sodium deoxycholate, 1% NP-40, 0.1% SDS and 25X complete protease inhibitor) without (RIPA buffer) or supplemented with 25 mM NEM (SUMO buffer).. For immunoprecipitation, cell lysates were precleared with protein G Sepharose beads (GE Healthcare) for 1 h at  $4^\circ\text{C}$ , incubated with FLAG primary antibody or IgG control overnight at  $4^\circ\text{C}$ . The immunocomplexes were then collected with protein G Sepharose beads. Immunoprecipitates or supernatants were separated by SDS-PAGE, blotted onto PVDF membranes and immunostained with SUMO antibody.

## 4.3 Results

### 4.3.1 Expression of AP-2 transcription factors in GBM

AP-2 RNA levels in a panel of 10 adherent GBM cell lines cultured under standard conditions was examined by semi-quantitative RT-PCR. *AP-2 $\alpha$*  was expressed at similar levels across all 10 cell lines (Figure 1A). There was a trend towards higher *AP-2 $\beta$*  levels in B-FABP<sup>+ve</sup> compared to B-FABP<sup>-ve</sup> MG cell lines. B-FABP is a marker for cell migration, invasion and stemness in GBM<sup>210, 298, 299</sup>. *AP-2 $\gamma$*  RNA levels were high in all MG cell lines tested with the exception of A172 and U87. *AP-2 $\delta$*  RNA was not detected in any of the cell lines tested, while *AP-2 $\epsilon$*  was expressed in T98, M021, M103 and U373 (Figure 4.1A). As *AP-2 $\alpha$* , *AP-2 $\beta$*  and *AP-2 $\gamma$*  were widely expressed in MG cell lines, western blot analysis was carried out to examine AP-2 protein levels in MG cell lines. As AP-2 proteins share structural similarities, we first examined the specificity of our AP-2 antibodies by western blot analysis of HeLa cells transfected with different AP-2 expression constructs. Based on western blotting, AP-2 $\alpha$ , AP-2 $\beta$ , AP-2 $\gamma$  antibodies are highly specific, mainly recognizing their target AP-2 proteins (Figure 4.1B). The presence of doublet bands suggests post-translational modification of ectopic AP-2 proteins. Immunoblotting of our panel of 10 MG cell lines using anti-AP-2 $\beta$  and anti-AP-2 $\gamma$  antibodies revealed reasonably good consistency between RNA and protein levels. However, there were some significant discrepancies in AP-2 $\alpha$  RNA and protein levels, with barely detectable AP-2 $\alpha$  protein in A172, U87 and M021 (Figure 4.1C).

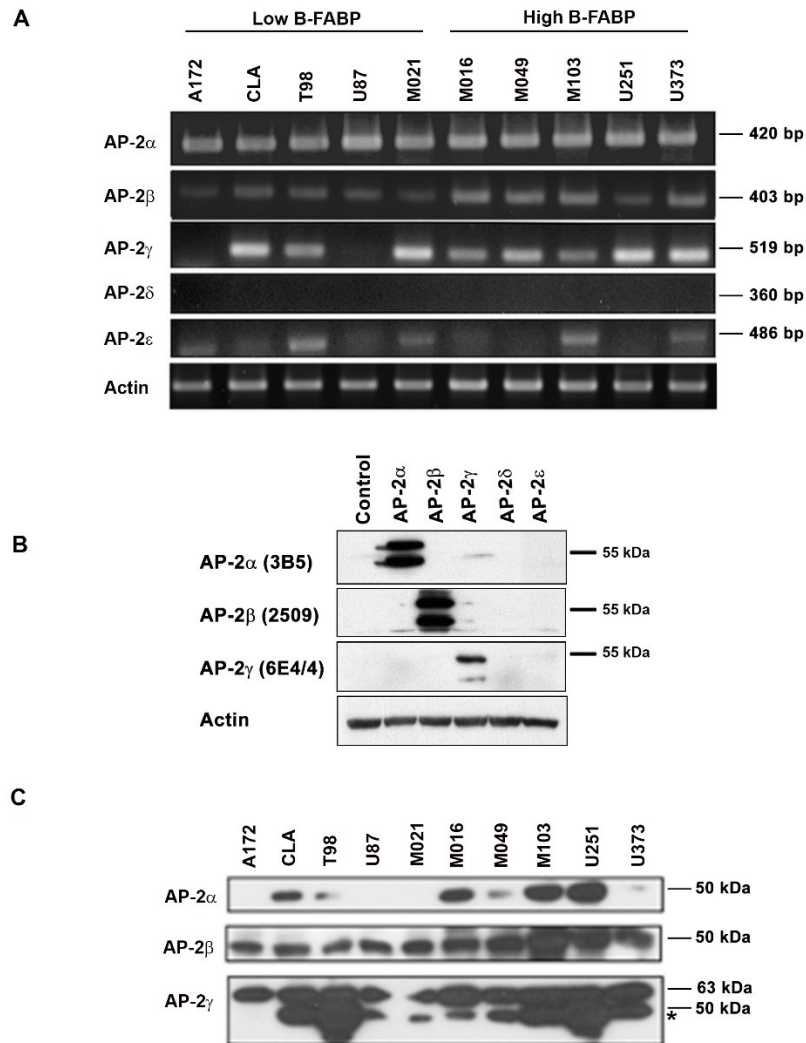


**Figure 4.1 RT-PCR analysis of AP-2 transcription factors in GBM cell lines.**

**(A)** RT-PCR was used to amplify AP-2 $\alpha$ ,  $\beta$ ,  $\gamma$ ,  $\delta$  and  $\epsilon$  from a panel of 10 GBM cell lines. Actin was used as a loading control. PCR products were loaded on 1% agarose gels. Primers used for RT-PCR are listed in Table 4.1. **(B)** Western blot analysis of AP-2 antibodies. HeLa cells were transfected with vector control, AP-2 $\alpha$ , AP-2 $\beta$ , AP-2 $\gamma$ , AP-2 $\delta$  or AP-2 $\epsilon$  expression constructs. Blots were immunostained with antibodies to AP-2 $\alpha$ , AP-2 $\beta$  or AP-2 $\gamma$ . **(C)** Western blot analysis of AP-2 $\alpha$ , AP-2 $\beta$  and AP-2 $\gamma$  in a panel of 10 GBM cell lines. Forty  $\mu$ g cell lysates were electrophoresed in a 10% SDS-polyacrylamide gel. Proteins were transferred to a nitrocellulose membrane and immunostained with specific AP-2 antibodies. AP-2 $\beta$  and AP-2 $\gamma$  protein levels mostly coincide with RNA levels.

RNA expression of *AP-2 $\alpha$* , *AP-2 $\beta$*  and *AP-2 $\gamma$*  was also examined in A4-004 patient-derived GBM cells by quantitative RT-PCR (qRT-PCR). We compared the expression of these genes in A4-004 cells cultured under standard vs neurosphere conditions. While no difference in *AP-2 $\alpha$*  mRNA levels was observed under these two conditions, *AP-2 $\beta$*  (55-fold) and *AP-2 $\gamma$*  (4-fold) were expressed at higher levels in cells cultured under neurosphere conditions compared to adherent conditions (Figure 4.2).

As *AP-2 $\beta$*  is highly upregulated under neurosphere conditions, and GBM cancer stem cells are believed to drive GBM malignancy, we focused on *AP-2 $\beta$*  in subsequent experiments. First, qRT-PCR analysis was carried out to confirm the levels of *AP-2 $\beta$*  in our panel of 10 adherent GBM cell lines. Although the trend observed by semi-quantitative RT-PCR was still clear, there was considerable variation in *AP-2 $\beta$*  levels, with highest levels in B-FABP<sup>ve</sup> M016, M103 and U373 (Figure 4.3A). We also examined *AP-2 $\beta$*  expression in a second set of paired adherent/neurosphere cultures derived from patient A4-007. Similar to A4-004, *AP-2 $\beta$*  RNA levels were considerably higher in the neurosphere culture compared to adherent culture (Figure 4.3B). These results were confirmed by semi-quantitative RT-PCR (allowing visualization of the correct size band) (Figure 4.3C). Western blot analysis further demonstrated a strong correlation between *AP-2 $\beta$*  RNA and protein levels in both A4-004 and A4-007 cells with higher expression in neurospheres compared to adherent cultures (Figure 4.3D). As neurosphere cultures have a higher percentage of cells with stem-like properties, higher *AP-2 $\beta$*  expression in neurosphere cultures suggests an association between *AP-2 $\beta$*  and stemness in GBM.

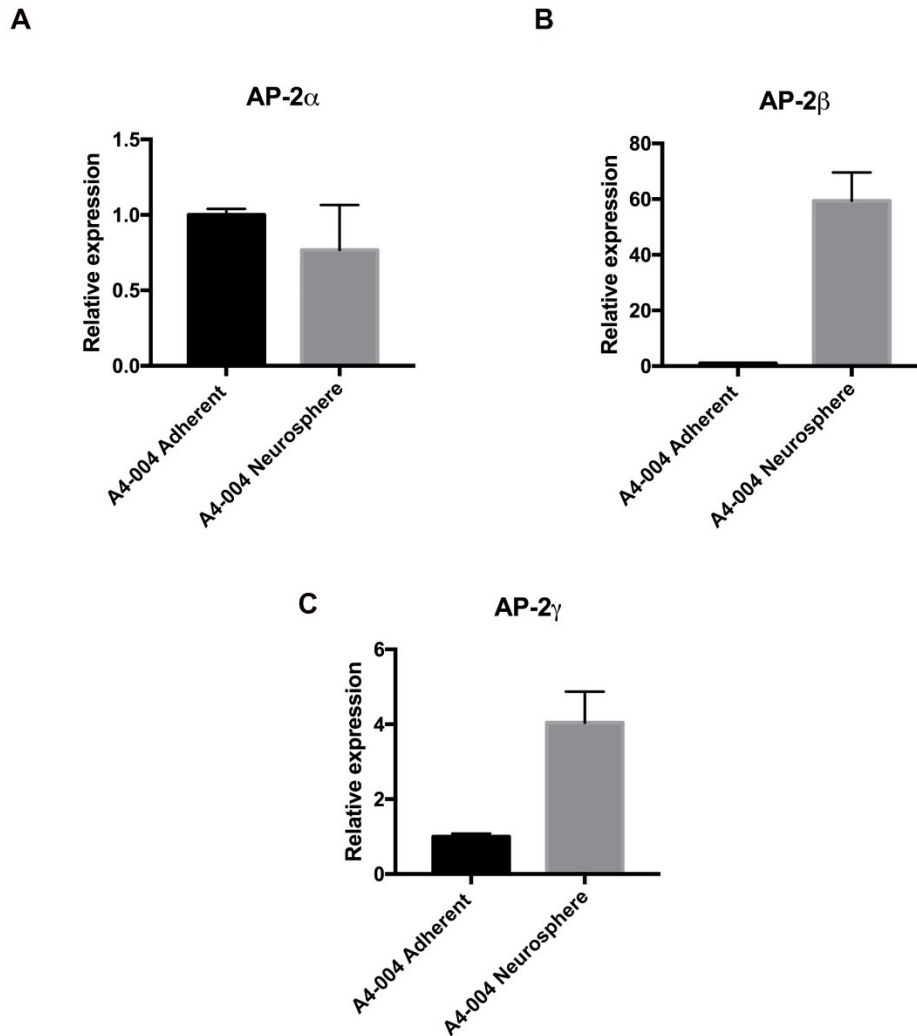


**Figure 4.2 Expression of AP-2 in A4-004 adherent vs neurospheres.**

**(A-C)** Quantitative RT- PCR *AP-2 $\alpha$*  (A), *AP-2 $\beta$*  (B) and *AP-2 $\gamma$*  (C) RNA levels in A4-004 adherent and A4-004 neurosphere cultures. Expression levels were normalized to *GAPDH*. Primers used for quantitative PCR are listed in Table 4.2.

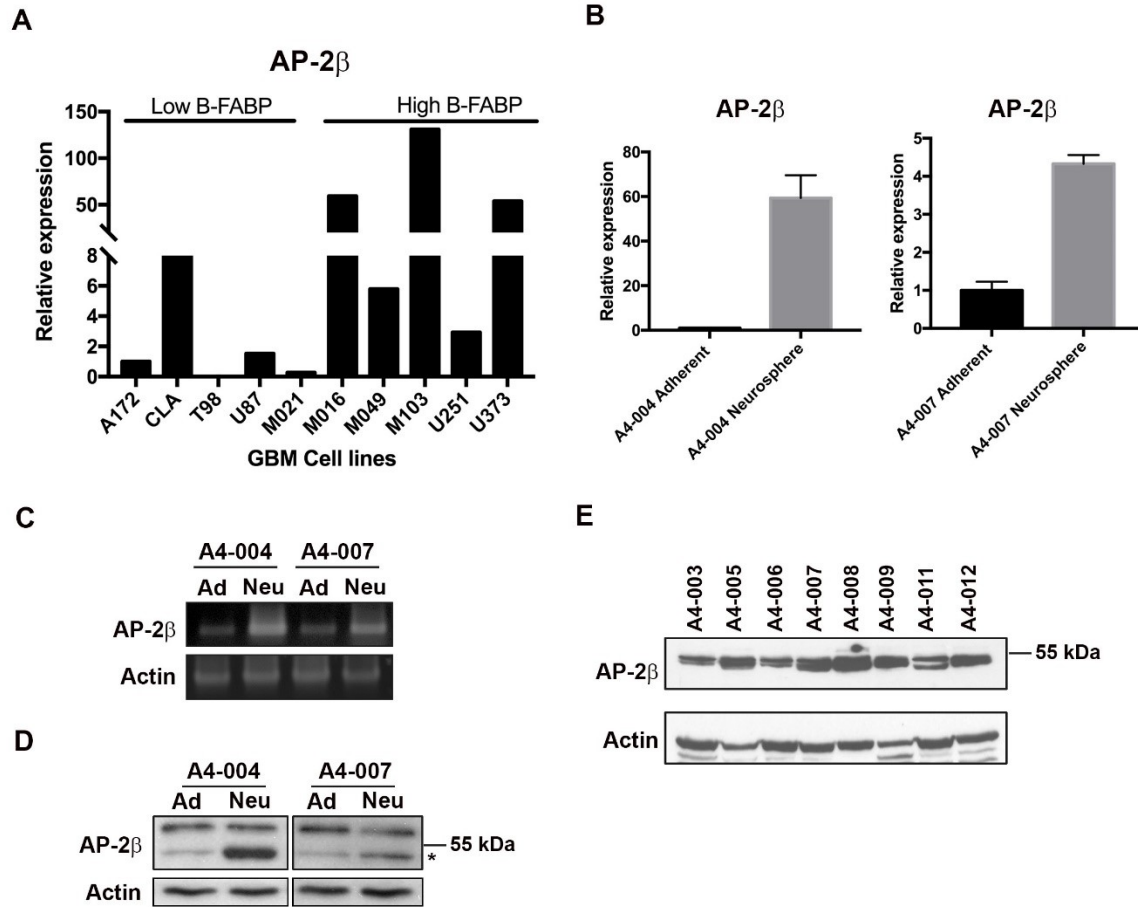


**Figure 4.3 AP-2 $\beta$  RNA levels in GBM cell lines.**

(A) qPCR analysis showing *AP-2 $\beta$*  mRNA levels in a panel of 10 GBM cells. The first five cell lines do not express B-FABP and the last five cell lines express B-FABP. (B) qPCR analysis showing *AP-2 $\beta$*  mRNA levels in A4-004 and A4-007 GBM cells cultured under standard and neurosphere culture conditions. (C) Semi-quantitative RT-PCR analysis showing *AP-2 $\beta$*  mRNA levels in A4-004 and A4-007 GBM cells cultured under standard and neurosphere culture conditions. (D) Western blot analysis of AP-2 $\beta$  in A4-004 and A4-007 GBM cells cultured under standard and neurosphere culture conditions. The asterisk on the right points to the AP-2 $\beta$  protein band. (E) Western blot analysis of AP-2 $\beta$  in eight patient-derived GBM tumour tissues.

To ensure that AP-2 $\beta$  expression is not a tissue culture artefact, we next carried out western blot analysis of a panel of 8 GBM tumour tissues. Abundant AP-2 $\beta$  protein was observed in all tumour tissues tested (Figure 4.3E). Two bands of ~50 kDa and ~63 kDa were observed in most samples. The lower band is the correct size for the unmodified AP-2 $\beta$  protein. The higher band may be a post-translationally modified form of AP-2 $\beta$ . Next, we immunostained a panel of patient tissue sections (A4-001, A4-002, A4-003, A4-004, A4-005, A4-006, A4-007, A4-008, A4-009, A4-010, A4-012). Variable AP-2 $\beta$  expression was detected in these tissue sections, with high expression in A4-004, A4-005, A4-006, A4-008 and A4-009 (Figure 4.4). With few exceptions, AP-2 $\beta$  localized to the nucleus.

#### **4.3.2 Expression of AP-2 $\beta$ correlates with survival in low grade gliomas and is associated with proneural GBM subtype**

Analysis of a TCGA dataset (Brain low grade glioma, TCGA provisional) revealed an inverse correlation ( $P < 0.0001$ ) between high levels of AP-2 $\beta$  and glioma patient survival (Figure 5A). No correlation was observed between either AP-2 $\alpha$  or AP-2 $\gamma$  RNA levels, and patient survival, using the same TCGA dataset (Figures 4.5B, C). Next, we examined the GBM subtype-specific expression of AP-2 $\beta$  using the TCGA GBM database (TCGA Cell 2013)<sup>319</sup>. AP-2 $\beta$  levels were considerably higher in the pro-neural GBM subtype compared to mesenchymal, neural and classical subtypes (Figure 4.5D). The pro-neural subtype is associated with stem cell markers in GBM<sup>320</sup>. We therefore carried out RT-PCR analysis of AP-2 $\beta$ , and two markers of neural stem cells, *Nestin* and *B-FABP* in A4-004 and A4-007 adherent and neurosphere cultures. Similar to AP-2 $\beta$ , both *B-FABP*

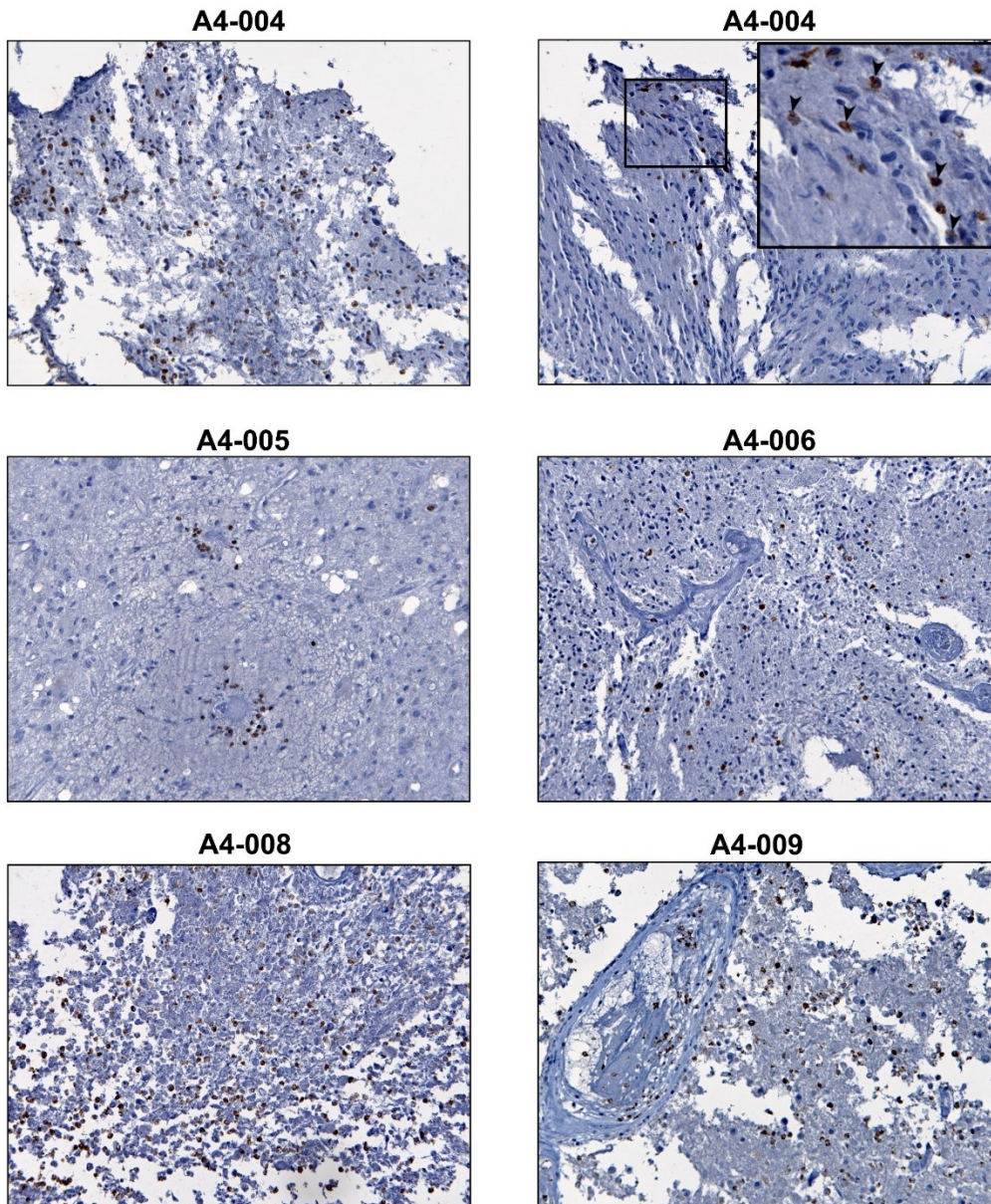


**Figure 4.4 Immunohistochemical analysis of AP-2 $\beta$  in GBM patient tumour tissues.**

A4-004, A4-005, A4-006, A4-008 and A4-009 GBM tissue sections were fixed in formalin and paraffin-embedded. Tissue sections were immunostained with rabbit anti-AP-2 $\beta$  antibody (1:1,500, generated by Dr. Markus Moser, Max Plank Institute of Biochemistry). Positive cells are stained brown. The arrowheads in A4-004 top right point to cytoplasmic AP-2 $\beta$ .

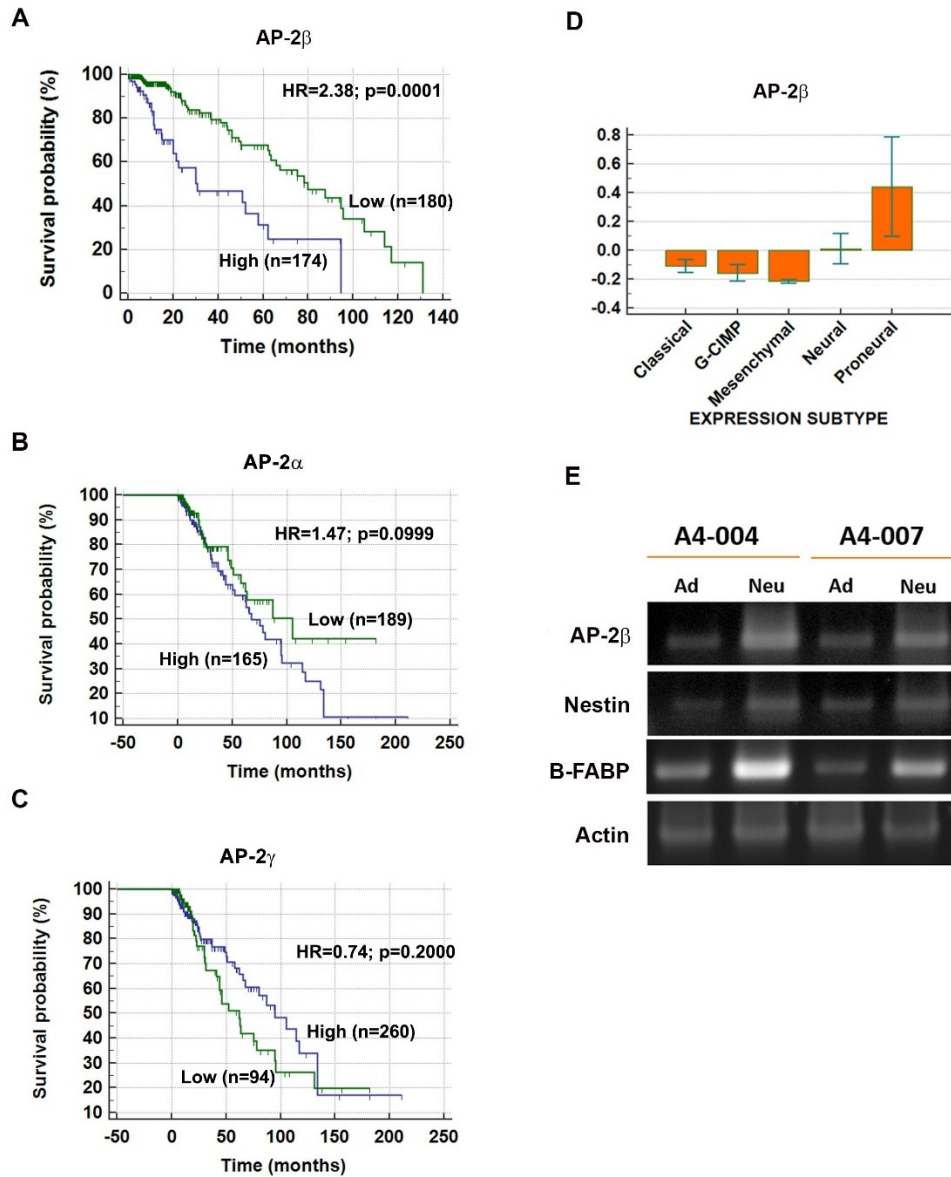


**Figure 4.5 Expression of *AP-2 $\beta$*  correlates with survival in glioma patients.**

**(A-C)** Kaplan-Meier curve obtained using a TCGA brain low grade glioma database showing that high levels of *AP-2 $\beta$*  mRNA (A), but not *AP-2 $\alpha$*  (B) and *AP-2 $\gamma$*  (C), significantly correlates with lower survival in lower-grade astrocytomas. **(D)** Analysis of TCGA database (TCGA, Cell 2013<sup>319</sup>) showing that *AP-2 $\beta$*  RNA levels are higher in the proneural GBM subtype compared to the other subtypes. **(E)** RT-PCR analysis showing up-regulation of *AP-2 $\beta$* , *Nestin* and *B-FABP* (stem cell markers) in A4-004 and A4-007 GBM cells cultured under standard or neurosphere culture conditions.

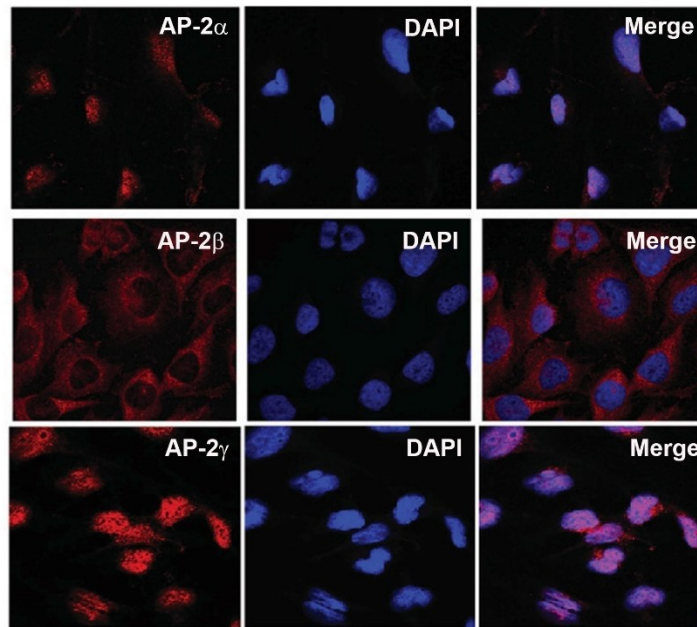
and *Nestin* were expressed at higher levels in neurosphere cultures compared to adherent cultures in both A4-004 and A4-007 (Figure 4.5E).

### **4.3.3 AP-2 $\beta$ localizes to the cytoplasm of adherent GBM cells**

As AP-2s are transcription factors, they are expected to localize to the nucleus. We carried out immunofluorescence analysis of AP-2 $\beta$  in U251 GBM cells using an AP-2 $\beta$ -specific antibody. AP-2 $\beta$  was almost exclusively found in the cytoplasm of these cells (Figure 6A). We therefore examined the subcellular location of AP-2 $\alpha$  and AP-2 $\gamma$  in U251 cells. In contrast to AP-2 $\beta$ , both AP-2 $\alpha$  and AP-2 $\gamma$  were found in the nucleus (Figure 4.6A). To confirm our immunofluorescence results, we carried out nuclear-cytoplasmic fractionation of 4 different GBM cell lines (U251, M049, T98 and A172) followed by western blotting. AP-2 $\beta$  was exclusively found in the cytoplasm of U251, M049 and T98. The only signal detected in A172 was the higher molecular weight band which was restricted to the cytoplasm (Figure 4.6B). The identity of this band remains to be determined. We used lamin A and  $\alpha$ -tubulin to ensure that our nuclear and cytoplasmic fractions, respectively, were reasonably pure. While there was some cytoplasmic contamination of the nuclear fractions, there appeared to be little to no contamination of the cytoplasmic fractions (Figure 4.6B).

Next, we carried out immunofluorescence analysis of AP-2 $\beta$  in patient-derived A4-004 adherent and neurosphere cultures. AP-2 $\beta$  was primarily found in the nucleus of A4-004 neurosphere cultures but was primarily found in the cytoplasm of A4-004 adherent cultures (Figure 4.7A). Nuclear and cytoplasmic fractionations show similar levels of AP-2 $\beta$  in the cytoplasm and nucleus of A4-004 neurosphere cultures (Figure 4.7B). The AP-

A



B

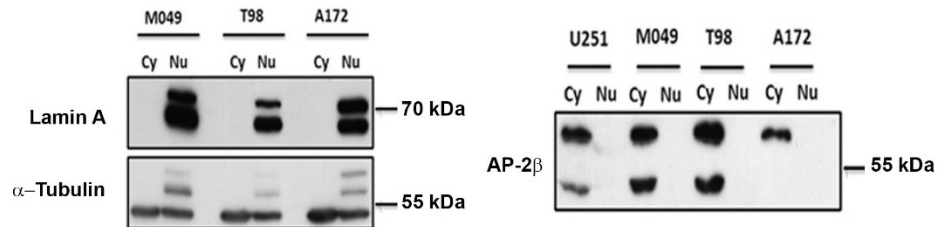


**Figure 4.6 Subcellular localization of AP-2 transcription factors.**

**(A)** Immunofluorescence analysis of AP-2 ( $\alpha$ ,  $\beta$  and  $\gamma$ ) in U251 GBM cells. Cells were fixed with 4% paraformaldehyde and immunostained with mouse anti-AP-2 $\alpha$  (3B5), rabbit anti-AP-2 $\beta$  (#2509), and mouse anti-AP-2 $\gamma$  (6E4/4). Cy3-conjugated secondary antibodies were used for immunodetection. Nuclei were stained with DAPI and images acquired by confocal microscopy using a 40x/1.3 oil immersion lens. All images are representative of the majority of cells observed.

**(B)** Nuclear and cytoplasmic fractions prepared from four GBM cell lines were electrophoresed through a 10% SDS-polyacrylamide gel. Proteins were transferred to a nitrocellulose membrane and immunostained with anti-AP-2 $\beta$  antibody. Lamin A was used as a loading control for nuclear fractions and  $\alpha$ -tubulin served as the loading control for cytoplasmic fractions. The band indicated by the arrow may be a post-translationally modified form of AP-2 $\beta$  or a non-specific band. This band was observed with every anti-AP-2 $\beta$  antibody tested. Cy = Cytoplasmic fraction and Nu = nuclear fraction.

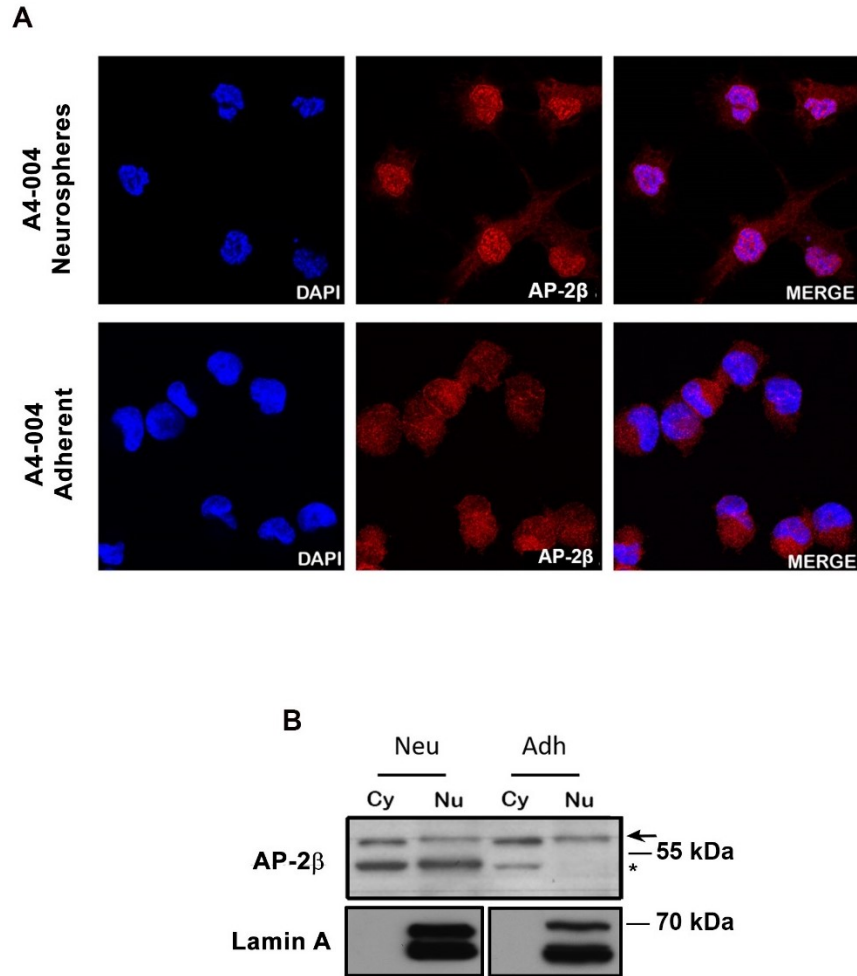


**Figure 4.7 Subcellular localization of AP-2β in A4-004 adherent and neurosphere cultures.**

(A) Immunofluorescence analysis of AP-2β in A4-004 GBM cells cultured under standard or neurosphere culture conditions. Cells were fixed with 4% paraformaldehyde and immunostained with a rabbit polyclonal anti-AP-2β antibody (#2509) followed by Cy-3 conjugated secondary antibody. Nuclei were stained with DAPI and images acquired by confocal microscopy using a 40x/1.3 oil immersion lens. All images are representative of the majority of cells observed under each condition. (B) Nuclear-cytoplasmic fractions of A4-004 cells were generated using NE-PER Nuclear and Cytoplasmic Extraction kit. Fifty μg of each fraction was loaded on a 10% SDS-polyacrylamide gel. The gel was electrophoresed and transferred to a nitrocellulose membrane and immunostained with specific AP-2β antibody. LaminA was used as a nuclear fraction control and α-tubulin was used as a cytoplasmic fraction control. The band indicated by the asterisk is AP-2β. The band indicated by the arrow may be a post-translationally modified form of AP-2β or a non-specific band. Cy= Cytoplasmic fraction and Nu= nuclear fraction.

2 $\beta$  signal is considerably weaker in A4-004 adherent cells compared to A4-004 neurosphere cultures and is mostly cytoplasmic (Figure 4.7B).

#### **4.3.4 Effect of AP-2 $\beta$ on GBM cell growth properties**

A4-004 neurospheres were transfected with scrambled siRNA or siRNAs targeting AP-2 $\beta$  (two pooled siRNAs). Based on qRT-PCR, AP-2 $\beta$  mRNA levels were reduced by 80% in these cells (Figure 4.8A) compared to cells transfected with a single siRNA targeting AP-2 $\beta$  which produced <2X decreases in AP-2 $\beta$  RNA levels. To measure cell proliferation, 25,000 cells/well were plated using 24-well plates. Cells in triplicate wells were counted every 24 h for a period of 96 h. No significant difference was observed in cells transfected with scrambled siRNA and AP-2 $\beta$  siRNAs. These results indicate that AP-2 $\beta$  does not affect A4-004 neurosphere cell proliferation (Figure 4.8B).

The migration of A4-004 neurospheres transfected with either scrambled or AP-2 $\beta$  siRNAs was examined using the scratch (wound healing) assay. The scratch was introduced once the cells had reached confluence. Cells were then allowed to migrate into the scratch for 18 h, with the filling-in of the scratched area measured by time-lapse photography. A significant reduction in A4-004 neurosphere cell motility was observed upon AP-2 $\beta$ -depletion compared to control cells (Figure 4.8C).

Next, we used the Transwell assay to examine the effect of AP-2 $\beta$  depletion on cell migration. A4-004 neurosphere cells were plated in the upper chamber and allowed to migrate across a PET membrane over a period of 24 h. In agreement with the scratch assay, AP-2 $\beta$  depletion resulted in a significant decrease in the number cells that migrated across the PET membrane compared to control cells (Figure 4.8D).

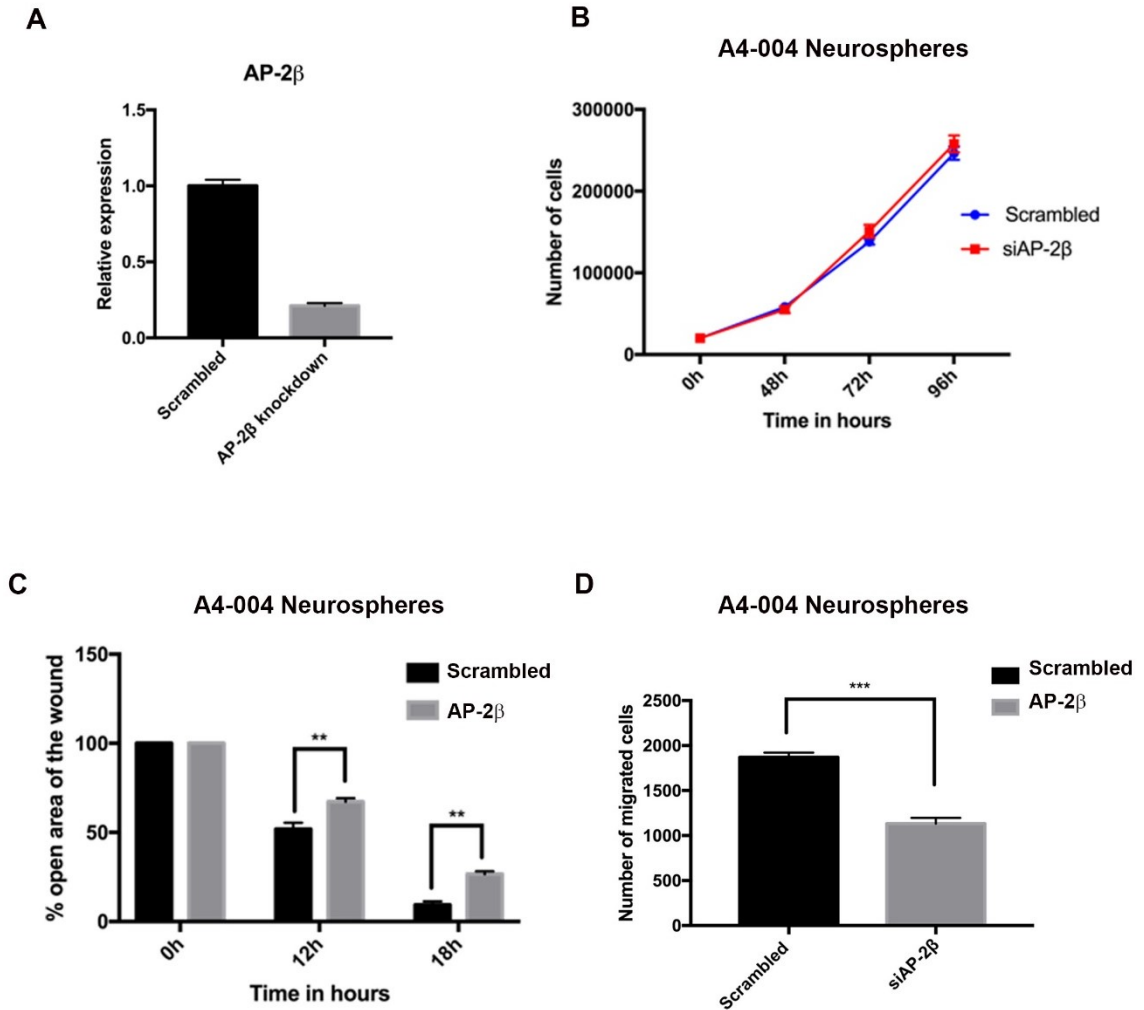


**Figure 4.8 Effect of AP-2 $\beta$  depletion on cell proliferation and migration in GBM cells.**

A4-004 cells cultured under neurosphere conditions were transfected with either scrambled siRNAs or siRNAs targeting AP-2 $\beta$ . **(A)** qPCR analysis of AP-2 $\beta$  in control and AP-2 $\beta$  knockdown cells. **(B)** Cell proliferation was measured by counting cells every 24 h for a period of 96 h using a Coulter counter. Thirty thousand cells per well were seeded in triplicate. **(C)** Cell migration was measured using the scratch (wound healing) assay. Cells were allowed to migrate into the scratch over a period of 18 h with live cell monitoring. Graphs represent percentage open area of the scratch. The data shown in the graphs represent an average of three independent experiments. **(D)** Transwell cell migration assay showing reduced cell migration upon AP-2 $\beta$  knockdown. Twenty-five thousand cells were seeded in the upper chamber and allowed to migrate across a PET membrane towards medium supplemented with 10% FCS over a period of 24 h. Migrated cells were fixed, stained and counted using Metamorph imaging software. The data shown in the graphs represent an average of two different experiments. The unpaired t-test was used to measure statistical significance. \*\*\* represents  $p < 0.001$ . Experiments were repeated 3 times for each cell line.

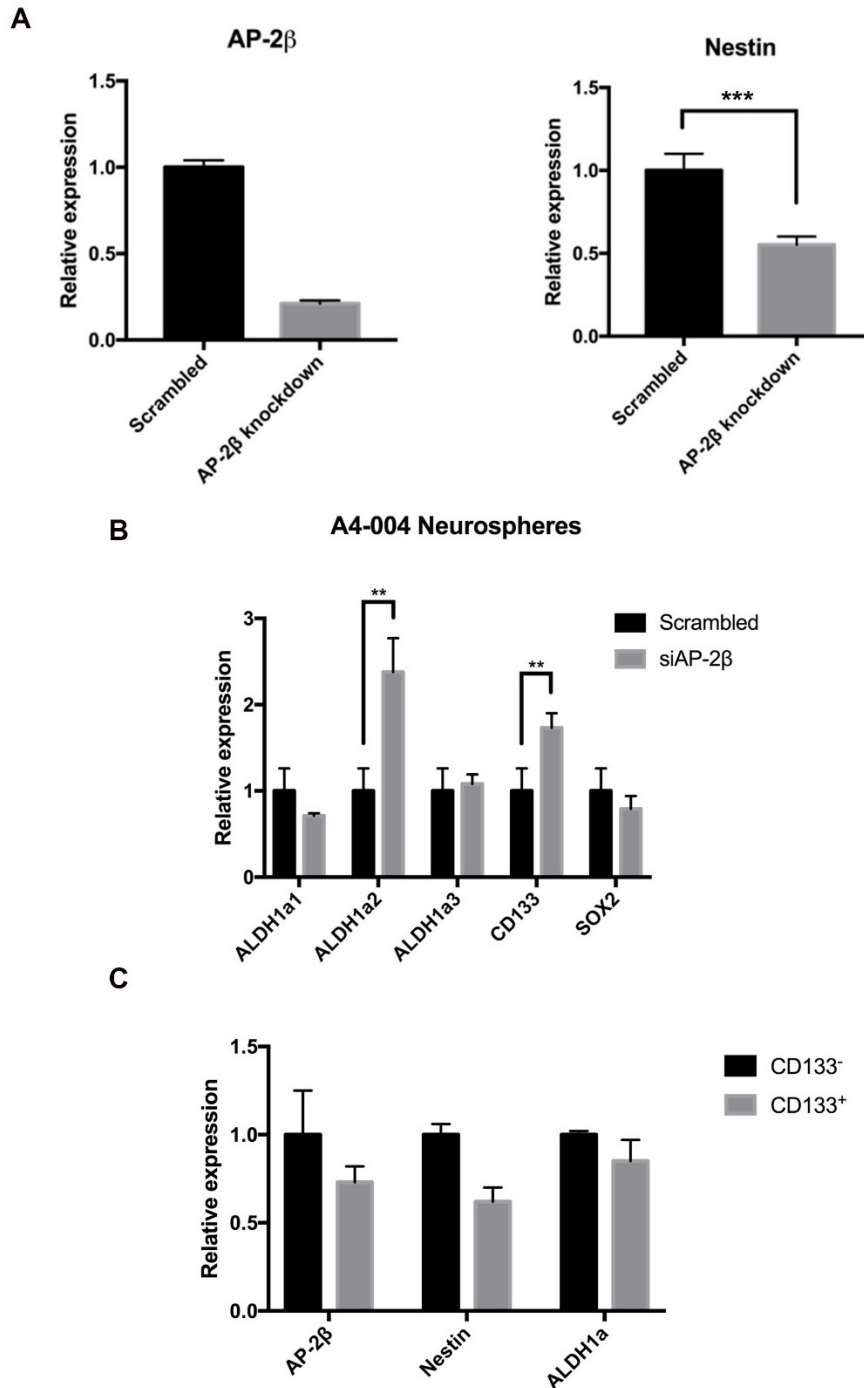


**Figure 4.9 Effect of AP-2β knockdown on stem cell markers in GBM cells.**

A4-004 cells cultured under neurosphere conditions were transfected with either scrambled siRNAs or siRNAs targeting AP-2β. **(A)** qPCR analysis of *Nestin* mRNA in control and AP-2β-depleted cells. **(B)** qPCR analysis *ALDH1a1*, *ALDH1a2*, *ALDH1a3*, *CD133* and *Sox2* in control and AP-2β-depleted cells. **(C)** Cell sorting was carried out using CD133 antibody, followed by qPCR analysis to determine *AP-2β*, *Nestin* and *ALDH1a1* RNA levels in CD133<sup>-</sup> vs CD133<sup>+</sup> cells.

#### **4.3.5 Effect of AP-2 $\beta$ on GBM stem cell markers**

Quantitative RT-PCR was carried out to investigate the effect of AP-2 $\beta$  depletion on the expression of stem cell markers in A4-004 neurospheres. A significant reduction in *Nestin* RNA levels (~50%) was observed upon AP-2 $\beta$  depletion (Figure 4.9A). None of the other stem markers tested showed a decrease in RNA levels upon AP-2 $\beta$  depletion. In fact, the expression of two stem cell markers *ALDH1a2* and *CD133*, was significantly increased upon AP-2 $\beta$  depletion (Figure 4.9B).

The different effect of AP-2 $\beta$  depletion on various neural stem cell markers suggest either a role for AP-2 $\beta$  in a subset of GBM neural stem-like cell populations and/or a specialized role for this transcription factor in specific stem cell properties. To examine the former, we used A4-004 neurosphere cultures to sort out CD133<sup>+</sup> from CD133<sup>-</sup> cells with a FACS sorter. We then carried out qRT-PCR analysis on these two populations of cells. Our results indicate that both AP-2 $\beta$  and *Nestin* are expressed at higher levels in CD133<sup>-</sup> compared to CD133<sup>+</sup> cells, with no change in *ALDH1* levels (Figure 4.9C). We also used the ALDEFLUOR reagent to detect aldehyde dehydrogenase production, a measure of stemness, in A4-004 neurosphere cultures. SK-Br3 was used as a positive control for these experiments. In contrast to SK-Br3, no significant difference was observed in the presence or absence of DEAB, an inhibitor of ALDH activity, in A4-004 neurospheres cultured under either normoxic or hypoxic conditions, indicating that there little to no cells with ALDH activity in these cultures (Figures 4.10A, B, C).

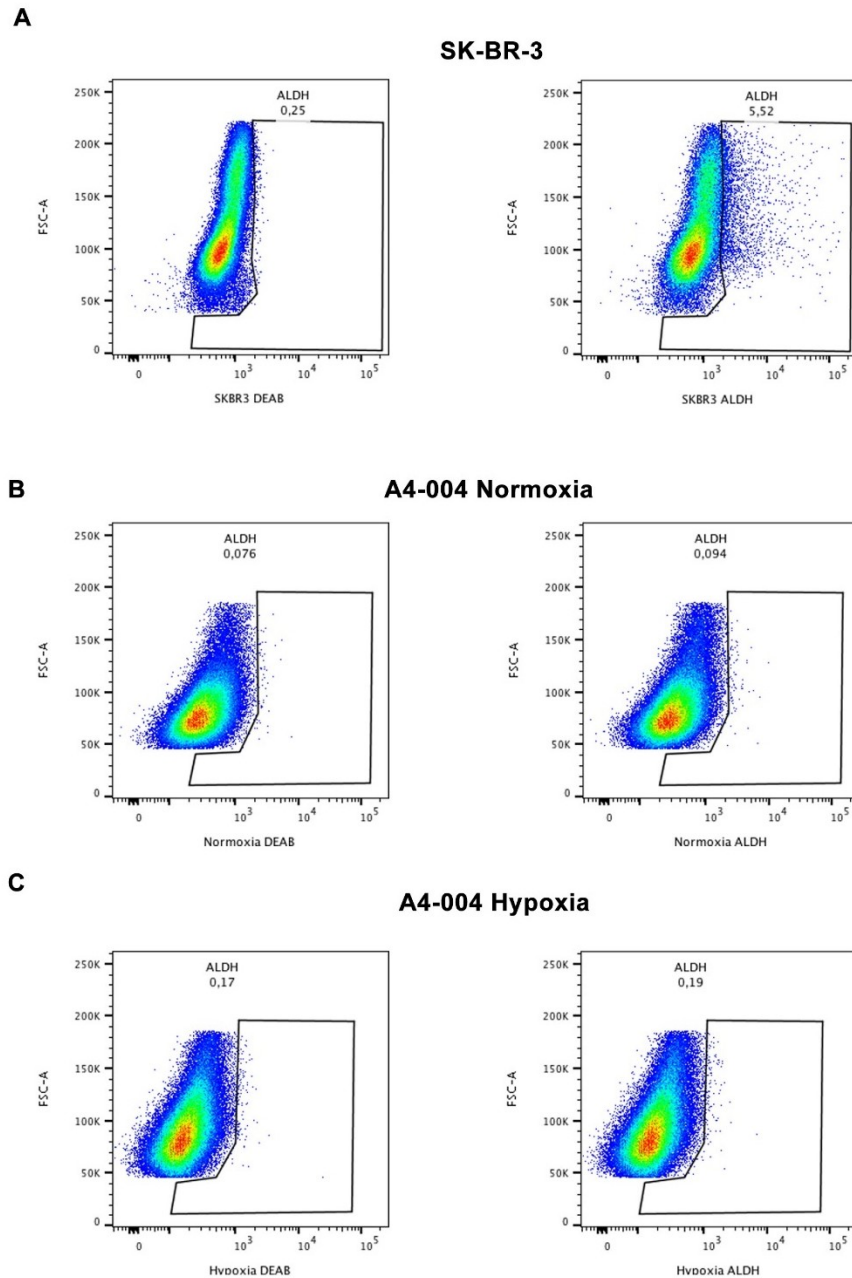


**Figure 4.10 A4-004 cell sorting based on ALDH activity.**

Analysis of ALDH activity in **(A)** SK-BR3 cells **(B)** A4-004 cells cultured under normoxic conditions and **(C)** A4-004 cells cultured under hypoxic (0.5% O<sub>2</sub>) conditions. Cells were resuspended in ALDEFLOUR assay buffer. ALDEFLOUR DEAB reagent was added to the “control” tube and activated ALDEFLOUR reagent was added to the “test” tube. Samples were analyzed in a FACSCanto II analyzer.

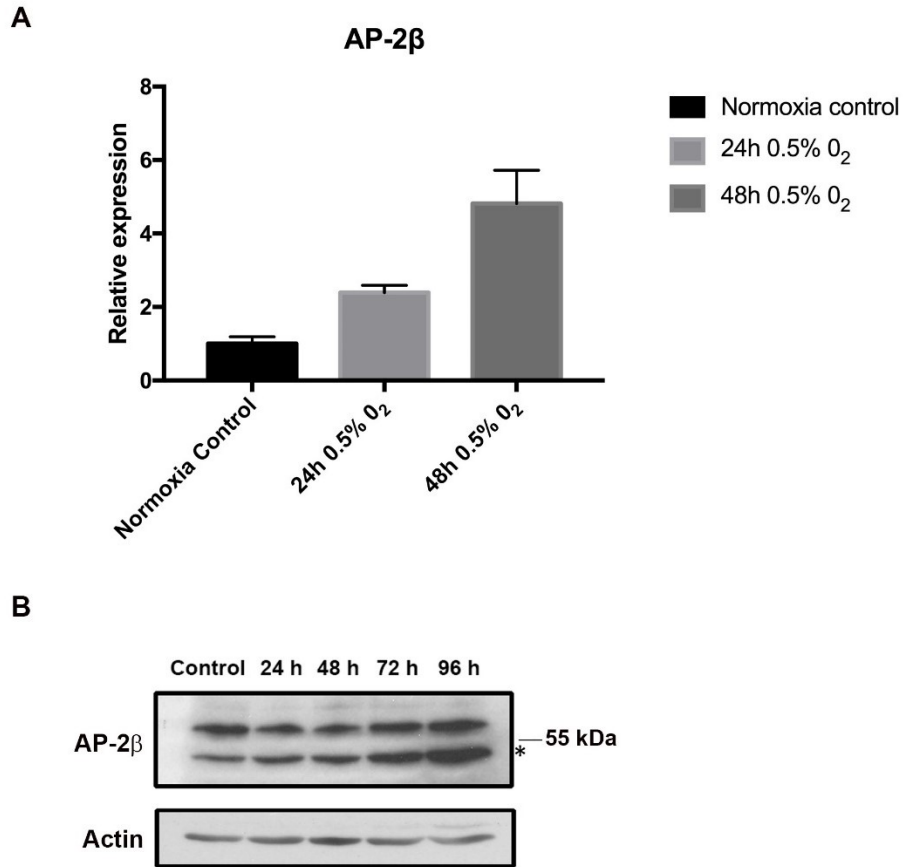


**Figure 4.11 AP-2 $\beta$  mRNA and protein are induced under hypoxia.**

**(A)** qPCR analysis of *AP-2 $\beta$*  in A4-004 cells cultured under normoxic (20% O<sub>2</sub>) or hypoxic (0.5% O<sub>2</sub>) conditions for 24 h and 48 h. **(B)** Western blot analysis showing AP-2 $\beta$  protein levels in cells cultured under either normoxic (20% O<sub>2</sub>) or hypoxic (0.5% O<sub>2</sub>) conditions after 24 h, 48 h, 72 h and 96 h.

#### **4.3.6 Hypoxia induces AP-2 $\beta$ expression**

GBM tumours are very hypoxic and hypoxia has been associated with induction of stem cells in GBM<sup>321</sup>. To examine if hypoxia affects the expression of AP-2 $\beta$ , we cultured A4-004 adherent cells which express low levels of AP-2 $\beta$  under hypoxic conditions (0.5% O<sub>2</sub>) for a period of 48 h, harvesting cells after 24 h and 48 h. A gradual increase in AP-2 $\beta$  RNA levels over time was observed based on qRT-PCR (Figure 4.11A). Western blot analysis was carried out to determine whether AP-2 $\beta$  protein levels are also increased under hypoxia. Cells were cultured under hypoxia (0.5% O<sub>2</sub>) and harvested every 24 h for a period of 96 h. Similar to RNA levels, AP-2 $\beta$  protein levels gradually increased with increasing time under hypoxia (Figure 4.11B – lower band marked by the asterisk).

As AP-2 $\beta$  depletion results in reduced cell migration, we then transfected A4-004 neurosphere cells with scrambled control and AP-2 $\beta$  siRNAs to examine the effect of AP-2 $\beta$  depletion on genes associated with migration under normoxic and hypoxic conditions. Western blot analysis revealed reduction in phospho-Smad and vimentin upon AP-2 $\beta$  knockdown under both normoxic (20% O<sub>2</sub>) and hypoxic (0.5% O<sub>2</sub> 72 h) conditions (Figure 4.12A). We also tested the effect of AP-2 $\beta$  depletion on other proteins including SOX2, a marker of stem cells and EGFR. A reduction in both SOX2 and EGFR expression was observed upon AP-2 $\beta$  knockdown under both hypoxic and normoxic conditions (Figure 4.12B).

#### **4.3.7 Post-translational modification of AP-2 $\beta$**

To date, we have tested three different AP-2 $\beta$  antibodies targeting different regions of the AP-2 $\beta$  protein. All three antibodies detected two prominent bands (one migrating at the expected ~50 kDa for AP-2 $\beta$ , and a slower migrating band) (Figure 13A). These

data suggest that the slower migrating band may represent a post-translationally modified version of AP-2 $\beta$ . To determine if AP-2 $\beta$  is post-translationally modified, we focused on two different types of post-translation modification: phosphorylation and sumoylation. To address phosphorylation, we prepared whole cell lysates from U251 and U87 GBM cells and then treated the lysates with lambda phosphatase. There was no change in the migration of the two bands using this assay suggesting that AP-2 $\beta$  may not be phosphorylated in these cell lines (Figure 4.13B). We also carried out 2D gel electrophoresis using A4-004 adherent and neurosphere cells; however, the results were inconclusive.

AP-2 has been shown to be sumoylated in breast cancer and colorectal cancer cells <sup>113</sup>. We therefore investigated AP-2 sumoylation in GBM cells. For these experiments, we first immunoprecipitated SUMO from U251 and A4-004 neurosphere cells using an anti-SUMO antibody. We then carried out western blot analysis of the IP supernatant and immunoprecipitate using anti-AP-2 $\beta$  antibody. The high molecular weight putative AP-2 $\beta$  band was not immunoprecipitated with the SUMO antibody (Figure 4.13C). When we used an anti-AP-2 $\gamma$  antibody for western blot analysis, we detected a weak high molecular weight band (Figure 4.13D), suggesting that AP-2 $\gamma$  may be sumoylated in GBM cells. Interestingly, we also found that inhibition of sumoylation by ginkgolic acid (an inhibitor of E1 ligases) in A4-004 cells cultured under neurosphere conditions is accompanied by a change in the localization of AP-2 $\beta$ , from nuclear to the cytoplasm (Figure 4.14).

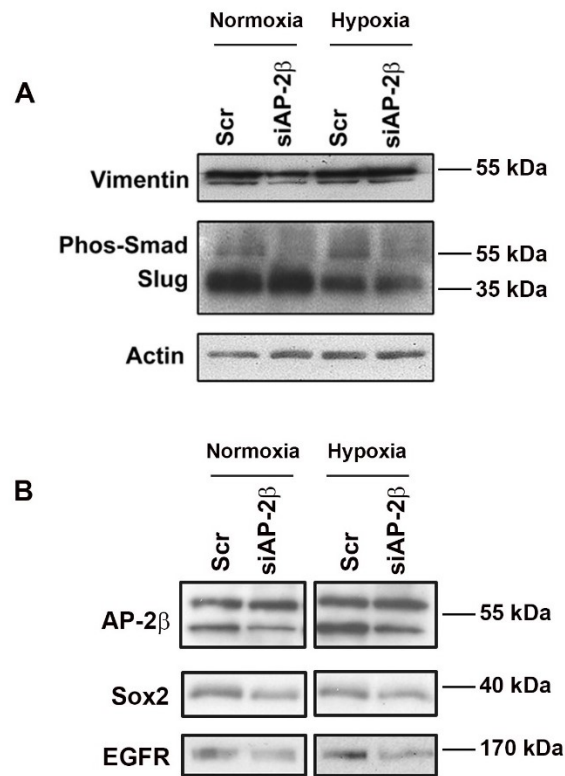


**Figure 4.12 Effect of AP-2β on target genes in GBM cells.**

A4-004 cells cultured under neurosphere conditions were transfected with either scrambled siRNAs or siRNAs targeting AP-2β. To examine efficiency of AP-2β knockdown, western blot analysis was carried out to determine AP-2β protein levels under normoxic (20% O<sub>2</sub>) or hypoxic (0.5% O<sub>2</sub> 72 h) conditions (top). (A) Western blot analysis of proteins associated with cell migration (vimentin, phospho-Smad and Slug). (B) Western blot analysis of SOX2 (stem cell marker) and EGFR. Actin was used as a loading control.

#### 4.4 Discussion

The AP-2 family of transcription factors plays key roles in several malignancies by regulating the transcription of genes associated with cell cycle, migration and invasion. Here, we show that four of the five members of the AP-2 family are expressed in GBM. The role of AP-2 $\beta$  in GBM appears to be at least partly regulated through its subcellular localization, being found in the cytoplasm of GBM cells that show reduced expression of neural stem cell markers. We propose that expression of AP-2 $\beta$ , especially nuclear AP-2 $\beta$ , is associated with GBM neural stem cell properties.

Our data indicate that elevated levels of *AP-2 $\beta$*  RNA in tumour tissue from lower grade astrocytomas are associated with reduced patient survival. In keeping with an association with more aggressive tumours, *AP-2 $\beta$*  is most highly expressed in the proneural subtype in GBM. The proneural subtype is associated with neural stem cells and patients with this subtype generally respond poorly to chemotherapy<sup>57, 59</sup>. Stem cell markers associated with proneural GBM include OLIG2 and SOX2<sup>57, 58</sup>. Although we did not look at OLIG2 association with AP-2 $\beta$ , we show that AP-2 $\beta$  knockdown in GBM cells results in reduced SOX2 expression. These results indicate an association between AP-2 $\beta$  and GBM stem cell properties and suggest a possible transcription regulatory link between AP-2 $\beta$  and GBM stem cell markers.

Transcription factors are classically believed to function by regulating the expression of their target genes. The subcellular localization of AP-2 $\beta$  suggests an additional mechanism for regulating gene expression through subcellular localization. AP-2 $\beta$  was enriched in the cytoplasm of adherent GBM cell lines, as well as adherent A4-004 cells derived from a GBM patient. However, when A4-004 cells were cultured under

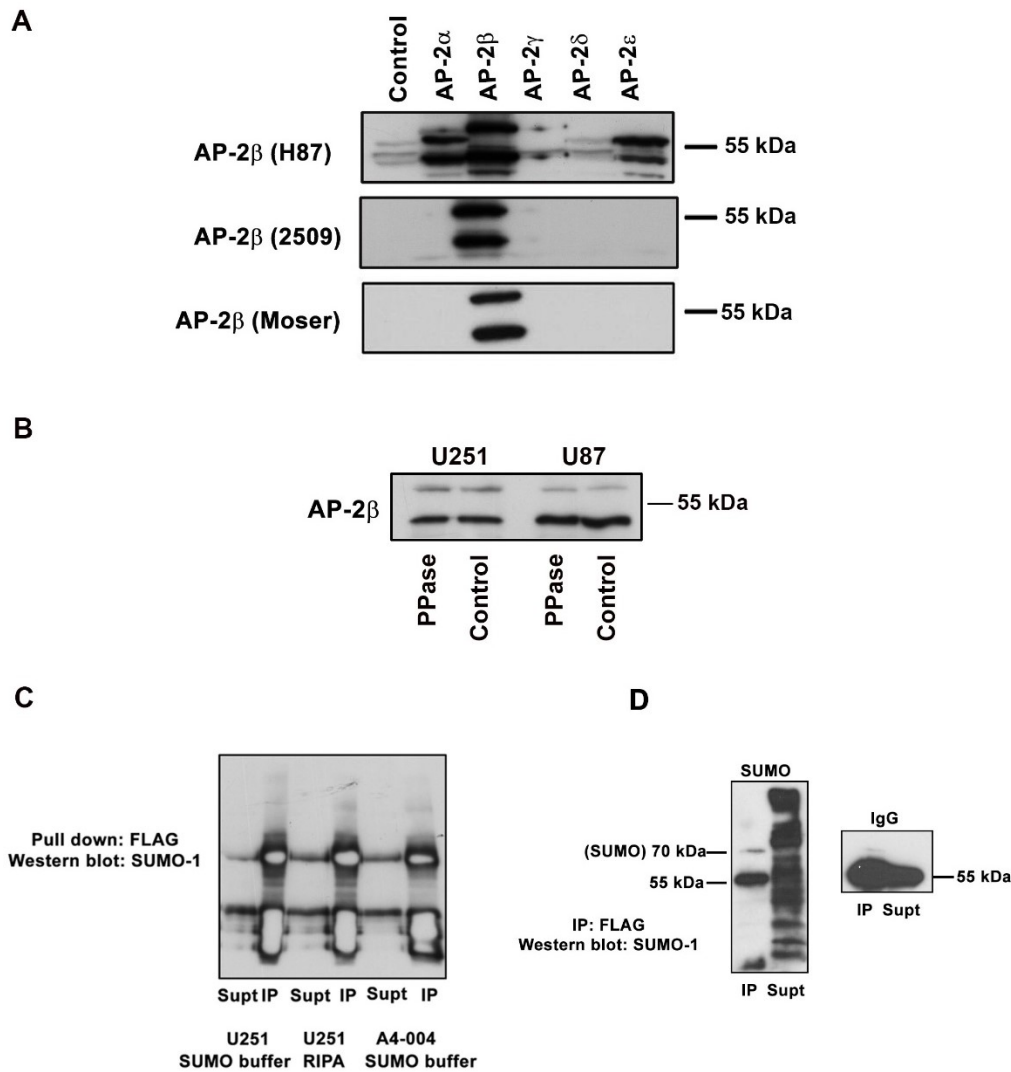


**Figure 4.13 Analysis of AP-2 $\beta$  post-translational modification.**

**(A)** Western blot analysis of different AP-2 $\beta$  antibodies. HeLa cells were transfected with vector control, AP-2 $\alpha$ , AP-2 $\beta$ , AP-2 $\gamma$ , AP-2 $\delta$  or AP-2 $\epsilon$  expression constructs. Blots were immunostained with 3 different AP-2 $\beta$  antibodies, each of which recognized two bands. **(B)** Phosphatase assay for detection of AP-2 $\beta$  phosphorylation. Cells lysed in RIPA buffer were treated with lambda protein phosphatase followed by western blot analysis with AP-2 $\beta$  antibody. Controls are identically-treated cells with no lambda phosphatase treatment. **(C, D)** Sumoylation assay for detection of AP-2 $\beta$  and AP-2 $\gamma$  sumoylation. Cells transfected with Flag-tagged AP-2 $\beta$  or AP-2 $\gamma$  expression constructs were lysed with RIPA buffer or modified RIPA (SUMO) buffer. Immunoprecipitations were carried out with the FLAG antibody followed by western blot analysis with the SUMO antibody.

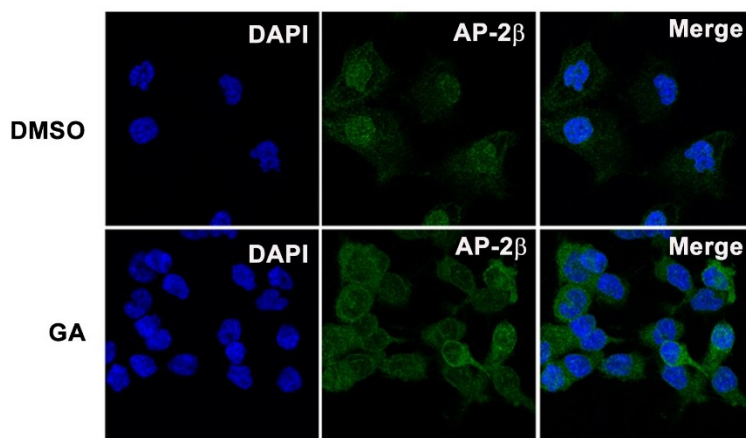


**Figure 4.14 Inhibition of sumoylation affects AP-2 $\beta$  subcellular localization.**

Immunofluorescence analysis of AP-2 $\beta$  in A4-004 GBM cells cultured in neurosphere conditions treated with either DMSO or GA. Cells were fixed with 4% paraformaldehyde and immunostained with a rabbit polyclonal anti-AP-2 $\beta$  antibody (#2509) followed by Alexa 488-conjugated secondary antibody. Nuclei were stained with DAPI and images acquired by confocal microscopy using a 40x/1.3 oil immersion lens. All images are representative of the majority of cells observed under each condition.

neurosphere conditions which promote the expression of GBM stem markers, AP-2 $\beta$  was present in the nucleus. These results suggest that shunting of AP-2 $\beta$  from the nucleus to the cytoplasm may control the expression of AP-2 $\beta$  target genes, particularly those associated with GBM stem cells.

Subcellular localization of AP-2 transcription factors has previously been observed in a number of malignancies; for example, cytoplasmic AP-2 $\alpha$  has been observed in melanoma where it is associated with melanoma progression, in ovarian cancer where it is associated with poor survival and in breast carcinomas where it is associated with aggressive properties <sup>154-157</sup>. A previous study in GBM tumours showed that AP-2 $\alpha$  was primarily localized to the cytoplasm. In contrast, AP-2 $\alpha$  was mostly found in the nucleus of low grade gliomas <sup>168, 169</sup>. This may reflect the fact that the bulk of GBM tumour cells are not stem cell-like. Although we did not examine the subcellular distribution of AP-2 $\alpha$  in GBM patient tissue, we observed a nuclear pattern for AP-2 $\alpha$  in all GBM cell lines tested using the same antibody as the previous group. Thus, the difference in AP-2 $\alpha$  subcellular localization is most likely due to the use of tumour tissue versus cell lines for analysis. Analysis of the subcellular localization of AP-2 $\beta$  in GBM patient tissues revealed a primarily nuclear distribution in localized regions of the tumours, with cytoplasmic AP-2 $\beta$  observed in sparse cells in tumour tissues. Thus, AP-2 $\beta$  may have different roles in GBM depending on whether it's expressed in the nucleus or cytoplasm. Co-immunostaining analysis will be required to determine whether there is an association between nuclear AP-2 $\beta$  and expression of GBM stem cell markers.

The mechanisms regulating the subcellular localization of AP-2s have not been well studied. To date, no nuclear localization signal (NLS) sequences have been reported

in AP-2 proteins. However, there is one study that shows that the subcellular localization of AP-2 $\gamma$  is regulated by physical interaction with the tumour suppressor gene, WWOX<sup>322</sup>. When WWOX is present, AP-2 $\gamma$  is sequestered to the cytoplasm<sup>322</sup>. Interestingly, mutations in the DNA binding region of AP-2 $\alpha$  are associated with Branchio-Oculo-Facial Syndrome (BOFS)<sup>132</sup>. In these patients, AP-2 $\alpha$  localizes to the cytoplasm rather than the nucleus. Limited sequencing analysis of AP-2 $\beta$  RNA in GBM cell lines revealed no mutations.

Post-translation modifications such as phosphorylation and sumoylation can regulate subcellular localization of proteins<sup>323, 324</sup>. AP-2 is phosphorylated by cAMP dependent Protein Kinase A (PKA)<sup>108, 325</sup>. Phosphorylation of AP-2 increases AP-2 transcriptional activity<sup>112</sup>. We were unable to find clear evidence of AP-2 phosphorylation in our study using two different approaches: phosphatase treatment and 2D gel electrophoresis. Our preliminary data show that elevation of cAMP levels by Rolipram, a phosphodiesterase type 4 inhibitor, in A4-004 adherent cells results in a change in the localization of AP-2 $\gamma$ , from the cytoplasm to the nucleus (Figure 4.15A). However, Rolipram had no effect on AP-2 $\beta$  (Figure 4.15B). We also tested the effect of Rolipram on the regulation of *B-FABP* by AP-2. We found that overexpression of AP-2, especially AP-2 $\beta$ , in the presence of Rolipram results in decreased expression of B-FABP (Figure 4.15C). These results suggest that cAMP-dependent phosphorylation of AP-2 may affect its transcription regulatory activity.

Another form of post-translational modification associated with AP-2 is sumoylation. Both AP-2 $\alpha$  and AP-2 $\gamma$  have been shown to be sumoylated, with sumoylation of AP-2 associated with maintenance of stem cells in breast and colorectal

cancer <sup>110, 113</sup>. There are no studies so far indicating that AP-2 $\beta$  is sumoylated, although the predicted sumoylation sites at lysine 10 (AP-2 $\alpha$  and AP-2 $\gamma$ ) and lysine 21 (AP-2 $\beta$ ) are conserved. Our preliminary work to address AP-2 $\beta$  sumoylation by immunoprecipitating sumoylated proteins followed by western blot analysis did not reveal AP-2 $\beta$  sumoylation, although we did obtain evidence of AP-2 $\gamma$  sumoylation using this approach. These results are not conclusive as proteins are rapidly desumoylated after cell lysis. Another approach involving over-expression of tagged SUMOs will be used to further address AP-2 $\beta$  sumoylation. Preliminary data using lysates prepared from SUMO-overexpressing HeLa cells (kind gift from Andrew Locke) indicate that AP-2 $\beta$  can indeed be sumoylated under these conditions. However, we found no evidence that sumoylation of AP-2 $\beta$  affected its subcellular localization in HeLa cells. Thus, further studies are required to determine how AP-2 $\beta$  subcellular localization is controlled in GBM cells. There is a possibility that physical interaction of AP-2 $\beta$  with some proteins may sequester AP-2 $\beta$  to the cytoplasm of GBM cells that are not “stem cell-like”. In GBM neurospheres, pathways involved in maintaining stem cell properties may block these interactions allowing AP-2 $\beta$  to translocate to the nucleus.

Recent studies have shown the co-occurrence of different types of GBM stem cells within one tumour population giving rise to intratumoural heterogeneity <sup>320</sup>. GBM stem cell heterogeneity is detected by using several markers characteristically associated with GBM stem cells to look individual cells within a single tumour. *In vitro* analysis also shows that GBM stem cells can give rise to different types of stem cells as well as differentiate into non-stem-like cells <sup>320</sup>. In turn, a differentiated cell can reacquire stem-cell like characteristics under specific environmental conditions such as hypoxia, thereby adding

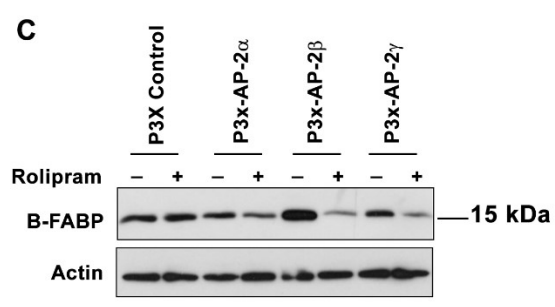
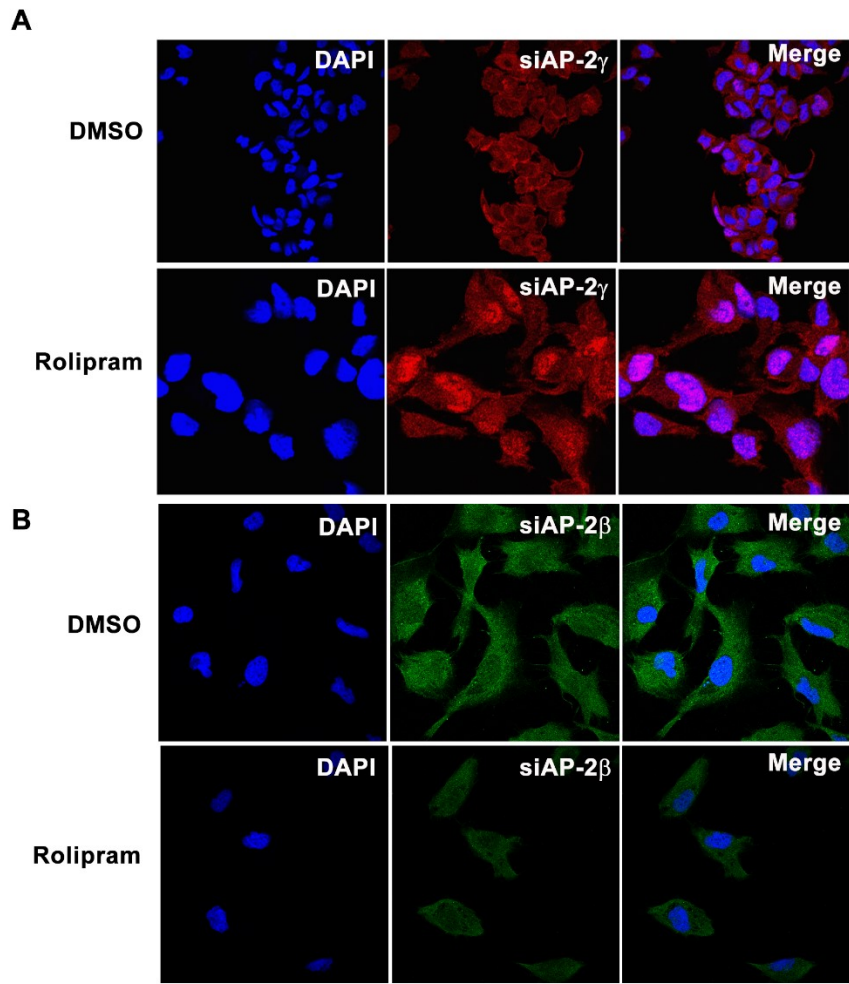


**Figure 4.15 Effect of Rolipram on AP-2 proteins.**

**(A, B)** Immunofluorescence analysis of AP-2 $\gamma$  **(A)** and AP-2 $\beta$  **(B)** in A4-004 GBM cells cultured in adherent conditions treated with either DMSO or Rolipram. Cells were fixed with 4% paraformaldehyde and immunostained with a rabbit polyclonal anti-AP-2 $\gamma$  antibody (#6E4/4) **(A)** or rabbit polyclonal AP-2 $\beta$  antibody (#2509) **(B)**, followed by Cy-3(or Alexa 488)-conjugated secondary antibody. Nuclei were stained with DAPI and images acquired by confocal microscopy using a 40x/1.3 oil immersion lens. All images are representative of the majority of cells observed under each condition. **(C)** Western blot analysis showing the effect of Rolipram on B-FABP expression. Cells transfected with control vector, AP-2 $\alpha$ , AP-2 $\beta$  or AP-2 $\gamma$  expression constructs were cultured in the absence or presence of Rolipram. Immunoblotting was carried out with polyclonal B-FABP antibody (made in house).

to the complexity of intratumoural heterogeneity. Thus, targeting a specific type of GBM stem cell may not be sufficient for treatment as other types of stem-like cells may either co-exist or be induced within the same tumour. It is possible that AP-2 $\beta$  plays a role in expression of specific stem cell markers in GBM cells. For example, AP-2 $\beta$  knockdown resulted in a significant decrease in the expression of stem cell marker Nestin; however, levels of another stem cell marker, CD133, were increased. Furthermore, CD133+ve cells enriched by cell sorting showed higher expression levels of both AP-2 $\beta$  and Nestin. These apparent discrepancies in stem cell marker expression may be explained by AP-2 $\beta$  association with a certain type of stem cells. Another explanation is that there is a compensatory mechanism at play, with a decrease in the levels of one stem cell marker (e.g. Nestin) resulting in an increase in another stem cell marker (e.g. CD133). More studies are needed to understand the mechanism for maintenance of different types of stem cells in GBM.

SOX2 mRNA levels did not significantly change upon AP-2 $\beta$  knockdown although SOX2 protein levels were reduced. The lack of effect at the mRNA level may be due to induction of a feedback pathway resulting from reduced SOX2 protein levels. Also, an important issue to be considered here is that AP-2 proteins bind to the promoters of their target genes as homodimers or heterodimers (amongst their family members), thus the expression level of other AP-2 proteins may affect the results we see in AP-2 $\beta$ -depleted cells. In addition, the effect of AP-2 $\beta$  depletion may be compensated for by other AP-2 family members. To begin to address the latter, we examined SOX2 expression upon combined knockdown of AP-2 $\beta$  and AP-2 $\alpha$  or AP-2 $\beta$  and AP-2 $\gamma$  in A4-004 neurosphere cultures. Western blot analysis showed a significant decrease in SOX2 protein levels

upon combined knockdown of AP-2 $\beta$  and AP-2 $\gamma$  (Figure 4.16). This suggests that AP-2 $\beta$ /AP-2 $\gamma$  heterodimers may bind to the *SOX2* promoter and regulate its expression.

Structurally, AP-2 proteins have a highly conserved DNA binding and dimerization domain at the carboxy terminus and they bind to a consensus recognition element GCCNNNGGC as homodimers or heterodimers<sup>96</sup>. The amino terminus consists of a transactivation domain, which is not well conserved. These conserved and variable structural entities in AP-2 proteins may allow different protein-protein and protein-DNA interactions and may govern AP-2 target gene specificity. For example, AP-2 $\alpha$ , AP-2 $\beta$  and AP-2 $\gamma$  can all bind as either homodimers or heterodimers to an AP-2 recognition site in the *c-erbB2* promoter; however, AP-2 $\alpha$  and AP-2 $\gamma$  are four times more active than AP-2 $\beta$  at activating a *c-erbB2*-driven reporter construct.

Given that AP-2 proteins can bind to similar target sequences as either homodimers or heterodimers, we also tested the effect of AP-2 $\alpha$  and AP-2 $\gamma$  knockdown on GBM cell motility (scratch assay). In contrast to AP-2 $\beta$  knockdown which resulted in reduced cell motility and migration, knockdown of either AP-2 $\alpha$  or AP-2 $\gamma$  resulted in increased cell motility compared to the scrambled control (Figure 4.17A). Furthermore, we observed different effects on cell proliferation and colony formation depending on which AP-2 was knockdown, with AP-2 $\beta$  or AP-2 $\gamma$  knockdown having no effect on cell proliferation, but AP-2 $\alpha$  knockdown resulting in a significant decrease in cell proliferation and colony formation (Figures 4.17B, C). Further studies are required involving co-depletion of two or more AP-2s to fully address the interplay of AP-2 transcription factors in GBM cells.

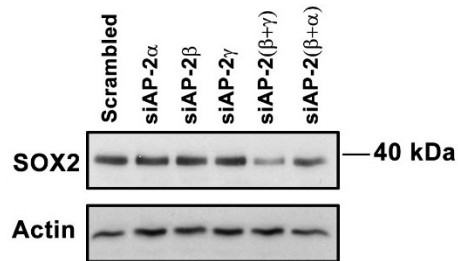


**Figure 4.16** Western blot analysis showing the effect of AP-2 knockdown on SOX2 expression.

A4-004 cells cultured under neurosphere conditions were transfected with vector control or AP-2 $\alpha$ , AP-2 $\beta$  or AP-2 $\gamma$ , expression constructs either individually or in combination. Immunoblotting was carried out using a polyclonal SOX2 antibody (#2748).

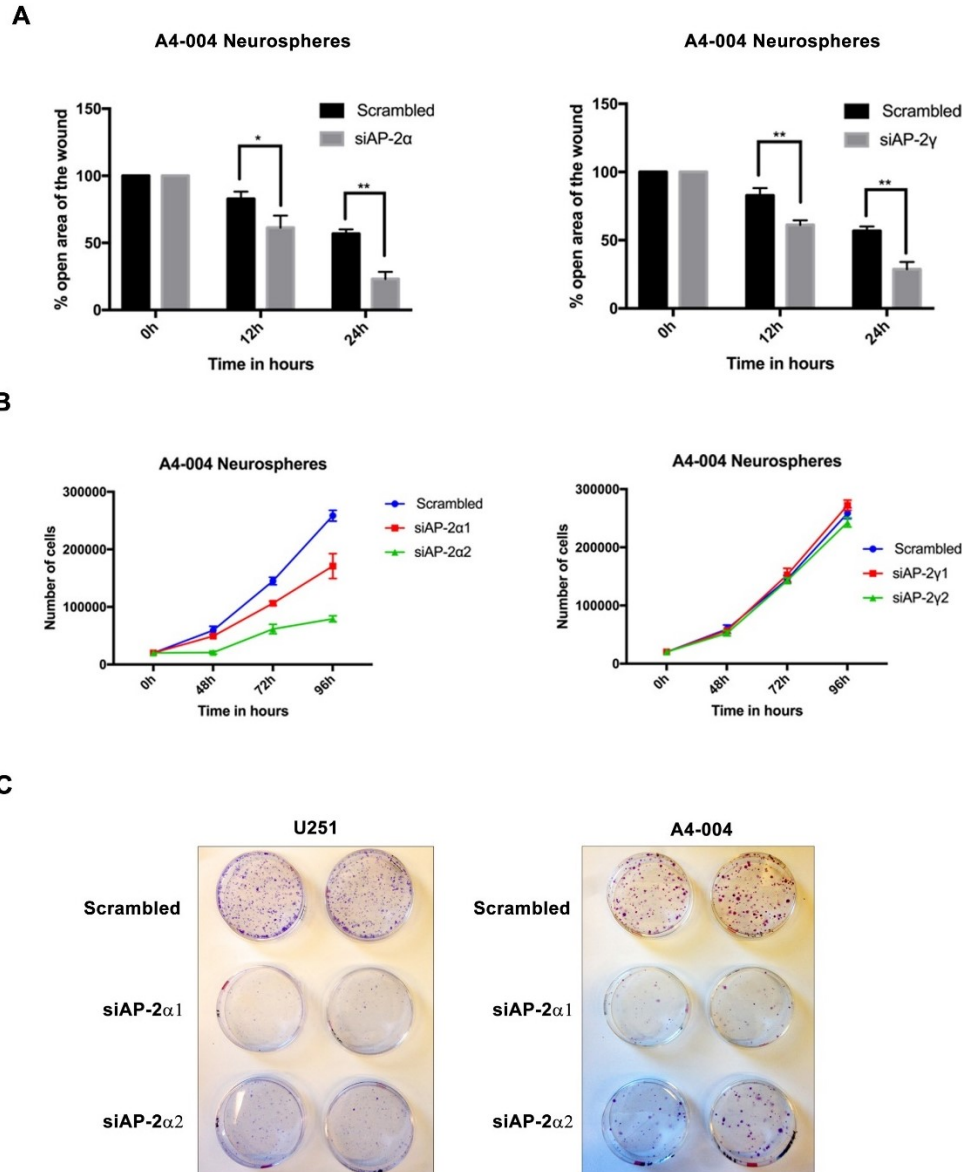


**Figure 4.17 AP-2 $\alpha$  and AP-2 $\gamma$  affects GBM growth properties.**

A4-004 cells cultured under neurosphere conditions were transfected with either scrambled siRNAs or siRNAs targeting AP-2 $\alpha$  or AP-2 $\gamma$ . **(A)** Cell migration was measured using the scratch (wound healing) assay. Cells were allowed to migrate into the scratch over a period of 18 h with live cell monitoring. Graphs represent percentage open area of the scratch. The data shown in the graphs represent an average of three independent experiments. **(B)** Cell proliferation was measured by counting cells every 24 h for a period of 96 h using a Coulter counter. Thirty thousand cells per well were seeded in triplicate. **(C)** Colony formation was measured by seeding U251 and A4-004 cells at low density (500 cells/6 cm plates) and counting colonies after 12 days in culture. Cells were stained with crystal violet. The unpaired t-test was used to measure statistical significance. \*\*\* represents  $p < 0.001$ . Experiments were repeated 3 times for each cell line.

In conclusion, we show that AP-2 $\beta$  is expressed in GBM cell lines and patient tissues. High levels of AP-2 $\beta$  mRNA are associated with reduced survival in glioma patients and AP-2 $\beta$  is preferentially expressed in the proneural GBM subtype, which is associated with stem cells in GBM. We found that AP-2 $\beta$  is highly expressed in patient-derived neurosphere cultures compared to adherent cultures and is localized to the nucleus of neurosphere cells in contrast to the cytoplasmic localization found in adherent cells cultured under standard conditions. AP-2 $\beta$  depletion results in reduction in the expression of stem cell markers Nestin and SOX2. Moreover, AP-2 $\beta$  expression is induced by hypoxia, a condition that favors stem cell survival. These results suggest that AP-2 $\beta$  is associated with stem cell maintenance in GBM. Furthermore, AP-2 $\beta$  knockdown in GBM cells leads to decreased cell migration, suggesting a link between AP-2 $\beta$  expression and increased motility/migration/infiltration. Overall, our study points to a role for AP-2 $\beta$  in GBM tumour progression.

## **Chapter 5 Discussion and Future directions**

Many hallmarks of early embryonic development are shared by cells undergoing malignant transformation. Embryonic development begins from a single cell which then undergoes proliferation, migration, differentiation while also interacting with other cells and the microenvironment. These characteristic features also apply to cancer. For example, spatial and temporal activation of key signaling pathways such as Wnt<sup>326</sup>, Hedgehog<sup>327</sup> and Notch, is necessary for embryonic development<sup>228</sup>. Aberrant regulation of these signaling pathways in adult cells has been associated with tumour progression and metastasis<sup>328</sup>.

Transcription factors are an integral part of cellular signaling pathways and play a key role in gene regulation during early embryonic development and in cancer<sup>329</sup>. Spatial and temporal coordination of transcription factor expression regulates key steps in embryonic development and cancer formation<sup>329</sup>. In this thesis, we explore the role of two transcription factor families, AP-2 and NFI, in development and cancer. Both AP-2 and NFI transcription factors are important for embryonic development and are associated with several malignancies. The work described in this thesis focuses on three main projects. In Chapter 2, we study the expression of AP-2 $\epsilon$  in the amacrine cells of the retina. In Chapter 3, we focus on the role of NFI transcription factors in glioblastoma and in Chapter 4, we examine how AP-2s affect glioblastoma cell growth properties.

## 5.1 Summary and key findings

AP-2 transcription factors play important roles in the regulation of gene expression during development. Four of the five members of the AP-2 family (AP-2 $\alpha$ , AP-2 $\beta$ , AP-2 $\gamma$  and AP-2 $\delta$ ) have previously been shown to be expressed in developing retina<sup>134-136</sup>. In Chapter 2, we showed for the first time that the fifth member of the AP-2 family, AP-2 $\epsilon$ , is also expressed in amacrine cells in developing mammalian and chicken retina. We used RT-PCR and immunostaining to demonstrate that the expression of AP-2 $\epsilon$  varies with developmental stages in mice and chick retina, with maximum expression at P1 in mice and ED10 in chicken. We further showed that AP-2 $\epsilon$  is co-expressed in subsets of AP-2 $\alpha$ , AP-2 $\beta$  and AP-2 $\gamma$ -positive amacrine cells during retinal development. The highest percentage of co-expressing cells was observed for AP-2 $\epsilon$ /AP-2 $\alpha$  and for AP-2 $\epsilon$ /AP-2 $\beta$ , with peak co-expression in P1 mouse retina, an early stage of retinal differentiation. In contrast, very little co-localization was observed between AP-2 $\epsilon$  and AP-2 $\gamma$ . We also found that AP-2 $\epsilon$  expression is associated with GABAergic rather than glycinergic amacrine cells. GABAergic amacrine cells are born earlier than the glycinergic amacrine cells. These results indicate that AP-2 $\epsilon$  is most likely involved in the development of early born amacrine cells. Interestingly, AP-2 $\epsilon$  RNA was also detected in a subset of retinoblastoma cell lines. As other members of the AP-2 family have previously been shown to be expressed in retinoblastoma cells<sup>146</sup>, our AP-2 $\epsilon$  data further support a link between amacrine cells and retinoblastoma. Thus, AP-2 expression patterns in retinoblastoma cell lines may reflect developmentally-regulated amacrine cell differentiation patterns. Overall, our study supports the idea that different combinations of

AP-2s in amacrine cells drives at least some of the functional diversity within this diverse subpopulation of retinal cells.

In addition to regulating important genes associated with cell proliferation, migration and differentiation during early embryonic development, aberrant regulation of AP-2 proteins has been associated with several malignancies. AP-2 transcription factors play important roles in CNS development<sup>96</sup>. Whereas AP-2s are normally found in the nucleus of the cell, as expected for transcription factors, AP-2s have also been found in the cytoplasm of GBM cells<sup>168, 169</sup>. In Chapter 4, we studied various aspects of AP-2 expression and function in GBM. First, we examined whether there was a correlation between AP-2 RNA levels and prognosis in GBM patients, and showed that *AP-2 $\beta$*  mRNA expression correlates with poor survival of glioma patients. In GBM tumours, *AP-2 $\beta$*  expression was associated with the proneural subtype (a subtype known for its elevated stem cell population compared to other subtypes). We also demonstrated that at least three AP-2 family members (*AP-2 $\alpha$* , *AP-2 $\beta$*  and *AP-2 $\gamma$* ) affect the growth properties of GBM cells and that *AP-2 $\beta$*  is highly expressed at both the RNA and protein levels in patient-derived GBM neurospheres and tissue extracts. Furthermore, by manipulating *AP-2 $\beta$*  levels, we found that *AP-2 $\beta$*  promotes neurosphere formation and cell migration in GBM cells. We also showed that *AP-2 $\beta$*  expression is induced under hypoxia and knockdown of *AP-2 $\beta$*  results in decreased expression of stem cell markers, nestin and SOX2, under both hypoxic and normoxic conditions. These results suggest that *AP-2 $\beta$*  is associated with maintenance of GBM stem cells and may thus promote GBM growth.

Finally, in Chapter 3, we examined the role of another transcription factor, NFI, in GBM cells. Like AP-2, NFI is a family of transcription factors that plays important roles in

CNS development<sup>198, 200</sup>. NFIs are important for the onset of gliogenesis and are known to regulate the expression of the astrocyte intermediate filament protein gene, *GFAP*<sup>198</sup>. Our lab had previously shown that NFIs regulate the expression of *GFAP* and *B-FABP* in GBM cells<sup>182</sup>. To further elucidate the role of NFIs in GBM, we carried out a ChIP-on-chip analysis to identify additional NFI target genes. Out of ~400 putative target genes obtained, we were particularly interested in *HEY1*, a Notch effector gene, as the Notch pathway has also been linked to gliogenesis and GBM malignancy. We showed that all four NFI family members can bind to the *HEY1* promoter and repress its transcription in GBM cells. Furthermore, we showed that HEY1 knockdown results in decreased proliferation and increased migration of GBM cells. These results support a role for NFIs in controlling GBM growth properties through regulation of its target genes.

## 5.2 Regulation of AP-2 transcription factor activity

AP-2 transcription factors show spatial and temporal cell-specific expression during embryogenesis<sup>96, 257</sup>. As AP-2 family members have highly conserved DNA binding and dimerization domains, they can bind to the same target genes<sup>96</sup>. However, there is considerable divergence in the transactivation domains of AP-2 family members. This variability in the transactivation domain likely accounts for the variation in gene regulation associated with different AP-2s. Thus, AP-2 activity is primarily regulated through physical interactions with other proteins as well as by epigenetic modification of the promoter regions of AP-2 target genes as shown by a number of labs<sup>96, 105, 141, 330, 331</sup>.

### 5.2.1 Activation of AP-2 by retinoic acid and cAMP

AP-2 mRNA levels, protein levels and transcriptional activity are induced by retinoic acid, a vitamin A derivative, in some cell types such as P19 and NT2 cells<sup>114</sup>. There is evidence suggesting that retinoic acid-induced neural cell differentiation in P19 is mediated through transcriptional activation of AP-2 target genes. Retinoic acid is also important for eye development and is synthesized in a dorsoventral gradient in the embryonic eye through oxidation of retinaldehyde by aldehyde dehydrogenases<sup>332</sup>. In light of the connection between retinoic acid and AP-2, and AP-2 expression in amacrine cells, it is possible that induction of AP-2 expression in the developing retina is dependent on retinoic acid. Retinoic acid effects are mediated through: (i) retinoic acid receptors (RARs and RXRs), transcription factors whose activity is regulated by retinoic acid, and (ii) retinoic acid binding proteins such as cellular retinoic acid binding proteins (CRABP1 and CRABP2). AP-2 regulates *CRABP2* expression in human mammary epithelial cells and breast cancer cells<sup>333</sup>. Our lab has previously shown that in GBM cells, cytoplasmic

CRABP2 levels are associated with poor survival, leading to the hypothesis that CRABP2 sequesters retinoic acid in the cytoplasm, with CRABP2 knockdown in GBM cells resulting in decreased cell proliferation and induction of retinoic acid-mediated RAR activation<sup>334</sup>. Attempts to investigate the effect of AP-2 on CRABP2 expression in U251 and T98 GBM cells were not successful as we were not able to detect CRABP2 in these cell lines.

AP-2 has also been shown to be activated by cAMP<sup>112, 114</sup>. While elevated cAMP levels do not increase AP-2 mRNA levels, they do lead to increased AP-2 transcriptional activity<sup>112</sup>. When cAMP levels are elevated, the transcription of genes containing both AP-2 and cAMP response elements is induced by AP-2<sup>112</sup>. In GBM cells, levels of cAMP are reduced compared to normal brain<sup>335</sup>. Phosphodiesterase 4 converts cAMP into adenylyl cyclase. Upregulation of the cAMP-PKA pathway by Rolipram, a PDE4 inhibitor, reduces cell proliferation, induces differentiation and subsequent apoptosis in GBM cells<sup>336-338</sup>. Rolipram has also been shown to reduce tumour formation and increase survival in a mouse orthotopic model of GBM<sup>337</sup>. The mechanism behind increased cAMP levels in Rolipram-treated GBM is still unknown. In light of AP-2's effects of cAMP, one possibility is that Rolipram acts through AP-2. We therefore investigated the effect of Rolipram on AP-2s in GBM cells. Our preliminary results indicate that Rolipram changes the subcellular localization of AP-2 $\gamma$  in GBM, from a primarily cytoplasmic localization to a primarily nuclear localization (Figure 4.15). In contrast to AP-2 $\gamma$ , the subcellular localization of AP-2 $\alpha$  and AP-2 $\beta$  was not affected by Rolipram. These results were obtained with patient-derived A4-004 GBM cells cultured under standard conditions (DMEM supplemented with 10% fetal calf serum). These data suggest a specific role for

PDE4 and cAMP in determining the subcellular localization of AP-2 $\gamma$ . As cAMP activates PKA, activated PKA may phosphorylate AP-2 $\gamma$ , and thus phosphorylation of AP-2 $\gamma$  may be responsible for its subcellular localization. Additional GBM cell lines, as well as investigations of the phosphorylation status of AP-2 $\gamma$  compared to the other AP-2s will need to be examined in order to test this hypothesis.

### **5.2.2 AP-2 dimerization and binding specificity**

AP-2 family members have conserved DNA binding and dimerization domains at the C-terminus and can bind to similar DNA binding elements based on *in vitro* studies. In contrast, the transactivation domain at the N-terminus of AP-2s is poorly conserved and likely accounts for the variation in gene regulation observed amongst the different AP-2 family members<sup>96, 339</sup>. AP-2 proteins bind to a GC-rich binding site, with the following consensus binding sequence: 5'-GCCN<sub>3</sub>GGC-3'<sup>339</sup>. A SELEX-based binding site assay revealed flexibility in the AP-2 binding site and identified additional AP-2 binding sites, including 5'-GCCN<sub>3</sub>GGC-3', 5'-GCCN<sub>4</sub>GGC-3' and 5'-GCCN<sub>3/4</sub>GGG-3'<sup>95</sup>. AP-2 proteins bind to their target genes as either homodimers or heterodimers, with different combinations of AP-2 proteins binding to various GC-rich elements with variable affinities. For example, AP-2 $\alpha$ , AP-2 $\beta$  and AP-2 $\gamma$  can all bind to an AP-2 binding site in the *c-erbB2* promoter; however, AP-2 $\alpha$  and AP-2 $\gamma$  demonstrate higher transcriptional activation of *c-erbB2* compared to AP-2 $\beta$ <sup>331</sup>.

Gene regulation by AP-2 is further complicated because of AP-2 isoforms. AP-2 $\alpha$  isoforms 1a, 1b and 1c are conserved across species<sup>313</sup>. These isoforms are alternatively spliced products differing in exon 1 (N.B. AP-2 $\alpha$  has 7 exons)<sup>313, 340</sup>. AP-2 $\alpha$  isoforms show

specific spatio-temporal expression patterns in mouse embryos<sup>340</sup>. In breast epithelium, AP-2 $\alpha$  isoforms 1a and 1c are expressed at similar protein levels whereas isoform 1b is expressed at lower levels. In breast cancer, higher levels of AP-2 $\alpha$  isoform 1c were observed in tamoxifen-resistant cell lines and tissues<sup>340</sup>. The functional variability in these isoforms arises from amino acid differences in the extreme N-terminal region. Isoform 1a is capable of repressing the cyclin D3 promoter in a sumoylation-dependent manner, as it contains a unique sumoylation motif which is not present in isoforms 1b and 1c. Also, isoforms 1b and 1c show higher transcriptional activation of the *ERBB2* promoter compared to isoform 1a, indicating that different AP-2 $\alpha$  isoforms have different transactivation potential<sup>340</sup>. In addition to AP-2 isoforms, another level of complexity arises from post-translational modification of AP-2. For example, sumoylation of AP-2 suppresses its transcriptional activity<sup>113</sup>. In support of a role for AP-2 sumoylation in GBM cells, our data indicate that AP-2 overexpression in U251 GBM cells does not affect B-FABP expression levels; however, overexpression of AP-2 along with inhibition of sumoylation results in decreased B-FABP expression in these cells. B-FABP has previously been shown to be a target of AP-2 in chicken<sup>265</sup>.

How sumoylation affects AP-2 transcriptional repression is not yet known. However, it is possible that sumoylation could affect AP-2 dimerization or binding potential. Alternatively, sumoylation may inhibit AP-2 activity by shuttling this transcription factor to the cytoplasm. In support of the latter, our preliminary results indicate that inhibition of sumoylation in A4-004 adherent cells results in shuttling of AP-2 $\beta$  from the cytoplasm to the nucleus. Additional studies will be required to characterize the role of AP-2 sumoylation in GBM.

### 5.3 AP-2 family members show redundant roles during amacrine cell development

Retina development is a complex process, which requires several spatially and temporally specific cues to direct the differentiation of retinal progenitor cells into neuronal and glial cells. A wide array of transcription factors play key roles in this process. Reports from our lab and other labs have shown that AP-2s are important for the differentiation of amacrine, horizontal and ganglion cells<sup>134-136, 138, 139, 264</sup>. In developing mouse and chicken retina, AP-2 $\alpha$  is expressed in amacrine cells whereas AP-2 $\beta$  is expressed in both amacrine and horizontal cells<sup>135</sup>. AP-2 $\gamma$  is expressed in amacrine cell populations that are partially distinct from those expressing AP-2 $\alpha$  and AP-2 $\beta$ <sup>134</sup>. In contrast to the other AP-2s, AP-2 $\delta$  is restricted to a subset of ganglion cells in the retina<sup>341</sup>. Co-expression has been previously reported for AP-2 $\alpha$ /AP-2 $\beta$  and AP-2 $\beta$ /AP-2 $\gamma$  in the amacrine cells of mouse retina<sup>134</sup>. In this thesis, we show that AP-2 $\alpha$  and AP-2 $\gamma$  are also co-expressed in a subset of amacrine cells. Thus, the overlapping and diverging expression patterns for the different members of the AP-2 family suggest both redundant and non-redundant functions for AP-2 family members in retina. Conditional (retina-specific) AP-2 $\alpha$  and AP-2 $\beta$  knockout mice show horizontal and amacrine cell defects that were not detected upon knockout of either AP-2 by itself<sup>134</sup>. While horizontal and amacrine cell numbers were not affected in AP-2 $\alpha$ /AP-2 $\beta$  double knockouts, aberrant amacrine cell mosaic formations were observed<sup>138</sup>. Our discovery that AP-2 $\epsilon$  can co-localize with all three AP-2 members previously reported to be expressed in amacrine cells further supports the complexity of AP-2 target gene regulation in differentiating amacrine cells. As mentioned earlier, AP-2 family members have well-conserved DNA binding and dimerization domains. Diversity

in target gene regulation is therefore likely to come from the divergent transactivation domains of AP-2s.

#### 5.4 AP-2 and NFI in glioblastoma

GBMs are highly aggressive tumours that are difficult to treat. Despite recent advances in surgical techniques, radiotherapy and chemotherapy (temozolomide), the median survival for GBM patients is approximately 15 months, with a poor quality of life during this time<sup>68</sup>. High throughput sequencing approaches have provided comprehensive molecular and genetic information about the biology of GBM but these advances have not resulted in improved patient survival<sup>57, 58</sup>. The major challenge with the treatment of GBM is the existence of highly infiltrative cells. These infiltrative cells evade standard treatment modalities and are believed to be the main reason for tumour recurrence.

The cell-of-origin of GBM remains unclear. Some studies indicate that a neural stem cell is the most probable cell-of-origin, while other studies suggest that GBM may also arise from dedifferentiation of terminally differentiated cells such as astrocytes<sup>342-344</sup>. Results from our lab have led us to propose that GBMs originate from B-FABP-expressing radial glial cells<sup>210</sup>. Several studies have drawn parallels between normal brain development and gliomagenesis<sup>343</sup>. Furthermore, a number of signaling pathways involved in the maintenance of the balance between the generation of progenitor cells and their differentiation are believed to play parallel roles in GBM cells, particularly as related to promotion of tumour growth versus migration/infiltration<sup>72</sup>. For example, Wnt/ $\beta$ -catenin signaling plays an essential role during brain development and is required for the regulation of cell proliferation, self-renewal and differentiation of neural progenitor cells during development<sup>326</sup>. Aberrant activation of Wnt signaling has been associated with GBM progression, with the Wnt/ $\beta$ -catenin pathway shown to be necessary for proliferation

and self-renewal of GSCs in GBM<sup>81</sup>. Upregulation of Wnt5a, a non-canonical Wnt ligand, promotes glioblastoma stem cell infiltration by upregulating the expression of MMPs<sup>83, 345</sup>. Aberrant TGF- $\beta$  signaling results in increased invasiveness in GBM cells by regulating the expression of SMAD2 and ZEB1<sup>79, 346, 347</sup>. Similar to these signaling pathways, the AP-2 and NFI transcription factors may play key roles in the regulation of GBM growth properties.

In this thesis, we show that both AP-2 and NFI may be involved in the maintenance of stem cells within the bulk of GBM tumour cells. Elevated levels of both AP-2 $\beta$  and NFI target gene *HEY1* are associated with elevated levels of B-FABP, a marker of GBM stem cells<sup>210, 298, 299</sup>. *HEY1* induction by NFIs is also associated with decreased levels of the astrocyte differentiation marker *GFAP*, suggesting an inverse relationship in the NFI target genes that govern proliferation versus differentiation. Although we did not directly examine the Wnt and TGF $\beta$  signaling pathways, AP-2 has been reported to function downstream of these signaling pathways, suggesting complex links between various transcription and signaling pathways in GBM<sup>348, 349</sup>.

Cell migration is an important component of development, with extensive cell migration occurring during CNS development. Radial glial cells form the scaffold along which neurons migrate in order to reach their final destination in the brain<sup>350</sup>. Radial glial cells are neural stem/progenitor cells that can differentiate into both neurons and glia<sup>351</sup>. Glioblastoma stem cells share radial glial cell properties, with the ability to self-renew and give rise to other cell types. Our lab has previously shown that the genes encoding radial glial cell marker B-FABP and glial differentiation marker *GFAP* are both targets of NFI<sup>182</sup>. However, preliminary evidence presented in this thesis suggests that B-FABP and *GFAP*

are rarely co-expressed in GBM neurosphere cultures, reflecting the heterogeneity associated with GBM tumours. We suggest that the complement of NFIs expressed in individual GBM cells contributes to GBM heterogeneity by determining which NFI target genes will be expressed, with expression of B-FABP promoting cell migration and stem cell properties, expression of HEY1 associated with stem cell maintenance but decreased cell migration and expression of GFAP associated with differentiation

## 5.5 NFI-HEY1-Notch

As mentioned earlier, NFIs play important roles in gliogenesis<sup>198</sup>. In Chapter 3, we show that NFI represses *HEY1* in GBM cells. *HEY1* is an effector of Notch signaling that promotes the maintenance of neural precursor cells in developing brain<sup>233</sup>. In GBM, elevated *HEY1* RNA levels are associated with decreased survival of patients<sup>254</sup>. Notch, NFI and *HEY1* have a complex relationship, with Notch shown to activate both NFI and *HEY1*<sup>200, 352</sup>. In developing brain, Notch signaling promotes maintenance of neural progenitor cells and prevents neuronal differentiation<sup>351</sup>. In GBM, Notch signaling activates the expression of *HEY1*, *HES1* (*HEY* related protein), *GFAP*, *nestin*, *TNC*, etc.<sup>219, 287, 353, 354</sup>. Notch has also been shown to induce *EGFR* expression in a p53-dependent manner<sup>355</sup>. Moreover, Notch signaling is activated under hypoxia and is associated with upregulation of *HEY1* expression in an *HIF1 $\alpha$* -dependent manner<sup>287, 356</sup>. These data suggest a complex balance in Notch activation of NFI and *HEY1*, with *HEY1* repression by NFI allowing fine-tuning of the balance between self-renewal and differentiation during brain development and in GBM cells. Our data in GBM support this idea, as we find a decrease in the formation of GBM neurospheres when *HEY1* is depleted.

## 5.6 Targeting transcription factors for cancer treatment

Our results suggest that AP-2 could serve as an effective target to inhibit the growth of cancer stem cells. Transcription factors are key regulators of gene expression. They govern essential processes such as cell proliferation, differentiation and apoptosis. Deregulation of transcription factors is very common in cancers. For example, TP53 and MYC are the most common genes that are aberrantly regulated in cancer. Major signal transduction pathways alter the expression of transcription factors, leading to aberrant gene regulation thereby affecting cancer formation and progression. As transcription factors can simultaneously affect the expression of numerous genes involved in various aspects of cancer growth, efficient targeting of these transcription factors would open new therapeutic avenues.

The inhibition of transcription factor function by small molecules is complicated by the strong interactions between transcription factors and their DNA targets. Different strategies have been used to target transcription factor function, such as targeting the physical interaction of transcription factors with essential co-factors, targeting dimerization partners or targeting proteins which regulate the subcellular localization of transcription factors. For example, Nutlin-3 inhibits the interaction between MDM2 and p53 and stabilizes p53<sup>357</sup>. Similarly, MYC inhibitors Mycro 1 and 2 inhibit the dimerization of MYC with its co-transcription factor MAX<sup>358</sup>. THS-044 has been used to inhibit the heterodimerization of HIF1 subunits<sup>359</sup>. Similar strategies could also be applied to target AP-2s. As mentioned before, AP-2 transcriptional activity is regulated by physical interactions with various proteins. The most feasible way of targeting AP-2 would be through inhibition of AP-2 interaction with CITED2,4 domains to prevent association with

p300/CEBP co-factors. As AP-2 proteins function as either homodimers or heterodimers, specifically targeting the dimerization domain would inhibit dimerization and subsequent DNA binding. Another strategy would be to prevent post-translation modification of AP-2. For example, inhibition of sumoylation would prevent the repressive activity of AP-2 transcription factors. Although these strategies could be applied, it will be challenging to specifically inhibit individual AP-2s. The differences in the N-terminal transactivation domain of AP-2 proteins could be exploited to address this issue.

Similarly, targeting NFI transcription factors may be of benefit in the treatment of GBM but as NFI can regulate genes which contribute to stem cell maintenance as well as differentiation, targeting specific NFI targets associated with increased migration and stem cell maintenance might be more beneficial. In the case of NFI, it may be possible to target NFI through its phosphorylation state as we have found that the activity of NFIs depends on its phosphorylated state<sup>181</sup>. Prevention of NFI phosphorylation by inhibiting specific kinases would keep NFI in the hypo-phosphorylated (activated) state and may promote some aspects of gliogenesis in GBM tumours.

## 5.7 Future directions

### 5.7.1 Validation of target genes and identification of additional AP-2 target genes

A number of target genes have already been identified for AP-2s, many of which are expressed in retina. AP-2 target genes identified to date include tyrosine hydroxylase<sup>360</sup>, choline acetyltransferase<sup>361</sup>, dopamine hydroxylase<sup>360</sup>. We generated a list of putative AP-2 $\epsilon$  target genes in P14 mouse retina using high throughput RNA sequencing data obtained from single cells<sup>49</sup>. Cluster-based analysis using these drop-seq data resulted in a list of putative AP-2 $\epsilon$  target genes based on shared expression profiles with AP-2 $\epsilon$ . Validation of these target genes would help in determining the function of AP-2 $\epsilon$  in the retina. We also generated a list of additional putative AP-2 $\epsilon$  target genes using cDNA microarray data obtained from colorectal cancer cells that expressed or didn't express AP-2 $\epsilon$ <sup>151</sup>. One of the genes preferentially expressed in AP-2 $\epsilon$ -positive colorectal cancer cells was Tenascin C, a gene known to be expressed in chick retina<sup>362</sup>. Immunofluorescence analysis and co-localization studies could be used to see whether there is up-regulation or down-regulation of known targets of AP-2s in cells that co-express specific AP-2s or combinations of AP-2s. A 3-colour immunofluorescence analysis would allow direct examination of different combinations of AP-2s in amacrine cells and their co-expression with the proteins encoded by putative target genes. Targets up-regulated or down-regulated based on the expression of specific AP-2s could be further analysed using primary retinal cultures as these would provide a more natural context for expression analysis. Gel shift, chromatin immunoprecipitation and reporter gene assays would be used to validate the binding and activity of AP-2 proteins. As there are variations in the sequence of AP-2 binding sites located in the promoters of different

AP-2 target genes, these experiments would shed light on whether specific combinations of AP-2s preferentially recognize certain AP-2 binding sites. As a complementary approach, we would carry out RNA Seq experiments with the goal of identifying additional AP-2 targets. Primary retinal cell cultures transfected with individual AP-2s or combinations of AP-2s would be used for these experiments. These combined experiments would help in gaining a better understanding of the role of AP-2 in retinal development, particularly as related to amacrine cell function.

### **5.7.2 To study the functional significance of AP-2 $\epsilon$ in retinal development**

Expression of AP-2 $\epsilon$  in the amacrine cells of chick and mammalian retina suggests that it may play a role in regulating genes expressed in these cells during their differentiation. AP-2 $\epsilon$  knockout mouse have been generated but have not been analysed for retinal defects. We could obtain these mice from Dr. Trevor Williams in order to determine whether AP-2 $\epsilon$  knockout results in structural or functional retinal defects. We would use a similar approach to that utilized in our lab to characterize the AP-2 $\delta$  knockout mice<sup>266</sup>. Briefly, electrophysiology experiments would be used to functionally analyse the eyes of AP-2 $\epsilon$  knockout mice for defects in visual function. For these experiments, a primary electrode is attached to the cornea and a reference electrode is attached subdermally in the temporal ridge. Photopic responses, a measure of cone activity and dark adaptation responses, a measure of rod activity, will be examined. Visual potential response (VER), a measure of the visual cortex function, could be analyzed by placing the primary electrode in the occipital lobe and the reference electrode between the two eyes. In addition to these experiments, we would analyse the relative location of amacrine

cells, and the number of amacrine cells, in the developing eye. There is a possibility that we will not see any significant defects associated with *AP-2 $\epsilon$*  knockout mice as the function of *AP-2 $\epsilon$*  may be compensated by other *AP-2* family members. However, the relatively unique pattern of *AP-2 $\epsilon$*  expression in amacrine cells suggests some unique functions in these cells. We could also generate double knock-out mice (*AP-2 $\alpha$* , *AP-2 $\beta$*  and/or *AP-2 $\gamma$* ) to further analyse the role of *AP-2* in the retina.

### **5.7.3 Validation of additional NFI targets**

Our ChIP-on-chip analysis revealed NFI binding to approximately 400 putative target genes. We validated *HEY1* as an NFI target gene in Chapter 3. PANTHER gene ontology enrichment analysis revealed that putative NFI target genes identified by our ChIP-on-chip analysis were associated with various biological processes related to development (nervous system, skeletal and cardiovascular), morphogenesis and differentiation, and cell-to-cell communication. Interestingly, many of the genes were related to metabolism; e.g., positive and negative regulation of cellular metabolic processes including RNA metabolism, nitrogen based metabolic processes, macromolecule synthesis process, and lipid metabolism. In this regard, it is interesting to note that NFI transcription factors modulate prostate cancer metabolism upon interaction with FOXA1 and several studies have shown that *IDH* mutations in GBM result in production of the oncometabolite 2-HG (2-hydroxyglutamate), associated with poor prognosis in GBM <sup>363</sup>. Thus, it will be interesting to validate NFI targets associated with cellular metabolism in GBM. A microarray analysis based on expression or non-expression of individual NFIs would reveal additional NFI target genes in GBM.

#### **5.7.4 Examination of specific NFI family members involved in *HEY1* expression**

In Chapter 3, we showed that NFI transcription factors repress *HEY1* in GBM cells. We also showed that NFI family members bind to different NFI binding sites (794 bp, 411 bp and 332 bp) located upstream of the *HEY1* transcription start site. We still do not know whether all three NFI binding sites are required for NFI transcriptional activity. To shed light on this aspect of *HEY1* regulation, we would prepare luciferase reporter constructs (pGL3 vector) with mutations in individual or combined NFI binding sites. GBM cells could then be transfected with control (scrambled), *NFIA*, *NFIB*, *NFIC*, *NFIX*, or combinations of NFI siRNAs, along with pGL3 constructs containing wild-type and mutated *HEY1* promoter regions. This analysis would shed light on which particular NFI binding site or combination of binding sites is necessary for *HEY1* transcriptional regulation.

#### **5.7.5 Characterization of AP-2 sumoylation in GBM cells**

AP-2 proteins (AP-2 $\alpha$  and AP-2 $\gamma$ ) have been found to be sumoylated in breast and colorectal cancers, with sumoylation associated with maintenance of stem cells<sup>110, 113</sup>. We have shown by His-tag-mediated pull down of SUMO from SUMO-overexpressing HeLa cells that AP-2 $\beta$  may also be sumoylated. We will carry out additional immunoprecipitation experiments with SUMO antibodies using A4-004 GBM cells, in order to determine the sumoylation status of AP-2 $\beta$  in GBM cells. We will determine whether sumoylation of AP-2 affects its regulation of endogenous target gene expression. As we have already shown that AP-2 $\beta$  knockdown induces the expression of stem cell markers, it will be interesting to see if the sumoylation status of AP-2 affects the expression of these stem cell genes.

We will also carry out reporter gene assays to assess the effect of AP-2 sumoylation on its transcriptional activity. We have prepared an AP-2 $\beta$  flag-tagged construct mutated at a sumoylation site located at lysine 20 which can be utilized for these experiments. As sumoylation has previously been shown to affect protein subcellular localization <sup>364</sup>, we will examine the effect of sumoylation on AP-2 subcellular localization using wild-type and mutated AP-2 $\beta$  expression constructs. The inhibitors of sumoylation, ginkgolic acid (GA) and anachardic acid (AA), will be incorporated into these experiments. Our preliminary results show that inhibition of sumoylation results in the shuttling of AP-2 $\beta$  from the cytoplasm to the nucleus of A4-004 cells cultured under standard conditions. Additional experiments are needed to confirm these results.

#### ***5.7.6 To further characterize the role of AP-2 $\beta$ in GBM cells and mouse models***

Knockdowns using siRNAs or shRNAs are deemed successful if RNA levels are reduced by at least 80-85%. We have found transient knockdown of AP-2 $\beta$  in GBM cells to be inefficient using several different siRNAs and lentiviral-shRNA constructs. Also, it is difficult to knockdown AP-2 $\beta$  under hypoxic condition as hypoxia results in induction of AP-2 $\beta$ . Thus, to study the effect of AP-2 $\beta$  knockdown in GBM cells, we generated AP-2 $\beta$  CRISPR knockout cells. Several of the clonal populations generated using this approach have little to no AP-2 $\beta$  expression. Future experiments will involve testing the effect of AP-2 knockout using a variety of assays, including the Transwell assay to measure cell migration, cell counts to measure cell proliferation, and an orthotopic mouse brain model of GBM. For the latter, control and AP-2 $\beta$  knockout clonal lines will be injected in a stereotactic manner and tumour formation monitored over time. When the mice start

losing weight, a sign of tumour growth, we will carry out immunostaining analysis of the brain to examine tumour growth and infiltration.

AP-2 proteins have previously been associated with chemoresistance in cancers. As AP-2 $\beta$  expression is associated with stem cells in GBM, and stem cells are believed to be a major cause of chemoresistance in GBM, it will be interesting to see if AP-2 $\beta$  is associated with chemoresistance in GBM cells. For these experiments, we will test the effect of temozolomide on control and AP-2 $\beta$ -depleted GBM cells. Furthermore, to better understand the role of AP-2 $\beta$  in GBM, we could identify additional AP-2 $\beta$  targets in GBM cells using a combination of CHIP analysis and RNA-seq analysis of control versus AP-2 $\beta$ -depleted GBM cells.

Recently Pastor *et. al.*<sup>365</sup> showed that AP-2 $\gamma$  maintains naïve human pluripotency and represses neuroectodermal differentiation by binding to enhancers and facilitating the binding of pluripotency factors by opening the enhancers in human embryonic stem cells. This suggests that AP-2 $\gamma$  could potentially play a role in maintenance of stem cells in GBM as well. Our results show that apart from AP-2 $\beta$ , AP-2 $\alpha$  and AP-2 $\gamma$  also alter the growth properties of GBM. Further studies should be carried out to study the mechanisms of action of these AP-2 family members in GBM, particularly as related to AP-2 $\gamma$ . As AP-2s function as heterodimers as well as homodimers, it will be important to address the complexity of AP-2 target gene regulation in GBM cells using techniques such as CHIP-re-chip using two antibodies to different AP-2s along with AP-2 co-expression studies.

## References

1. F. J. Livesey, C. L. Cepko, Vertebrate neural cell-fate determination: lessons from the retina. *Nat Rev Neurosci* **2**, 109-118 (2001).
2. C. L. Cepko, C. P. Austin, X. Yang, M. Alexiades, D. Ezzeddine, Cell fate determination in the vertebrate retina. *Proceedings of the National Academy of Sciences of the United States of America* **93**, 589-595 (1996).
3. R. L. Chow, R. A. Lang, Early eye development in vertebrates. *Annu Rev Cell Dev Biol* **17**, 255-296 (2001).
4. D. L. Turner, E. Y. Snyder, C. L. Cepko, Lineage-independent determination of cell type in the embryonic mouse retina. *Neuron* **4**, 833-845 (1990).
5. C. E. Holt, T. W. Bertsch, H. M. Ellis, W. A. Harris, Cellular determination in the *Xenopus* retina is independent of lineage and birth date. *Neuron* **1**, 15-26 (1988).
6. R. W. Young, Cell differentiation in the retina of the mouse. *Anat Rec* **212**, 199-205 (1985).
7. T. Marquardt *et al.*, Pax6 is required for the multipotent state of retinal progenitor cells. *Cell* **105**, 43-55 (2001).
8. O. V. Taranova *et al.*, SOX2 is a dose-dependent regulator of retinal neural progenitor competence. *Genes Dev* **20**, 1187-1202 (2006).
9. M. E. Zuber, G. Gestri, A. S. Viczian, G. Barsacchi, W. A. Harris, Specification of the vertebrate eye by a network of eye field transcription factors. *Development* **130**, 5155-5167 (2003).
10. T. Miyawaki *et al.*, Tlx, an orphan nuclear receptor, regulates cell numbers and astrocyte development in the developing retina. *J Neurosci* **24**, 8124-8134 (2004).
11. N. A. Zaghoul, S. A. Moody, Alterations of rx1 and pax6 expression levels at neural plate stages differentially affect the production of retinal cell types and maintenance of retinal stem cell qualities. *Dev Biol* **306**, 222-240 (2007).
12. M. E. Zuber, M. Perron, A. Philpott, A. Bang, W. A. Harris, Giant eyes in *Xenopus laevis* by overexpression of XOptx2. *Cell* **98**, 341-352 (1999).
13. G. Gestri *et al.*, Six3 functions in anterior neural plate specification by promoting cell proliferation and inhibiting Bmp4 expression. *Development* **132**, 2401-2413 (2005).
14. M. Bylund, E. Andersson, B. G. Novitsch, J. Muhr, Vertebrate neurogenesis is counteracted by Sox1-3 activity. *Nature neuroscience* **6**, 1162-1168 (2003).
15. V. Graham, J. Khudyakov, P. Ellis, L. Pevny, SOX2 functions to maintain neural progenitor identity. *Neuron* **39**, 749-765 (2003).
16. M. A. Dyer, C. L. Cepko, Regulating proliferation during retinal development. *Nat Rev Neurosci* **2**, 333-342 (2001).
17. P. Sicinski *et al.*, Cyclin D1 provides a link between development and oncogenesis in the retina and breast. *Cell* **82**, 621-630 (1995).
18. D. Chen *et al.*, Division and apoptosis of E2f-deficient retinal progenitors. *Nature* **462**, 925-929 (2009).
19. T. J. Van Raay, M. L. Vetter, Wnt/frizzled signaling during vertebrate retinal development. *Dev Neurosci* **26**, 352-358 (2004).

20. M. Perron, W. A. Harris, Determination of vertebrate retinal progenitor cell fate by the Notch pathway and basic helix-loop-helix transcription factors. *Cell Mol Life Sci* **57**, 215-223 (2000).
21. T. Hashimoto, X. M. Zhang, B. Y. Chen, X. J. Yang, VEGF activates divergent intracellular signaling components to regulate retinal progenitor cell proliferation and neuronal differentiation. *Development* **133**, 2201-2210 (2006).
22. M. Hu, S. S. Easter, Retinal neurogenesis: the formation of the initial central patch of postmitotic cells. *Dev Biol* **207**, 309-321 (1999).
23. J. R. Martinez-Morales *et al.*, Differentiation of the vertebrate retina is coordinated by an FGF signaling center. *Developmental cell* **8**, 565-574 (2005).
24. C. J. Neumann, C. Nüsslein-Volhard, Patterning of the zebrafish retina by a wave of sonic hedgehog activity. *Science* **289**, 2137-2139 (2000).
25. A. Shkumatava, C. J. Neumann, Shh directs cell-cycle exit by activating p57Kip2 in the zebrafish retina. *EMBO Rep* **6**, 563-569 (2005).
26. D. L. Stenkamp, R. A. Frey, Extraretinal and retinal hedgehog signaling sequentially regulate retinal differentiation in zebrafish. *Dev Biol* **258**, 349-363 (2003).
27. J. Zhang *et al.*, Rb regulates proliferation and rod photoreceptor development in the mouse retina. *Nat Genet* **36**, 351-360 (2004).
28. T. Marquardt, P. Gruss, Generating neuronal diversity in the retina: one for nearly all. *Trends Neurosci* **25**, 32-38 (2002).
29. S. Ohnuma, A. Philpott, K. Wang, C. E. Holt, W. A. Harris, p27Xic1, a Cdk inhibitor, promotes the determination of glial cells in *Xenopus* retina. *Cell* **99**, 499-510 (1999).
30. M. R. Alexiades, C. Cepko, Quantitative analysis of proliferation and cell cycle length during development of the rat retina. *Dev Dyn* **205**, 293-307 (1996).
31. S. Decembrini, M. Andreazzoli, R. Vignali, G. Barsacchi, F. Cremisi, Timing the generation of distinct retinal cells by homeobox proteins. *PLoS Biol* **4**, e272 (2006).
32. R. Ohsawa, R. Kageyama, Regulation of retinal cell fate specification by multiple transcription factors. *Brain Res* **1192**, 90-98 (2008).
33. N. L. Brown, S. Patel, J. Brzezinski, T. Glaser, Math5 is required for retinal ganglion cell and optic nerve formation. *Development* **128**, 2497-2508 (2001).
34. A. J. Mears *et al.*, Nrl is required for rod photoreceptor development. *Nat Genet* **29**, 447-452 (2001).
35. M. Burmeister *et al.*, Ocular retardation mouse caused by Chx10 homeobox null allele: impaired retinal progenitor proliferation and bipolar cell differentiation. *Nat Genet* **12**, 376-384 (1996).
36. M. L. Vetter, N. L. Brown, The role of basic helix-loop-helix genes in vertebrate retinogenesis. *Semin Cell Dev Biol* **12**, 491-498 (2001).
37. W. Liu, Z. Mo, M. Xiang, The Ath5 proneural genes function upstream of Brn3 POU domain transcription factor genes to promote retinal ganglion cell development. *Proc Natl Acad Sci U S A* **98**, 1649-1654 (2001).
38. T. Kondo, Epigenetic alchemy for cell fate conversion. *Curr Opin Genet Dev* **16**, 502-507 (2006).
39. M. Agathocleous, W. A. Harris, From progenitors to differentiated cells in the vertebrate retina. *Annu Rev Cell Dev Biol* **25**, 45-69 (2009).

40. B. Chen, C. L. Cepko, Requirement of histone deacetylase activity for the expression of critical photoreceptor genes. *BMC Dev Biol* **7**, 78 (2007).
41. J. I. Wu, J. Lessard, G. R. Crabtree, Understanding the words of chromatin regulation. *Cell* **136**, 200-206 (2009).
42. A. V. Das *et al.*, SWI/SNF chromatin remodeling ATPase Brm regulates the differentiation of early retinal stem cells/progenitors by influencing Brn3b expression and Notch signaling. *J Biol Chem* **282**, 35187-35201 (2007).
43. M. A. MacNeil, J. K. Heussy, R. F. Dacheux, E. Raviola, R. H. Masland, The shapes and numbers of amacrine cells: matching of photofilled with Golgi-stained cells in the rabbit retina and comparison with other mammalian species. *J Comp Neurol* **413**, 305-326 (1999).
44. R. H. Masland, The neuronal organization of the retina. *Neuron* **76**, 266-280 (2012).
45. H. Kolb, The morphology of the bipolar cells, amacrine cells and ganglion cells in the retina of the turtle *Pseudemys scripta elegans*. *Philos Trans R Soc Lond B Biol Sci* **298**, 355-393 (1982).
46. H. Kolb, K. A. Linberg, S. K. Fisher, Neurons of the human retina: a Golgi study. *J Comp Neurol* **318**, 147-187 (1992).
47. J. M. Trimarchi *et al.*, Molecular heterogeneity of developing retinal ganglion and amacrine cells revealed through single cell gene expression profiling. *The Journal of comparative neurology* **502**, 1047-1065 (2007).
48. T. J. Cherry, J. M. Trimarchi, M. B. Stadler, C. L. Cepko, Development and diversification of retinal amacrine interneurons at single cell resolution. *Proc Natl Acad Sci U S A* **106**, 9495-9500 (2009).
49. E. Z. Macosko *et al.*, Highly Parallel Genome-wide Expression Profiling of Individual Cells Using Nanoliter Droplets. *Cell* **161**, 1202-1214 (2015).
50. A. Jemal, R. Siegel, J. Xu, E. Ward, Cancer statistics, 2010. *CA Cancer J Clin* **60**, 277-300 (2010).
51. G. Reifenberger, H. G. Wirsching, C. B. Knobbe-Thomsen, M. Weller, Advances in the molecular genetics of gliomas - implications for classification and therapy. *Nat Rev Clin Oncol* **14**, 434-452 (2017).
52. D. N. Louis *et al.*, The 2016 World Health Organization Classification of Tumors of the Central Nervous System: a summary. *Acta Neuropathol* **131**, 803-820 (2016).
53. M. Sanson *et al.*, Isocitrate dehydrogenase 1 codon 132 mutation is an important prognostic biomarker in gliomas. *J Clin Oncol* **27**, 4150-4154 (2009).
54. S. Nobusawa, T. Watanabe, P. Kleihues, H. Ohgaki, IDH1 mutations as molecular signature and predictive factor of secondary glioblastomas. *Clin Cancer Res* **15**, 6002-6007 (2009).
55. D. W. Parsons *et al.*, An integrated genomic analysis of human glioblastoma multiforme. *Science* **321**, 1807-1812 (2008).
56. M. E. Hegi *et al.*, MGMT gene silencing and benefit from temozolomide in glioblastoma. *N Engl J Med* **352**, 997-1003 (2005).
57. H. S. Phillips *et al.*, Molecular subclasses of high-grade glioma predict prognosis, delineate a pattern of disease progression, and resemble stages in neurogenesis. *Cancer Cell* **9**, 157-173 (2006).

58. R. G. Verhaak *et al.*, Integrated genomic analysis identifies clinically relevant subtypes of glioblastoma characterized by abnormalities in PDGFRA, IDH1, EGFR, and NF1. *Cancer Cell* **17**, 98-110 (2010).
59. J. Bartek, Jr. *et al.*, Key concepts in glioblastoma therapy. *J Neurol Neurosurg Psychiatry* **83**, 753-760 (2012).
60. J. Wang, C. Bettegowda, Genomic discoveries in adult astrocytoma. *Curr Opin Genet Dev* **30C**, 17-24 (2015).
61. S. Phuphanich, S. Ferrall, H. Greenberg, Long-term survival in malignant glioma. Prognostic factors. *J Fla Med Assoc* **80**, 181-184 (1993).
62. H. Ohgaki, P. Kleihues, Population-based studies on incidence, survival rates, and genetic alterations in astrocytic and oligodendroglial gliomas. *Journal of neuropathology and experimental neurology* **64**, 479-489 (2005).
63. C. Sarkar, A. Jain, V. Suri, Current concepts in the pathology and genetics of gliomas. *Indian J Cancer* **46**, 108-119 (2009).
64. P. Y. Wen, S. Kesari, Malignant gliomas in adults. *N Engl J Med* **359**, 492-507 (2008).
65. H. Ohgaki, P. Kleihues, Epidemiology and etiology of gliomas. *Acta Neuropathol* **109**, 93-108 (2005).
66. Q. T. Ostrom *et al.*, CBTRUS Statistical Report: Primary Brain and Central Nervous System Tumors Diagnosed in the United States in 2008-2012. *Neuro Oncol* **17 Suppl 4**, iv1-iv62 (2015).
67. R. Stupp *et al.*, Effects of radiotherapy with concomitant and adjuvant temozolomide versus radiotherapy alone on survival in glioblastoma in a randomised phase III study: 5-year analysis of the EORTC-NCIC trial. *Lancet Oncol* **10**, 459-466 (2009).
68. R. Stupp *et al.*, Radiotherapy plus concomitant and adjuvant temozolomide for glioblastoma. *N Engl J Med* **352**, 987-996 (2005).
69. A. A. Brandes, D. Lacombe, C. Vecht, Future trends in the treatment of brain tumours. *Eur J Cancer* **37**, 2297-2301 (2001).
70. E. G. Van Meir, A. Bellail, S. Phuphanich, Emerging molecular therapies for brain tumors. *Semin Oncol* **31**, 38-46 (2004).
71. M. C. Chamberlain, Temozolomide: therapeutic limitations in the treatment of adult high-grade gliomas. *Expert Rev Neurother* **10**, 1537-1544 (2010).
72. S. Mehta, C. Lo Cascio, Developmentally regulated signaling pathways in glioma invasion. *Cell Mol Life Sci* **75**, 385-402 (2018).
73. C. Richichi, P. Brescia, V. Alberizzi, L. Fornasari, G. Pelicci, Marker-independent method for isolating slow-dividing cancer stem cells in human glioblastoma. *Neoplasia* **15**, 840-847 (2013).
74. J. Halliday *et al.*, In vivo radiation response of proneural glioma characterized by protective p53 transcriptional program and proneural-mesenchymal shift. *Proc Natl Acad Sci U S A* **111**, 5248-5253 (2014).
75. J. F. de Groot *et al.*, Tumor invasion after treatment of glioblastoma with bevacizumab: radiographic and pathologic correlation in humans and mice. *Neuro Oncol* **12**, 233-242 (2010).
76. B. Ortensi, M. Setti, D. Osti, G. Pelicci, Cancer stem cell contribution to glioblastoma invasiveness. *Stem Cell Res Ther* **4**, 18 (2013).

77. A. Inoue *et al.*, Cancer stem-like cells of glioblastoma characteristically express MMP-13 and display highly invasive activity. *Int J Oncol* **37**, 1121-1131 (2010).
78. C. Calabrese *et al.*, A perivascular niche for brain tumor stem cells. *Cancer Cell* **11**, 69-82 (2007).
79. U. Wellner *et al.*, The EMT-activator ZEB1 promotes tumorigenicity by repressing stemness-inhibiting microRNAs. *Nat Cell Biol* **11**, 1487-1495 (2009).
80. F. A. Siebzehnrubl *et al.*, The ZEB1 pathway links glioblastoma initiation, invasion and chemoresistance. *EMBO Mol Med* **5**, 1196-1212 (2013).
81. X. Jin *et al.*, Frizzled 4 regulates stemness and invasiveness of migrating glioma cells established by serial intracranial transplantation. *Cancer Res* **71**, 3066-3075 (2011).
82. Y. Lee, J. K. Lee, S. H. Ahn, J. Lee, D. H. Nam, WNT signaling in glioblastoma and therapeutic opportunities. *Lab Invest* **96**, 137-150 (2016).
83. E. Binda *et al.*, Wnt5a Drives an Invasive Phenotype in Human Glioblastoma Stem-like Cells. *Cancer Res* **77**, 996-1007 (2017).
84. A. Giese *et al.*, Dichotomy of astrocytoma migration and proliferation. *Int J Cancer* **67**, 275-282 (1996).
85. A. Giese, Glioma invasion--pattern of dissemination by mechanisms of invasion and surgical intervention, pattern of gene expression and its regulatory control by tumor suppressor p53 and proto-oncogene ETS-1. *Acta Neurochir Suppl* **88**, 153-162 (2003).
86. A. Farin *et al.*, Transplanted glioma cells migrate and proliferate on host brain vasculature: a dynamic analysis. *Glia* **53**, 799-808 (2006).
87. J. Godlewski, A. Bronisz, M. O. Nowicki, E. A. Chiocca, S. Lawler, microRNA-451: A conditional switch controlling glioma cell proliferation and migration. *Cell Cycle* **9**, 2742-2748 (2010).
88. J. Godlewski *et al.*, MicroRNA-451 regulates LKB1/AMPK signaling and allows adaptation to metabolic stress in glioma cells. *Mol Cell* **37**, 620-632 (2010).
89. P. J. Mitchell, C. Wang, R. Tjian, Positive and negative regulation of transcription in vitro: enhancer-binding protein AP-2 is inhibited by SV40 T antigen. *Cell* **50**, 847-861 (1987).
90. T. Williams, A. Admon, B. Luscher, R. Tjian, Cloning and expression of AP-2, a cell-type-specific transcription factor that activates inducible enhancer elements. *Genes Dev* **2**, 1557-1569 (1988).
91. M. Moser *et al.*, Cloning and characterization of a second AP-2 transcription factor: AP-2 beta. *Development* **121**, 2779-2788 (1995).
92. C. Chazaud *et al.*, AP-2.2, a novel gene related to AP-2, is expressed in the forebrain, limbs and face during mouse embryogenesis. *Mech Dev* **54**, 83-94 (1996).
93. F. Zhao, M. Satoda, J. D. Licht, Y. Hayashizaki, B. D. Gelb, Cloning and characterization of a novel mouse AP-2 transcription factor, AP-2delta, with unique DNA binding and transactivation properties. *J Biol Chem* **276**, 40755-40760 (2001).
94. W. Feng, T. Williams, Cloning and characterization of the mouse AP-2 epsilon gene: a novel family member expressed in the developing olfactory bulb. *Mol Cell Neurosci* **24**, 460-475 (2003).

95. N. Mohibullah, A. Donner, J. A. Ippolito, T. Williams, SELEX and missing phosphate contact analyses reveal flexibility within the AP-2[alpha] protein: DNA binding complex. *Nucleic Acids Res* **27**, 2760-2769 (1999).
96. D. Eckert, S. Buhl, S. Weber, R. Jager, H. Schorle, The AP-2 family of transcription factors. *Genome Biol* **6**, 246 (2005).
97. Y. X. Zeng, K. Somasundaram, W. S. el-Deiry, AP2 inhibits cancer cell growth and activates p21WAF1/CIP1 expression. *Nat Genet* **15**, 78-82 (1997).
98. L. A. McPherson, A. V. Loktev, R. J. Weigel, Tumor suppressor activity of AP2alpha mediated through a direct interaction with p53. *J Biol Chem* **277**, 45028-45033 (2002).
99. P. R. Mertens, M. A. Alfonso-Jaume, K. Steinmann, D. H. Lovett, A synergistic interaction of transcription factors AP2 and YB-1 regulates gelatinase A enhancer-dependent transcription. *J Biol Chem* **273**, 32957-32965 (1998).
100. P. Pena *et al.*, Activator protein-2 mediates transcriptional activation of the CYP11A1 gene by interaction with Sp1 rather than binding to DNA. *Mol Endocrinol* **13**, 1402-1416 (1999).
101. J. M. Sivak, J. A. West-Mays, A. Yee, T. Williams, M. E. Fini, Transcription Factors Pax6 and AP-2alpha Interact To Coordinate Corneal Epithelial Repair by Controlling Expression of Matrix Metalloproteinase Gelatinase B. *Mol Cell Biol* **24**, 245-257 (2004).
102. K. Somasundaram *et al.*, Repression of a matrix metalloprotease gene by E1A correlates with its ability to bind to cell type-specific transcription factor AP-2. *Proc Natl Acad Sci U S A* **93**, 3088-3093 (1996).
103. F. Wu, A. S. Lee, Identification of AP-2 as an interactive target of Rb and a regulator of the G1/S control element of the hamster histone H3.2 promoter. *Nucleic Acids Res* **26**, 4837-4845 (1998).
104. P. Kannan, Y. Yu, S. Wankhade, M. A. Tainsky, PolyADP-ribose polymerase is a coactivator for AP-2-mediated transcriptional activation. *Nucleic Acids Res* **27**, 866-874 (1999).
105. J. Braganca *et al.*, Human CREB-binding protein/p300-interacting transactivator with ED-rich tail (CITED) 4, a new member of the CITED family, functions as a co-activator for transcription factor AP-2. *J Biol Chem* **277**, 8559-8565 (2002).
106. S. Gaubatz *et al.*, Transcriptional activation by Myc is under negative control by the transcription factor AP-2. *EMBO J* **14**, 1508-1519 (1995).
107. E. Batsche, C. Muchardt, J. Behrens, H. C. Hurst, C. Cremisi, RB and c-Myc activate expression of the E-cadherin gene in epithelial cells through interaction with transcription factor AP-2. *Mol Cell Biol* **18**, 3647-3658 (1998).
108. M. A. Garcia, M. Campillos, A. Marina, F. Valdivieso, J. Vazquez, Transcription factor AP-2 activity is modulated by protein kinase A-mediated phosphorylation. *FEBS Lett* **444**, 27-31 (1999).
109. J. J. Eloranta, H. C. Hurst, Transcription factor AP-2 interacts with the SUMO-conjugating enzyme UBC9 and is sumolated in vivo. *J Biol Chem* **277**, 30798-30804 (2002).
110. M. V. Bogachek *et al.*, Sumoylation pathway is required to maintain the basal breast cancer subtype. *Cancer Cell* **25**, 748-761 (2014).
111. A. K. Wenke, A. K. Bosserhoff, Roles of AP-2 transcription factors in the regulation of cartilage and skeletal development. *Febs J* **277**, 894-902 (2010).

112. M. Imagawa, R. Chiu, M. Karin, Transcription factor AP-2 mediates induction by two different signal-transduction pathways: protein kinase C and cAMP. *Cell* **51**, 251-260 (1987).
113. M. V. Bogachek *et al.*, Inhibiting the SUMO Pathway Represses the Cancer Stem Cell Population in Breast and Colorectal Carcinomas. *Stem Cell Reports* **7**, 1140-1151 (2016).
114. B. Luscher, P. J. Mitchell, T. Williams, R. Tjian, Regulation of transcription factor AP-2 by the morphogen retinoic acid and by second messengers. *Genes Dev* **3**, 1507-1517 (1989).
115. L. F. Doerksen, A. Bhattacharya, P. Kannan, D. Pratt, M. A. Tainsky, Functional interaction between a RARE and an AP-2 binding site in the regulation of the human HOX A4 gene promoter. *Nucleic Acids Res* **24**, 2849-2856 (1996).
116. M. Schmidt *et al.*, The transcription factors AP-2beta and AP-2alpha are required for survival of sympathetic progenitors and differentiated sympathetic neurons. *Dev Biol* **355**, 89-100 (2011).
117. A. Rada-Iglesias *et al.*, Epigenomic annotation of enhancers predicts transcriptional regulators of human neural crest. *Cell Stem Cell* **11**, 633-648 (2012).
118. E. Van Otterloo *et al.*, Novel Tfp2-mediated control of soxE expression facilitated the evolutionary emergence of the neural crest. *Development* **139**, 720-730 (2012).
119. V. E. Zarelli, I. B. Dawid, Inhibition of neural crest formation by Kctd15 involves regulation of transcription factor AP-2. *Proc Natl Acad Sci U S A* **110**, 2870-2875 (2013).
120. M. Moser, J. Ruschoff, R. Buettner, Comparative analysis of AP-2 alpha and AP-2 beta gene expression during murine embryogenesis. *Dev Dyn* **208**, 115-124 (1997).
121. F. Zhao, T. Lufkin, B. D. Gelb, Expression of Tfp2d, the gene encoding the transcription factor Ap-2 delta, during mouse embryogenesis. *Gene Expr Patterns* **3**, 213-217 (2003).
122. H. V. Wang, K. Vaupel, R. Buettner, A. K. Bosserhoff, M. Moser, Identification and embryonic expression of a new AP-2 transcription factor, AP-2 epsilon. *Dev Dyn* **231**, 128-135 (2004).
123. T. Nottoli, S. Hagopian-Donaldson, J. Zhang, A. Perkins, T. Williams, AP-2-null cells disrupt morphogenesis of the eye, face, and limbs in chimeric mice. *Proc Natl Acad Sci U S A* **95**, 13714-13719 (1998).
124. H. Schorle, P. Meier, M. Buchert, R. Jaenisch, P. J. Mitchell, Transcription factor AP-2 essential for cranial closure and craniofacial development. *Nature* **381**, 235-238 (1996).
125. J. Zhang *et al.*, Neural tube, skeletal and body wall defects in mice lacking transcription factor AP-2. *Nature* **381**, 238-241 (1996).
126. M. Moser *et al.*, Terminal renal failure in mice lacking transcription factor AP-2 beta. *Lab Invest* **83**, 571-578 (2003).
127. M. Moser *et al.*, Enhanced apoptotic cell death of renal epithelial cells in mice lacking transcription factor AP-2beta. *Genes Dev* **11**, 1938-1948 (1997).
128. H. J. Auman *et al.*, Transcription factor AP-2gamma is essential in the extra-embryonic lineages for early postimplantation development. *Development* **129**, 2733-2747 (2002).
129. U. Werling, H. Schorle, Transcription factor gene AP-2 gamma essential for early murine development. *Mol Cell Biol* **22**, 3149-3156 (2002).
130. K. Hesse *et al.*, AP-2delta is a crucial transcriptional regulator of the posterior midbrain. *PLoS One* **6**, e23483 (2011).

131. W. Feng, F. Simoes-de-Souza, T. E. Finger, D. Restrepo, T. Williams, Disorganized olfactory bulb lamination in mice deficient for transcription factor AP-2epsilon. *Mol Cell Neurosci* **42**, 161-171 (2009).
132. H. Li, R. Sheridan, T. Williams, Analysis of TFAP2A mutations in Branchio-Oculo-Facial Syndrome indicates functional complexity within the AP-2alpha DNA-binding domain. *Hum Mol Genet* **22**, 3195-3206 (2013).
133. M. Satoda *et al.*, Mutations in TFAP2B cause Char syndrome, a familial form of patent ductus arteriosus. *Nat Genet* **25**, 42-46 (2000).
134. E. A. Bassett *et al.*, Overlapping expression patterns and redundant roles for AP-2 transcription factors in the developing mammalian retina. *Dev Dyn* **241**, 814-829 (2012).
135. E. A. Bassett *et al.*, Conditional deletion of activating protein 2alpha (AP-2alpha) in the developing retina demonstrates non-cell-autonomous roles for AP-2alpha in optic cup development. *Mol Cell Biol* **27**, 7497-7510 (2007).
136. D. A. Bisgrove, R. Godbout, Differential expression of AP-2alpha and AP-2beta in the developing chick retina: repression of R-FABP promoter activity by AP-2. *Dev Dyn* **214**, 195-206 (1999).
137. X. Li, D. D. Glubrecht, R. Mita, R. Godbout, Expression of AP-2delta in the developing chick retina. *Dev Dyn* **237**, 3210-3221 (2008).
138. E. A. Hicks *et al.*, Conditional Deletion of AP-2alpha and AP-2beta in the Developing Murine Retina Leads to Altered Amacrine Cell Mosaics and Disrupted Visual Function. *Invest Ophthalmol Vis Sci* **59**, 2229-2239 (2018).
139. X. Li, E. A. Monckton, R. Godbout, Ectopic expression of transcription factor AP-2delta in developing retina: effect on PSA-NCAM and axon routing. *J Neurochem* **129**, 72-84 (2014).
140. X. Li, A. R. Persad, E. A. Monckton, R. Godbout, Transcription factor AP-2delta regulates the expression of polysialyltransferase ST8SIA2 in chick retina. *FEBS Lett* **588**, 770-775 (2014).
141. A. Allouche *et al.*, The combined immunodetection of AP-2alpha and YY1 transcription factors is associated with ERBB2 gene overexpression in primary breast tumors. *Breast Cancer Res* **10**, R9 (2008).
142. N. Wajapeyee, R. Britto, H. M. Ravishankar, K. Somasundaram, Apoptosis induction by activator protein 2alpha involves transcriptional repression of Bcl-2. *J Biol Chem* **281**, 16207-16219 (2006).
143. S. Huang, D. Jean, M. Luca, M. A. Tainsky, M. Bar-Eli, Loss of AP-2 results in downregulation of c-KIT and enhancement of melanoma tumorigenicity and metastasis. *EMBO J* **17**, 4358-4369 (1998).
144. D. Jean *et al.*, Loss of AP-2 results in up-regulation of MCAM/MUC18 and an increase in tumor growth and metastasis of human melanoma cells. *J Biol Chem* **273**, 16501-16508 (1998).
145. D. Shi *et al.*, TFAP2A regulates nasopharyngeal carcinoma growth and survival by targeting HIF-1alpha signaling pathway. *Cancer Prev Res (Phila)* **7**, 266-277 (2014).
146. X. Li, D. D. Glubrecht, R. Godbout, AP2 transcription factor induces apoptosis in retinoblastoma cells. *Genes Chromosomes Cancer* **49**, 819-830 (2010).

147. J. Zhang, S. Brewer, J. Huang, T. Williams, Overexpression of transcription factor AP-2alpha suppresses mammary gland growth and morphogenesis. *Dev Biol* **256**, 127-145 (2003).
148. R. Jager, U. Werling, S. Rimpf, A. Jacob, H. Schorle, Transcription factor AP-2gamma stimulates proliferation and apoptosis and impairs differentiation in a transgenic model. *Mol Cancer Res* **1**, 921-929 (2003).
149. F. Orso *et al.*, AP-2alpha and AP-2gamma regulate tumor progression via specific genetic programs. *FASEB J* **22**, 2702-2714 (2008).
150. G. W. Woodfield, A. D. Horan, Y. Chen, R. J. Weigel, TFAP2C controls hormone response in breast cancer cells through multiple pathways of estrogen signaling. *Cancer Res* **67**, 8439-8443 (2007).
151. M. P. Ebert *et al.*, TFAP2E-DKK4 and chemoresistance in colorectal cancer. *N Engl J Med* **366**, 44-53 (2012).
152. O. Murcia *et al.*, TFAP2E Methylation and Expression Status Does Not Predict Response to 5-FU-based Chemotherapy in Colorectal Cancer. *Clin Cancer Res* **24**, 2820-2827 (2018).
153. S. J. Park *et al.*, TFAP2E methylation status and prognosis of patients with radically resected colorectal cancer. *Oncology* **88**, 122-132 (2015).
154. J. M. Karjalainen, J. K. Kellokoski, M. J. Eskelinen, E. M. Alhava, V. M. Kosma, Downregulation of transcription factor AP-2 predicts poor survival in stage I cutaneous malignant melanoma. *J Clin Oncol* **16**, 3584-3591 (1998).
155. M. A. Anttila *et al.*, Expression of transcription factor AP-2alpha predicts survival in epithelial ovarian cancer. *Br J Cancer* **82**, 1974-1983 (2000).
156. P. Lipponen, S. Aaltomaa, J. Kellokoski, M. Ala-Opas, V. Kosma, Expression of activator protein 2 in prostate cancer is related to tumor differentiation and cell proliferation. *Eur Urol* **37**, 573-578 (2000).
157. K. M. Ropponen *et al.*, Expression of transcription factor AP-2 in colorectal adenomas and adenocarcinomas; comparison of immunohistochemistry and in situ hybridisation. *J Clin Pathol* **54**, 533-538 (2001).
158. E. Odegaard *et al.*, The AP-2gamma transcription factor is upregulated in advanced-stage ovarian carcinoma. *Gynecol Oncol* **100**, 462-468 (2006).
159. K. M. Ropponen *et al.*, p22/WAF1 expression in human colorectal carcinoma: association with p53, transcription factor AP-2 and prognosis. *Br J Cancer* **81**, 133-140 (1999).
160. M. Bar-Eli, Gene regulation in melanoma progression by the AP-2 transcription factor. *Pigment Cell Res* **14**, 78-85 (2001).
161. C. Tellez, M. McCarty, M. Ruiz, M. Bar-Eli, Loss of activator protein-2alpha results in overexpression of protease-activated receptor-1 and correlates with the malignant phenotype of human melanoma. *J Biol Chem* **278**, 46632-46642 (2003).
162. S. Sumigama *et al.*, Suppression of invasion and peritoneal carcinomatosis of ovarian cancer cells by overexpression of AP-2alpha. *Oncogene* **23**, 5496-5504 (2004).
163. J. Pellikainen *et al.*, Expression of HER2 and its association with AP-2 in breast cancer. *Eur J Cancer* **40**, 1485-1495 (2004).

164. N. Friedrichs *et al.*, Distinct spatial expression patterns of AP-2alpha and AP-2gamma in non-neoplastic human breast and breast cancer. *Mod Pathol* **18**, 431-438 (2005).
165. J. M. Gee, J. F. Robertson, I. O. Ellis, R. I. Nicholson, H. C. Hurst, Immunohistochemical analysis reveals a tumour suppressor-like role for the transcription factor AP-2 in invasive breast cancer. *J Pathol* **189**, 514-520 (1999).
166. B. C. Turner *et al.*, Expression of AP-2 transcription factors in human breast cancer correlates with the regulation of multiple growth factor signalling pathways. *Cancer Res* **58**, 5466-5472 (1998).
167. M. Li *et al.*, The human transcription factor activation protein-2 gamma (AP-2gamma): gene structure, promoter, and expression in mammary carcinoma cell lines. *Gene* **301**, 43-51 (2002).
168. A. B. Heimberger *et al.*, Loss of the AP-2alpha transcription factor is associated with the grade of human gliomas. *Clin Cancer Res* **11**, 267-272 (2005).
169. R. Britto *et al.*, Shift in AP-2alpha localization characterizes astrocytoma progression. *Cancer Biol Ther* **6**, 413-418 (2007).
170. M. Ruiz *et al.*, Activator protein 2alpha inhibits tumorigenicity and represses vascular endothelial growth factor transcription in prostate cancer cells. *Cancer Res* **64**, 631-638 (2004).
171. W. Su *et al.*, Ectopic expression of AP-2alpha transcription factor suppresses glioma progression. *Int J Clin Exp Pathol* **7**, 8666-8674 (2014).
172. K. Nagata, R. A. Guggenheimer, T. Enomoto, J. H. Lichy, J. Hurwitz, Adenovirus DNA replication in vitro: identification of a host factor that stimulates synthesis of the preterminal protein-dCMP complex. *Proc Natl Acad Sci U S A* **79**, 6438-6442 (1982).
173. K. Nagata, R. A. Guggenheimer, J. Hurwitz, Specific binding of a cellular DNA replication protein to the origin of replication of adenovirus DNA. *Proc Natl Acad Sci U S A* **80**, 6177-6181 (1983).
174. S. Mason, M. Piper, R. M. Gronostajski, L. J. Richards, Nuclear factor one transcription factors in CNS development. *Mol Neurobiol* **39**, 10-23 (2009).
175. R. M. Gronostajski, Roles of the NFI/CTF gene family in transcription and development. *Gene* **249**, 31-45 (2000).
176. R. M. Gronostajski, Analysis of nuclear factor I binding to DNA using degenerate oligonucleotides. *Nucleic Acids Res* **14**, 9117-9132 (1986).
177. P. A. Leegwater, W. van Driel, P. C. van der Vliet, Recognition site of nuclear factor I, a sequence-specific DNA-binding protein from HeLa cells that stimulates adenovirus DNA replication. *EMBO J* **4**, 1515-1521 (1985).
178. Y. Liu, H. U. Bernard, D. Apt, NFI-B3, a novel transcriptional repressor of the nuclear factor I family, is generated by alternative RNA processing. *J Biol Chem* **272**, 10739-10745 (1997).
179. S. S. Mukhopadhyay, S. L. Wyszomierski, R. M. Gronostajski, J. M. Rosen, Differential interactions of specific nuclear factor I isoforms with the glucocorticoid receptor and STAT5 in the cooperative regulation of WAP gene transcription. *Mol Cell Biol* **21**, 6859-6869 (2001).

180. S. K. Singh *et al.*, The unique transcriptional activation domain of nuclear factor-I-X3 is critical to specifically induce marker gene expression in astrocytes. *J Biol Chem* **286**, 7315-7326 (2011).
181. D. A. Bisgrove, E. A. Monckton, M. Packer, R. Godbout, Regulation of brain fatty acid-binding protein expression by differential phosphorylation of nuclear factor I in malignant glioma cell lines. *J Biol Chem* **275**, 30668-30676 (2000).
182. M. Brun *et al.*, Nuclear factor I regulates brain fatty acid-binding protein and glial fibrillary acidic protein gene expression in malignant glioma cell lines. *Journal of molecular biology* **391**, 282-300 (2009).
183. S. H. Yang, A. Galanis, J. Witty, A. D. Sharrocks, An extended consensus motif enhances the specificity of substrate modification by SUMO. *EMBO J* **25**, 5083-5093 (2006).
184. P. V. Hornbeck *et al.*, PhosphoSitePlus, 2014: mutations, PTMs and recalibrations. *Nucleic Acids Res* **43**, D512-520 (2015).
185. Y. H. Heng *et al.*, NFIX regulates neural progenitor cell differentiation during hippocampal morphogenesis. *Cereb Cortex* **24**, 261-279 (2014).
186. M. Piper *et al.*, NFIA controls telencephalic progenitor cell differentiation through repression of the Notch effector Hes1. *J Neurosci* **30**, 9127-9139 (2010).
187. M. Piper *et al.*, NFIB-mediated repression of the epigenetic factor Ezh2 regulates cortical development. *J Neurosci* **34**, 2921-2930 (2014).
188. G. Steele-Perkins *et al.*, The transcription factor gene Nfib is essential for both lung maturation and brain development. *Mol Cell Biol* **25**, 685-698 (2005).
189. A. Z. Chaudhry, G. E. Lyons, R. M. Gronostajski, Expression patterns of the four nuclear factor I genes during mouse embryogenesis indicate a potential role in development. *Dev Dyn* **208**, 313-325 (1997).
190. K. S. Chen *et al.*, Differential neuronal and glial expression of nuclear factor I proteins in the cerebral cortex of adult mice. *J Comp Neurol* **525**, 2465-2483 (2017).
191. L. das Neves *et al.*, Disruption of the murine nuclear factor I-A gene (Nfia) results in perinatal lethality, hydrocephalus, and agenesis of the corpus callosum. *Proc Natl Acad Sci U S A* **96**, 11946-11951 (1999).
192. K. Driller *et al.*, Nuclear factor I X deficiency causes brain malformation and severe skeletal defects. *Mol Cell Biol* **27**, 3855-3867 (2007).
193. T. Shu, K. G. Butz, C. Plachez, R. M. Gronostajski, L. J. Richards, Abnormal development of forebrain midline glia and commissural projections in Nfia knock-out mice. *J Neurosci* **23**, 203-212 (2003).
194. W. Lu *et al.*, NFIA haploinsufficiency is associated with a CNS malformation syndrome and urinary tract defects. *PLoS genetics* **3**, e80 (2007).
195. G. Steele-Perkins *et al.*, Essential role for NFI-C/CTF transcription-replication factor in tooth root development. *Mol Cell Biol* **23**, 1075-1084 (2003).
196. C. E. Campbell *et al.*, The transcription factor Nfix is essential for normal brain development. *BMC Dev Biol* **8**, 52 (2008).
197. M. Piper *et al.*, Nuclear factor one X regulates the development of multiple cellular populations in the postnatal cerebellum. *J Comp Neurol* **519**, 3532-3548 (2011).
198. B. Deneen *et al.*, The transcription factor NFIA controls the onset of gliogenesis in the developing spinal cord. *Neuron* **52**, 953-968 (2006).

199. P. Kang *et al.*, Sox9 and NFIA coordinate a transcriptional regulatory cascade during the initiation of gliogenesis. *Neuron* **74**, 79-94 (2012).
200. M. Namihira *et al.*, Committed neuronal precursors confer astrocytic potential on residual neural precursor cells. *Developmental cell* **16**, 245-255 (2009).
201. B. Cebolla, M. Vallejo, Nuclear factor-I regulates glial fibrillary acidic protein gene expression in astrocytes differentiated from cortical precursor cells. *J Neurochem* **97**, 1057-1070 (2006).
202. E. Matuzelski *et al.*, Transcriptional regulation of Nfix by NFIB drives astrocytic maturation within the developing spinal cord. *Dev Biol* **432**, 286-297 (2017).
203. L. Harris, L. A. Genovesi, R. M. Gronostajski, B. J. Wainwright, M. Piper, Nuclear factor one transcription factors: Divergent functions in developmental versus adult stem cell populations. *Dev Dyn* **244**, 227-238 (2015).
204. B. Martynoga *et al.*, Epigenomic enhancer annotation reveals a key role for NFIX in neural stem cell quiescence. *Genes Dev* **27**, 1769-1786 (2013).
205. H. R. Song *et al.*, Nuclear factor IA is expressed in astrocytomas and is associated with improved survival. *Neuro Oncol* **12**, 122-132 (2010).
206. J. S. Lee *et al.*, A novel tumor-promoting role for nuclear factor IA in glioblastomas is mediated through negative regulation of p53, p21, and PAI1. *Neuro Oncol* **16**, 191-203 (2014).
207. S. M. Glasgow *et al.*, The miR-223/nuclear factor I-A axis regulates glial precursor proliferation and tumorigenesis in the CNS. *J Neurosci* **33**, 13560-13568 (2013).
208. S. M. Glasgow *et al.*, Mutual antagonism between Sox10 and NFIA regulates diversification of glial lineages and glioma subtypes. *Nature neuroscience* **17**, 1322-1329 (2014).
209. B. W. Stringer *et al.*, Nuclear factor one B (NFIB) encodes a subtype-specific tumour suppressor in glioblastoma. *Oncotarget* **7**, 29306-29320 (2016).
210. R. Mita *et al.*, B-FABP-expressing radial glial cells: the malignant glioma cell of origin? *Neoplasia* **9**, 734-744 (2007).
211. O. Nakagawa, M. Nakagawa, J. A. Richardson, E. N. Olson, D. Srivastava, HRT1, HRT2, and HRT3: a new subclass of bHLH transcription factors marking specific cardiac, somitic, and pharyngeal arch segments. *Dev Biol* **216**, 72-84 (1999).
212. M. T. Chin *et al.*, Cardiovascular basic helix loop helix factor 1, a novel transcriptional repressor expressed preferentially in the developing and adult cardiovascular system. *J Biol Chem* **275**, 6381-6387 (2000).
213. D. Weber, C. Wiese, M. Gessler, Hey bHLH transcription factors. *Curr Top Dev Biol* **110**, 285-315 (2014).
214. C. Steidl *et al.*, Characterization of the human and mouse HEY1, HEY2, and HEYL genes: cloning, mapping, and mutation screening of a new bHLH gene family. *Genomics* **66**, 195-203 (2000).
215. T. Iso, L. Kedes, Y. Hamamori, HES and HERP families: multiple effectors of the Notch signaling pathway. *J Cell Physiol* **194**, 237-255 (2003).
216. J. Heisig *et al.*, Target gene analysis by microarrays and chromatin immunoprecipitation identifies HEY proteins as highly redundant bHLH repressors. *PLoS genetics* **8**, e1002728 (2012).

217. A. Fischer, M. Gessler, Delta-Notch--and then? Protein interactions and proposed modes of repression by Hes and Hey bHLH factors. *Nucleic Acids Res* **35**, 4583-4596 (2007).
218. T. Iso *et al.*, HERP, a novel heterodimer partner of HES/E(spl) in Notch signaling. *Mol Cell Biol* **21**, 6080-6089 (2001).
219. C. Leimeister, A. Externbrink, B. Klamt, M. Gessler, Hey genes: a novel subfamily of hairy- and Enhancer of split related genes specifically expressed during mouse embryogenesis. *Mech Dev* **85**, 173-177 (1999).
220. J. L. Ables, J. J. Breunig, A. J. Eisch, P. Rakic, Not(ch) just development: Notch signalling in the adult brain. *Nat Rev Neurosci* **12**, 269-283 (2011).
221. T. Iso *et al.*, HERP, a new primary target of Notch regulated by ligand binding. *Mol Cell Biol* **21**, 6071-6079 (2001).
222. M. M. Maier, M. Gessler, Comparative analysis of the human and mouse Hey1 promoter: Hey genes are new Notch target genes. *Biochemical and biophysical research communications* **275**, 652-660 (2000).
223. T. Iso, G. Chung, Y. Hamamori, L. Kedes, HERP1 is a cell type-specific primary target of Notch. *J Biol Chem* **277**, 6598-6607 (2002).
224. S. Kamakura *et al.*, Hes binding to STAT3 mediates crosstalk between Notch and JAK-STAT signalling. *Nat Cell Biol* **6**, 547-554 (2004).
225. H. Hayashi, T. Kume, Foxc transcription factors directly regulate Dll4 and Hey2 expression by interacting with the VEGF-Notch signaling pathways in endothelial cells. *PLoS One* **3**, e2401 (2008).
226. K. A. Sharff *et al.*, Hey1 basic helix-loop-helix protein plays an important role in mediating BMP9-induced osteogenic differentiation of mesenchymal progenitor cells. *J Biol Chem* **284**, 649-659 (2009).
227. C. Dahlqvist *et al.*, Functional Notch signaling is required for BMP4-induced inhibition of myogenic differentiation. *Development* **130**, 6089-6099 (2003).
228. S. J. Morrison *et al.*, Transient Notch activation initiates an irreversible switch from neurogenesis to gliogenesis by neural crest stem cells. *Cell* **101**, 499-510 (2000).
229. S. Fukada *et al.*, Hesr1 and Hesr3 are essential to generate undifferentiated quiescent satellite cells and to maintain satellite cell numbers. *Development* **138**, 4609-4619 (2011).
230. T. P. Zhong, M. Rosenberg, M. A. Mohideen, B. Weinstein, M. C. Fishman, gridlock, an HLH gene required for assembly of the aorta in zebrafish. *Science* **287**, 1820-1824 (2000).
231. Y. Li *et al.*, Smooth muscle Notch1 mediates neointimal formation after vascular injury. *Circulation* **119**, 2686-2692 (2009).
232. T. Satow *et al.*, The basic helix-loop-helix gene hesr2 promotes gliogenesis in mouse retina. *J Neurosci* **21**, 1265-1273 (2001).
233. M. Sakamoto, H. Hirata, T. Ohtsuka, Y. Bessho, R. Kageyama, The basic helix-loop-helix genes Hesr1/Hey1 and Hesr2/Hey2 regulate maintenance of neural precursor cells in the brain. *J Biol Chem* **278**, 44808-44815 (2003).
234. N. Malik *et al.*, Comparison of the gene expression profiles of human fetal cortical astrocytes with pluripotent stem cell derived neural stem cells identifies human

- astrocyte markers and signaling pathways and transcription factors active in human astrocytes. *PLoS One* **9**, e96139 (2014).
235. F. Culpier *et al.*, Novel features of boundary cap cells revealed by the analysis of newly identified molecular markers. *Glia* **57**, 1450-1457 (2009).
  236. A. Mukhopadhyay, J. Jarrett, T. Chlon, J. A. Kessler, HeyL regulates the number of TrkC neurons in dorsal root ganglia. *Dev Biol* **334**, 142-151 (2009).
  237. A. Jalali *et al.*, HeyL promotes neuronal differentiation of neural progenitor cells. *J Neurosci Res* **89**, 299-309 (2011).
  238. N. El Hindy *et al.*, Implications of Dll4-Notch signaling activation in primary glioblastoma multiforme. *Neuro Oncol* **15**, 1366-1378 (2013).
  239. P. A. Candy *et al.*, Notch-induced transcription factors are predictive of survival and 5-fluorouracil response in colorectal cancer patients. *Br J Cancer* **109**, 1023-1030 (2013).
  240. M. M. Forghanifard, S. Taleb, M. R. Abbaszadegan, Notch Signaling Target Genes are Directly Correlated to Esophageal Squamous Cell Carcinoma Tumorigenesis. *Pathol Oncol Res* **21**, 463-467 (2015).
  241. F. Engin *et al.*, Notch signaling contributes to the pathogenesis of human osteosarcomas. *Hum Mol Genet* **18**, 1464-1470 (2009).
  242. M. E. Mullendore *et al.*, Ligand-dependent Notch signaling is involved in tumor initiation and tumor maintenance in pancreatic cancer. *Clin Cancer Res* **15**, 2291-2301 (2009).
  243. A. Tsuru *et al.*, Hairy/enhancer-of-split related with YRPW motif protein 1 promotes osteosarcoma metastasis via matrix metalloproteinase 9 expression. *Br J Cancer* **112**, 1232-1240 (2015).
  244. A. Fischer *et al.*, Combined loss of Hey1 and HeyL causes congenital heart defects because of impaired epithelial to mesenchymal transition. *Circ Res* **100**, 856-863 (2007).
  245. J. Zavadil, L. Cermak, N. Soto-Nieves, E. P. Bottinger, Integration of TGF-beta/Smad and Jagged1/Notch signalling in epithelial-to-mesenchymal transition. *EMBO J* **23**, 1155-1165 (2004).
  246. L. Han *et al.*, The Notch pathway inhibits TGFbeta signaling in breast cancer through HEYL-mediated crosstalk. *Cancer Res* **74**, 6509-6518 (2014).
  247. M. Yamamoto *et al.*, NF-kappaB non-cell-autonomously regulates cancer stem cell populations in the basal-like breast cancer subtype. *Nat Commun* **4**, 2299 (2013).
  248. E. Y. Lau *et al.*, Cancer-Associated Fibroblasts Regulate Tumor-Initiating Cell Plasticity in Hepatocellular Carcinoma through c-Met/FRA1/HEY1 Signaling. *Cell Rep* **15**, 1175-1189 (2016).
  249. Z. Liu *et al.*, Hey Factors at the Crossroad of Tumorigenesis and Clinical Therapeutic Modulation of Hey for Anticancer Treatment. *Mol Cancer Ther* **16**, 775-786 (2017).
  250. V. Bolos *et al.*, Notch activation stimulates migration of breast cancer cells and promotes tumor growth. *Breast Cancer Res* **15**, R54 (2013).
  251. P. Xu *et al.*, Differential expression of Notch family members in astrocytomas and medulloblastomas. *Pathol Oncol Res* **15**, 703-710 (2009).
  252. P. Dell'albani *et al.*, Differential patterns of NOTCH1-4 receptor expression are markers of glioma cell differentiation. *Neuro Oncol* **16**, 204-216 (2014).
  253. B. W. Purow *et al.*, Expression of Notch-1 and its ligands, Delta-like-1 and Jagged-1, is critical for glioma cell survival and proliferation. *Cancer Res* **65**, 2353-2363 (2005).

254. E. Hulleman *et al.*, A role for the transcription factor HEY1 in glioblastoma. *Journal of cellular and molecular medicine* **13**, 136-146 (2009).
255. A. J. Tsung *et al.*, Methylation regulates HEY1 expression in glioblastoma. *Oncotarget* **8**, 44398-44409 (2017).
256. C. L. Cepko, The roles of intrinsic and extrinsic cues and bHLH genes in the determination of retinal cell fates. *Curr Opin Neurobiol* **9**, 37-46 (1999).
257. K. Hilger-Eversheim, M. Moser, H. Schorle, R. Buettner, Regulatory roles of AP-2 transcription factors in vertebrate development, apoptosis and cell-cycle control. *Gene* **260**, 1-12 (2000).
258. P. J. Mitchell, P. M. Timmons, J. M. Hebert, P. W. Rigby, R. Tjian, Transcription factor AP-2 is expressed in neural crest cell lineages during mouse embryogenesis. *Genes Dev* **5**, 105-119 (1991).
259. R. Tummala, R. A. Romano, E. Fuchs, S. Sinha, Molecular cloning and characterization of AP-2 epsilon, a fifth member of the AP-2 family. *Gene* **321**, 93-102 (2003).
260. X. Li *et al.*, Loss of AP-2delta reduces retinal ganglion cell numbers and axonal projections to the superior colliculus. *Mol Brain* **9**, 62 (2016).
261. J. A. West-Mays *et al.*, AP-2alpha transcription factor is required for early morphogenesis of the lens vesicle. *Dev Biol* **206**, 46-62 (1999).
262. D. J. Dwivedi *et al.*, Targeted deletion of AP-2alpha leads to disruption in corneal epithelial cell integrity and defects in the corneal stroma. *Invest Ophthalmol Vis Sci* **46**, 3623-3630 (2005).
263. G. F. Pontoriero *et al.*, Cell autonomous roles for AP-2alpha in lens vesicle separation and maintenance of the lens epithelial cell phenotype. *Developmental dynamics : an official publication of the American Association of Anatomists* **237**, 602-617 (2008).
264. E. A. Bassett *et al.*, AP-2alpha knockout mice exhibit optic cup patterning defects and failure of optic stalk morphogenesis. *Hum Mol Genet* **19**, 1791-1804 (2010).
265. D. A. Bisgrove, E. A. Monckton, R. Godbout, Involvement of AP-2 in regulation of the R-FABP gene in the developing chick retina. *Mol Cell Biol* **17**, 5935-5945 (1997).
266. X. Li, E. A. Monckton, R. Godbout, Ectopic expression of transcription factor AP-2delta in developing retina: effect on PSA-NCAM and axon routing. *Journal of neurochemistry* **129**, 72-84 (2014).
267. C. J. Jeon, E. Strettoi, R. H. Masland, The major cell populations of the mouse retina. *J Neurosci* **18**, 8936-8946 (1998).
268. S. Katyal, R. Godbout, Alternative splicing modulates Disabled-1 (Dab1) function in the developing chick retina. *EMBO J* **23**, 1878-1888 (2004).
269. Z. Gao *et al.*, Splice-mediated motif switching regulates disabled-1 phosphorylation and SH2 domain interactions. *Mol Cell Biol* **32**, 2794-2808 (2012).
270. D. D. Glubrecht, J. H. Kim, L. Russell, J. S. Bamforth, R. Godbout, Differential CRX and OTX2 expression in human retina and retinoblastoma. *J Neurochem* **111**, 250-263 (2009).
271. C. Prada, J. Puga, L. Perez-Mendez, R. Lopez, G. Ramirez, Spatial and Temporal Patterns of Neurogenesis in the Chick Retina. *Eur J Neurosci* **3**, 559-569 (1991).
272. P. G. Layer, G. Vollmer, Lucifer yellow stains displaced amacrine cells of the chicken retina during embryonic development. *Neurosci Lett* **31**, 99-104 (1982).

273. C. Prada, L. Puelles, J. M. Genis-Galvez, G. Ramirez, Two modes of free migration of amacrine cell neuroblasts in the chick retina. *Anat Embryol (Berl)* **175**, 281-287 (1987).
274. L. Li *et al.*, Role for RIF1-interacting partner DDX1 in BLM recruitment to DNA double-strand breaks. *DNA Repair (Amst)* **55**, 47-63 (2017).
275. D. M. Lam, Neurotransmitters in the vertebrate retina. *Investigative ophthalmology & visual science* **38**, 553-556 (1997).
276. T. A. Dolecek, J. M. Propp, N. E. Stroup, C. Kruchko, CBTRUS statistical report: primary brain and central nervous system tumors diagnosed in the United States in 2005-2009. *Neuro Oncol* **14 Suppl 5**, v1-49 (2012).
277. W. P. Mason *et al.*, Canadian recommendations for the treatment of glioblastoma multiforme. *Curr Oncol* **14**, 110-117 (2007).
278. T. F. Cloughesy, W. K. Cavenee, P. S. Mischel, Glioblastoma: from molecular pathology to targeted treatment. *Annu Rev Pathol* **9**, 1-25 (2014).
279. H. Wang *et al.*, The challenges and the promise of molecular targeted therapy in malignant gliomas. *Neoplasia* **17**, 239-255 (2015).
280. U. Kruse, F. Qian, A. E. Sippel, Identification of a fourth nuclear factor I gene in chicken by cDNA cloning: NFI-X. *Nucleic Acids Res* **19**, 6641 (1991).
281. U. Kruse, A. E. Sippel, Transcription factor nuclear factor I proteins form stable homo- and heterodimers. *FEBS Lett* **348**, 46-50 (1994).
282. A. Z. Chaudhry, A. D. Vitullo, R. M. Gronostajski, Nuclear factor I (NFI) isoforms differentially activate simple versus complex NFI-responsive promoters. *J Biol Chem* **273**, 18538-18546 (1998).
283. K. Amemiya, R. Traub, L. Durham, E. O. Major, Adjacent nuclear factor-1 and activator protein binding sites in the enhancer of the neurotropic JC virus. A common characteristic of many brain-specific genes. *J Biol Chem* **267**, 14204-14211 (1992).
284. J. Betancourt, S. Katzman, B. Chen, Nuclear factor one B regulates neural stem cell differentiation and axonal projection of corticofugal neurons. *J Comp Neurol* **522**, 6-35 (2014).
285. Y. W. Wong *et al.*, Gene expression analysis of nuclear factor I-A deficient mice indicates delayed brain maturation. *Genome Biol* **8**, R72 (2007).
286. N. S. Bayin *et al.*, Patient-Specific Screening Using High-Grade Glioma Explants to Determine Potential Radiosensitization by a TGF-beta Small Molecule Inhibitor. *Neoplasia* **18**, 795-805 (2016).
287. M. M. Lino, A. Merlo, J. L. Boulay, Notch signaling in glioblastoma: a developmental drug target? *BMC Med* **8**, 72 (2010).
288. R. Godbout, D. A. Bisgrove, D. Shkolny, R. S. Day, 3rd, Correlation of B-FABP and GFAP expression in malignant glioma. *Oncogene* **16**, 1955-1962 (1998).
289. S. Pillai, P. Dasgupta, S. P. Chellappan, Chromatin immunoprecipitation assays: analyzing transcription factor binding and histone modifications in vivo. *Methods Mol Biol* **523**, 323-339 (2009).
290. R. M. O'Brien *et al.*, Hepatic nuclear factor 3- and hormone-regulated expression of the phosphoenolpyruvate carboxykinase and insulin-like growth factor-binding protein 1 genes. *Mol Cell Biol* **15**, 1747-1758 (1995).

291. R. J. Roy, P. Gosselin, S. L. Guerin, A short protocol for micro-purification of nuclear proteins from whole animal tissue. *BioTechniques* **11**, 770-777 (1991).
292. S. Bleoo *et al.*, Association of human DEAD box protein DDX1 with a cleavage stimulation factor involved in 3'-end processing of pre-mRNA. *Molecular biology of the cell* **12**, 3046-3059 (2001).
293. S. M. Gopalan, K. M. Wilczynska, B. S. Konik, L. Bryan, T. Kordula, Nuclear factor-1-X regulates astrocyte-specific expression of the alpha1-antichymotrypsin and glial fibrillary acidic protein genes. *J Biol Chem* **281**, 13126-13133 (2006).
294. S. Ouellet *et al.*, Transcriptional regulation of the cyclin-dependent kinase inhibitor 1A (p21) gene by NF1 in proliferating human cells. *Nucleic Acids Res* **34**, 6472-6487 (2006).
295. M. Ashburner *et al.*, Gene ontology: tool for the unification of biology. The Gene Ontology Consortium. *Nat Genet* **25**, 25-29 (2000).
296. Gene Ontology Consortium: going forward. *Nucleic Acids Res* **43**, D1049-1056 (2015).
297. H. Mi, A. Muruganujan, P. D. Thomas, PANTHER in 2013: modeling the evolution of gene function, and other gene attributes, in the context of phylogenetic trees. *Nucleic Acids Res* **41**, D377-386 (2013).
298. Y. Morihiro *et al.*, Fatty acid binding protein 7 as a marker of glioma stem cells. *Pathol Int* **63**, 546-553 (2013).
299. A. De Rosa *et al.*, A radial glia gene marker, fatty acid binding protein 7 (FABP7), is involved in proliferation and invasion of glioblastoma cells. *PLoS One* **7**, e52113 (2012).
300. Y. Yasumoto *et al.*, Inhibition of Fatty Acid Synthase Decreases Expression of Stemness Markers in Glioma Stem Cells. *PLoS One* **11**, e0147717 (2016).
301. S. Osada *et al.*, Expression, DNA-binding specificity and transcriptional regulation of nuclear factor 1 family proteins from rat. *The Biochemical journal* **342 ( Pt 1)**, 189-198 (1999).
302. T. K. Archer, P. Lefebvre, R. G. Wolford, G. L. Hager, Transcription factor loading on the MMTV promoter: a bimodal mechanism for promoter activation. *Science* **255**, 1573-1576 (1992).
303. P. B. Hebbar, T. K. Archer, Altered histone H1 stoichiometry and an absence of nucleosome positioning on transfected DNA. *J Biol Chem* **283**, 4595-4601 (2008).
304. P. Gaetani *et al.*, Expression of the transcription factor HEY1 in glioblastoma: a preliminary clinical study. *Tumori* **96**, 97-102 (2010).
305. K. M. Wilczynska *et al.*, Nuclear factor I isoforms regulate gene expression during the differentiation of human neural progenitors to astrocytes. *Stem Cells* **27**, 1173-1181 (2009).
306. T. Y. Lee *et al.*, Disruption of Nfic causes dissociation of odontoblasts by interfering with the formation of intercellular junctions and aberrant odontoblast differentiation. *J Histochem Cytochem* **57**, 469-476 (2009).
307. K. S. Chen, J. W. C. Lim, L. J. Richards, J. Bunt, The convergent roles of the nuclear factor I transcription factors in development and cancer. *Cancer Lett* **410**, 124-138 (2017).
308. D. Beier *et al.*, CD133(+) and CD133(-) glioblastoma-derived cancer stem cells show differential growth characteristics and molecular profiles. *Cancer Res* **67**, 4010-4015 (2007).

309. A. D. Berezovsky *et al.*, Sox2 promotes malignancy in glioblastoma by regulating plasticity and astrocytic differentiation. *Neoplasia* **16**, 193-206, 206 e119-125 (2014).
310. S. K. Singh *et al.*, Identification of a cancer stem cell in human brain tumors. *Cancer Res* **63**, 5821-5828 (2003).
311. J. M. Pellikainen, V. M. Kosma, Activator protein-2 in carcinogenesis with a special reference to breast cancer--a mini review. *Int J Cancer* **120**, 2061-2067 (2007).
312. J. Pellikainen *et al.*, Reduced nuclear expression of transcription factor AP-2 associates with aggressive breast cancer. *Clin Cancer Res* **8**, 3487-3495 (2002).
313. C. Berlato *et al.*, Alternative TFAP2A isoforms have distinct activities in breast cancer. *Breast Cancer Res* **13**, R23 (2011).
314. C. M. Williams *et al.*, AP-2gamma promotes proliferation in breast tumour cells by direct repression of the CDKN1A gene. *EMBO J* **28**, 3591-3601 (2009).
315. C. Zhao *et al.*, Elevated expression levels of NCOA3, TOP1, and TFAP2C in breast tumors as predictors of poor prognosis. *Cancer* **98**, 18-23 (2003).
316. L. Fu *et al.*, TFAP2B overexpression contributes to tumor growth and a poor prognosis of human lung adenocarcinoma through modulation of ERK and VEGF/PEDF signaling. *Mol Cancer* **13**, 89 (2014).
317. H. Wu, J. Zhang, Decreased expression of TFAP2B in endometrial cancer predicts poor prognosis: A study based on TCGA data. *Gynecol Oncol* **149**, 592-597 (2018).
318. W. Su *et al.*, Ectopic expression of AP-2alpha transcription factor suppresses glioma progression. *Int J Clin Exp Pathol* **7**, 8666-8674 (2014).
319. C. W. Brennan *et al.*, The somatic genomic landscape of glioblastoma. *Cell* **155**, 462-477 (2013).
320. B. E. Stopschinski, C. P. Beier, D. Beier, Glioblastoma cancer stem cells--from concept to clinical application. *Cancer Lett* **338**, 32-40 (2013).
321. L. Yang, C. Lin, L. Wang, H. Guo, X. Wang, Hypoxia and hypoxia-inducible factors in glioblastoma multiforme progression and therapeutic implications. *Exp Cell Res* **318**, 2417-2426 (2012).
322. H. R. Qin *et al.*, Wwox suppresses prostate cancer cell growth through modulation of ErbB2-mediated androgen receptor signaling. *Mol Cancer Res* **5**, 957-965 (2007).
323. J. D. Nardozi, K. Lott, G. Cingolani, Phosphorylation meets nuclear import: a review. *Cell Commun Signal* **8**, 32 (2010).
324. R. T. Hay, SUMO: a history of modification. *Mol Cell* **18**, 1-12 (2005).
325. K. Park, K. H. Kim, The site of cAMP action in the insulin induction of gene expression of acetyl-CoA carboxylase is AP-2. *J Biol Chem* **268**, 17811-17819 (1993).
326. N. C. Inestrosa, E. Arenas, Emerging roles of Wnts in the adult nervous system. *Nat Rev Neurosci* **11**, 77-86 (2010).
327. P. W. Ingham, A. P. McMahon, Hedgehog signaling in animal development: paradigms and principles. *Genes Dev* **15**, 3059-3087 (2001).
328. J. M. Vaquerizas, S. K. Kummerfeld, S. A. Teichmann, N. M. Luscombe, A census of human transcription factors: function, expression and evolution. *Nat Rev Genet* **10**, 252-263 (2009).
329. T. I. Lee, R. A. Young, Transcriptional regulation and its misregulation in disease. *Cell* **152**, 1237-1251 (2013).

330. R. I. Aqeilan *et al.*, Physical and functional interactions between the Wwox tumor suppressor protein and the AP-2gamma transcription factor. *Cancer Res* **64**, 8256-8261 (2004).
331. J. M. Boshier, N. F. Totty, J. J. Hsuan, T. Williams, H. C. Hurst, A family of AP-2 proteins regulates c-erbB-2 expression in mammary carcinoma. *Oncogene* **13**, 1701-1707 (1996).
332. G. A. Hyatt, J. E. Dowling, Retinoic acid. A key molecule for eye and photoreceptor development. *Invest Ophthalmol Vis Sci* **38**, 1471-1475 (1997).
333. L. A. McPherson, G. W. Woodfield, R. J. Weigel, AP2 transcription factors regulate expression of CRABP2 in hormone responsive breast carcinoma. *J Surg Res* **138**, 71-78 (2007).
334. R. Z. Liu *et al.*, Association between cytoplasmic CRABP2, altered retinoic acid signaling, and poor prognosis in glioblastoma. *Glia* **64**, 963-976 (2016).
335. F. Odreman *et al.*, Proteomic studies on low- and high-grade human brain astrocytomas. *J Proteome Res* **4**, 698-708 (2005).
336. T. C. Chen, D. R. Hinton, R. Zidovetzki, F. M. Hofman, Up-regulation of the cAMP/PKA pathway inhibits proliferation, induces differentiation, and leads to apoptosis in malignant gliomas. *Lab Invest* **78**, 165-174 (1998).
337. P. Goldhoff *et al.*, Targeted inhibition of cyclic AMP phosphodiesterase-4 promotes brain tumor regression. *Clin Cancer Res* **14**, 7717-7725 (2008).
338. T. C. Chen *et al.*, The type IV phosphodiesterase inhibitor rolipram induces expression of the cell cycle inhibitors p21(Cip1) and p27(Kip1), resulting in growth inhibition, increased differentiation, and subsequent apoptosis of malignant A-172 glioma cells. *Cancer Biol Ther* **1**, 268-276 (2002).
339. T. Williams, R. Tjian, Analysis of the DNA-binding and activation properties of the human transcription factor AP-2. *Genes Dev* **5**, 670-682 (1991).
340. P. Meier, M. Koedood, J. Philipp, A. Fontana, P. J. Mitchell, Alternative mRNAs encode multiple isoforms of transcription factor AP-2 during murine embryogenesis. *Dev Biol* **169**, 1-14 (1995).
341. X. Li *et al.*, Loss of AP-2delta reduces retinal ganglion cell numbers and axonal projections to the superior colliculus. *Mol Brain* **9**, 62 (2016).
342. S. Alcantara Llaguno *et al.*, Malignant astrocytomas originate from neural stem/progenitor cells in a somatic tumor suppressor mouse model. *Cancer Cell* **15**, 45-56 (2009).
343. C. Liu *et al.*, Mosaic analysis with double markers reveals tumor cell of origin in glioma. *Cell* **146**, 209-221 (2011).
344. N. Sanai, A. Alvarez-Buylla, M. S. Berger, Neural stem cells and the origin of gliomas. *N Engl J Med* **353**, 811-822 (2005).
345. M. Kamino *et al.*, Wnt-5a signaling is correlated with infiltrative activity in human glioma by inducing cellular migration and MMP-2. *Cancer Sci* **102**, 540-548 (2011).
346. N. Golestaneh, B. Mishra, TGF-beta, neuronal stem cells and glioblastoma. *Oncogene* **24**, 5722-5730 (2005).
347. J. N. Rich, The role of transforming growth factor-beta in primary brain tumors. *Front Biosci* **8**, e245-260 (2003).

348. D. Koinuma *et al.*, Chromatin immunoprecipitation on microarray analysis of Smad2/3 binding sites reveals roles of ETS1 and TFAP2A in transforming growth factor beta signaling. *Mol Cell Biol* **29**, 172-186 (2009).
349. W. D. Wang, D. B. Melville, M. Montero-Balaguer, A. K. Hatzopoulos, E. W. Knapik, Tfp2a and Foxd3 regulate early steps in the development of the neural crest progenitor population. *Dev Biol* **360**, 173-185 (2011).
350. P. Rakic, Specification of cerebral cortical areas. *Science* **241**, 170-176 (1988).
351. T. E. Anthony, C. Klein, G. Fishell, N. Heintz, Radial glia serve as neuronal progenitors in all regions of the central nervous system. *Neuron* **41**, 881-890 (2004).
352. O. Nakagawa *et al.*, Members of the HRT family of basic helix-loop-helix proteins act as transcriptional repressors downstream of Notch signaling. *Proc Natl Acad Sci U S A* **97**, 13655-13660 (2000).
353. W. Ge *et al.*, Notch signaling promotes astroglialogenesis via direct CSL-mediated glial gene activation. *J Neurosci Res* **69**, 848-860 (2002).
354. A. H. Shih, E. C. Holland, Notch signaling enhances nestin expression in gliomas. *Neoplasia* **8**, 1072-1082 (2006).
355. B. W. Purow *et al.*, Notch-1 regulates transcription of the epidermal growth factor receptor through p53. *Carcinogenesis* **29**, 918-925 (2008).
356. M. V. Gustafsson *et al.*, Hypoxia requires notch signaling to maintain the undifferentiated cell state. *Developmental cell* **9**, 617-628 (2005).
357. C. Zhan *et al.*, An ultrahigh affinity d-peptide antagonist Of MDM2. *J Med Chem* **55**, 6237-6241 (2012).
358. A. Kiessling, B. Sperl, A. Hollis, D. Eick, T. Berg, Selective inhibition of c-Myc/Max dimerization and DNA binding by small molecules. *Chem Biol* **13**, 745-751 (2006).
359. T. H. Scheuermann *et al.*, Allosteric inhibition of hypoxia inducible factor-2 with small molecules. *Nat Chem Biol* **9**, 271-276 (2013).
360. H. S. Kim, S. J. Hong, M. S. LeDoux, K. S. Kim, Regulation of the tyrosine hydroxylase and dopamine beta-hydroxylase genes by the transcription factor AP-2. *J Neurochem* **76**, 280-294 (2001).
361. C. Quirin-Stricker, C. Mauvais, M. Schmitt, Transcriptional activation of human choline acetyltransferase by AP2- and NGF-induced factors. *Brain Res Mol Brain Res* **49**, 165-174 (1997).
362. S. Bartsch, K. Husmann, M. Schachner, U. Bartsch, The extracellular matrix molecule tenascin: expression in the developing chick retinotectal system and substrate properties for retinal ganglion cell neurites in vitro. *Eur J Neurosci* **7**, 907-916 (1995).
363. F. Ducray *et al.*, Predictive and prognostic factors for gliomas. *Expert Rev Anticancer Ther* **11**, 781-789 (2011).
364. A. Pichler, F. Melchior, Ubiquitin-related modifier SUMO1 and nucleocytoplasmic transport. *Traffic* **3**, 381-387 (2002).
365. W. A. Pastor *et al.*, TFAP2C regulates transcription in human naive pluripotency by opening enhancers. *Nat Cell Biol* **20**, 553-564 (2018).